Supporting Information for:

Highly Nucleophilic Dipropanolamine Chelated Boron Reagents for Aryl-Transmetallation to Iron Complexes

*Jay J. Dunsford, Ewan R. Clark and Michael J. Ingleson**

School of Chemistry, University of Manchester, Manchester, M13 9PL, U.K.

Table of Contents

1. General Remarks

Unless otherwise stated, all manipulations were carried out using standard Schlenk techniques under argon, or in an MBraun UniLab glovebox, under an atmosphere of argon (< 0.1 ppm O_2/H_2O). Unless otherwise indicated, solvents were distilled from appropriate drying agents: tetrahydrofuran (potassium); toluene (potassium); *n*-hexane (NaK); and dichloromethane (CaH_2). Tetrahydrofuran and dichloromethane were stored over activated 3Å molecular sieves while toluene and *n*-hexane were stored over potassium mirrors. 3,3'-azanediyl*bis*(propan-1-ol),[1] [Fe(dppe)Cl_2],[2] [Fe(dpbz)$_2$$Cl_2$][3] and [Fe(dpbz)$_2$(*p*-Tol)],[4] were all prepared according to previously reported literature procedures. All other compounds were purchased from commercial sources and used as received. NMR spectra were recorded on Bruker AvanceIII-400, Bruker AvanceII-500 or Bruker Ascend-400 spectrometers. Chemical shifts are reported as dimensionless δ values and are frequency referenced relative to residual *protio*- impurities in the NMR solvents for ^{1}H and $^{13}C\{^{1}H\}$ respectively, while $^{11}B\{^{1}H\}$, $^{19}F\{^{1}H\}$ and ^{7}Li shifts are referenced relative to external BF_3-etherate, hexafluorobenzene and LiCl, respectively. Coupling constants *J* are given in Hertz (Hz) as positive values regardless of their real individual signs. The multiplicity of the signals are indicated as “s”, “d”, “t” “pent”, “sept” or “m” for singlet, doublet, triplet, pentet, septet or multiplet, respectively. High resolution mass spectra (HRMS) were recorded on a Waters QTOF mass spectrometer. GC-MS analysis was performed on an Agilent Technologies 7890A GC system equipped with an Agilent Technologies 5975C inert XL EI/CI MSD with triple axis detector. The column employed was an Agilent J&W HP-5ms ((5%-Phenyl)-methylpolysiloxane) of dimensions: length, 30 m; internal diameter, 0.250 mm; film, 0.25 μm. Microanalysis was performed by Mr Stephen Boyer at the London Metropolitan University microanalytical service. X-band CW-EPR spectra were recorded at 120K on a Bruker EMXmicro spectrometer operating at 9.35 GHz field modulation, 2 mW microwave power and equipped with a high sensitivity Bruker cavity (ER 4119HS).

2. Synthesis of Compounds 1a-1q

General Procedure for the Synthesis of 1a-1q: Under ambient conditions, with no additional precautions taken to exclude air or moisture, a round bottom flask was charged with 3,3'-azanediyl*bis*(propan-1-ol) (1.1 equiv.) and tetrahydrofuran. To this stirred solution was added the appropriate boronic acid (1 equiv.) and the reaction mixture stirred at ambient temperature. Typically, the desired products **1a**-**1q** began to deposit from solution after stirring for between 5 and 30 minutes, however in examples where this was not the case, stirring was continued at ambient temperature for 16h. Isolation of the insoluble material by filtration followed by washing with cold tetrahydrofuran typically afforded **1a**-**1q** as colourless free-flowing solids of sufficient purity to be used without further purification. Alternatively, **1a**-**1q** can be recrystallized from hot acetone.

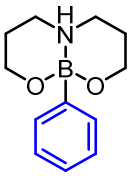

2a. 10-phenyloctahydro-[1,3,2]oxazaborinino[2,3-*b*][1,3,2]oxazaborinin-5-ium-10-uide[5] (1a): Prepared according to the general procedure. Phenylboronic acid (6.10 g, 50.0 mmol) and 3,3'-azanediyl*bis*(propan-1-ol) (7.33 g, 55.0 mmol) in tetrahydrofuran (200 mL) afforded **1a** as a free-flowing white solid (9.74 g, 89%). ^{1}H NMR (400 MHz, DMSO-d_6, 298 K): 7.39 (2H, d, J = 6.7 Hz, *o*-C*H*); 7.19 (2H, t, J = 7.5 Hz, *m*-C*H*); 7.09 (1H, t, J = 7.5 Hz, *p*-C*H*); 5.90 (1H, bs, N*H*); 3.76-3.70 (2H, m, CH_2); 3.50-3.44 (2H, m, CH_2); 3.09-3.02 (2H, m, CH_2); 2.86-2.80 (2H, m, CH_2); 1.81-1.72 (2H, m, CH_2); 1.51-1.42 ppm (2H, m, CH_2). ^{13}C{^{1}H} NMR (100 MHz, DMSO-d_6, 298 K): 131.8; 126.9; 125.5; 59.7; 46.0; 24.3 ppm. ^{11}B{^{1}H} NMR (128.4 MHz, DMSO-d_6, 298 K): 3.2 ppm. HRMS (ESI) *m/z*: calculated for $[M+H]^+$, $C_{12}H_{19}BNO_2^+$, 220.1509, found: 220.1516. Crystals suitable for X-ray diffraction were grown by the slow evapouration of a concentrated acetone solution of **1a** at ambient temperature.

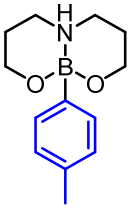

2b. 10-(*p*-tolyl)octahydro-[1,3,2]oxazaborinino[2,3-*b*][1,3,2]oxazaborinin-5-ium-10-uide (1b): Prepared according to the general procedure. *p*-tolylboronic acid (300 mg, 2.21 mmol) and 3,3'-azanediyl*bis*(propan-1-ol) (324 mg, 2.43 mmol) in tetrahydrofuran (50 mL) afforded **1b** as a free-flowing white solid (432 mg, 84%). ^{1}H NMR (400 MHz, DMSO-d_6, 298 K): 7.28 (2H, d, J = 7.9 Hz, C*H*); 7.00 (2H, d, J = 7.2 Hz, C*H*); 5.84 (1H, bs, N*H*); 3.75-3.69 (2H, m, CH_2); 3.50-3.44 (2H, m, CH_2); 3.07-2.99 (2H, m, CH_2); 2.84-2.79 (2H, m, CH_2); 2.24 (3H, s, CH_3); 1.79-1.72 (2H, m, CH_2); 1.49-1.42 ppm (2H, m, CH_2). ^{13}C{^{1}H} NMR (100 MHz, DMSO-d_6, 298 K): 134.0; 131.8; 127.6; 59.7; 46.0; 24.4; 20.9 ppm. ^{11}B{^{1}H} NMR (128.4 MHz, DMSO-d_6, 298 K): 3.3 ppm. HRMS (ESI) *m/z*: calculated for $[M+H]^+$, $C_{13}H_{21}BNO_2^+$, 234.1665, found: 234.1666. Crystals suitable for X-ray diffraction were grown by the slow evapouration of a concentrated acetone solution of **1b** at ambient temperature.

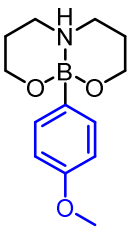

2c. 10-(4-methoxyphenyl)octahydro-[1,3,2]oxazaborinino[2,3-*b*][1,3,2]oxazaborinin-5-ium-10-uide (1c): Prepared according to the general procedure. 4-methoxypenylboronic acid (300 mg, 1.97 mmol) and 3,3'-azanediyl*bis*(propan-1-ol) (289 mg, 2.17 mmol) in tetrahydrofuran (30 mL) afforded **1c** as a free-flowing white solid (475 mg, 97%). ^{1}H NMR (400 MHz, DMSO-d_6, 298 K): 7.29 (2H, d, J = 8.3 Hz, *CH*); 6.77 (2H, d, J = 8.3 Hz, *CH*); 5.84 (1H, bs, N*H*); 3.75-

3.68 (5H, m, CH_2 + OCH_3); 3.51-3.44 (2H, m, CH_2); 3.08-2.98 (2H, m, CH_2); 2.87-2.78 (2H, m, CH_2); 1.77-1.72 (2H, m, CH_2); 1.50-1.40 (2H, m, CH_2) ppm. $^{13}C\{^1H\}$ NMR (100 MHz, DMSO-d_6, 298 K): 157.5; 132.9; 112.5; 59.7; 54.6; 46.0; 24.4 ppm. $^{11}B\{^1H\}$ NMR (128.4 MHz, DMSO-d_6, 298 K): 3.3 ppm. HRMS (ESI) *m/z*: calculated for $[M+Na]^+$, $C_{13}H_{20}BNO_3Na^+$, 272.1434, found: 272.1424.

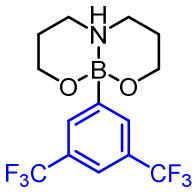

2d. 10-(3,5-bis(trifluoromethyl)phenyl)octahydro-[1,3,2]oxazaborinino [2,3-*b*][1,3,2]oxazaborinin-5-ium-10-uide (1d): Prepared according to the general procedure. 3,5-trichloromethylphenylboronic acid (300 mg, 1.16 mmol) and 3,3'-azanediyl*bis*(propan-1-ol) (171 mg, 1.28 mmol) in tetrahydrofuran (30 mL) afforded **1d** as a free-flowing white solid (377 mg, 83%). ^1H NMR (400 MHz, DMSO-d_6, 298 K): 8.03 (2H, s, *o*-C*H*); 7.78 (1H, s, *p*-C*H*); 6.40 (1H, bs, N*H*); 3.79-3.74 (2H, m, CH_2); 3.44-3.38 (2H, m, CH_2); 3.16-3.08 (2H, m, CH_2); 2.85-2.80 (2H, m, CH_2); 1.84-1.77 (2H, m, CH_2); 1.54-1.48 ppm (2H, m, CH_2). $^{13}C\{^1H\}$ NMR (100 MHz, DMSO-d_6, 298 K): 132.2; 128.7; 125.5; 122.8; 119.3; 59.9; 46.1; 24.0 ppm. $^{11}B\{^1H\}$ NMR (128.4 MHz, DMSO-d_6, 298 K): 2.6 ppm. $^{19}F\{^1H\}$ NMR (376.5 MHz, DMSO-d_6, 298 K): -61.10 ppm. HRMS (ESI) *m/z*: calculated for $[M+H]^+$, $C_{14}H_{17}BF_6NO_2^+$, 356.1257, found: 356.1262.

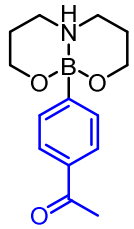

2e. 10-(4-ethane-1-onephenyl)octahydro-[1,3,2]oxazaborinino[2,3-*b*][1,3,2] oxazaborinin-5-ium-10-uide (1e): Prepared according to the general procedure. 4-acetylphenylboronic acid (300 mg, 1.83 mmol) and 3,3'-azanediyl*bis*(propan-1-ol) (268 mg, 2.01 mmol) in tetrahydrofuran (30 mL) afforded **1e** as a free-flowing white solid (440 mg, 92%). ^1H NMR (400 MHz, DMSO-d_6, 298 K): 7.80 (2H, d, J = 8.1 Hz, C*H*); 7.54 (2H, d, J = 8.1 Hz, C*H*); 6.06 (1H, bs, N*H*); 3.78-3.71 (2H, m, CH_2); 3.48-3.40 (2H, m, CH_2); 3.12-3.03 (2H, m, CH_2); 2.86-2.78 (2H, m, CH_2); 2.54 (3H, s, CH_3); 1.84-1.73 (2H, m, CH_2); 1.53-1.43 (2H, m, CH_2) ppm. $^{13}C\{^1H\}$ NMR (100 MHz, DMSO-d_6, 298 K): 198.1; 134.6; 132.0; 126.7; 59.7; 46.0; 26.6; 24.2 ppm. $^{11}B\{^1H\}$ NMR (128.4 MHz, DMSO-d_6, 298 K): 3.4 ppm. HRMS (ESI) *m/z*: calculated for $[M+H]^+$, $C_{14}H_{21}BNO_3^+$, 262.1604, found: 262.1624.

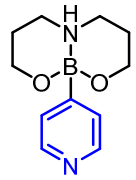

2f 10-(4-pyridyl)octahydro-[1,3,2]oxazaborinino[2,3-*b*][1,3,2]oxaza-borinin-5-ium-10-uide (1f): Prepared according to the general procedure. 4-pyridinylboronic acid (300 mg, 2.44 mmol) and 3,3'-azanediyl*bis*(propan-1-ol) (357 mg, 2.68 mmol) in tetrahydrofuran (30 mL) afforded **1f** as a free-flowing white solid (521 mg, 97%). ^1H NMR (500 MHz, DMSO-d_6, 298 K): 8.36 (2H, d, J = 5.5 Hz, C*H*); 7.35 (2H, d, J = 5.5 Hz, C*H*); 6.08 (1H, bs, N*H*); 3.77-3.70 (2H, m, CH_2); 3.46-3.39 (2H, m, CH_2); 3.21-3.04 (2H, m, CH_2); 2.86-2.79 (2H, m, CH_2); 1.82-1.73 (2H, m, CH_2); 1.52-1.44 (2H, m, CH_2) ppm. $^{13}C\{^1H\}$ NMR (125 MHz, DMSO-d_6, 298 K): 148.0; 127.4; 59.8; 46.1; 24.1 ppm. $^{11}B\{^1H\}$ NMR (160.5 MHz, DMSO-d_6, 298 K): 2.7 ppm. HRMS (ESI) *m/z*: calculated for $[M+H]^+$, $C_{11}H_{18}BN_2O_2^+$, 221.1470, found: 221.1461.

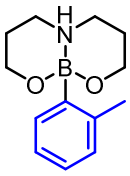

2g. 10-(*o*-tolyl)octahydro-[1,3,2]oxazaborinino[2,3-*b*][1,3,2]oxazaborinin-5-ium-10-uide (1g): Prepared according to the general procedure. *o*-tolyl phenylboronic acid (300 mg, 2.21 mmol), 3,3'-azanediylbis(propan-1-ol) (324 mg, 2.43 mmol) in THF (20 mL) afforded **1g** as a free-flowing white solid (457 mg, 89%). ^{1}H NMR (400 MHz, DMSO-d_6, 298 K): 7.23-7.15 (2H, m, C*H*); 7.07 (1H, t, *J* = 7.3 Hz, C*H*); 6.91 (1H, d, *J* = 7.1 Hz, C*H*); 5.86 (1H, bs, N*H*); 3.76-3.68 (2H, m, CH_2); 3.51-3.43 (2H, m, CH_2); 3.09-2.99 (2H, m, CH_2); 2.88-2.78 (2H, m, CH_2); 2.26 (3H, s, CH_3); 1.81-1.70 (2H, m, CH_2); 1.51-1.41 ppm (2H, m, CH_2). ^{13}C{^{1}H} NMR (100 MHz, DMSO-d_6, 298 K): 135.3; 132.6; 128.9; 126.8; 126.1; 59.7; 46.0; 24.3; 21.5 ppm. ^{11}B{^{1}H} NMR (128.4 MHz, DMSO-d_6, 298 K): 3.5 ppm. HRMS (ESI) *m/z*: calculated for [M+Na]$^+$, $C_{13}H_{20}BNO_2Na^+$, 256.1485, found: 256.1476.

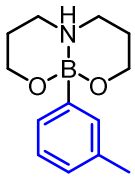

2h. 10-(*m*-tolyl)octahydro-[1,3,2]oxazaborinino[2,3-*b*][1,3,2]oxazaborinin-5-ium-10-uide (1h): Prepared according to the general procedure. *m*-tolyl phenylboronic acid (300 mg, 2.21 mmol), 3,3'-azanediylbis(propan-1-ol) (324 mg, 2.43 mmol) in THF (20 mL) afforded **1h** as a free-flowing white solid (374 mg, 74%). ^{1}H NMR (400 MHz, DMSO-d_6, 298 K): 7.29 (1H, s, *o*-C*H*); 7.04-6.91 (3H, m, C*H*); 5.86 (1H, bs, N*H*); 3.79-3.70 (2H, m, CH_2); 3.37-3.30 (2H, m, CH_2, *overlapping with* H_2O *from DMSO-*d_6); 3.14-3.04 (2H, m, CH_2); 3.02-2.92 (2H, m, CH_2); 2.32 (3H, s, CH_3); 1.83-1.71 (2H, m, CH_2); 1.52-1.41 ppm (2H, m, CH_2). ^{13}C{^{1}H} NMR (100 MHz, DMSO-d_6, 298 K): 141.6; 131.6; 129.6; 125.4; 123.9; 59.5; 46.3; 24.4; 21.7 ppm. ^{11}B{^{1}H} NMR (128.4 MHz, DMSO-d_6, 298 K): 4.2 ppm. HRMS (ESI) *m/z*: calculated for [M+Na]$^+$, $C_{13}H_{20}BNO_2Na^+$, 254.1485, found: 254.1488.

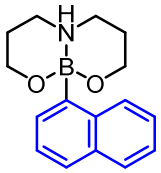

2i. 10-(1-naphthyl)octahydro-[1,3,2]oxazaborinino[2,3-*b*][1,3,2]oxazaborinin-5-ium-10-uide (1i): Prepared according to the general procedure. 1-napthylboronic acid (300 mg, 1.74 mmol), 3,3'-azanediylbis(propan-1-ol) (254 mg, 1.91 mmol) in THF (20 mL) afforded **1i** as a free-flowing white solid (393 mg, 84 %). ^{1}H NMR (400 MHz, DMSO-d_6, 298 K): 8.82 (1H, d, *J* = 8.4 Hz, C*H*); 7.74 (1H, d, *J* = 7.8 Hz, C*H*); 7.65 (1H, d, *J* = 7.8 Hz, C*H*); 7.53 (1H, d, *J* = 6.5 Hz, C*H*); 7.4-7.28 (3H, m, 3xC*H*); 6.16 (1H, bs, N*H*); 3.87-3.75 (2H, m, CH_2); 3.36-3.28 (2H, m, CH_2, *overlapping with* H_2O *from DMSO-*d_6); 3.21-3.03 (4H, m, 2xCH_2); 1.88-1.74 (2H, m, CH_2); 1.56-1.44 ppm (2H, m, CH_2). ^{13}C{^{1}H} NMR (100 MHz, DMSO-d_6, 298 K): 136.8; 133.3; 129.8; 128.8; 127.6; 126.0; 124.8; 124.4; 123.9; 59.8; 46.4; 24.4 ppm. ^{11}B{^{1}H} NMR (128.4 MHz, DMSO-d_6, 298 K): 4.5 ppm. HRMS (ESI) *m/z*: calculated for [M+Na]$^+$, $C_{16}H_{20}BNO_2Na^+$, 292.1485, found: 292.1483.

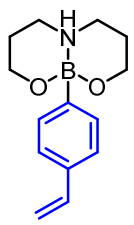

2j. 10-(4-vinylphenyl)octahydro-[1,3,2]oxazaborinino[2,3-*b*][1,3,2]oxazaborinin-5-ium-10-uide (1j): Prepared according to the general procedure. 4-vinylphenylboronic acid (300 mg, 2.03 mmol) and 3,3'-azanediyl*bis*(propan-1-ol) (297 mg, 2.23 mmol) in tetrahydrofuran (30 mL) afforded **1j** as a free-flowing white solid (418 mg, 84%). ^{1}H NMR (500 MHz, DMSO-d_6, 298 K): 7.38 (2H, d, *J* = 7.6 Hz, C*H*); 7.29 (2H, d, 7.9 Hz, C*H*); 6.67 (1H, dd, *J* = 17.7, 10.7 Hz, CH_2C*H*); 5.91 (1H, bs, N*H*); 5.74 (1H, d, *J* = 17.7 Hz, CH_2CH); 5.14 (1H, d, *J* =

11.0 Hz, CH_2CH); 3.78-3.69 (2H, m, CH_2); 3.52-3.43 (2H, m, CH_2); 3.10-3.00 (2H, m, CH_2); 2.88-2.78 (2H, m, CH_2); 1.82-1.72 (2H, m, CH_2); 1.52-1.42 ppm (2H, m, CH_2). ^{13}C{^{1}H} NMR (125 MHz, DMSO-d_6, 298 K): 137.4; 134.6; 132.1; 124.8; 112.2; 59.7; 46.0; 24.3 ppm. ^{11}B{^{1}H} NMR (160.5 MHz, DMSO-d_6, 298 K): 3.5 ppm. HRMS (ESI) *m/z*: calculated for $[M+H]^+$, $C_{14}H_{21}BNO_2^+$, 246.1668, found: 246.1677.

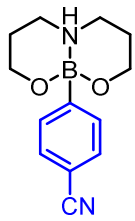

2k. 10-(4-cyanophenyl)octahydro-[1,3,2]oxazaborinino[2,3-*b*][1,3,2]oxazaborinin-5-ium-10-uide (1k): Prepared according to the general procedure. 4-cyanophenylboronic acid (300 mg, 2.0 mmol) and 3,3'-azanediyl*bis*(propan-1-ol) (278 mg, 2.1 mmol) in tetrahydrofuran (30 mL) afforded **1k** as a free-flowing white solid (449 mg, 92%). ^{1}H NMR (400 MHz, DMSO-d_6, 298 K): 7.63 (2H, d, *J* = 8.1 Hz, C*H*); 7.58 (2H, d, *J* = 8.1 Hz, C*H*); 6.12 (1H, bs, N*H*); 3.78-3.69 (2H, m, CH_2); 3.47-3.37 (2H, m, CH_2); 3.14-3.02 (2H, m, CH_2); 2.87-2.76 (2H, m, CH_2); 1.83-1.71 (2H, m, CH_2); 1.53-1.43 ppm (2H, m, CH_2). ^{13}C{^{1}H} NMR (100 MHz, DMSO-d_6, 298 K): 132.7; 130.5; 119.8; 108.2; 59.8; 46.1; 24.2 ppm. ^{11}B{^{1}H} NMR (128.4 MHz, DMSO-d_6, 298 K): 3.3 ppm. MS (ESI) *m/z*: calculated for $[M+H]^+$, $C_{13}H_{18}BN_2O_2^+$, 245.1, found: 245.1. HRMS (ESI) *m/z*: calculated for $[M+H]^+$, $C_{13}H_{18}BN_2O_2^+$, 245.1464, found: 245.1462.

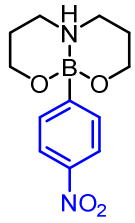

2l. 10-(4-nitrophenyl)octahydro-[1,3,2]oxazaborinino[2,3-*b*][1,3,2]oxazaborinin-5-ium-10-uide (1l): Prepared according to the general procedure. 4-nitrophenylboronic acid (300 mg, 1.80 mmol) and 3,3'-azanediyl*bis*(propan-1-ol) (264 mg, 1.98 mmol) in tetrahydrofuran (30 mL) afforded **1l** as a free-flowing pale yellow solid (349 mg, 83%). ^{1}H NMR (400 MHz, DMSO-d_6, 298 K): 8.07 (2H, d, *J* = 8.3 Hz, C*H*); 7.68 (2H, d, *J* = 8.3 Hz, C*H*); 6.21 (1H, bs, N*H*); 3.80-3.70 (2H, m, CH_2); 3.47-3.38 (2H, m, CH_2); 3.15-3.04 (2H, m, CH_2); 2.87-2.77 (2H, m, CH_2); 1.85-1.73 (2H, m, CH_2); 1.56-1.43 ppm (2H, m, CH_2). ^{13}C{^{1}H} NMR (100 MHz, DMSO-d_6, 298 K): 146.1; 132.9; 121.7; 59.8; 46.1; 24.1 ppm. ^{11}B{^{1}H} NMR (128.4 MHz, DMSO-d_6, 298 K): 2.8 ppm.

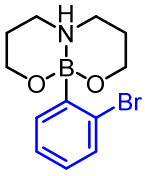

2m. 10-(2-bromophenyl)octahydro-[1,3,2]oxazaborinino[2,3-*b*][1,3,2]oxazaborinin-5-ium-10-uide (1m): Prepared according to the general procedure. 2-bromophenylboronic acid (500 mg, 2.49 mmol) and 3,3'-azanediyl*bis*(propan-1-ol) (365 mg, 2.74 mmol) in tetrahydrofuran (25 mL) afforded **1m** as a free-flowing white solid (611 mg, 82%). ^{1}H NMR (400 MHz, DMSO-d_6, 298 K): 7.45 (1H, dd, *J* = 7.3, 1.5 Hz, C*H*); 7.40 (1H, d, *J* = 7.8 Hz, C*H*); 7.22 (1H, t, *J* = 7.3 Hz, C*H*); 7.05 (1H, td, *J* = 7.6, 1.8 Hz, C*H*); 5.73 (1H, bs, N*H*); 3.75 (2H, m, CH_2); 3.46 (2H, m, CH_2); 3.14 (2H, m, CH_2); 2.90 (2H, m, CH_2); 1.79 (2H, m, CH_2); 1.51 ppm (2H, m, CH_2).^{13}C{^{1}H} NMR (100 MHz, DMSO-d_6, 298 K): 135.4; 132.7; 128.2; 127.8; 126.2; 59.8; 46.1; 24.0 ppm.^{11}B{^{1}H} NMR (128.4 MHz, DMSO-d_6, 298 K): 3.1 ppm.

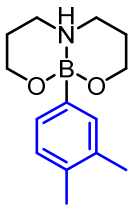

2o. 10-(3,4-dimethylphenyl)octahydro-[1,3,2]oxazaborinino[2,3-*b*][1,3,2]oxazaborinin-5-ium-10-uide (1n): Prepared according to the general procedure. 3,4-dimethylphenylboronic acid (500 mg, 3.33 mmol) and 3,3'-

azanediyl*bis*(propan-1-ol) (487 mg, 3.66 mmol) in tetrahydrofuran (33 mL) afforded **1n** as a free-flowing white solid (592 mg, 72%). ^{1}H NMR (400 MHz, DMSO-d_6, 298 K): 7.13 (1H, s, C*H*); 7.09 (1H, d, *J* = 7.3 Hz, C*H*); 6.94 (1H, d, d, *J* = 7.3 Hz, C*H*); 5.81 (1H, bs, N*H*); 3.71 (2H, m, CH_2); 3.47 (2H, m, CH_2); 3.02 (2H, m, CH_2); 2.82 (2H, m, CH_2); 2.17 (3H, s, CH_3); 2.15 (3H, s, CH_3); 1.74 (2H, m, CH_2); 1.45 ppm (2H, m, CH_2). ^{13}C{^{1}H} NMR (100 MHz, DMSO-d_6, 298 K): 134.0; 133.3; 132.6; 129.4; 128.2; 57.9; 46.0; 24.4; 19.6; 19.2 ppm. ^{11}B{^{1}H} NMR (128.4 MHz, DMSO-d_6, 298 K): 3.5 ppm.

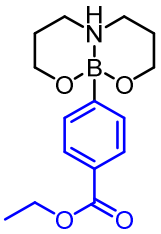

2p. 10-(ethylbenzoate)octahydro-[1,3,2]oxazaborinino[2,3-*b*][1,3,2]oxazaborinin-5-ium-10-uide (1o): Prepared according to the general procedure. 4-(ethoxycarbonyl)phenylboronic acid (500 mg, 2.58 mmol) and 3,3'-azanediyl*bis*(propan-1-ol) (378 mg, 2.84 mmol) in tetrahydrofuran (25 mL) afforded **1o** as a free flowing white solid (721 mg, 96%). ^{1}H NMR (400 MHz, DMSO-d_6, 298 K): 7.80 (2H, d, *J* = 8.1 Hz, C*H*); 7/54 (2H, d, *J* = 8.3 Hz, C*H*); 6.07 (1H, bs, N*H*); 4.28 (2H, q, *J* = 7.1 Hz, CH_2); 3.74 (2H, m, CH_2); 3.44 (2H, m, CH_2); 3.07 (2H, m, CH_2); 2.81 (2H, m, CH_2); 1.77 (2H, m, CH_2); 1.47 (2H, m, CH_2); 1.31 ppm (3H, t, *J* = 7.1 Hz, CH_3). ^{13}C{^{1}H} NMR (100 MHz, DMSO-d_6, 298 K): 166.4; 132.0; 127.6; 127.3; 60.2; 59.8; 46.1; 24.2; 14.3 ppm ^{11}B{^{1}H} NMR (128.4 MHz, DMSO-d_6, 298 K): 3.0 ppm.

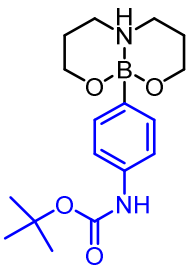

2q. 10-(*tert*-butylcarbamate)octahydro-[1,3,2]oxazaborinino[2,3-*b*][1,3,2]oxazaborinin-5-ium-10-uide (1p): Prepared according to the general procedure. 4-(*N*-boc-amino)phenylboronic acid (500 mg, 2.11 mmol) and 3,3'-azanediyl*bis*(propan-1-ol) (309 mg, 2.31 mmol) in tetrahydrofuran (20 mL) afforded **1p** as a free flowing white solid (537 mg, 76%). ^{1}H NMR (400 MHz, DMSO-d_6, 298 K): 9.04 (1H, bs, N*H*); 7.25 (4H, apparent s, C*H*); 5.84 (1H, bs, N*H*); 3.71 (2H, m, CH_2); 3.46 (2H, m, CH_2); 3.03 (2H, m, CH_2); 2.81 (2H, m, CH_2);1.75 (2H, m, CH_2); 1.46 ppm (11H, m, CH_2 + CH_3 overlapping). ^{13}C{^{1}H} NMR (100 MHz, DMSO-d_6, 298 K): 152.9; 137.0; 132.0; 117.3; 78.5; 59.7; 46.0; 28.2; 24.4 ppm ^{11}B{^{1}H} NMR (128.4 MHz, DMSO-d_6, 298 K): 3.5 ppm.

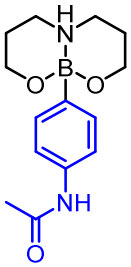

2r. 10-(*N*-acetamide)octahydro-[1,3,2]oxazaborinino[2,3-*b*][1,3,2]oxazaborinin-5-ium-10-uide (1q): Prepared according to the general procedure. 4-acetamidophenylboronic acid (500 mg, 2.79 mmol) and 3,3'-azanediyl*bis*(propan-1-ol) (409 mg, 3.07 mmol) in tetrahydrofuran (28 mL) afforded **1q** as a free-flowing white solid (693 mg, 90%). ^{1}H NMR (400 MHz, DMSO-d_6, 298 K): 9.70 (1H, bs, N*H*); 7.37 (2H, d, *J* = 8.3 Hz, C*H*); 7.29 (2H, d, *J* = 8.3 Hz, C*H*); 5.86 (1H, bs, N*H*); 3.71 (2H, m, CH_2); 3.46 (2H, m, CH_2); 3.03 (2H, m, CH_2); 2.82 (2H, m, CH_2); 2.00 (3H, s, CH_3); 1.75 (2H, m, CH_2); 1.46 ppm (2H, m, CH_2). ^{13}C{^{1}H} NMR (100 MHz, DMSO-d_6, 298 K): 167.8; 137.0; 132.0; 118.1; 59.7; 46.0; 24.4; 24.0 ppm ^{11}B{^{1}H} NMR (128.4 MHz, DMSO-d_6, 298 K): 3.4 ppm.

3. General Procedure for the Synthesis of M[2a] (M = K or Li)

A flame dried Schlenk tube was charged with **1a** (1 equiv.) and dried under vacuum for *ca.* 1h prior to the addition of anhydrous THF or toluene (X mL) under an argon atmosphere. To

this stirred suspension was added the appropriate base (1 equiv.) and the reaction mixture stirred at ambient temperature until the solution became homogeneous. Removal of the solvent generally afforded a pale residue which could be triturated with anhydrous *n*-hexane to afford M[**2a**] (M = K or Li) as a free-flowing white solid after isolation by filtration and drying under vacuum (*see Table S1 for isolated yields*).

K[2a]: Prepared according to the general procedure. **1a** (750.0 mg, 3.42 mmol) and KH (136.8 mg, 3.42 mmol) in tetrahydrofuran (10 mL) afforded K[**2a**] as a free-flowing white solid (862 mg, 98%).^{1}H NMR (400 MHz, THF-d_8, 298 K): 7.54 (2H, d, J = 6.9 Hz, *o*-CH); 7.09 (2H, t, J = 7.2 Hz, *m*-CH); 6.96 (1H, t, J = 7.5 Hz, *p*-CH); 3.61-3.56 (2H, m, CH_2); 3.52-3.43 (2H, m, CH_2); 3.34-3.25 (2H, m, CH_2); 2.74-2.66 (2H, m, CH_2); 1.88-1.75 (2H, m, CH_2); 1.36-1.26 (2H, m, CH_2) ppm. ^{13}C{^{1}H} NMR (100 MHz, THF-d_8, 298 K): 135.1; 127.1; 125.0; 62.6; 51.8; 31.1 ppm. ^{11}B{^{1}H} NMR (128.4 MHz, THF-d_8, 298 K): 2.5 ppm. Anal Calcd. for $C_{12}H_{18}BKNO_2$: C, 56.04; H, 6.66; N, 5.45. Found: C, 55.84; H, 6.49; N, 5.39. Crystals suitable for X-ray diffraction were grown by the slow evaporation of a concentrated THF solution of K[**2a**] at ambient temperature.

Li[2a]: Prepared according to the general procedure. **1a** (500.0 mg, 2.28 mmol) and solid *tert*-butyl lithium (146.0 mg, 2.28 mmol) in toluene (5 mL) afforded Li[**2a**] as a free-flowing white solid (508 mg, 99%)..^{1}H NMR (400 MHz, C_6D_6, 298 K): 7.77 (2H, d, J = 7.0 Hz, C*H*); 7.51 (2H, t, J = 7.5 Hz, C*H*); 7.35 (1H, t, J = 7.0 Hz, C*H*); 3.51 (4H, m, CH_2); 3.39 (2H, m, CH_2); 2.81 (2H, m, CH_2); 1.98 (2H, m, CH_2); 1.21 ppm (2H, m, CH_2).^{13}C{^{1}H} NMR (100 MHz, C_6D_6, 298 K): 134.4; 128.9; 127.0; 62.2; 49.7; 29.3 ppm. ^{11}B{^{1}H} NMR (128.4 MHz, C_6D_6, 298 K): 3.8 ppm. ^{7}Li NMR (155.51 MHz, C_6D_6, 298 K): 0.54 ppm.

Table S1. Screening of Bases for the Generation of M[**2a**]

Entry	Base	Time (mins)	Yield (%)[a]
1	KH	15	98
2	^{t}BuOK	5	97
3	KOMe	5	97
4	KOH	60	0
5	^{t}BuLi	5	99[c]

[a] Isolated yields.

4. Synthesis of hexahydro-[1,3,2]oxazaborinino[2,3-*b*][1,3,2]oxazaborinine, 3

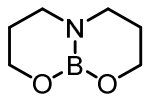

An oven dried Schlenk tube was loaded with 3,3'-azanediyl*bis*(propan-1-ol) (100 mg, 0.75 mmol) which was placed under vacuum for *ca*. 15 minutes and back-filled with argon prior to being taken up in anhydrous toluene (5 mL). To this stirred solution $Me_2S.BH_3$ (2M in toluene) (376 µL, 0.75 mmol) was added drop-wise at ambient temperature with significant gas evolution observed. After complete addition the reaction mixture was allowed to stir at ambient temperature for 3h prior to the removal of the solvent affording a colourless residue. The residue was triturated with anhydrous *n*-hexane to yield **3** as a sticky white solid (97 mg, 92 %). ^{1}H NMR (400 MHz, $CDCl_3$, 298 K): 3.92 (4H, t, $^{3}J_{HH}$ = 5.3 Hz, *CH*$_2$), 2.89 (4H, t, $^{3}J_{HH}$ = 6.1 Hz, *CH*$_2$), 1.88 ppm (4H, pent, $^{3}J_{HH}$ = 5.5 Hz, *CH*$_2$) ppm. ^{13}C{^{1}H} NMR (100 MHz, $CDCl_3$, 298 K): 62.9, 45.8, 27.2 ppm. ^{11}B{^{1}H} NMR (128.4 MHz, $CDCl_3$, 298 K): 20.4 ppm.

5. Modified Synthesis of 5[6]

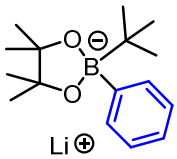

An oven dried Schlenk tube was loaded with phenylboronic acid pinacol ester (1.0 g, 4.90 mmol) and taken up in anhydrous hexanes (10 mL). In a separate oven dried Schlenk tube solid *tert*-butyl lithium (314 mg, 4.90 mmol) was taken up in hexanes (10 mL). The phenylboronic acid pinacol ester solution was added drop-wise to the *tert*-butyl lithium solution at -40°C and stirred for 30 minutes before warming to ambient temperature. The resulting colourless precipitate was isolated by filtration and dried under vacuum to afford **5** (1.13 g, 86%).^{1}H NMR (400 MHz, *protio*-THF (DMSO-d_6 capillary), 298 K): 7.34 (2H, d, *J* = 7.8 Hz, C*H*); 6.90 (2H, t, *J* = 7.4 Hz, C*H*); 6.77 (1H, m, C*H*); 1.10 (6H, s, C*H*$_{3\ pinacol}$); 0.80 (6H, s, C*H*$_{3\ pinacol}$); 0.60 ppm (9H, s, C*H*$_3$). ^{13}C{^{1}H} NMR (100 MHz, *protio*-THF (DMSO-d_6 capillary), 298 K): 131.9; 124.5; 121.9; 77.2; 29.6; 27.3; 26.8 ppm. ^{11}B{^{1}H} NMR (128.4 MHz, *protio*-THF (DMSO-d_6 capillary), 298 K): 7.8 ppm. ^{7}Li NMR (155.51 MHz, *protio*-THF (DMSO-d_6 capillary), 298 K): -0.14 ppm.

6. Phenyl Ion Affinity (PhIA) Calculations

Relative PhIAs were calculated from the isodesmic reactions between tetraphenylborate and the appropriate test Lewis acid (*Scheme S1*) at the M06-2X/6-311g+(d,p) level of theory with incorporation of a dichloromethane PCM solvent model. This methodology is analogous to our previous approach toward the calculation of hydride/chloride ion affinities (HIAs/CIAs) of borocations.[7]

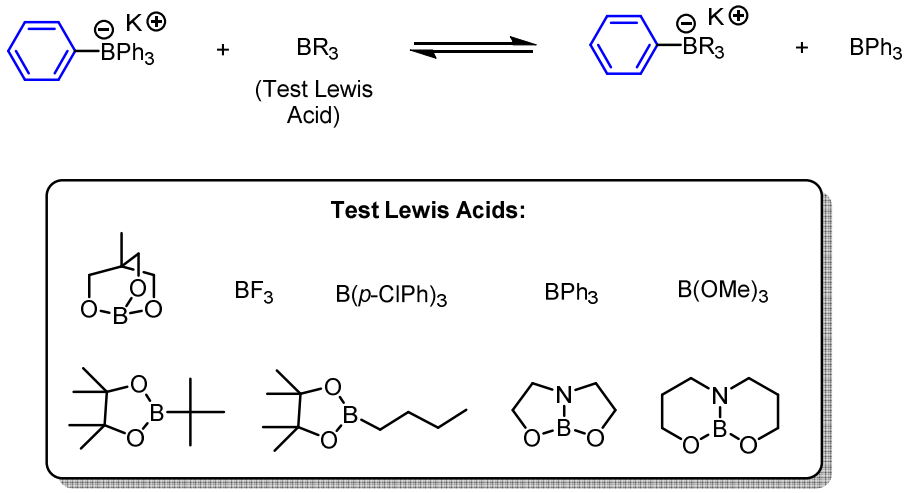

Scheme S1. The isodesmic reactions between tetraphenylborate and various test Lewis acids.

6a. Computational Details: Calculations were performed using the Gaussian09 suite of programmes.[8] Structures were pre-optimised at the HF/3-21G level followed by optimisation at the M06-2X/6-311G+(d,p) level with inclusion of a PCM model for solvent correction (DCM).[9] Structures were confirmed as minima by frequency analysis and the absence of imaginary frequencies. For *entry 8 (Table S2)*, a residual imaginary frequency associated with free-rotation about an unhindered B-C bond remained but optimisation was deemed to be complete on the basis of negligible residual forces. Full Cartesian coordinates for all M06-2X/6-311G+(d,p) structures can be found in **Section 18** (pages S96 – S128).

Table S2. Phenyl Ion Affinity (PhIA) Values of Borane Lewis Acids.

Entry	Lewis Acid	Abbreviation	PhIA (kcalMol^{-1})[a]
1	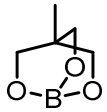	Triolborane	- 22.8
2	BF_3	-	- 16.3
3	B(*p*-ClPh)$_3$	-	- 5.5
4	BPh_3	-	0.0
5	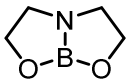	5,5-ONO	+ 17.0
6	$B(OMe)_3$	-	+ 22.7
7	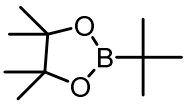	B(Pin)(^{t}Bu)	+ 23.2
8	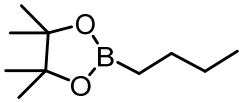	B(Pin)(^{n}Bu)	+ 23.9
9	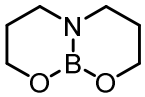	**3 (This Work)**	+ 36.3 (+ 31.3)[b]

[a] PhIAs calculated at the M06-2X/6-311G+(d,p) level of theory with incorporation of a dichloromethane PCM solvent model. [b] In parenthesis the PhIA is calculated using atomic coordinates from the solid state structure of K[**2a**].

7. Stoichiometric Phenyl Ion Transfer Experiments

General Procedure: In a glovebox a J. Youngs NMR tube equipped with a DMSO-d_6 capillary insert was loaded with K[**2a**] (30.0 mg, 0.117 mmol) and *protio*-THF (0.8 mL) prior to the addition of the appropriate Lewis acid (0.117 mmol). The reaction mixture was periodically monitored by $^{11}B\{^1H\}$ NMR spectroscopy to judge the progress of the phenyl ion transfer reactions.

7a. Phenyl Ion Transfer from K[2a] to 4-methyl-2,6,7-trioxa-1-borabicyclo[2.2.2]octane

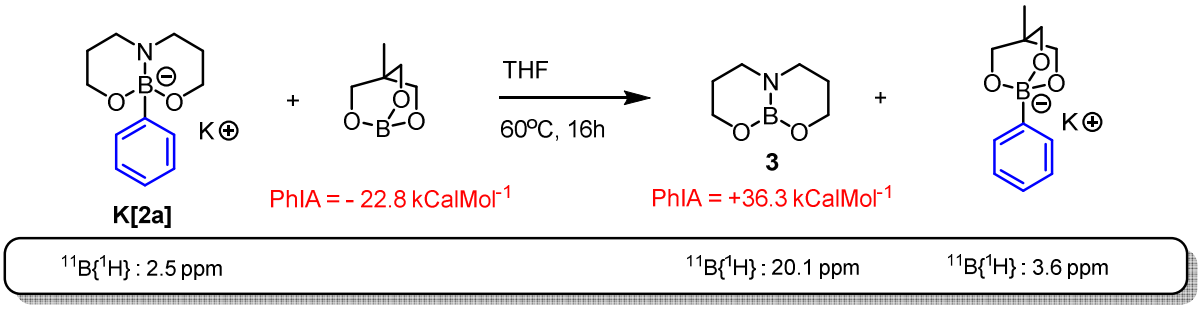

In a glovebox an oven dried J. Youngs NMR tube equipped with a DMSO-d_6 capillary insert was loaded with K[**2a**] (30.0 mg, 0.117 mmol), 4-methyl-2,6,7-trioxa-1-borabicyclo-[2.2.2]octane (15.0 mg, 0.117 mmol) and *protio*-THF (0.8 mL) then heated at 60°C for 16h. Minutes after borane addition the $^{11}B\{^1H\}$ NMR (*Figure S1, green*) demonstrated the presence of K[**2a**] (δ_{11B} = 2.5 ppm) and a new 4-coordinate resonance (δ_{11B} = 4.4 ppm). Free triolborane is not observed due to its poor solubility in THF. Heating the reaction mixture at 60°C for 16h led to the expected products of aryl transfer, **3** (δ_{11B} = 20.0 ppm) and the corresponding triolborate (δ_{11B} = 3.6 ppm) as well as a minor unidentified 4-coordinate resonance at δ_{11B} = 1.3 ppm (*Figure S1, red*).

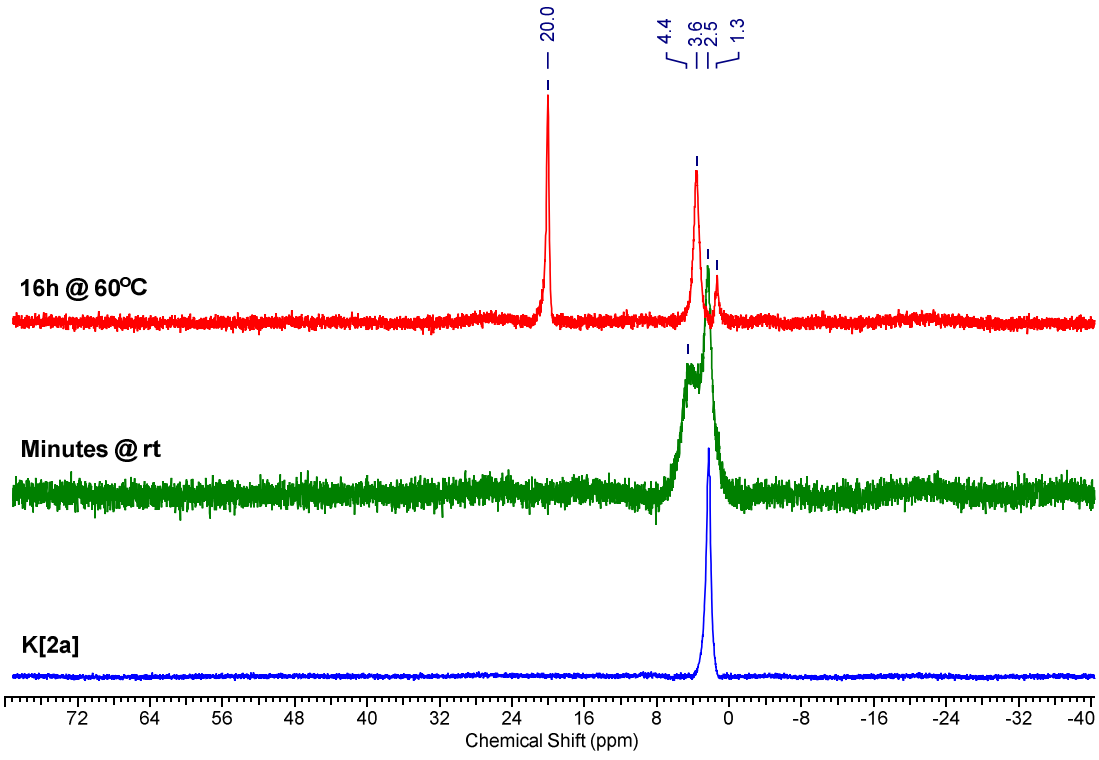

Figure S1. Collected $^{11}B\{^1H\}$ NMR spectra (baseline corrected): K[**2a**] (blue); reaction mixture minutes after the addition of 4-methyl-2,6,7-trioxa-1-borabicyclo[2.2.2]octane at ambient temperature (green); reaction mixture after 16h at 60°C (red).

7b. Phenyl Ion Transfer from K[2a] to BF_3-etherate

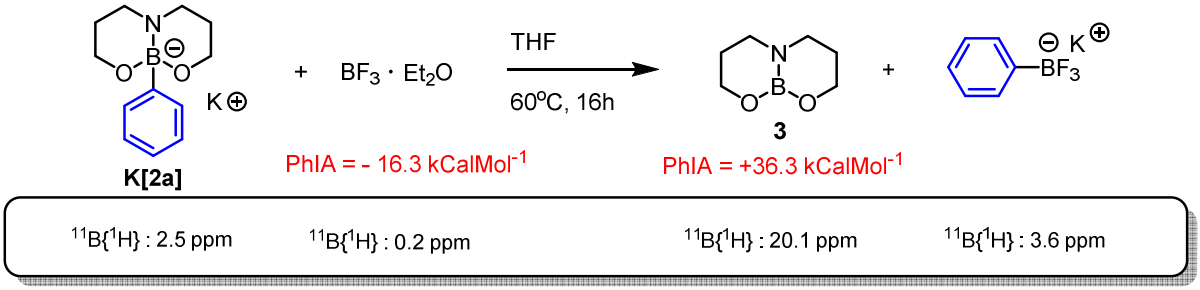

In a glovebox an oven dried J. Youngs NMR tube equipped with a DMSO-d_6 capillary insert was loaded with K[**2a**] (30.0 mg, 0.117 mmol), BF_3•Et_2O (14.4 µL, 0.117 mmol) and *protio*-THF (0.8 mL). The $^{11}B\{^1H\}$ NMR spectrum taken minutes after borane addition at ambient temperature (*Figure S2, green*) demonstrates the presence of **3** (δ_{11B} = 20.0 ppm), potassium trifluoro(phenyl)borate (δ_{11B} = 3.6 ppm) and a minor unidentified 4-coordinate resonance (δ_{11B} = 0.1 ppm). After 16h at 60°C, only the expected products of aryl transfer remain, **3** (δ_{11B} = 20.0 ppm) and potassium trifluoro(phenyl)borate (δ_{11B} = 3.6 ppm) (*Figure S2, red*).

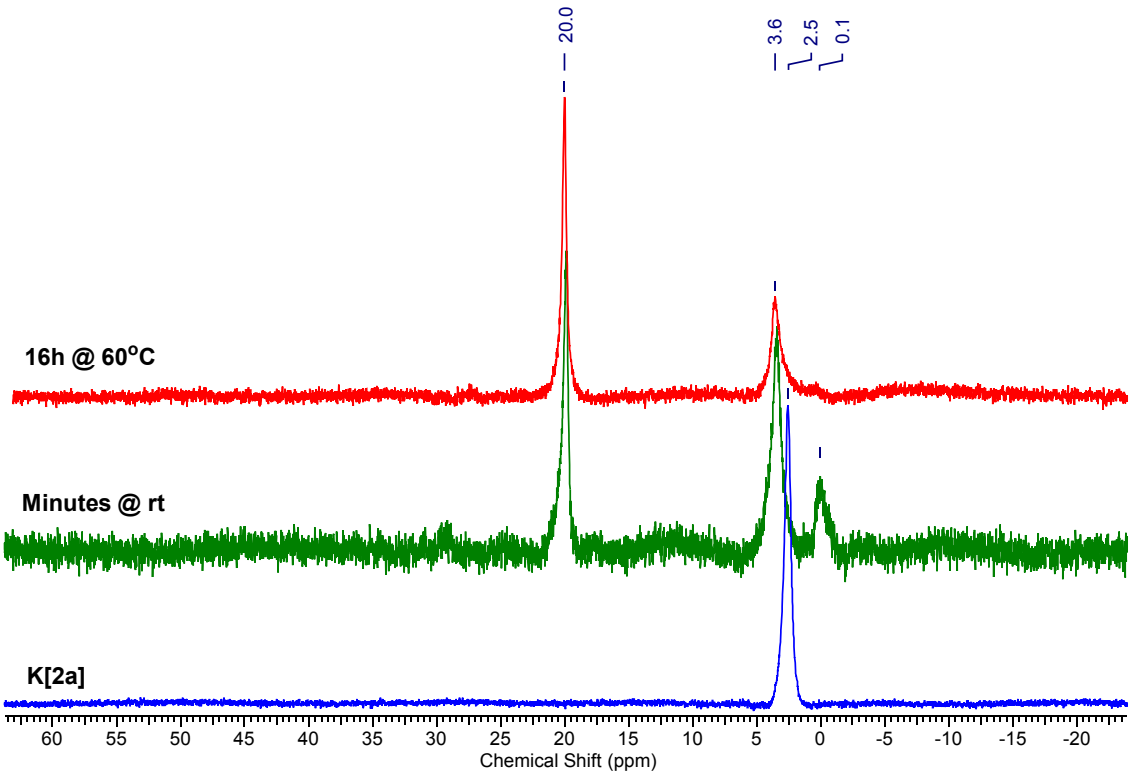

Figure S2. Collected $^{11}B\{^1H\}$ NMR spectra (baseline corrected): K[**2a**] (blue); reaction mixture minutes after the addition of BF_3-etherate at ambient temperature (green); reaction mixture after 16h at 60°C (red).

7c. Phenyl Ion Transfer from K[2a] to Triphenylborane (in THF)

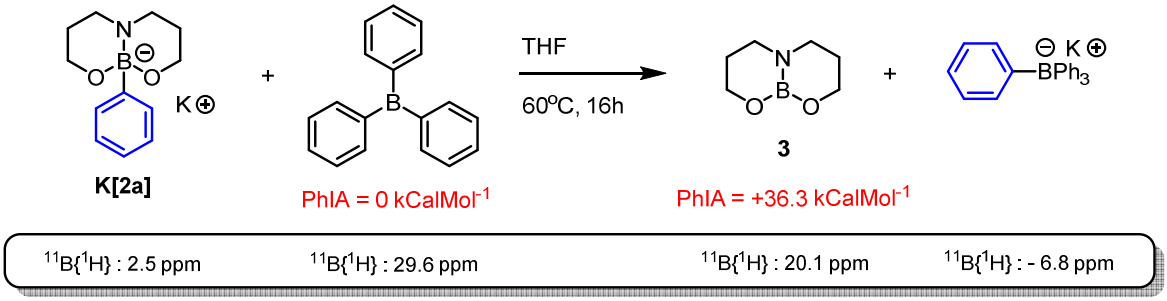

In a glovebox an oven dried J. Youngs NMR tube equipped with a DMSO-d_6 capillary insert was loaded with K[**2a**] (30.0 mg, 0.117 mmol), triphenylborane (28.0 mg, 0.117 mmol) and *protio*-THF (0.8 mL). The $^{11}B\{^1H\}$ NMR spectrum taken minutes after borane addition at ambient temperature (*Figure S3, green*) demonstrates the presence of BPh_3 / THF-BPh_3 (δ_{11B} = 29.6 ppm, in fast exchange), K[**2a**], a 4-coordinate species at δ_{11B} = 0.8 ppm, tentatively assigned as the K[**2a**]•triphenylborane adduct. Heating at 60°C for 16h affords no observable change (*Figure S3, red*). We propose that in this case coordination of K[**2a**] / THF to BPh_3 is preventing aryl transfer reactivity in this specific example.

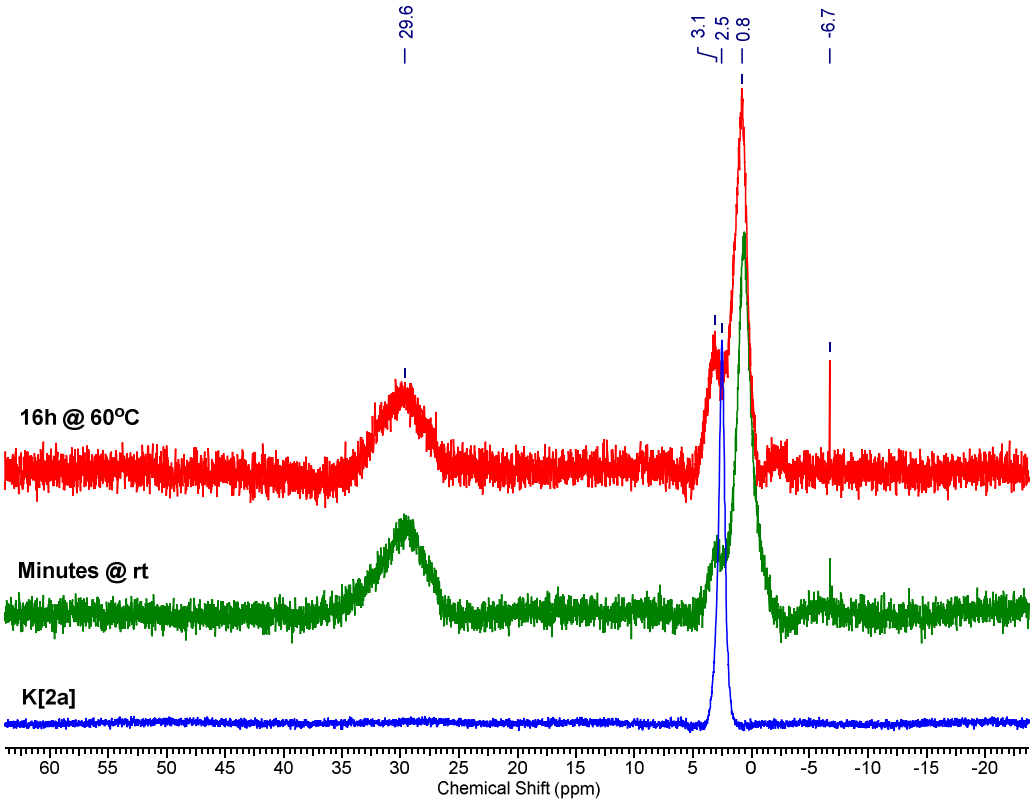

Figure S3. Collected $^{11}B\{^1H\}$ NMR spectra (baseline corrected): K[**2a**] (blue); reaction mixture minutes after the addition of BPh_3 at ambient temperature (green); reaction mixture after 16h at 60°C (red).

7d. Phenyl Ion Transfer from K[2a] to Triphenylborane (in DCM)

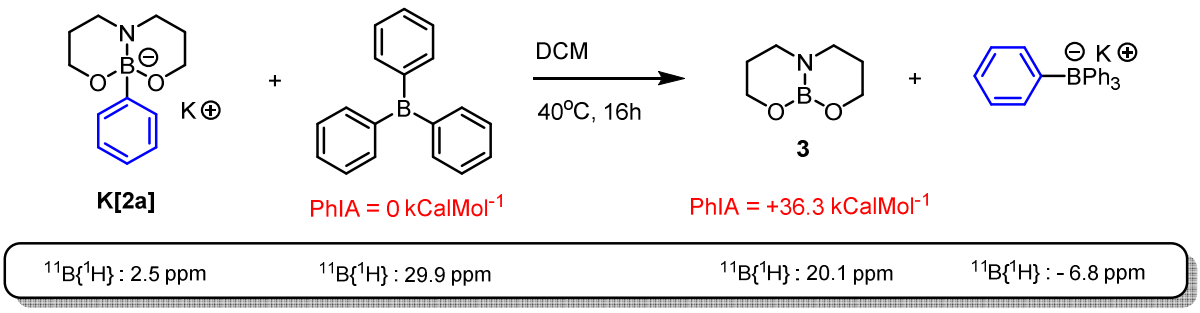

In a glovebox an oven dried J. Youngs NMR tube equipped with a DMSO-d_6 capillary insert was loaded with K[**2a**] (30.0 mg, 0.117 mmol), triphenylborane (28.0 mg, 0.117 mmol) and *protio*-DCM (0.8 mL). The reaction mixture was heated at 40°C for 16h to afford a sharp resonance at δ_{11B} = -6.8 characteristic of potassium tetraphenylborate, providing evidence for aryl transfer (*Figure S4*). The by-product of hydrocarbyl transfer, **3** was not observed due to its poor solubility in DCM. Again the resonance at *ca.* δ_{11B} = -0.5 ppm is observed which is tentatively assigned as the K[**2a**]-BPh_3 adduct.

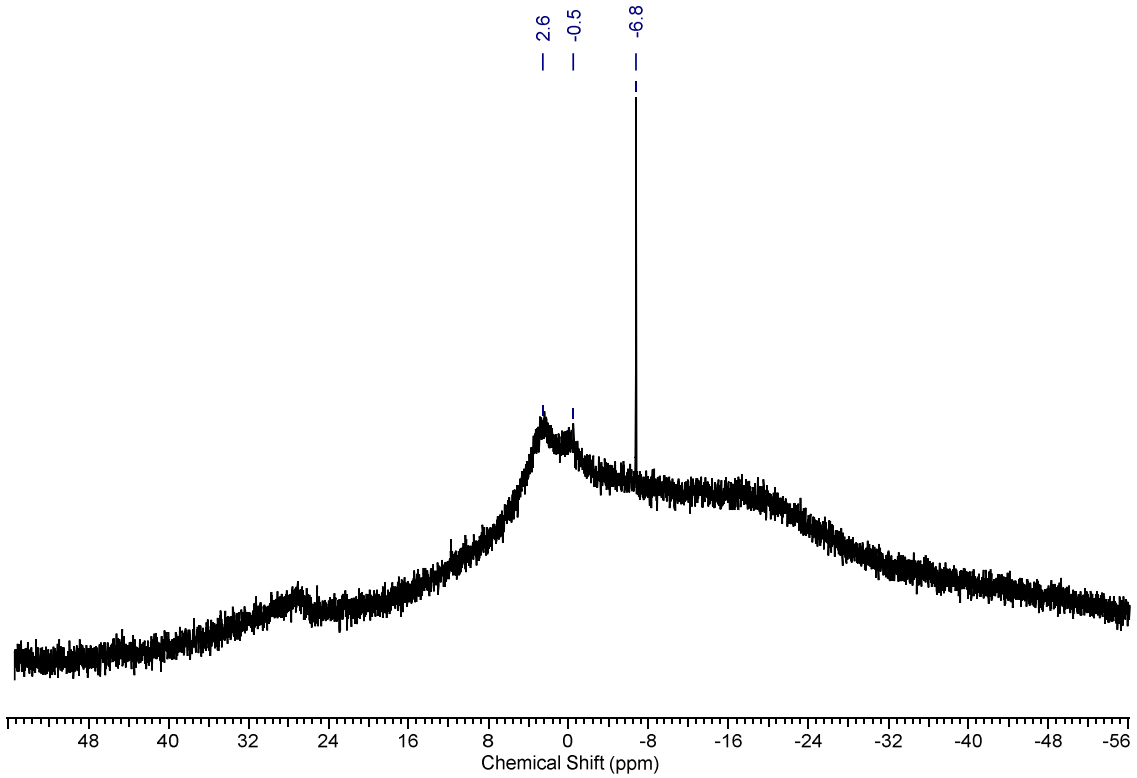

Figure S4. $^{11}B\{^1H\}$ NMR spectrum after heating at 40°C for 16h.

7e. Phenyl Ion Transfer from K[2a] to Trimethoxyborane

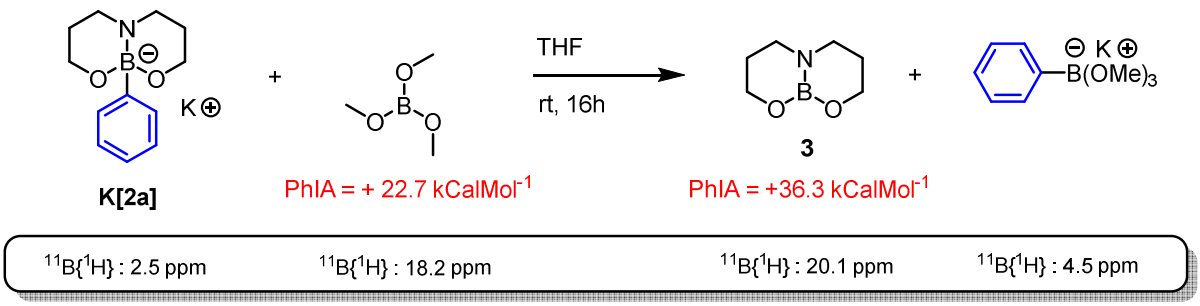

In a glovebox an oven dried J. Youngs NMR tube equipped with a DMSO-d_6 capillary insert was loaded with K[**2a**] (30.0 mg, 0.117 mmol), *protio*-THF (0.8 mL), trimethoxyborane (13.0 µL, 0.117 mmol) and agitated at ambient temperature for 16h. The $^{11}B\{^1H\}$ NMR spectrum taken minutes after borane (*Figure S5, pink*) addition demonstrates the presence of a new 4-coordinate compound at δ_{11B} = 3.1 ppm, along with the expected products of aryl transfer, **3** (δ_{11B} = 20.0 ppm) and $[PhB(OMe)_3]^-K^+$ (δ_{11B} = 4.5 ppm). Continued agitation at ambient temperature for 16h lead to complete aryl transfer (*Figure S5, red*).

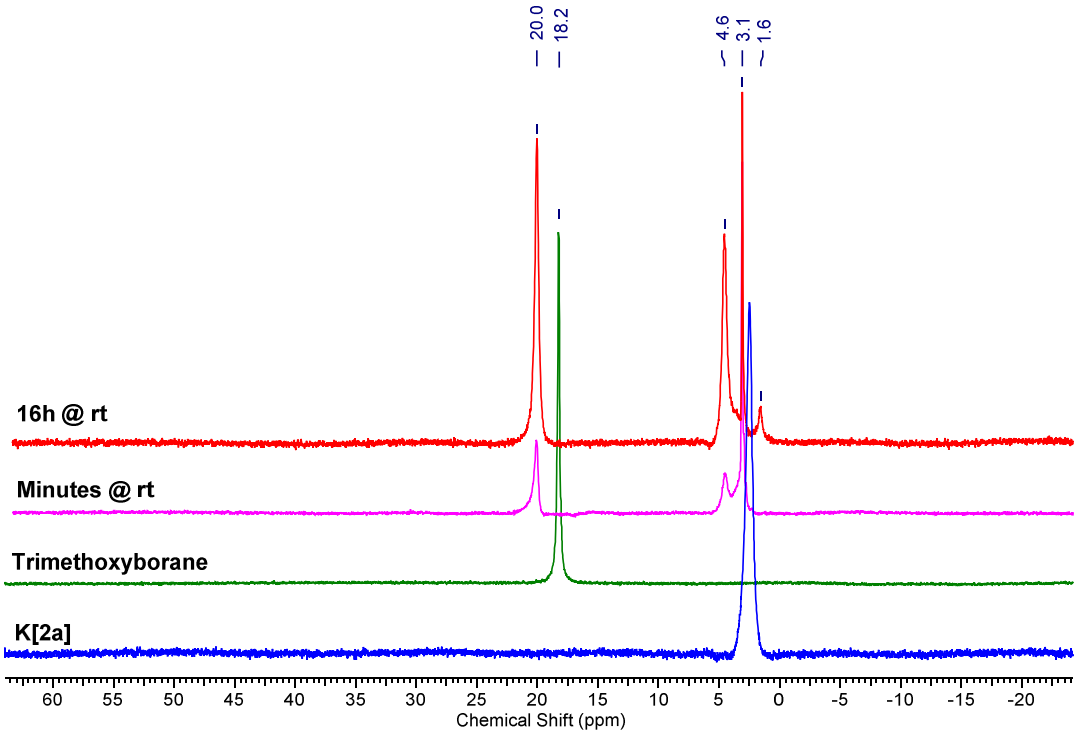

Figure S5. Collected $^{11}B\{^1H\}$ NMR spectra (baseline corrected): K[**2a**] (blue); trimethoxyborane (green); reaction mixture minutes after the addition of trimethoxyborane at ambient temperature (pink); reaction mixture after 16h at ambient temperature (red).

7f. Phenyl Ion Transfer from K[2a] to 2-butyl-4,4,5,5-tetramethyl-1,3,2-dioxaborolane

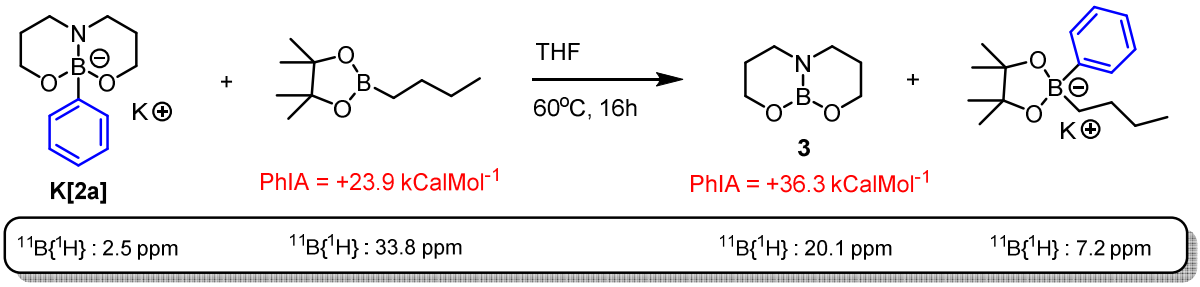

In a glovebox an oven dried J. Youngs NMR tube equipped with a DMSO-d_6 capillary insert was loaded with K[**2a**] (30.0 mg, 0.117 mmol), 2-butyl-4,4,5,5-tetramethyl-1,3,2-dioxaborolane (25.0 µL, 0.117 mmol) then *protio*-THF (0.8 mL) and heated to 60°C for 16h. The $^{11}B\{^1H\}$ NMR spectrum taken minutes after borane addition at ambient temperature (*Figure S6, pink*) demonstrates 2-butyl-4,4,5,5-tetramethyl-1,3,2-dioxaborolane (δ_{11B} = 33.8 ppm), K[**2a**] (δ_{11B} = 2.6 ppm) and a minor unidentified broad resonance at δ_{11B} = 7.4 ppm. Heating at 60°C for 16h confirmed that slow aryl transfer proceeds, as demonstrated by the presence of **3** (δ_{11B} = 20.0 ppm) and [^{n}BuB(Pin)(Ph)]$^-$K$^+$ (δ_{11B} = 7.2 ppm, overlapping with the minor unidentified resonance) (*Figure S6, red*).

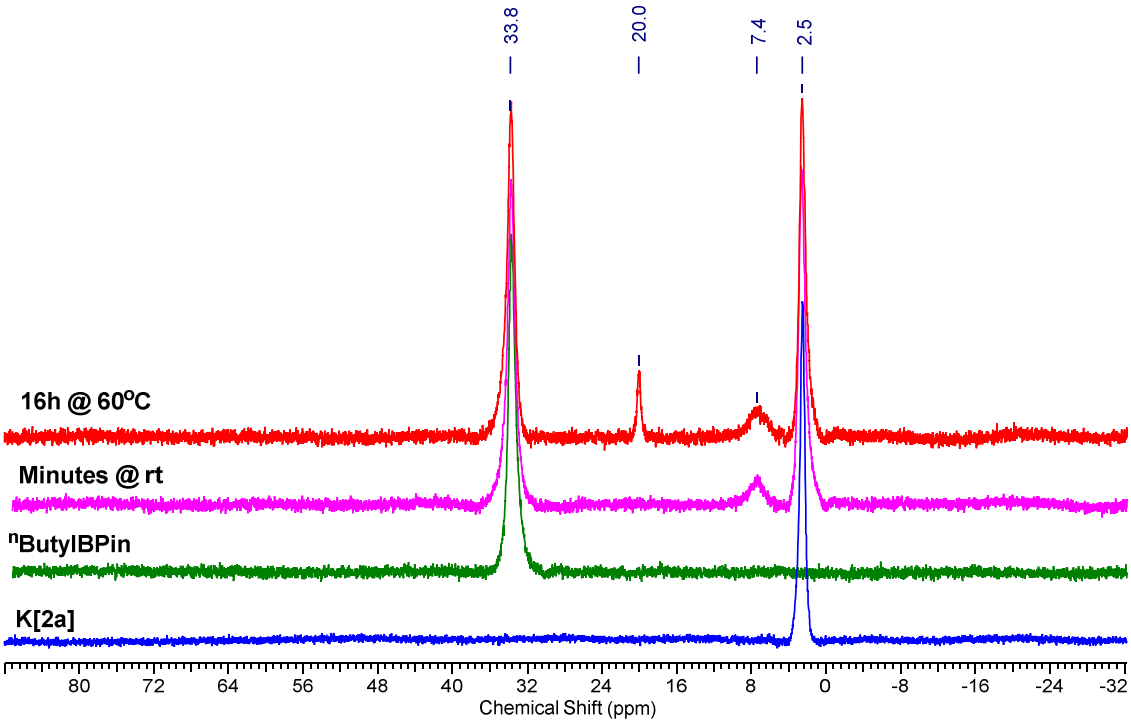

Figure S6. Collected $^{11}B\{^1H\}$ NMR spectra (baseline corrected): K[**2a**] (blue); 2-butyl-4,4,5,5-tetramethyl-1,3,2-dioxaborolane (green); reaction mixture minutes after the addition of trimethoxyborane at ambient temperature (pink); reaction mixture after 16h at 60°C (red).

7g. Phenyl Ion Transfer from [^{n}BuB(Pin)(Ph)]$^{-}$Li^{+} to 3

As aryl transfer from K[**2a**] to 2-butyl-4,4,5,5-tetramethyl-1,3,2-dioxaborolane was slow the complementary reaction was attempted to confirm that the minor degree of aryl transfer observed in *Figure S6* is not simply the equilibrium position for this reaction.

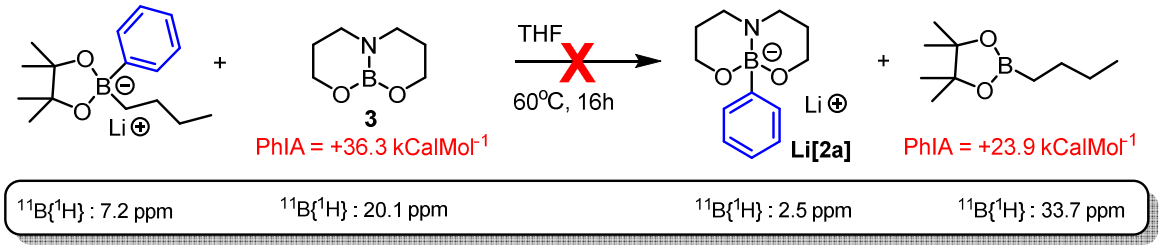

In a glovebox an oven dried J. Youngs NMR tube equipped with a DMSO-d_6 capillary insert was loaded with *n*-butylboronic acid pinacol ester (38.0 µL, 0.183 mmol), *protio*-THF (0.8 mL) and phenyl lithium (120.0 µL, 1.8M in dibutyl ether). The reaction mixture was subsequently analysed by ^{11}B{^{1}H} NMR spectroscopy revealing the expected boronate species, [^{n}BuB(Pin)(Ph)]$^{-}$Li^{+} (δ_{11B} = 7.2 ppm). To the *in-situ* generated [^{n}BuB(Pin)(Ph)]$^{-}$Li^{+} was added **3** (25.8 mg, 0.183 mmol) and the reaction mixture immediately analysed by ^{11}B{^{1}H} NMR. The ^{11}B{^{1}H} NMR spectra revealed the presence of [^{n}BuB(Pin)(Ph)]$^{-}$Li^{+} (δ_{11B} = 6.8 ppm), **3** (δ_{11B} = 20.0 ppm) and a minor amount of arylated **3** (δ_{11B} = 2.7 ppm), derived from a stoichiometric imbalance of phenyl lithium. Aryl transfer can be precluded as the by-product of aryl transfer from [^{n}BuB(Pin)(Ph)]$^{-}$Li^{+}, *n*-butylboronic acid pinacol ester cannot be observed at δ_{11B} = 33.7 ppm. Heating the reaction mixture at 60°C for 16h (*Figure S7, red*) afforded no further change.

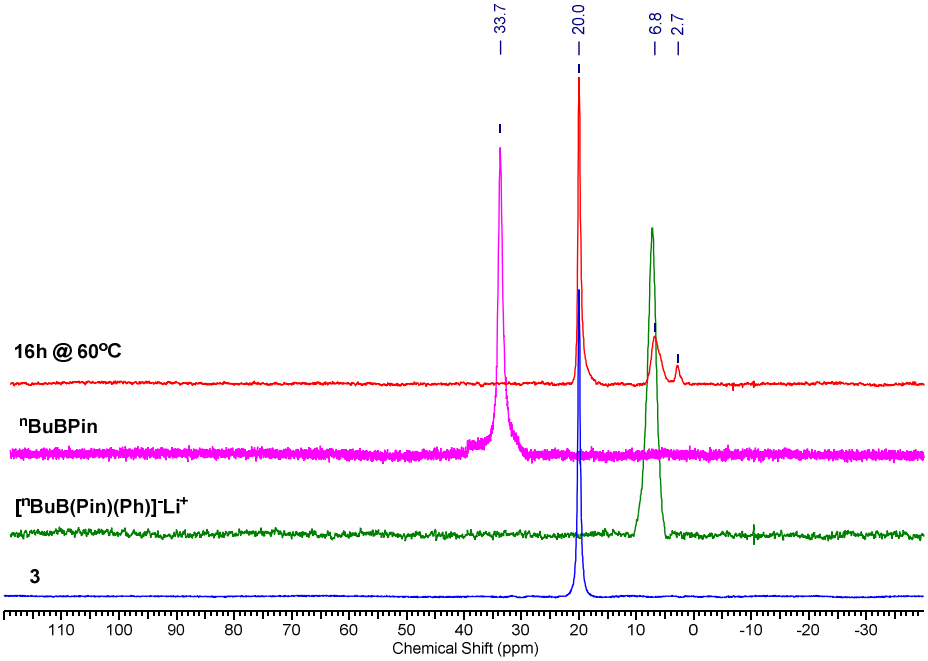

Figure S7. Collected ^{11}B{^{1}H} NMR spectra (baseline corrected): **3** (blue); [^{n}BuB(Pin)(Ph)]$^{-}$Li^{+} (green); ^{n}BuBPin (pink) reaction mixture after 16h at 60°C (red).

8. Stoichiometric Direct Boron-to-Iron Transmetallation Studies

8a. [Fe(dppe)Cl_2] (1 equiv.) + sodium 2-methoxy-2-(*p*-tolyl)-1,3,2-dioxaborolan-2-uide:[10]

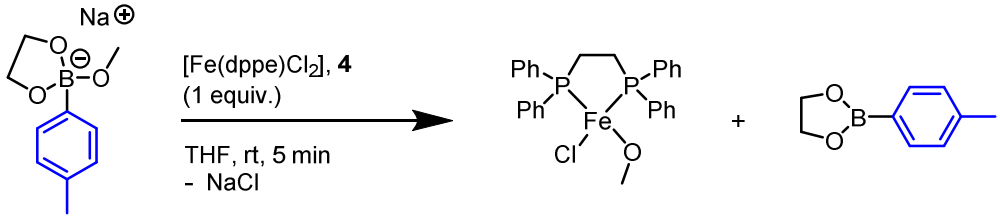

In a glovebox an oven dried J. Youngs NMR tube equipped with a DMSO-d_6 capillary insert was loaded with sodium 2-methoxy-2-(*p*-tolyl)-1,3,2-dioxaborolan-2-uide (8.2 mg, 0.038 mmol) and *protio*-THF (0.8 mL) followed by the addition of [Fe(dppe)Cl_2], **4** (20.0 mg, 0.038 mmol). The reaction mixture was agitated at ambient temperature for *ca.* 5 minutes prior to analysis by $^{11}B\{^1H\}$ NMR spectroscopy (*Figure S8, red*). The $^{11}B\{^1H\}$ NMR spectrum demonstrated the complete disappearance of the characteristic sodium 2-methoxy-2-(*p*-tolyl)-1,3,2-dioxaborolan-2-uide resonance (δ_{11B} = 8.2 ppm) and the presence of a single new resonance at δ_{11B} = 33.3 ppm, assigned as the neutral 3-coordinate borane derived from methoxide transfer to iron, 2-(*p*-tolyl)-1,3,2-dioxaborolane *via* its independent synthesis.[10]

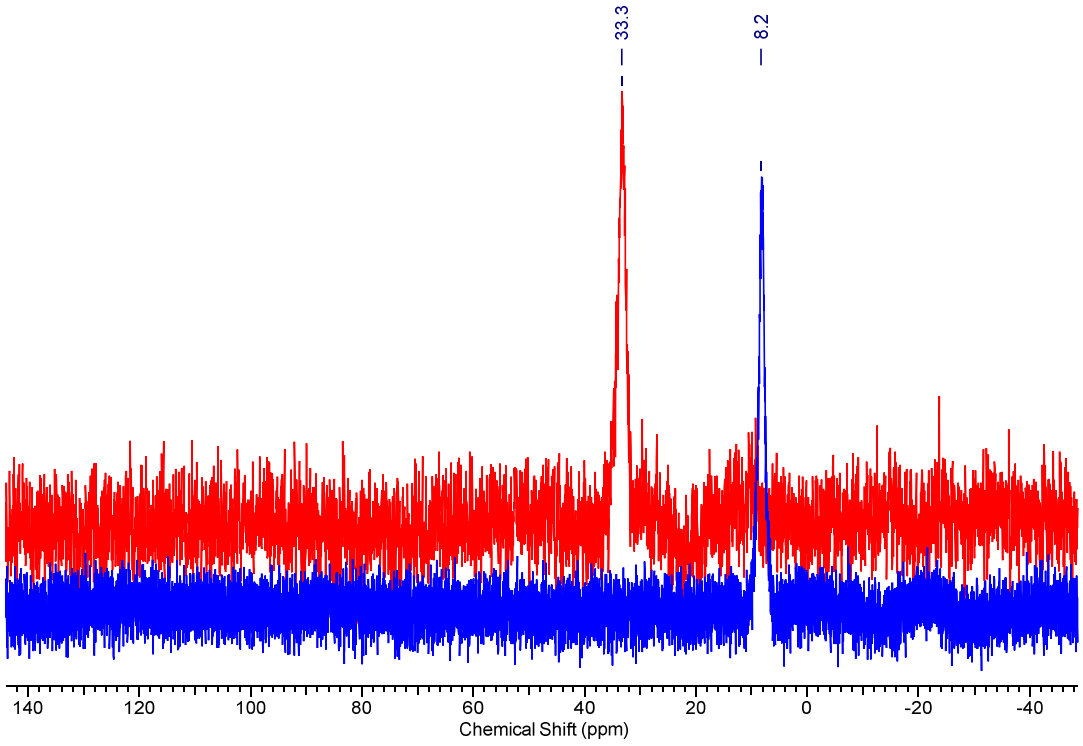

Figure S8. Collected $^{11}B\{^1H\}$ NMR spectra (baseline corrected): sodium 2-methoxy-2-(*p*-tolyl)-1,3,2-dioxaborolan-2-uide (blue); reaction mixture after 5 minutes at ambient temperature (red).

8b. [Fe(dppe)Cl_2] (0.5 equiv.) + K[2a] (isolated) in THF:

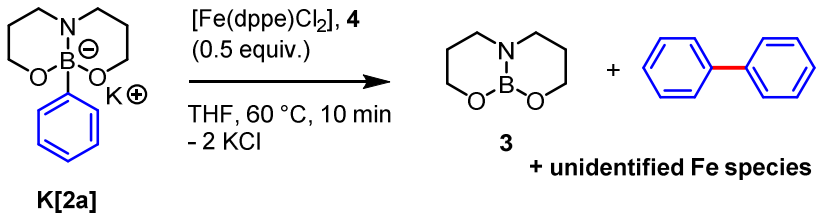

In a glovebox an oven dried J. Youngs NMR tube equipped with a DMSO-d_6 capillary insert was loaded with K[**2a**] (20.0 mg, 0.078 mmol) and *protio*-THF (0.8 mL) prior to the addition of [Fe(dppe)Cl_2], **4** (20.5 mg, 0.039 mmol), where upon the reaction mixture became opaque and pale green in colour. The reaction mixture was heated at 60°C for 10 minutes which led to a deep red solution with a fine colourless precipitate. Analysis of the reaction mixture by $^{11}B\{^1H\}$ NMR spectroscopy (*Figure S9, red*) revealed the complete consumption of K[**2a**] (δ_{11B} = 2.5 ppm), with **3** (δ_{11B} = 21.5 ppm) as the sole product of aryl transfer.

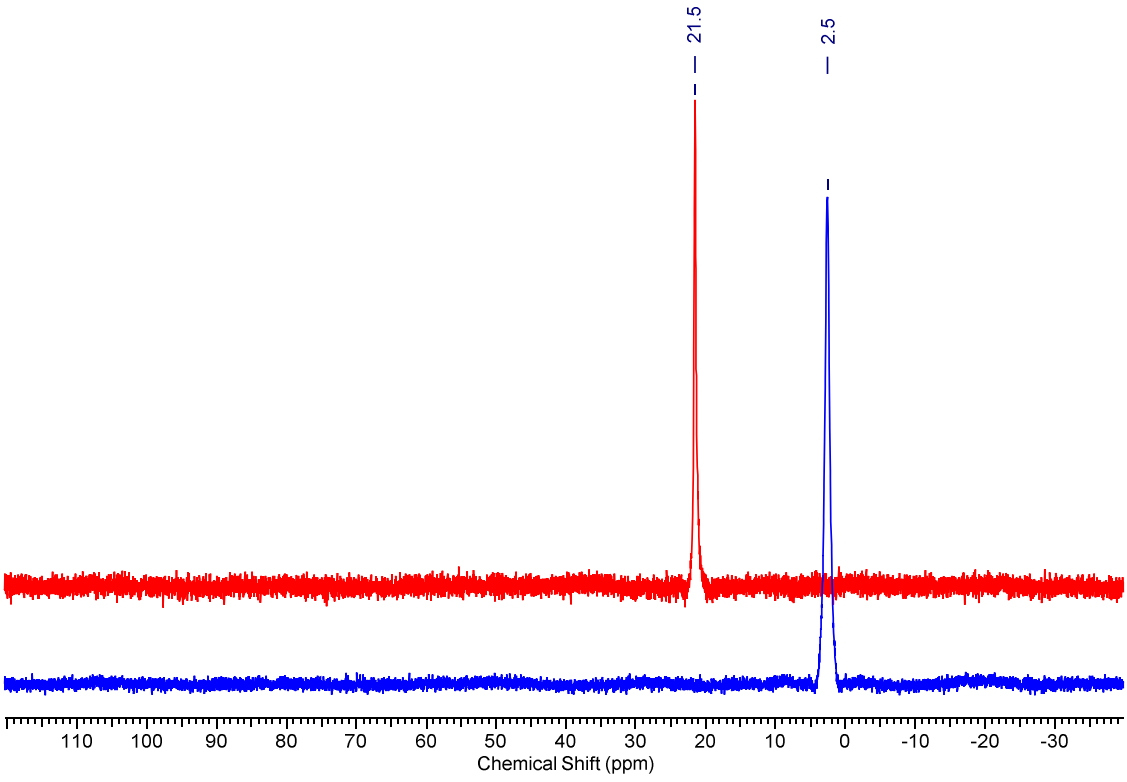

Figure S9. Collected $^{11}B\{^1H\}$ NMR spectra (baseline corrected): K[**2a**] (blue); K[**2a**] + [Fe(dppe)Cl_2], **4** after 10 minutes at 60°C (red).

8c. [Fe(dppe)Cl_2] (0.5 equiv.) + K[2a] (isolated) in Toluene:

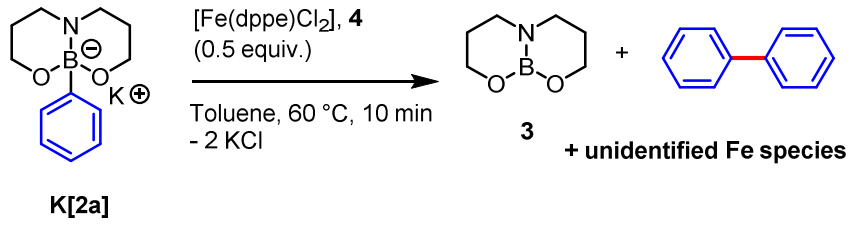

In a glovebox an oven dried J. Youngs NMR tube equipped with a DMSO-d_6 capillary insert was loaded with K[**2a**] (20.0 mg, 0.078 mmol) and *protio*-toluene (0.8 mL) prior to the addition of [Fe(dppe)Cl_2], **4** (20.5 mg, 0.039 mmol). The limited solubility of K[**2a**] in toluene leads to a colourless slurry which upon heating to 60°C for 10 minutes becomes deep red in colour with a colourless insoluble precipitate. Analysis of the reaction mixture by $^{11}B\{^1H\}$ NMR spectroscopy (*Figure S10, red*) reveals the complete consumption of K[**2a**] (δ_{11B} = 4.2 ppm), with **3** (δ_{11B} = 21.6 ppm) as the only boron containing species in solution.

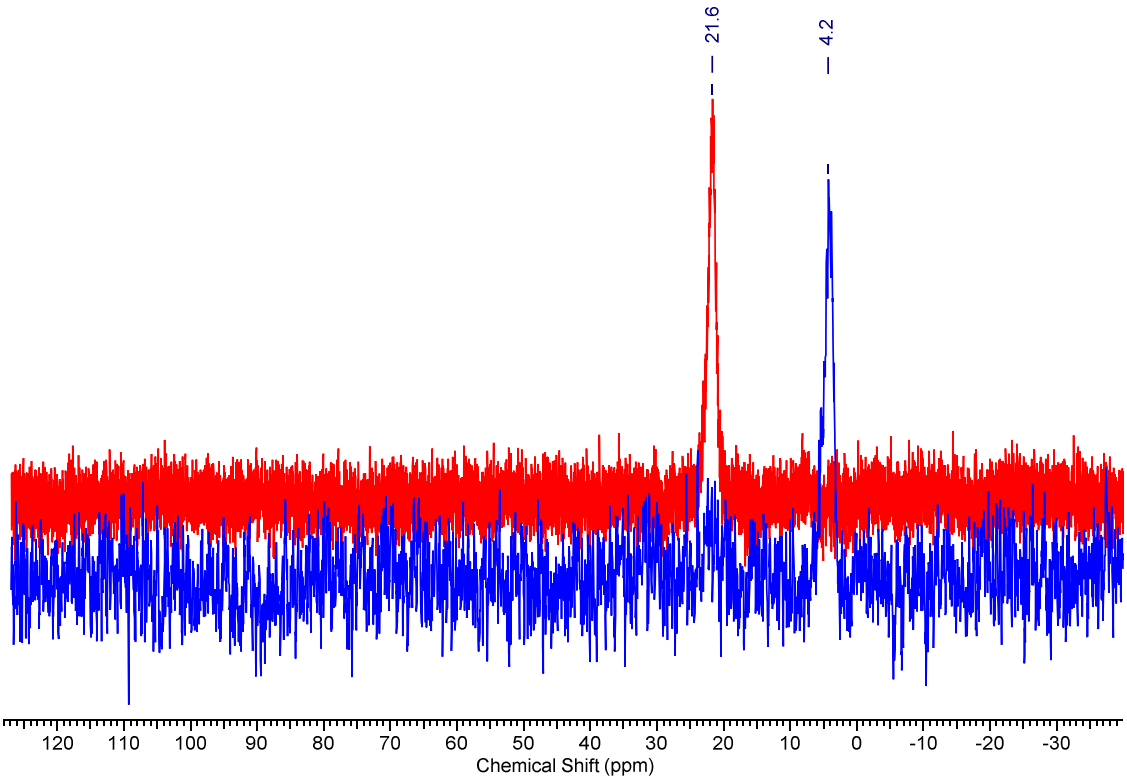

Figure S10. Collected $^{11}B\{^1H\}$ NMR spectra (baseline corrected): K[**2a**] (blue); K[**2a**] + [Fe(dppe)Cl_2], **4** after 10 minutes at 60°C (red).

8d. [Fe(dppe)Cl_2] (0.5 equiv.) + K[2a] (generated *in-situ* from KH):

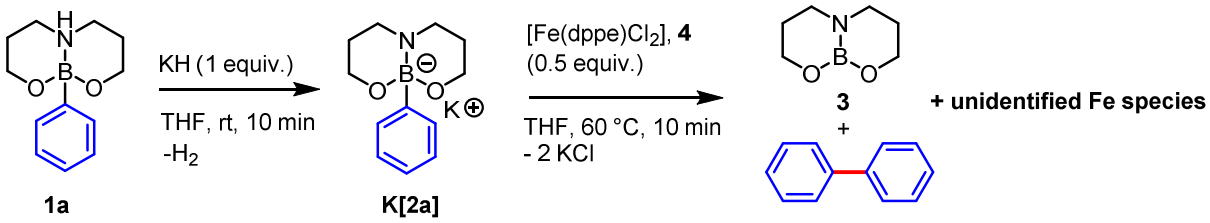

In a glovebox an oven dried J. Youngs NMR tube equipped with a DMSO-d_6 capillary insert was loaded with **1a** (40.0 mg, 0.183 mmol), KH (7.3 mg, 0.183 mmol) and *protio*-THF (0.8 mL) followed by agitation until the reaction mixture became completely homogeneous and hydrogen evolution had ceased (*ca.* 10-15 mins). After this time an $^{11}B\{^1H\}$ NMR spectrum was taken (*Figure S11, blue*) prior to the addition of [Fe(dppe)Cl_2], **4** (48.0 mg, 0.092 mmol). Heating the reaction mixture at 60°C for 10 minutes afforded a deep red solution with a fine precipitate. The reaction mixture was subsequently analysed by $^{11}B\{^1H\}$ NMR (*Figure S11, red*), revealing the quantitative conversion of K[**2a**] (δ_{11B} = 2.7 ppm) to the by-product of hydrocarbyl transmetallation, **3** (δ_{11B} = 23.9 ppm).

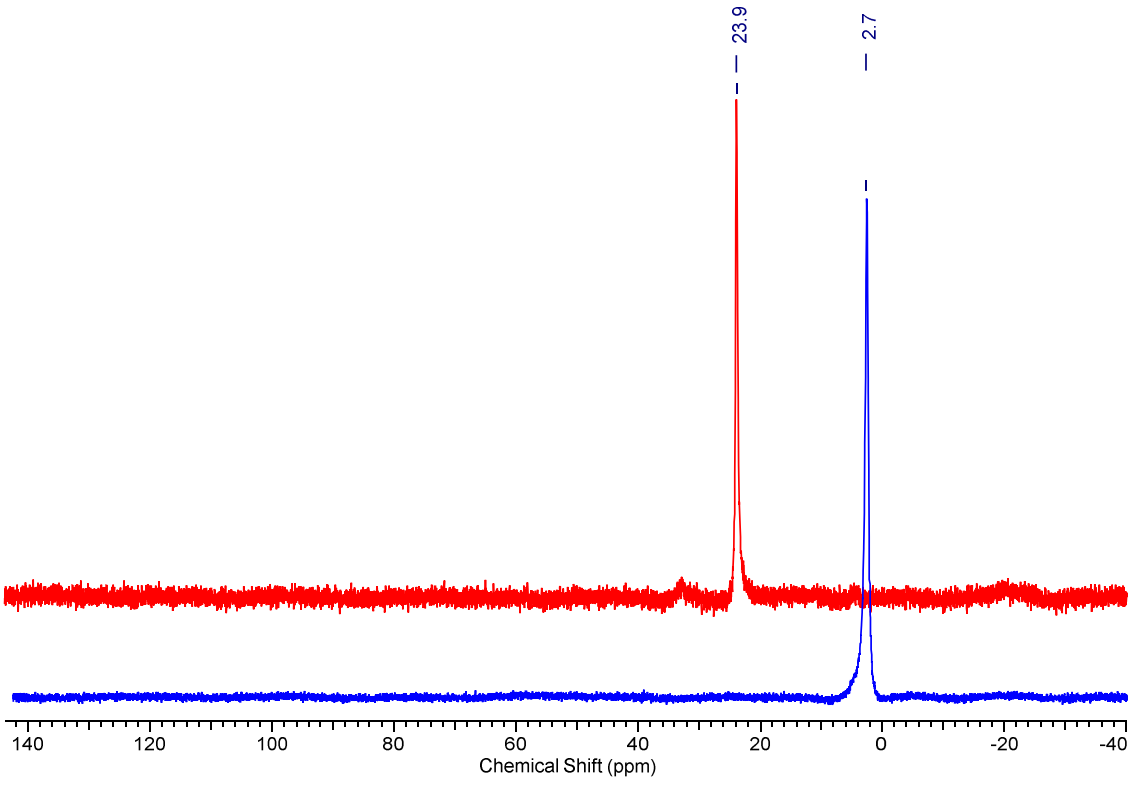

Figure S11. Collected $^{11}B\{^1H\}$ NMR spectra (baseline corrected): *In-situ* generated K[**2a**] (blue); reaction mixture after heating at 60°C for 10 minutes (red).

8e. [Fe(dppe)Cl_2] (0.5 equiv.) / dppe (0.5 equiv.) + K[2a] (generated *in-situ* from KH):

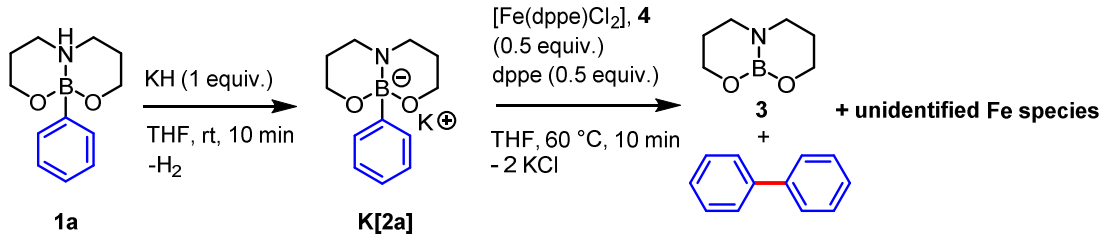

In a glovebox an oven dried J. Youngs NMR tube equipped with a DMSO-d_6 capillary insert was loaded with **1a** (40.0 mg, 0.183 mmol), KH (7.3 mg, 0.183 mmol) and *protio*-THF (0.8 mL) followed by agitation until the reaction mixture became completely homogeneous and hydrogen evolution had ceased (*ca.* 10-15 mins). After this time a $^{11}B\{^1H\}$ NMR spectrum was taken (*Figure S12, blue*) prior to the addition of [Fe(dppe)Cl_2], **4** (48.0 mg, 0.092 mmol) and dppe (37.0 mg, 0.092 mmol) in a glovebox. Heating the reaction mixture at 60°C for 10 minutes afforded a deep red solution with a fine precipitate. The reaction mixture was subsequently analysed by $^{11}B\{^1H\}$ NMR (*Figure S12, red*), revealing the conversion of K[**2a**] (δ_{11B} = 2.7 ppm) to the by-product of hydrocarbyl transmetallation, **3** (δ_{11B} = 24.3 ppm). Biphenyl ~0.5 equiv. was confirmed *via* GC-MS analysis against a calibrated internal standard.

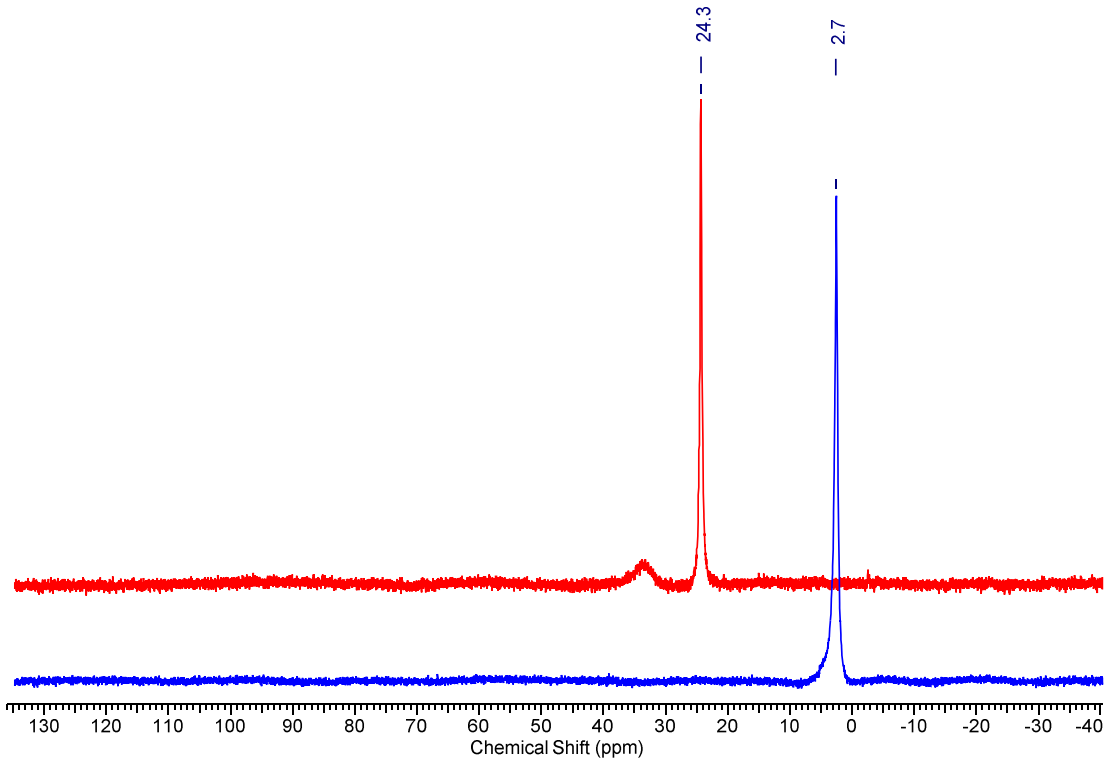

Figure S12. Collected $^{11}B\{^1H\}$ NMR spectra (baseline corrected): *In-situ* generated K[**2a**] (blue); reaction mixture after heating at 60°C for 10 minutes (red).

8f. [Fe(dppe)Cl_2] (0.5 equiv.) / dppe (0.5 equiv.) + K[2c] (generated *in-situ* from KH):

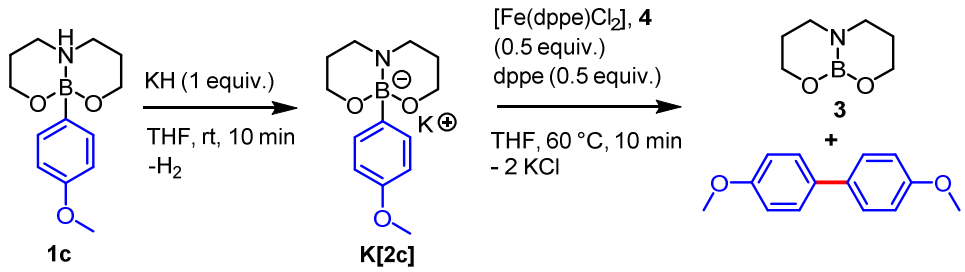

In a glovebox an oven dried J. Youngs NMR equipped with a DMSO-d_6 capillary insert tube was loaded with **1c** (46.0 mg, 0.183 mmol), KH (7.3 mg, 0.183 mmol) and *protio*-THF (0.8 mL) followed by agitation until the reaction mixture became completely homogeneous and hydrogen evolution had ceased (*ca.* 10-15 mins). After this time an $^{11}B\{^1H\}$ NMR spectrum was taken (*Figure S13, blue*) prior to the addition of [Fe(dppe)Cl_2], **4** (48.0 mg, 0.092 mmol) and dppe (37.0 mg, 0.092 mmol) in a glovebox. Heating the reaction mixture at 60°C for 10 minutes afforded a deep red solution with a fine precipitate. The reaction mixture was subsequently analysed by $^{11}B\{^1H\}$ NMR (*Figure S13, red*), revealing the quantitative conversion of K[**2c**] (δ_{11B} = 2.6 ppm) to the by-product of hydrocarbyl transmetallation, **3** (δ_{11B} = 21.2 ppm). 4,4'-dimethoxy-1,1'-biphenyl ~0.5 equiv. was confirmed *via* GC-MS analysis against a calibrated internal standard.

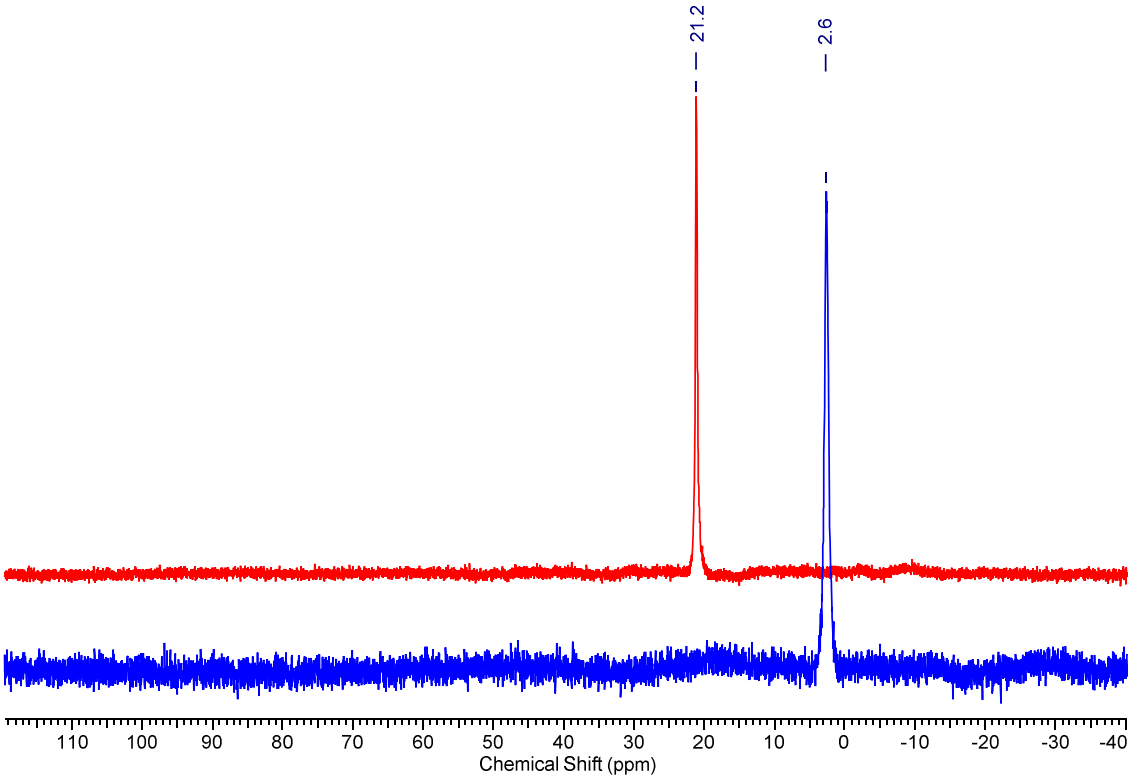

Figure S13. Collected $^{11}B\{^1H\}$ NMR spectra (baseline corrected): *In-situ* generated K[**2c**] (blue); reaction mixture after heating at 60°C for 10 minutes (red).

8g. [Fe(dppe)Cl_2] (0.5 equiv.) / dppe (0.5 equiv.) + K[2d] (generated *in-situ* from KH):

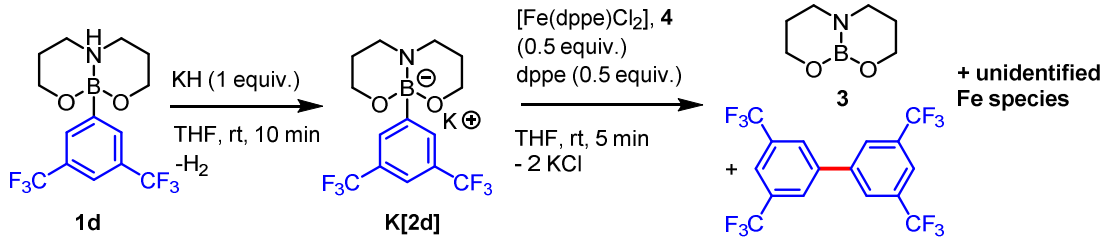

In a glovebox an oven dried J. Youngs NMR tube equipped with a DMSO-d_6 capillary insert was loaded with **1d** (65.0 mg, 0.183 mmol), KH (7.3 mg, 0.183 mmol) and *protio*-THF (0.8 mL) followed by agitation until the reaction mixture became completely homogeneous and hydrogen evolution had ceased (*ca.* 10-15 mins). After this time an $^{11}B\{^1H\}$ NMR spectrum was taken (*Figure S14, blue*) prior to the addition of [Fe(dppe)Cl_2], **4** (48.0 mg, 0.092 mmol) and dppe (37.0 mg, 0.092 mmol) in a glovebox. Agitation of the reaction mixture at ambient temperature quickly afforded a deep red solution with a fine precipitate (<5 minutes). The reaction mixture was subsequently analysed by $^{11}B\{^1H\}$ NMR (*Figure S14, red*), revealing the quantitative conversion of K[**2d**] (δ_{11B} = 2.0 ppm) to the by-product of hydrocarbyl transmetallation, **3** (δ_{11B} = 24.1 ppm). 3,3',5,5'-tetrakis(trifluoromethyl)-1,1'-biphenyl ~0.5 equiv. was confirmed *via* GC-MS analysis against a calibrated internal standard.

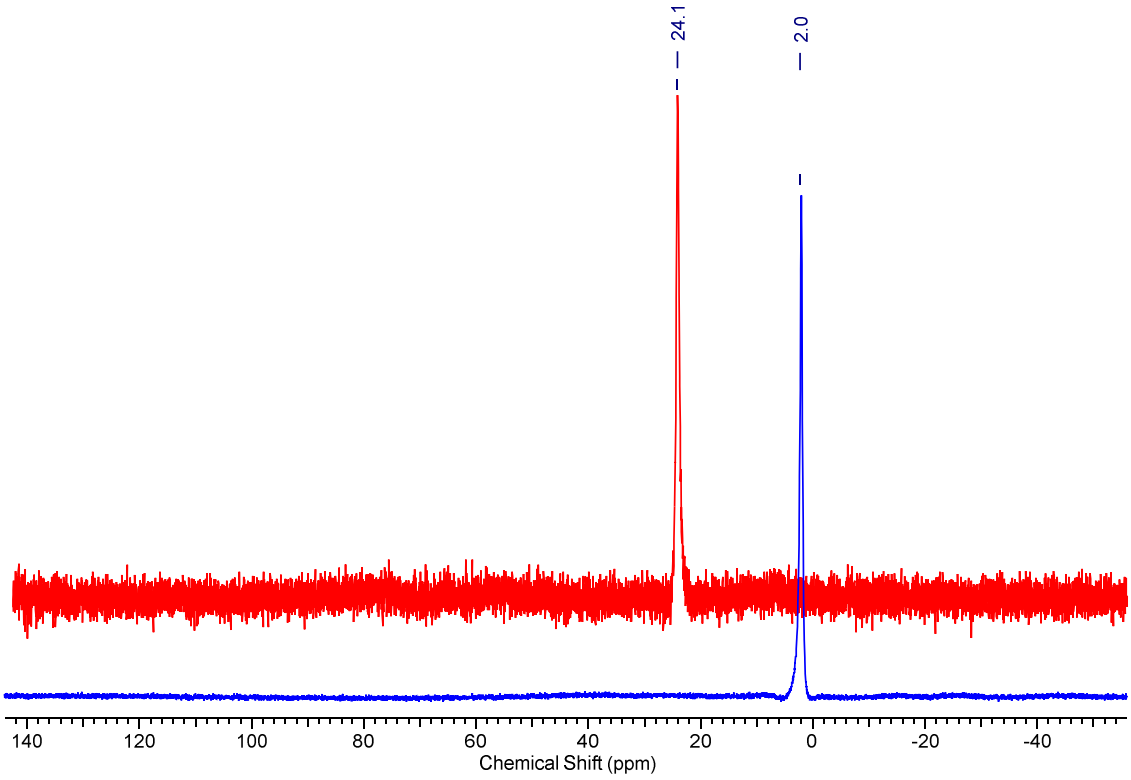

Figure S14. Collected $^{11}B\{^1H\}$ NMR spectra (baseline corrected): *In-situ* generated K[**2d**] (blue); reaction mixture after 5 minutes at ambient temperature (red).

8h. [Fe(dpbz)$_2$Cl$_2$] (0.5 equiv.) + K[2a] (generated *in-situ* from KH):

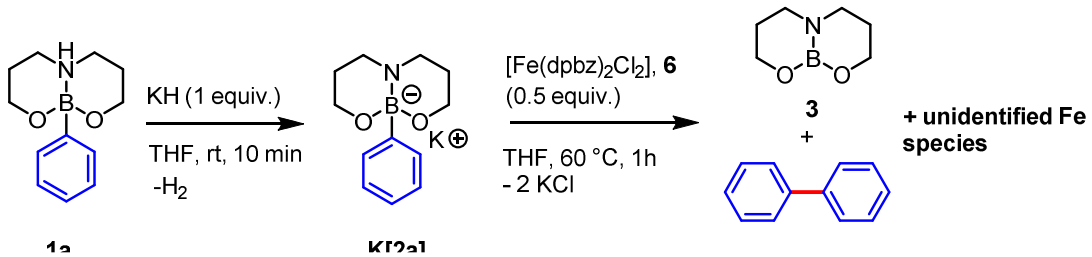

In a glovebox an oven dried J. Youngs NMR tube equipped with a DMSO-d_6 capillary insert was loaded with **1a** (40.0 mg, 0.183 mmol), KH (7.3 mg, 0.183 mmol) and *protio*-THF (0.8 mL) followed by agitation until the reaction mixture became completely homogeneous and hydrogen evolution had ceased (*ca.* 10-15 mins). After this time an $^{11}B\{^1H\}$ NMR spectrum was taken (*Figure S15, blue*) prior to the addition of [Fe(dpbz)$_2$Cl$_2$], **6** (86.8 mg, 0.092 mmol) in a glovebox. Heating the reaction mixture at 60°C for 1h afforded a deep red solution with a fine precipitate. The reaction mixture was subsequently analysed by $^{11}B\{^1H\}$ NMR (*Figure S15, red*), revealing the quantitative conversion of K[**2a**] (δ_{11B} = 2.5 ppm) to the by-product of hydrocarbyl transmetallation, **3** (δ_{11B} = 21.1 ppm). Biphenyl ~0.5 equiv. was confirmed *via* GC-MS analysis against a calibrated internal standard.

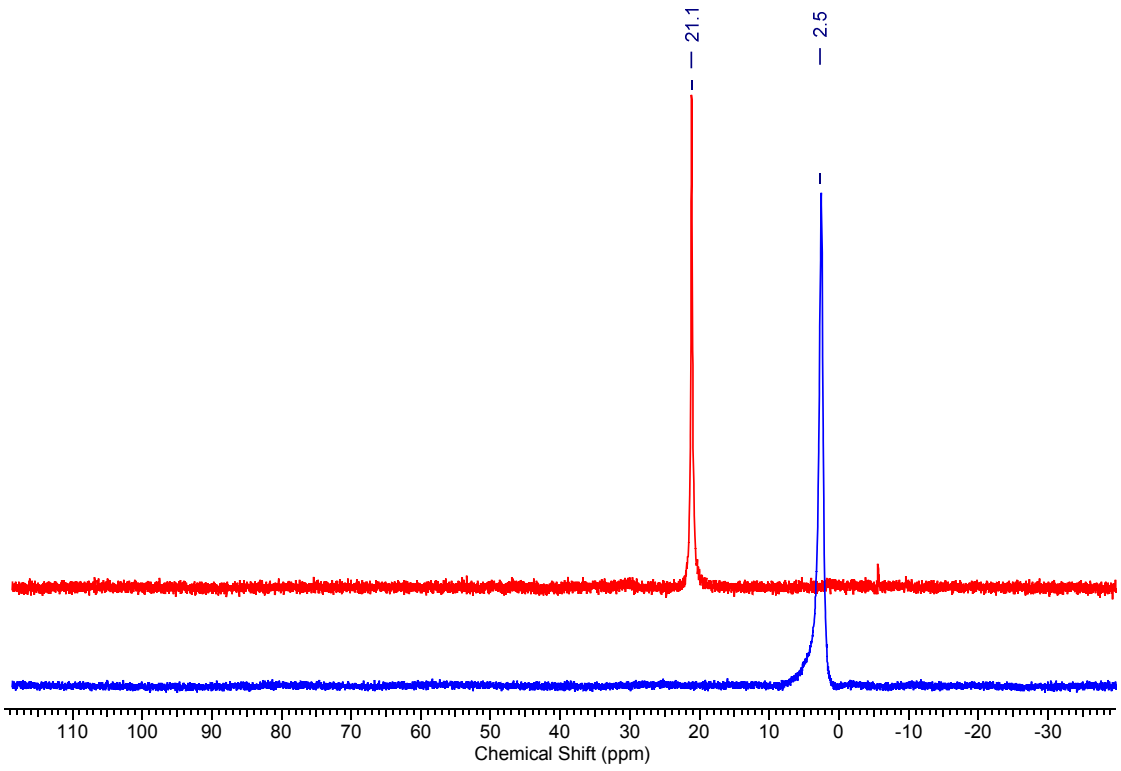

Figure S15. Collected $^{11}B\{^1H\}$ NMR spectra (baseline corrected): *In-situ* generated K[**2a**] (blue); reaction mixture after heating at 60°C for 1h (red).

8i. [Fe(dpbz)$_2$Cl$_2$] (0.5 equiv.) + K[2b] (generated *in-situ* from KH):

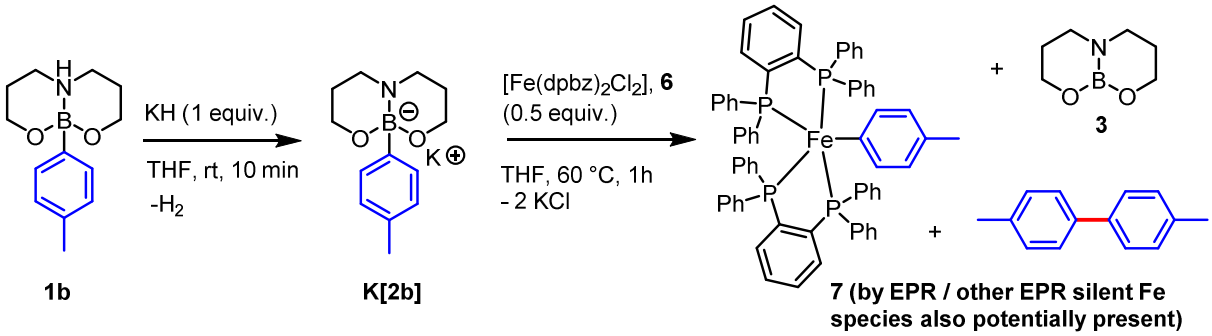

In a glovebox an oven dried J. Youngs NMR tube equipped with a DMSO-d_6 capillary insert was loaded with **1b** (43.0 mg, 0.183 mmol), KH (7.3 mg, 0.183 mmol) and *protio*-THF (0.8 mL) followed by agitation until the reaction mixture became completely homogeneous and hydrogen evolution had ceased (*ca.* 10-15 mins). After this time an $^{11}B\{^1H\}$ NMR spectrum was taken (*Figure S16, blue*) prior to the addition of [Fe(dpbz)$_2$Cl$_2$], **6** (86.8 mg, 0.092 mmol) in a glovebox. Heating the reaction mixture at 60°C for 1h afforded a deep red solution with a fine precipitate. The reaction mixture was subsequently analysed by $^{11}B\{^1H\}$ NMR (*Figure S16, red*), revealing the quantitative conversion of K[**2b**] (δ_{11B} = 4.5 ppm) to the by-product of hydrocarbyl transmetallation, **3** (δ_{11B} = 21.1 ppm). 4,4'-dimethyl-1,1'-biphenyl ~0.5 equiv. was confirmed *via* GC-MS analysis against a calibrated internal standard. **7** was confirmed by CW-EPR measurements (*Vide Infra*).

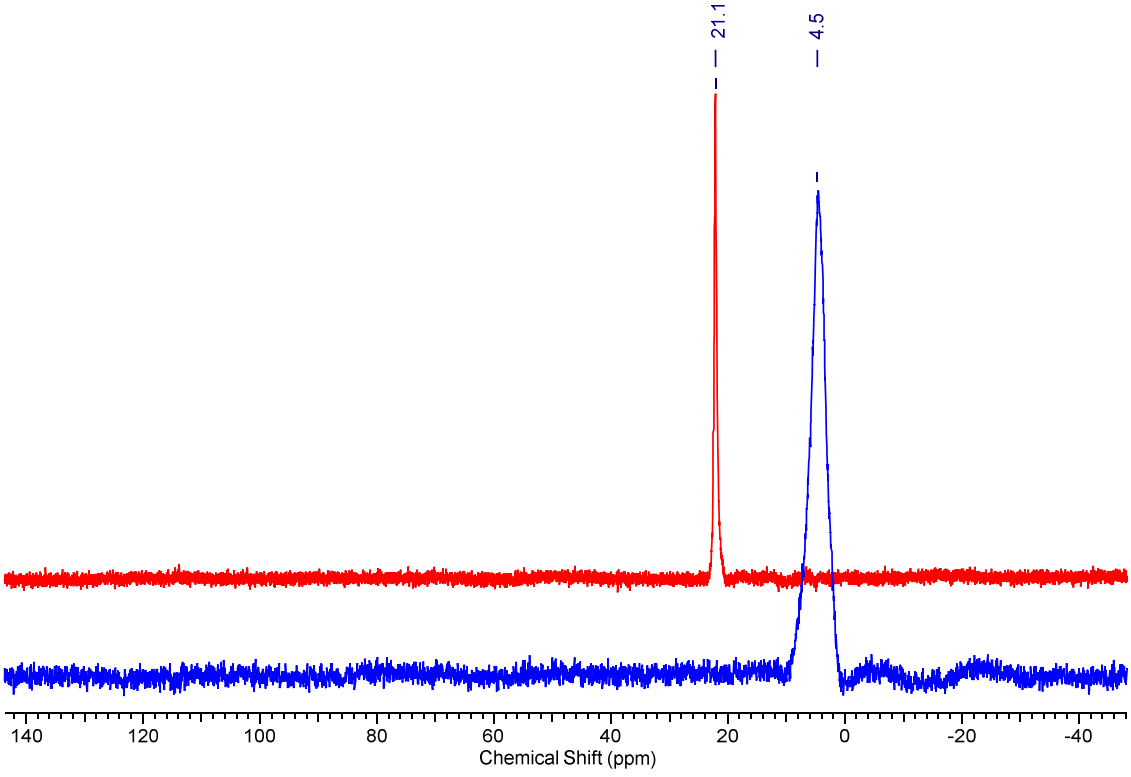

Figure S16. Collected $^{11}B\{^1H\}$ NMR spectra (baseline corrected): *In-situ* generated K[**2b**] (blue); reaction mixture after heating at 60°C for 1h (red).

8j. [Fe(dppe)Cl_2] + dppe + Li[2a] (generated *in-situ* from ^{t}BuLi) in C_6D_6:

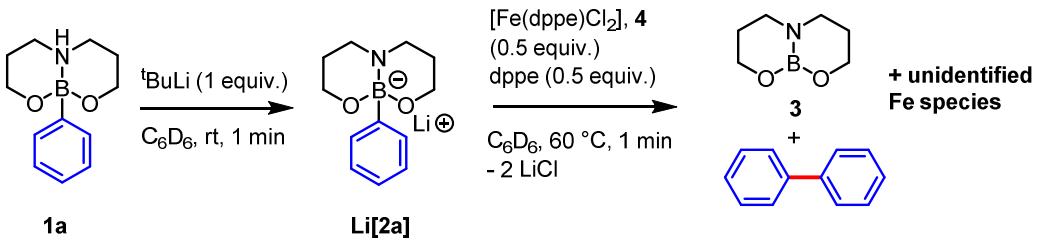

A J. Youngs NMR tube was loaded with **1a** (40.0 mg, 0.183 mmol) and *tert*-butyl lithium (11.7 mg, 0.183 mmol) prior to the addition of C_6D_6 (1 mL) and agitation at ambient temperature for 1 minute. After this period the solution became completely homogeneous (**1a** is insoluble in C_6D_6) and analysis of the reaction mixture by $^{11}B\{^1H\}$ NMR spectroscopy revealed the clean formation of Li[**2a**] (δ_{11B} = 3.8 ppm) (*Figure S17, blue*). Addition of [Fe(dppe)Cl_2], **4** (48.0 mg, 0.092 mmol) and dppe (37.0 mg, 0.092 mmol) to the reaction mixture in one portion lead to an orange solution which quickly became deep red upon heating to 60°C for 1 minute. Immediate analysis of the reaction mixture by $^{11}B\{^1H\}$ NMR spectroscopy (*Figure S17, red*) revealed the complete consumption of Li[**2a**] (δ_{11B} = 3.8 ppm) with the only observed boron containing species being the expected 3-coordinate borane of hydrocarbyl transmetallation, **3** (δ_{11B} = 20.9 ppm).

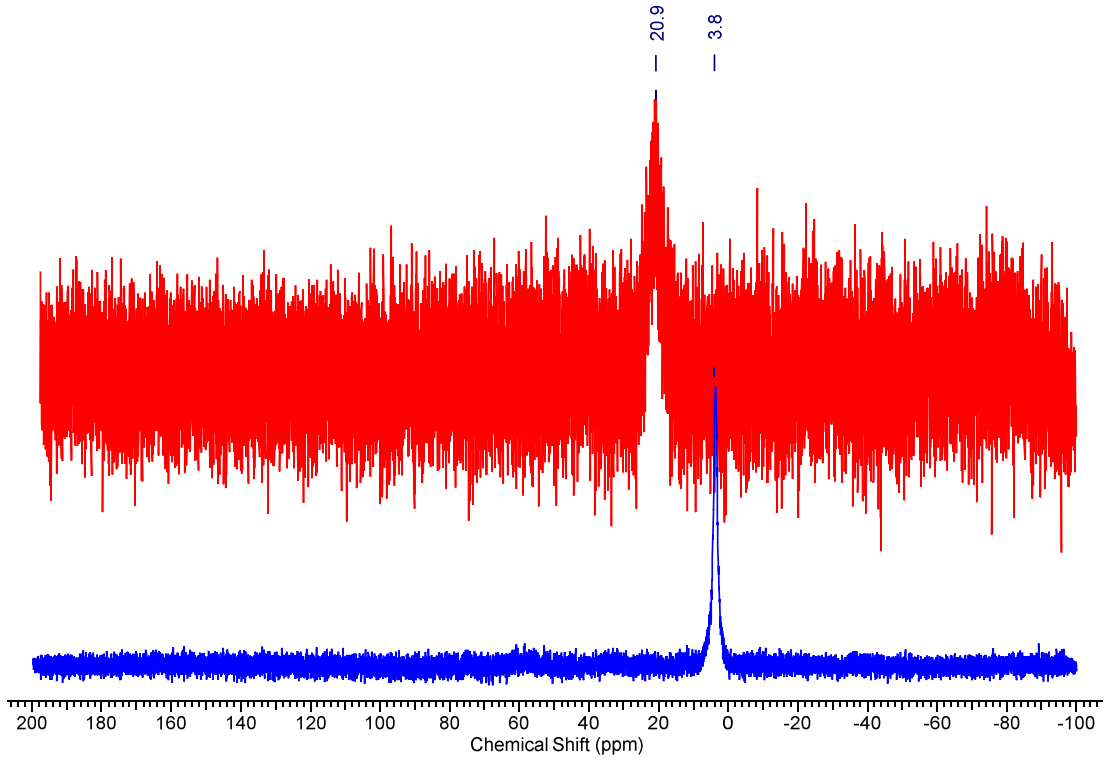

Figure S17. Collected $^{11}B\{^1H\}$ NMR spectra (baseline corrected): *In-situ* generated Li[**2a**] (blue); reaction mixture after heating at 60°C for 1 minute (red).

8k. [Fe(dppe)Cl_2] + dppe + Li[2a] (isolated) in THF:

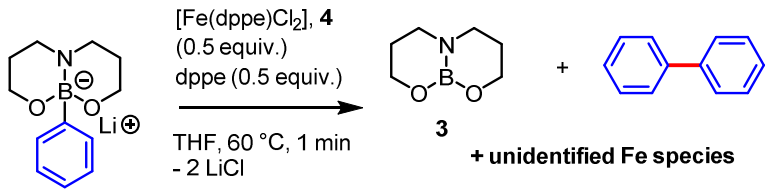

Li[2a]

A J. Youngs NMR tube equipped with a DMSO-d_6 capillary insert was loaded with Li[**2a**] (41.2 mg, 0.183 mmol), [Fe(dppe)Cl_2], **4** (48.0 mg, 0.092 mmol) and dppe (38.0 mg, 0.092 mmol) prior to the addition of *protio*-THF (1 mL). The reaction mixture became homogeneous and pale orange in colour. Heating the reaction mixture to 60°C for 5 minutes lead to the reaction mixture becoming deep red in colour and immediate analysis by $^{11}B\{^1H\}$ NMR spectroscopy (*Figure S18, red*) revealed the complete consumption of Li[**2a**] (δ_{11B} = 3.8 ppm) and the expected by-product of hydrocarbyl transmetallation, **3** (δ_{11B} = 22.9 ppm).

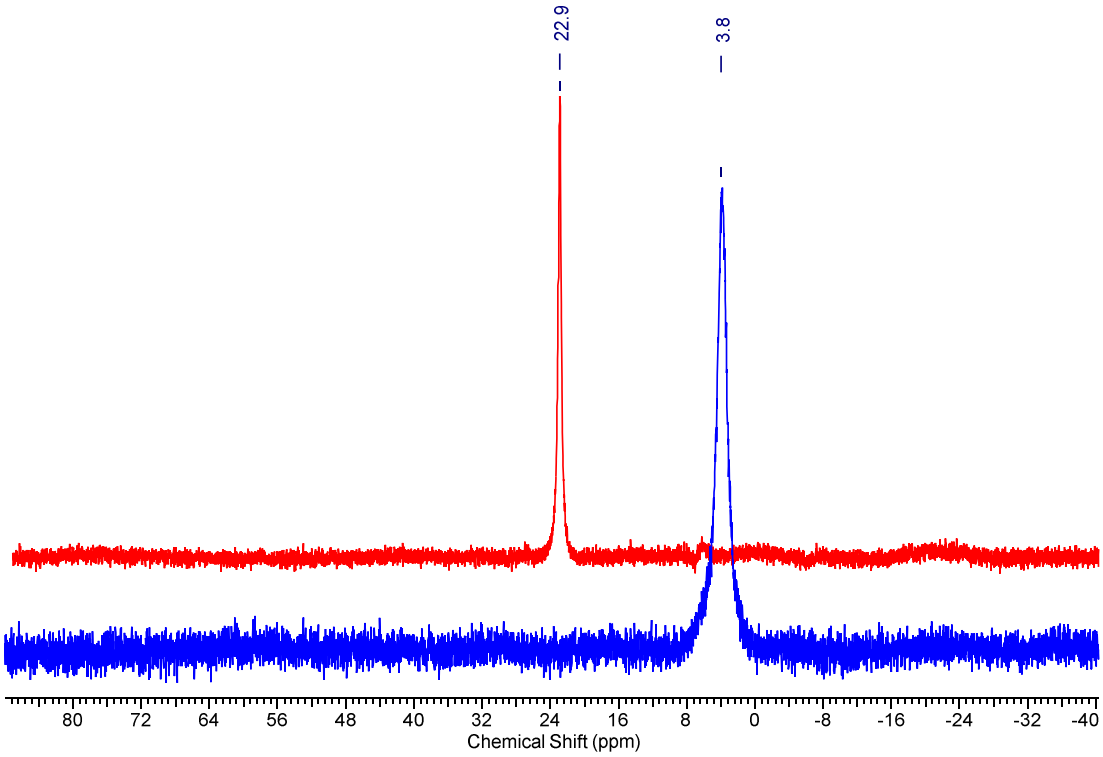

Figure S18. Collected $^{11}B\{^1H\}$ NMR spectra (baseline corrected): Li[**2a**] (blue); reaction mixture after heating at 60°C for 5 minutes (red).

8l. [Fe(dppe)Cl_2] + dppe + 9 in THF:

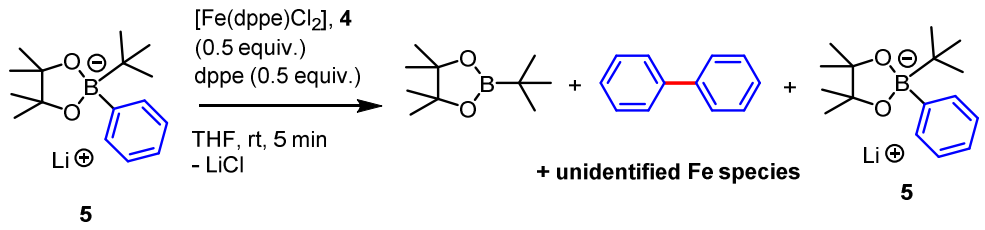

A J. Youngs NMR tube equipped with a DMSO-d_6 capillary insert was loaded with **5** (53.6 mg, 0.2 mmol), [Fe(dppe)Cl_2], **4** (52.5 mg, 0.1 mmol) and dppe (39.8 mg, 0.1 mmol) prior to the addition of THF. The reaction mixture became deep red in colour within 1 minute at ambient temperature. Immediate analysis of the reaction mixture by $^{11}B\{^1H\}$ NMR spectroscopy (*Figure S19*) demonstrated the presence of both the expected by-product of hydrocarbyl transmetallation, ^{t}BuBPin (δ_{11B} = 35.9 ppm) and **5** (δ_{11B} = 9.3 ppm). This observation is consistent with partial transmetallation to iron (one aryl equivalent) *in the absence of* MgX_2. It is noteworthy that heating of the reaction mixture to 60°C for 1h does lead to a reduction in the concentration of **5**, with an increase in the concentration of ^{t}BuBPin (*Figure S20*).

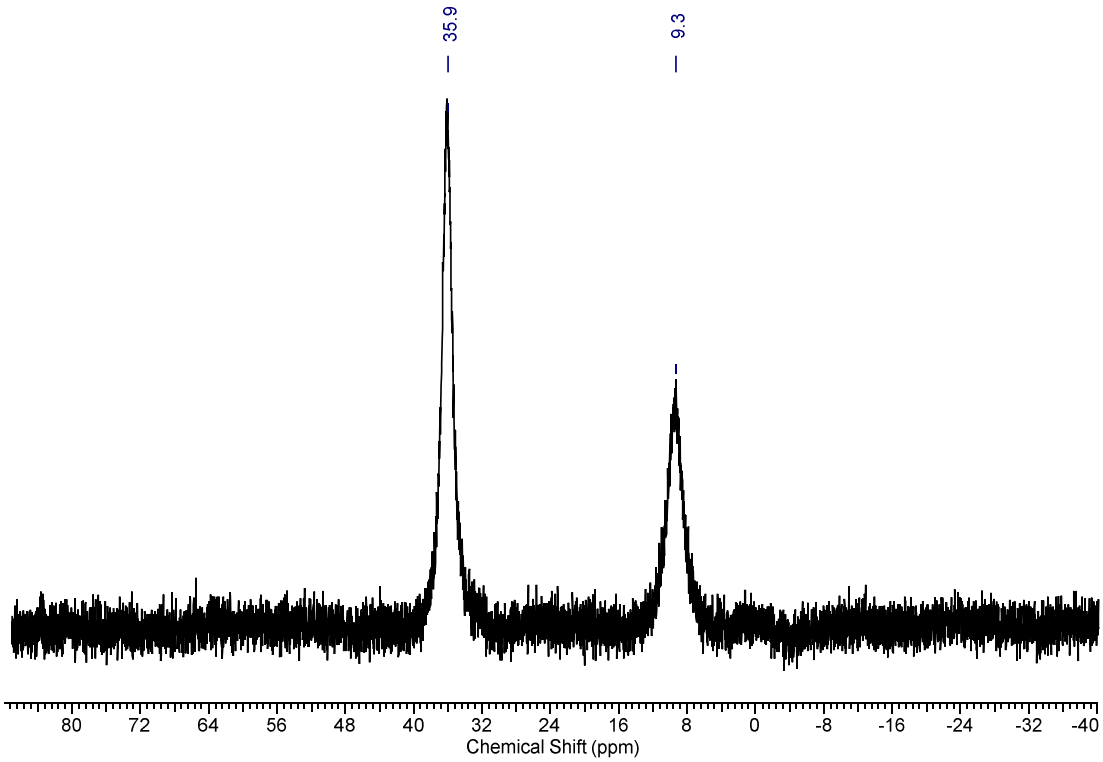

Figure S19. $^{11}B\{^1H\}$ NMR spectra (baseline corrected) of the reaction mixture after 5 minutes at ambient temperature.

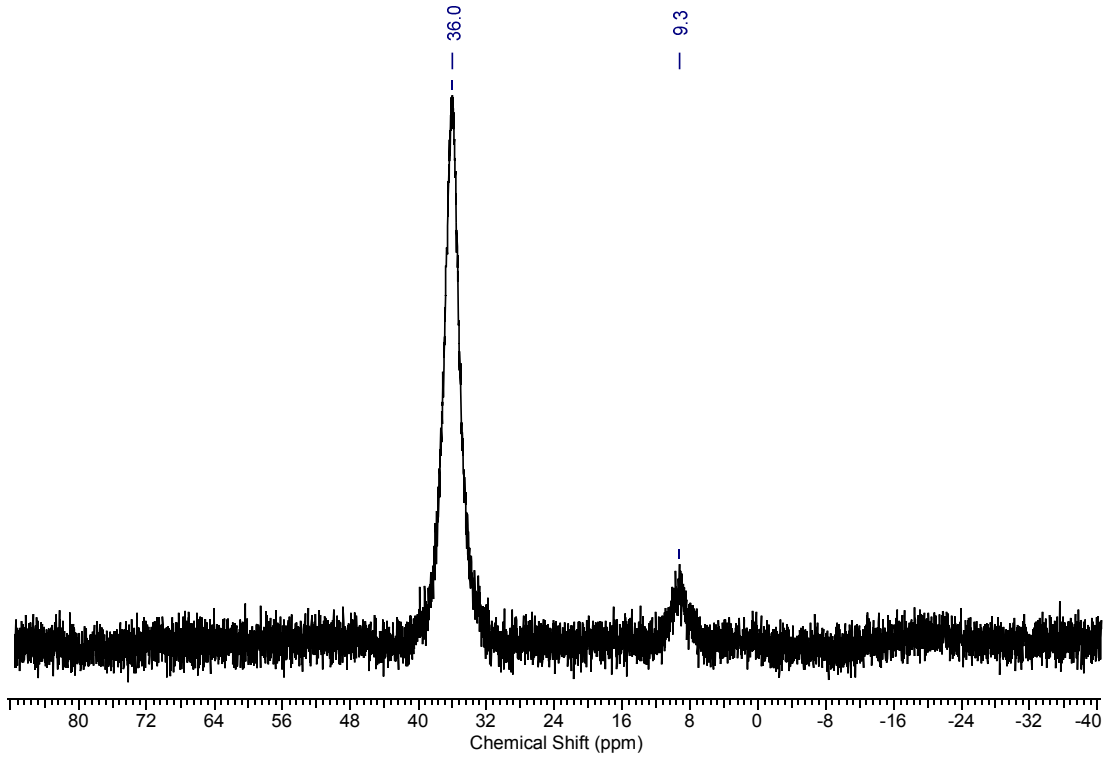

Figure S20. $^{11}B\{^{1}H\}$ NMR spectra (baseline corrected) of the reaction mixture after 1h at 60°C.

8m. [Fe(dppe)Cl_2] + K[2a] (generated *in-situ* from KH) 1:3:

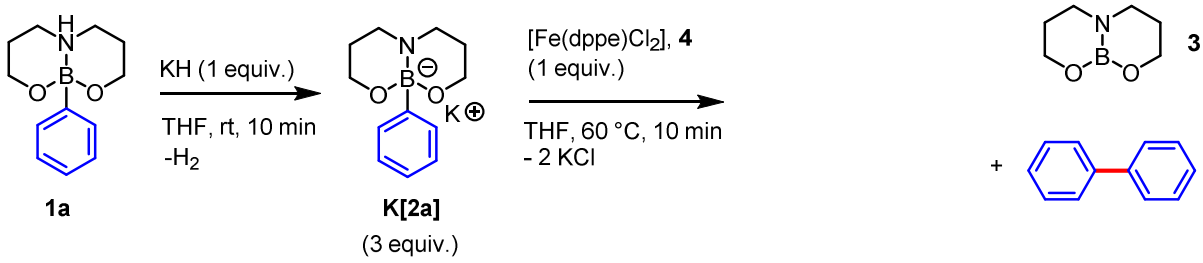

In a glovebox an oven dried J. Youngs NMR tube equipped with a DMSO-d_6 capillary insert was loaded with **1a** (60.0 mg, 0.275 mmol), KH (11.0 mg, 0.275 mmol) and *protio*-THF (0.8 mL) followed by agitation until the reaction mixture became completely homogeneous and hydrogen evolution had ceased (*ca.* 10-15 mins). After this time [Fe(dppe)Cl_2], **4** (48.0 mg, 0.092 mmol) was added and the reaction mixture heated at 60°C for 10 minutes to afford a deep red solution. The reaction mixture was subsequently analysed by $^{11}B\{^1H\}$ NMR (*Figure S21*), revealing the incomplete conversion of K[**2a**] (δ_{11B} = 3.6 ppm) and the by-product of hydrocarbyl transmetallation, **3** (δ_{11B} = 21.2 ppm).

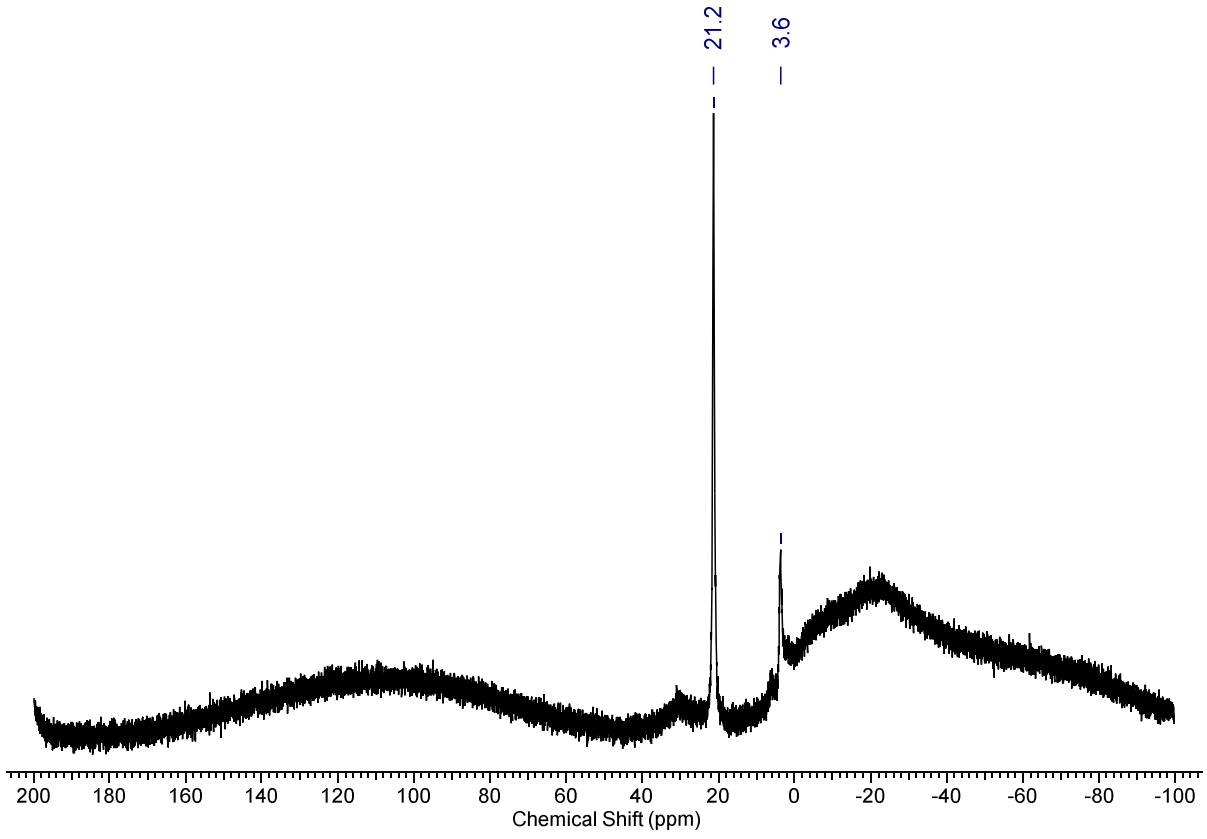

Figure S21. $^{11}B\{^1H\}$ NMR spectra of the reaction mixture after 10 minutes at 60°C.

8n. [Fe(dppe)Cl_2] + K[2a] (generated *in-situ* from KH) 1:4:

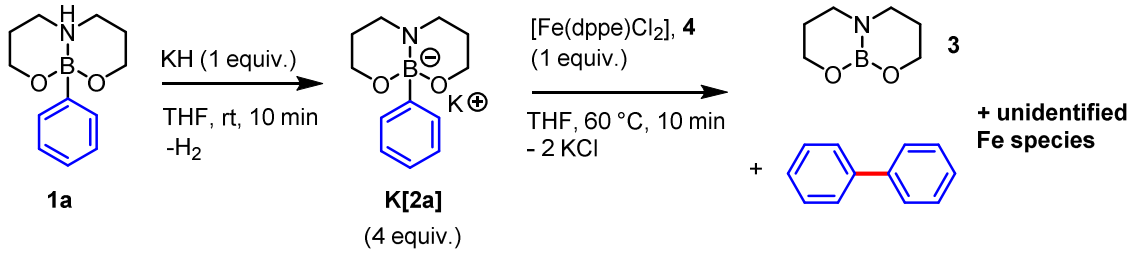

In a glovebox an oven dried J. Youngs NMR tube equipped with a DMSO-d_6 capillary insert was loaded with **1a** (80.0 mg, 0.366 mmol), KH (14.6 mg, 0.366 mmol) and *protio*-THF (0.8 mL) followed by agitation until the reaction mixture became completely homogeneous and hydrogen evolution had ceased (*ca.* 10-15 mins). After this time [Fe(dppe)Cl_2], **4** (48.0 mg, 0.092 mmol) was added and the reaction mixture heated at 60°C for 10 minutes to afford a deep red solution. The reaction mixture was subsequently analysed by $^{11}B\{^1H\}$ NMR (*Figure S22*), revealing the incomplete conversion of K[**2a**] (δ_{11B} = 3.9 ppm) and the by-product of hydrocarbyl transmetallation, **3** (δ_{11B} = 21.5 ppm).

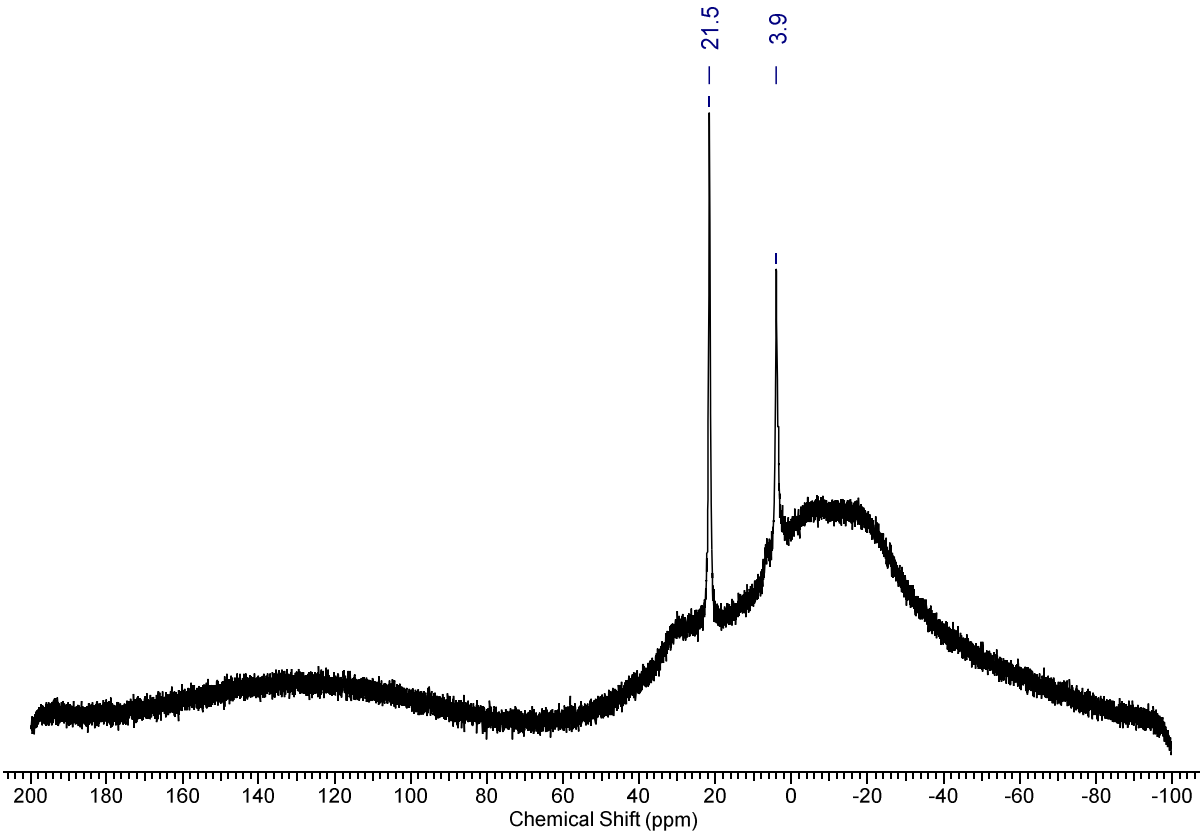

Figure S22. $^{11}B\{^1H\}$ NMR spectra of the reaction mixture after 10 minutes at 60°C.

9. Representative GC-MS Data

9a. GC-MS Sample Preparation: All samples for GC-MS analysis (0.1 mL) were taken directly from the corresponding reaction mixtures (with added mesitylene, 1 equiv. relative to boronate), diluted with HPLC grade dichloromethane (1.5 mL) and eluted through a small plug of silica prior to analysis.

9b. GC-MS Program of Analysis: Initial temperature at 40 ºC, held for 2.5 minutes, ramp 5 ºC/minute next 150 ºC, ramp 10 ºC/minute next 220 ºC, held for 10 minutes. The temperature of the injector and detector were maintained at 240 ºC.

9c. [Fe(dppe)Cl_2] (0.5 equiv.) / dppe (0.5 equiv.) + K[2a] (generated *in-situ*):

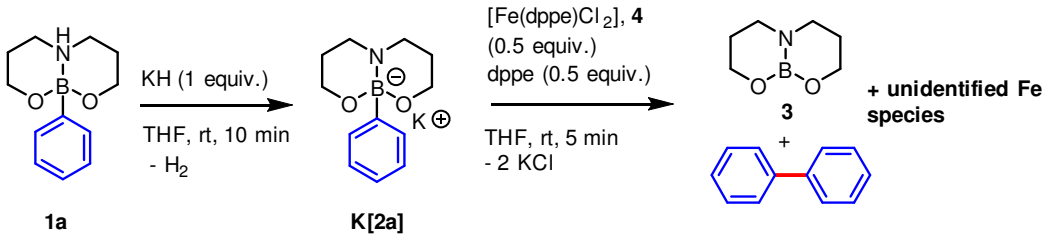

Analysis of the reaction mixture by GC-MS (*Figure S23*) reveals the presence of biphenyl (0.44 equiv., 0.082 mmol) along with a minor amount benzene derived from the hydrolysis of the [Fe(dppe)$_2$(Ph)] species during the sample preparation and also an *ortho*-dichlorobenzene impurity (18.10 minutes) carried over from a previous GC-MS experiment.

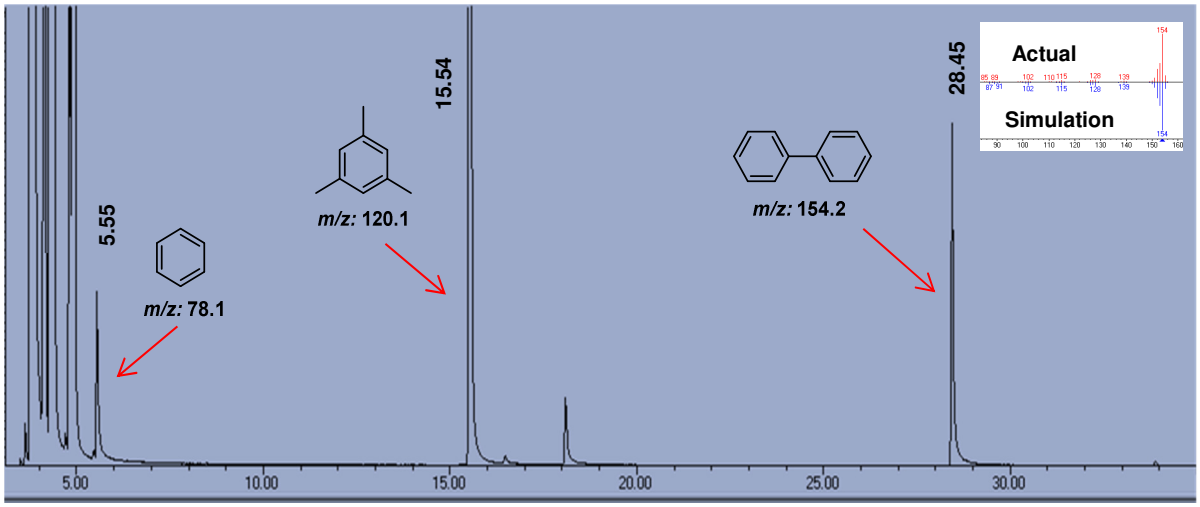

Figure S23. GC-MS trace of the reaction mixture. Retention times of analytes: benzene (5.55 minutes); mesitylene (15.54 minutes); biphenyl (28.45 minutes).

9d. [Fe(dppe)Cl_2] (0.5 equiv.) / dppe (0.5 equiv.) + K[2d] (generated *in-situ*):

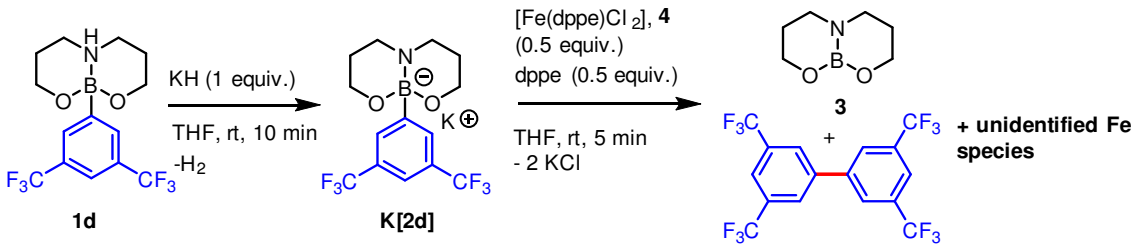

Analysis of the reaction mixture by GC-MS (*Figure S24*) reveals the presence of 3,3',5,5'-tetrakis (trifluoromethyl)biphenyl (0.43 equivalents, 0.079 mmol) along with a minor amount 3,5-trifluoromethylbenzene derived from the hydrolysis of the [Fe(dppe)$_2$(Ar)] species during the sample preparation.

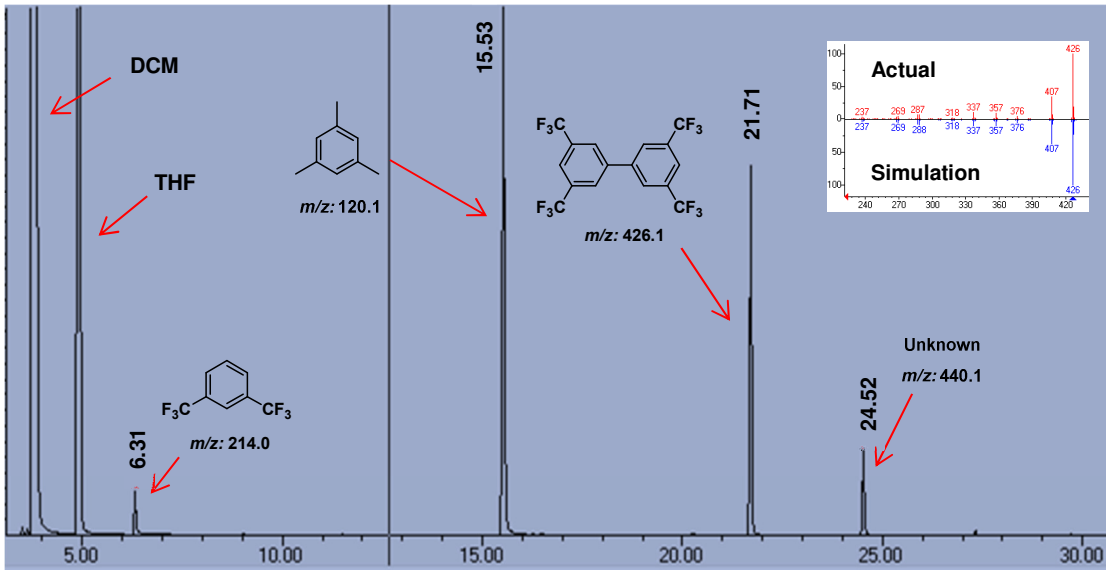

Figure S24. GC-MS trace of the reaction mixture. Retention times of analytes: 3,5-trifluoromethylbenzene (6.31 minutes); mesitylene (15.53 minutes); 3,3',5,5'-tetrakis(trifluoromethyl)biphenyl (21.71 minutes).

9e. [Fe(dpbz)$_2$Cl$_2$] (0.5 equiv.) + K[2b] (generated *in-situ*):

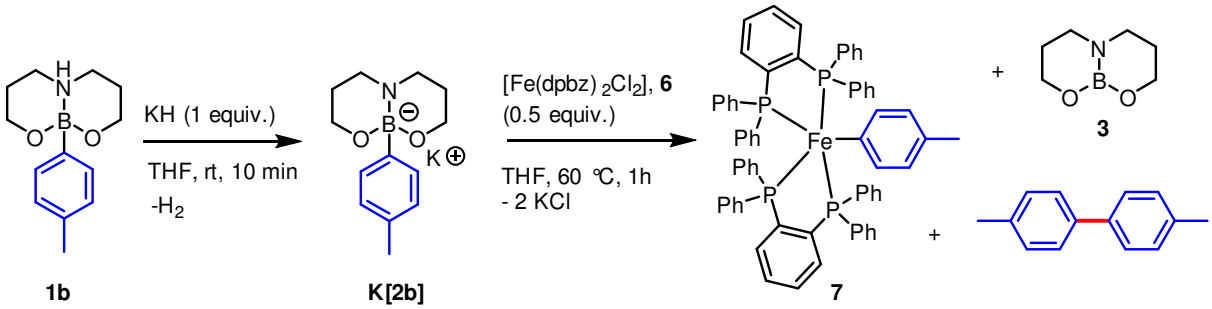

Analysis of the reaction mixture by GC-MS (*Figure S25*) reveals the presence of 4,4'-dimethylbiphenyl (0.39 equiv., 0.072 mmol) along with a minor amount toluene.

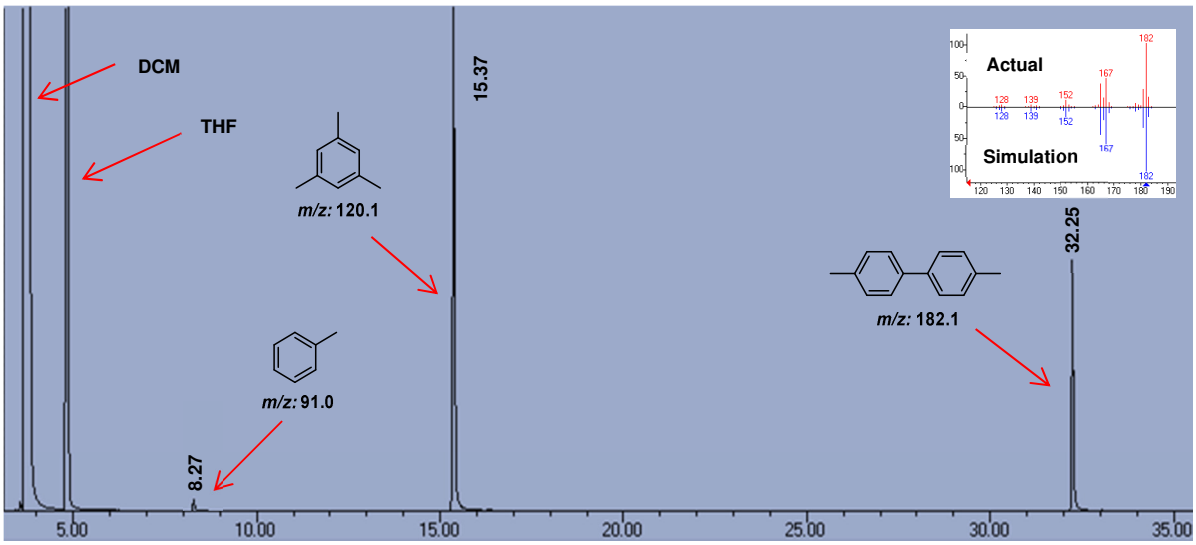

Figure S25. GC-MS trace of the reaction mixture. Retention times of analytes: toluene (8.27 minutes); mesitylene (15.37 minutes); 4,4'-dimethylbiphenyl (32.25 minutes).

10. EPR Data

10a. EPR spectra of *in-situ* generated 7b from K[2b] and 6 (0.5 equiv.)

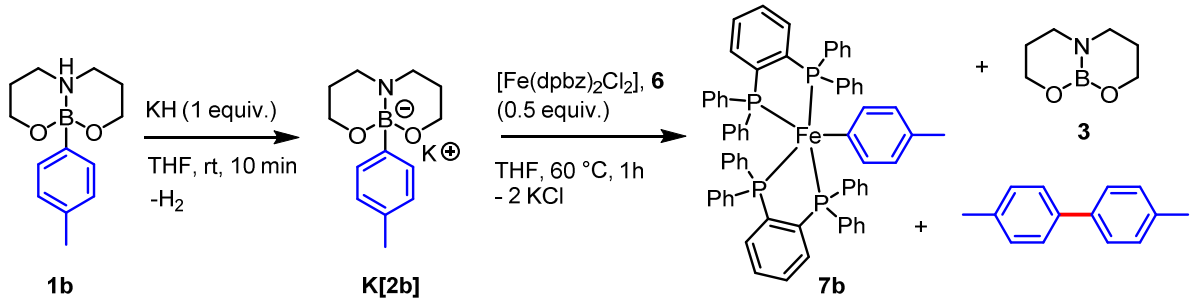

In a glovebox an oven dried J. Youngs NMR tube equipped with a DMSO-d_6 capillary insert was loaded with **1b** (43.0 mg, 0.183 mmol), KH (7.3 mg, 0.183 mmol) and *protio*-THF (0.8 mL) followed by agitation until the reaction mixture became completely homogeneous and hydrogen evolution had ceased (*ca.* 10-15 mins). After this time an $^{11}B\{^{1}H\}$ NMR spectrum was taken to confirm the clean generation of K[**2b**] prior to the addition of [Fe(dpbz)$_2$Cl$_2$], **6** (86.8 mg, 0.092 mmol) in a glovebox. Heating the reaction mixture at 60°C for 1h afforded a deep red solution with a fine precipitate. A portion of the reaction mixture was transferred directly into an oven dried quartz EPR tube (~2cm sample depth) equipped with a J. Youngs tap and evacuated *via* three consecutive freeze-pump-thaw cycles prior to analysis (*Figure S26*).

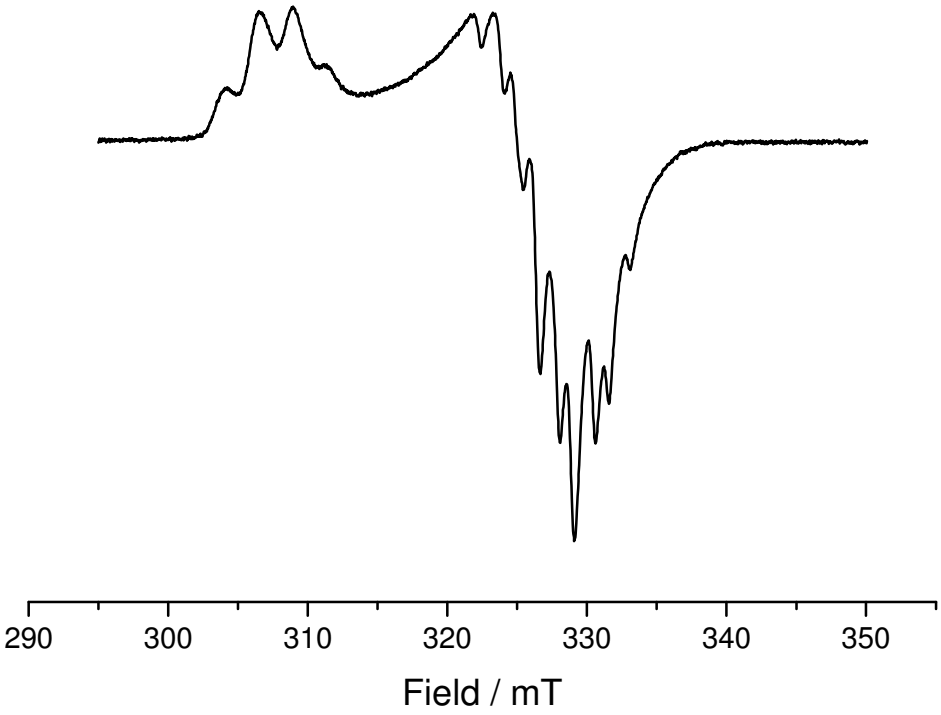

Figure S26. X-band CW-EPR spectrum of *in-situ* generated **7** recorded at 120K in THF.

10b. EPR spectra of *in-situ* generated 7b from *p*-TolMgBr (1M solution in THF) and 6 (0.5 equiv.)

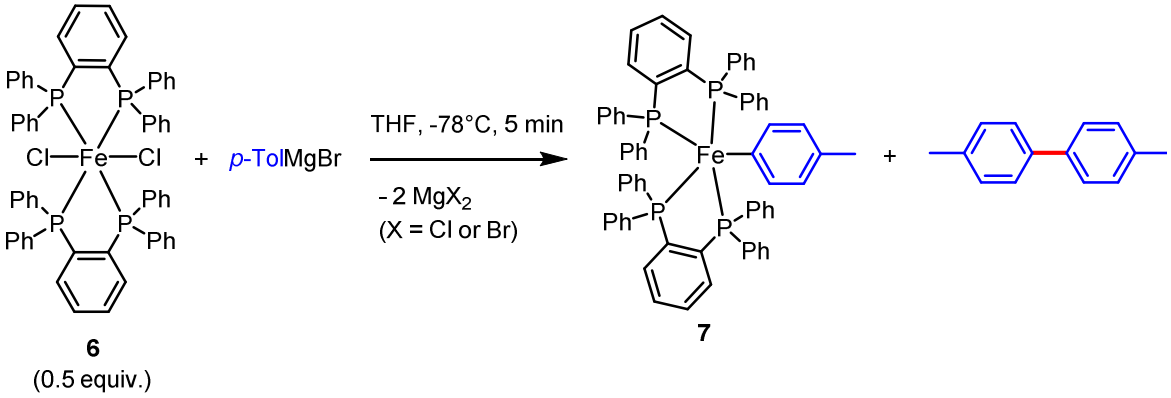

In a glovebox an oven dried J. Youngs ampule was loaded with [Fe(dpbz)$_2$Cl$_2$], **6** (86.8 mg, 0.092 mmol) and anhydrous *protio*-THF (0.8 mL) followed by the addition of *p*-TolMgBr (1 M solution in THF) (183 µL, 0.183 mmol) outside the glovebox under a nitrogen atomsphere at -78°C to afford an orange heterogeneous solution which, upon warming to ambient temperature became deep red in colour and homogeneous. A portion of the reaction mixture was transferred directly into a quartz EPR tube (2cm sample depth) equipped with a J. Youngs tap and evacuated *via* three consecutive freeze-pump-thaw cycles prior to analysis (*Figure S27*).

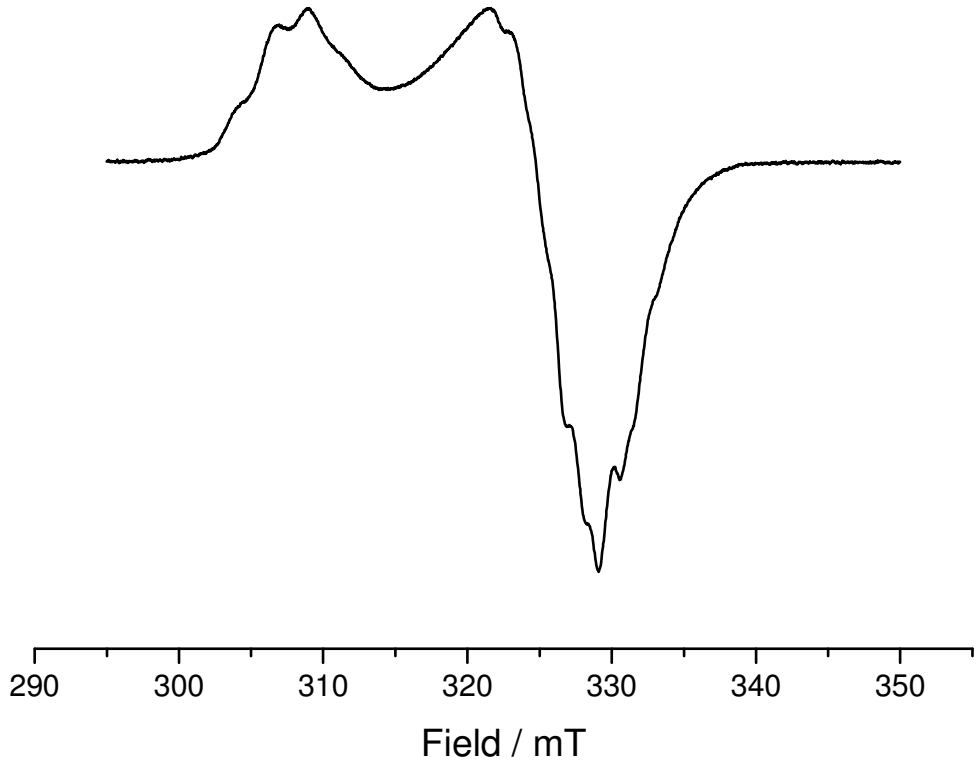

Figure S27. X-band CW-EPR spectrum of *in-situ* generated **7** recorded at 120K in THF.

10c. Collected EPR spectra of *in-situ* generated 7 from 6 and either K[2b] (2 equiv.) or *p*-TolMgBr (2 equiv.)

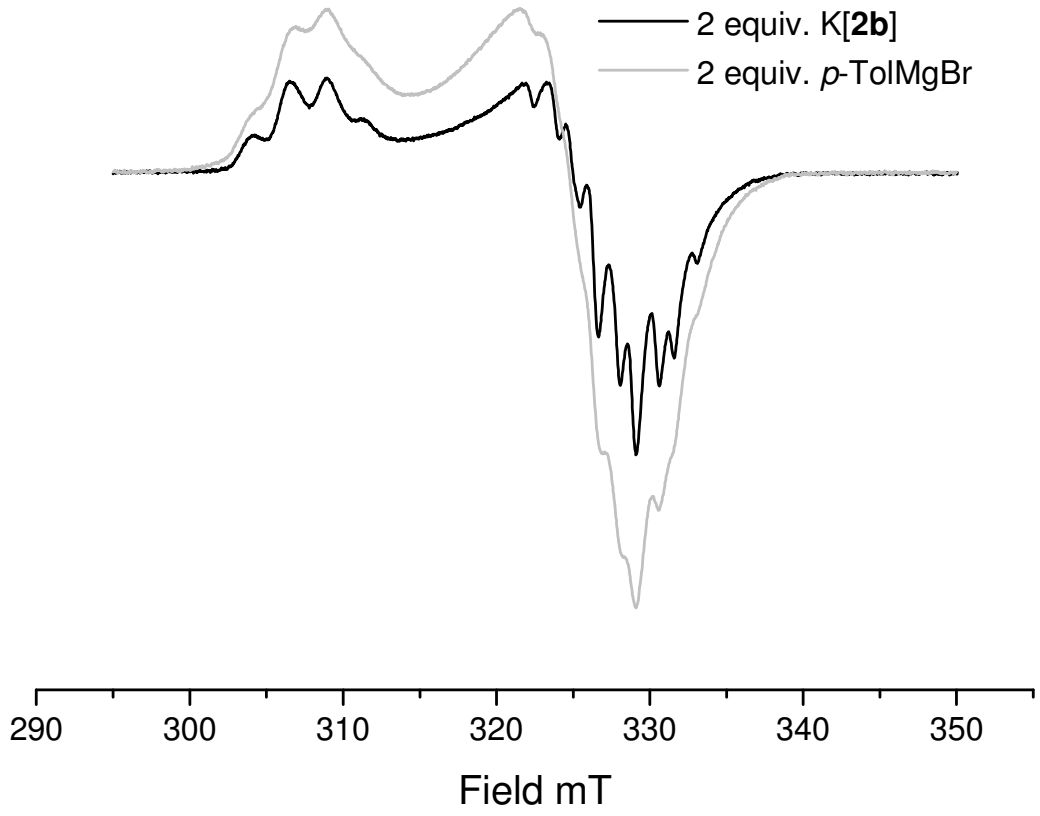

***Figure S28*.** Collected X-band CW-EPR spectrum of *in-situ* generated **7** generated *via* boronate (black) and Grignard (grey) routes recorded at 120K in THF.

11. Csp^2-Csp^3 Cross-Coupling Studies

11a. Li[2a] + 3-methoxybenzyl bromide with no added $MgBr_2$ in THF

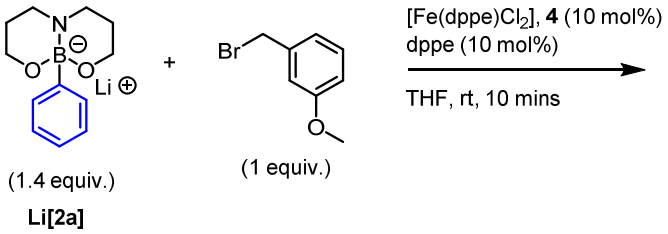

In a glovebox an oven dried J. Youngs NMR tube equipped with a DMSO-d_6 capillary insert was loaded with **Li[2a]** (63.0 mg, 0.28 mmol), [Fe(dppe)Cl_2] (10.5 mg, 0.02 mmol) and dppe (8.0 mg, 0.02 mmol) prior to the addition of THF (1.0 mL). To this reaction mixture was added 3-methoxybenzyl bromide (28 µL, 0.2 mmol). The reaction mixture was heated to 60°C for 30 minutes prior to analysis by $^{11}B\{^1H\}$ NMR spectroscopy (*Figure S29, green*) which revealed the minor formation of **3** (δ_{11B} = 20.7 ppm) and Li[**2a**] (δ_{11B} = 4.6 ppm). Continued heating at 60°C for 20h led to **3** (δ_{11B} = 20.7 ppm) as the major boron containing species along with the expected residual Li[**2a**] (*Figure S29, red*) as it is present in an excess of the limiting reagent, 3-methoxybenzyl bromide. Analysis of the reaction mixture by GC-MS revealed almost quantitative homocoupling of the 3-methoxybenzyl bromide starting material.

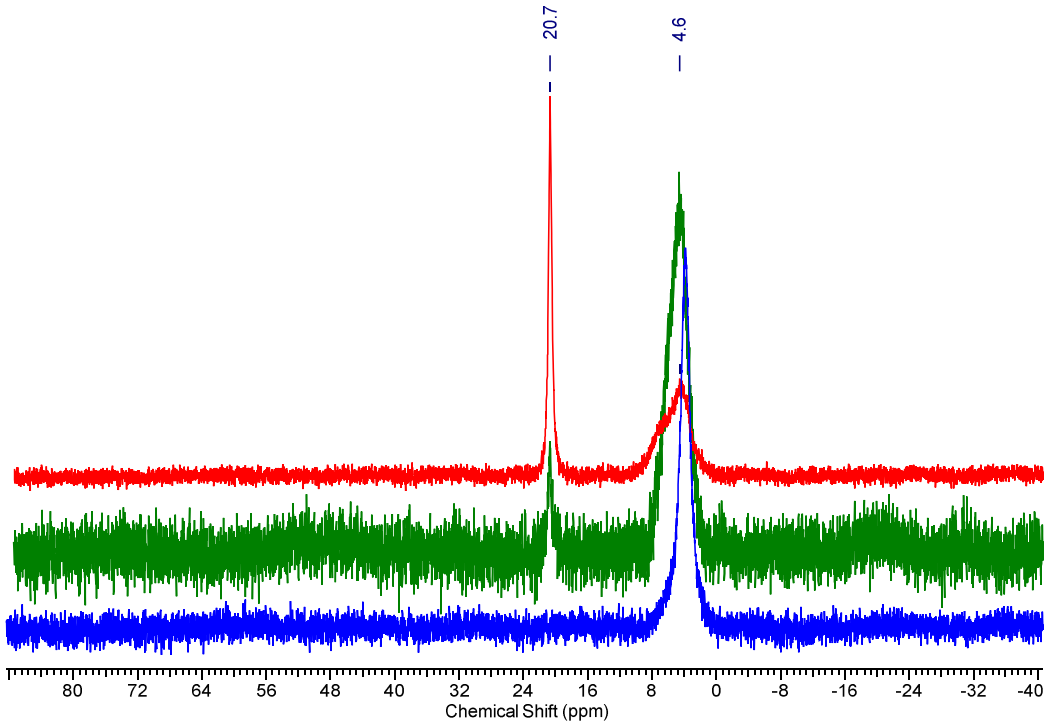

Figure S29. Collected $^{11}B\{^1H\}$ NMR spectra (baseline corrected): Li[**2a**] (blue); reaction mixture after 30 minutes at 60°C (green); reaction mixture after 20h at 60°C (red).

11b. Li[2a] + 3-methoxybenzyl bromide with added $MgBr_2$ in THF

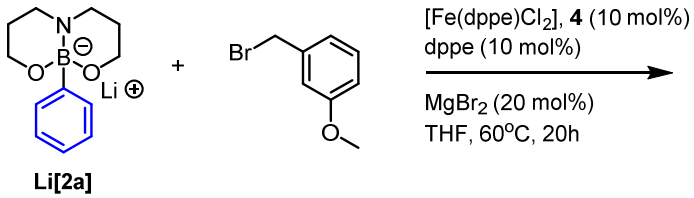

In a glovebox an oven dried J. Youngs NMR tube equipped with a DMSO-d_6 capillary insert was loaded with Li**[2a]** (63.0 mg, 0.28 mmol), [Fe(dppe)Cl_2] (10.5 mg, 0.02 mmol), dppe (8.0 mg, 0.02 mmol) and $MgBr_2$ (7.4 mg, 0.04 mmol) prior to the addition of THF (1.0 mL). To this reaction mixture was added 3-methoxybenzyl bromide (28 µL, 0.2 mmol). The reaction mixture was heated to 60°C for 30 minutes prior to analysis by $^{11}B\{^1H\}$ NMR spectroscopy (*Figure S30, green*) which revealed the minor formation of **3** (δ_{11B} = 20.7 ppm) and Li[**2a**] (δ_{11B} = 4.6 ppm). Continued heating at 60°C for 20h led to **3** (δ_{11B} = 20.7 ppm) along with the expected residual Li[**2a**] (*Figure S30, red*) as it is present in an excess of the limiting reagent, 3-methoxybenzyl bromide. Analysis of the reaction mixture by GC-MS revealed almost quantitative homocoupling of the 3-methoxybenzyl bromide starting material.

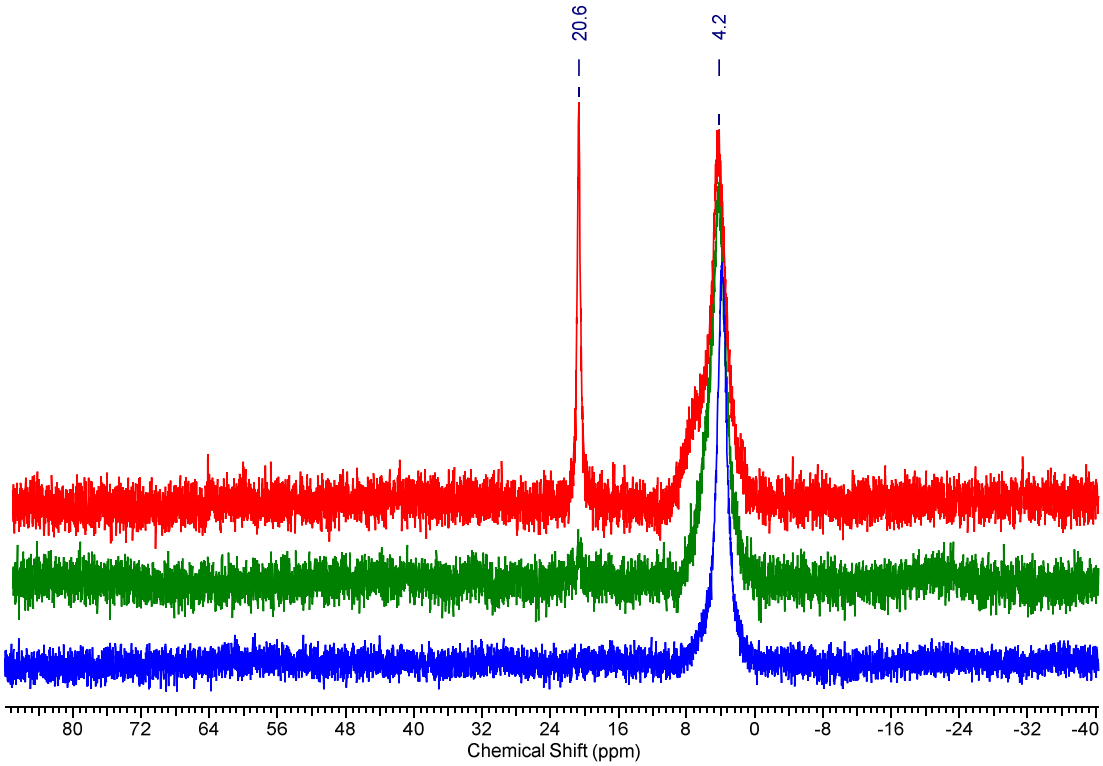

Figure S30. Collected $^{11}B\{^1H\}$ NMR spectra (baseline corrected): Li[**2a**] (blue); reaction mixture after 30 minutes at 60°C (green); reaction mixture after 20h at 60°C (red).

11c. 9 + 3-methoxybenzyl bromide in THF

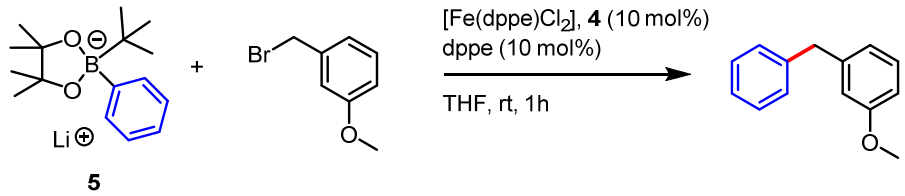

In a glovebox an oven dried J. Youngs NMR tube equipped with a DMSO-d_6 capillary insert was loaded with **5** (75.0 mg, 0.28 mmol), [Fe(dppe)Cl_2] (10.5 mg, 0.02 mmol) and dppe (8.0 mg, 0.02 mmol) prior to the addition of THF (1 mL). To this reaction mixture was added 3-methoxybenzyl bromide (28 µL, 0.2 mmol). The deep red reaction mixture agitated at ambient temperature for 10 minutes prior to analysis by $^{11}B\{^1H\}$ NMR spectroscopy (*Figure S31*). The $^{11}B\{^1H\}$ NMR spectra clearly indicated the presence of the expected by-product of hydrocarbyl transmetallation, ^{t}BuBPin (δ_{11B} = 35.3 ppm) and **5** (δ_{11B} = 8.5 ppm). The presence of **5** is to be expected even after the reaction has reached completion as it is present in an excess of the limiting reagent, 3-methoxybenzyl bromide. Agitation at ambient temperature was continued for 1h prior to quenching with HPLC grade dichloromethane (2.0 mL), the addition of mesitylene (27.8 µL, 0.2 mmol) and filtration through a small column of silica gel. Analysis by GC-MS revealed almost quantitative heterocoupling (*Figure S32*).

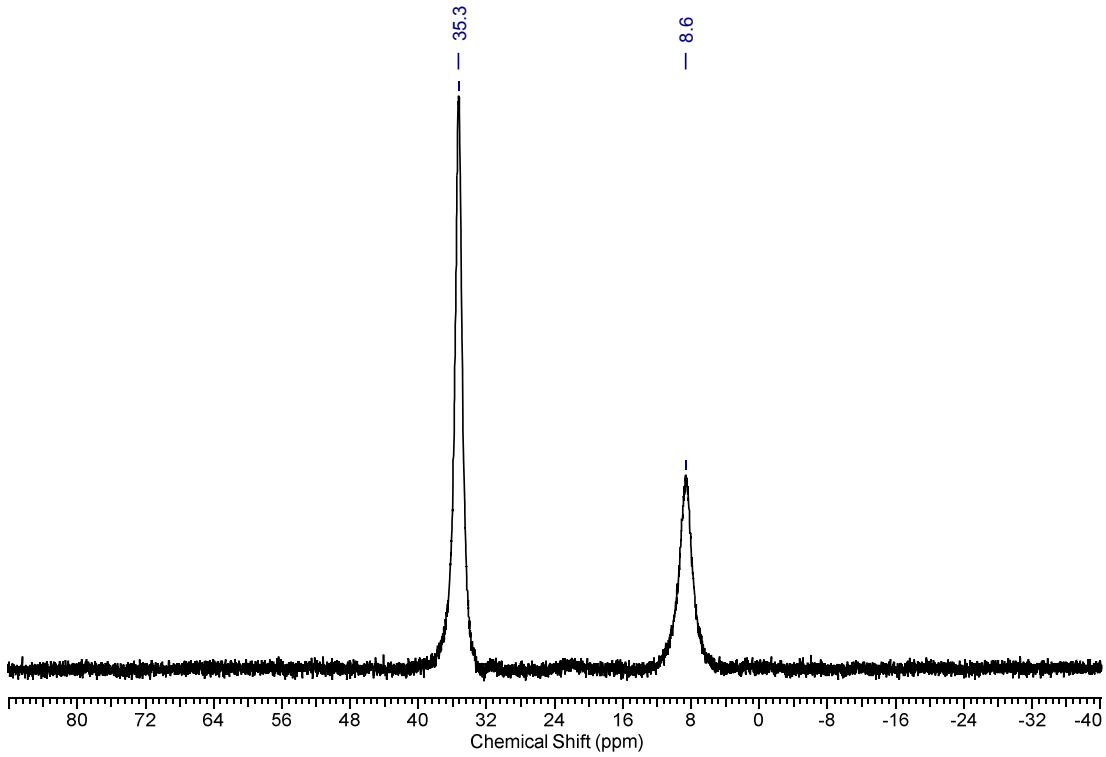

Figure S31. $^{11}B\{^1H\}$ NMR spectrum of the reaction mixture after 5 minutes at ambient temperature.

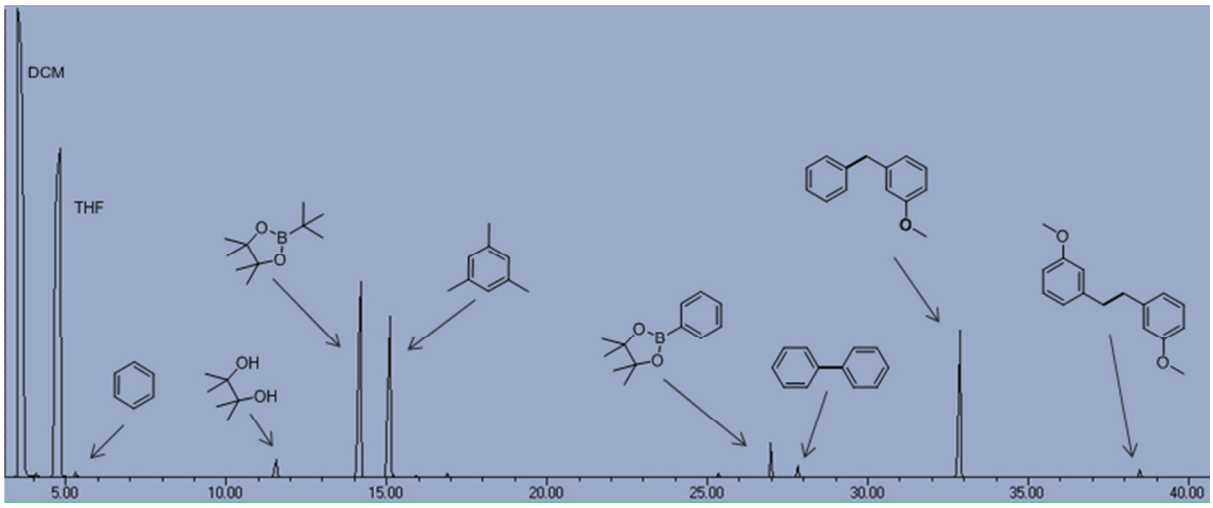

Figure S32. GC-MS trace of the quenched reaction mixture after 1h at ambient temperature. GC-MS retention times: 5.30 minutes, benzene; 11.53 minutes, pinacol; 14.15 minutes, ^{t}BuBPin; 15.06 minutes, mesitylene; 26.98 minutes, PhBPin; 27.81 minutes, biphenyl; 32.83 minutes, 1-benzyl-3-methoxybenzene; 1-benzyl-3-methoxybenzene; 38.47 minutes, 1,2-bis(3-methoxyphenyl)ethane.

11d. 9 + $MgBr_2$ (20 mol%) + 3-methoxybenzyl bromide in THF

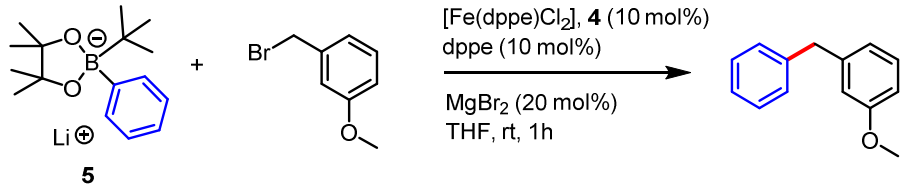

In a glovebox an oven dried J. Youngs NMR tube equipped with a DMSO-d_6 capillary insert was loaded with **5** (75.0 mg, 0.28 mmol), [Fe(dppe)Cl_2] (10.5 mg, 0.02 mmol), dppe (8.0 mg, 0.02 mmol) and $MgBr_2$ (7.4 mg, 0.04 mmol) prior to the addition of THF (1 mL). To this reaction mixture was added 3-methoxybenzyl bromide (28 µL, 0.2 mmol). The deep red reaction mixture agitated at ambient temperature for 10 minutes prior to analysis by $^{11}B\{^1H\}$ NMR spectroscopy (*Figure S33*). The $^{11}B\{^1H\}$ NMR spectra clearly indicated the presence of the expected by-product of hydrocarbyl transmetallation, ^{t}BuBPin (δ_{11B} = 35.1 ppm) and **5** (δ_{11B} = 8.4 ppm). The presence of **5** is to be expected even after the reaction has reached completion as it is present in an excess of the limiting reagent, 3-methoxybenzyl bromide. Agitation at ambient temperature was continued for 1h prior to quenching with HPLC grade dichloromethane (2 mL), the addition of mesitylene (27.8 µL, 0.2 mmol) and filtration through a small column of silica gel. Analysis by GC-MS revealed almost quantitative heterocoupling (*Figure S34*). It is noteworthy that the product distribution is almost identical between *Figure S32* and *Figure S34*.

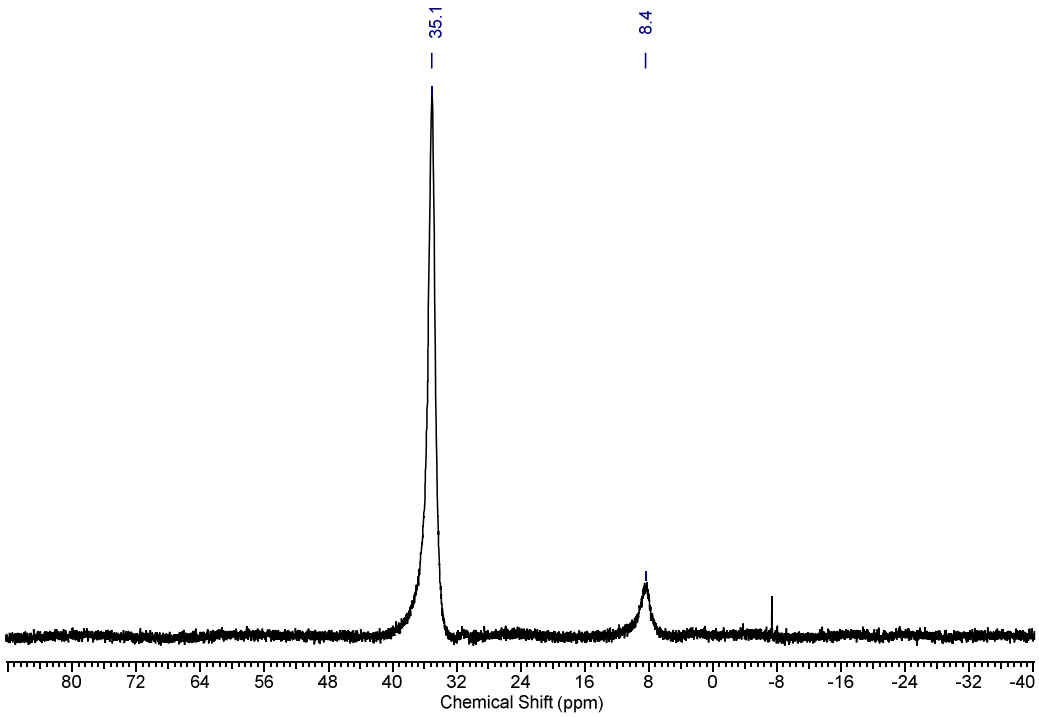

Figure S33. $^{11}B\{^1H\}$ NMR spectrum of the reaction mixture after 5 minutes at ambient temperature.

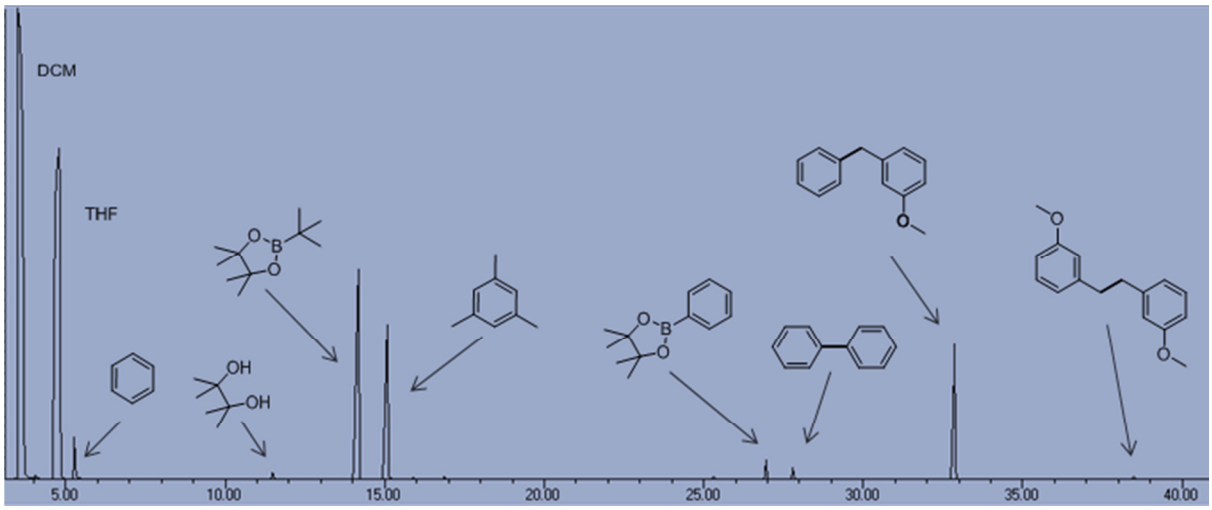

Figure S34. GC-MS trace of the quenched reaction mixture after 1h at ambient temperature. GC-MS retention times: 5.27 minutes, benzene; 11.49 minutes, pinacol; 14.13 minutes, ^{t}BuBPin; 15.07 minutes, mesitylene; 26.97 minutes, PhBPin; 27.81 minutes, biphenyl; 32.82 minutes, 1-benzyl-3-methoxybenzene; 1-benzyl-3-methoxybenzene; 38.48 minutes, 1,2-bis(3-methoxyphenyl)ethane.

11e. K[2a] + Zincate (10 mol%) + Bromocycloheptane in Toluene:

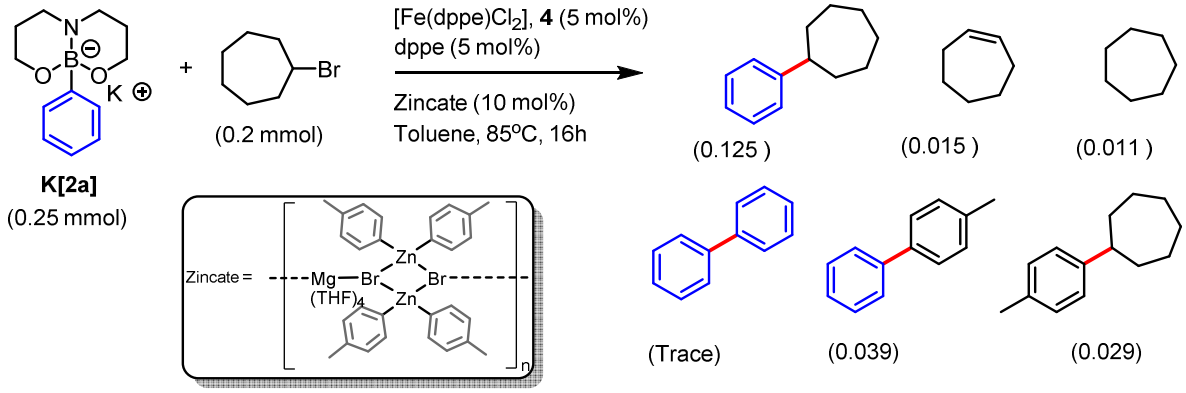

In a glovebox an oven dried J. Youngs NMR tube equipped with a DMSO-d_6 capillary insert was loaded with **K[2a]** (64.3 mg, 0.25 mmol), [Fe(dppe)Cl_2] (5.3 mg, 0.01 mmol), dppe (4.0 mg, 0.01 mmol) and toluene (1mL) prior to the addition of the zincate (0.25 M stock solution in THF) (160 µL, 0.04 mmol – equating to 10 mol% zincate and 0.08 mmol tolyl nucleophile). To this reaction mixture was added bromocycloheptane (27.7 µL, 0.2 mmol). The reaction mixture was heated at 85°C for 16h prior to quenching with HPLC grade DCM (2 mL), the addition of mesitylene (27.8 µL, 0.2 mmol), filtration through a small column of silica gel and analysis of the reaction mixture by GC-MS (*Figure S35*).

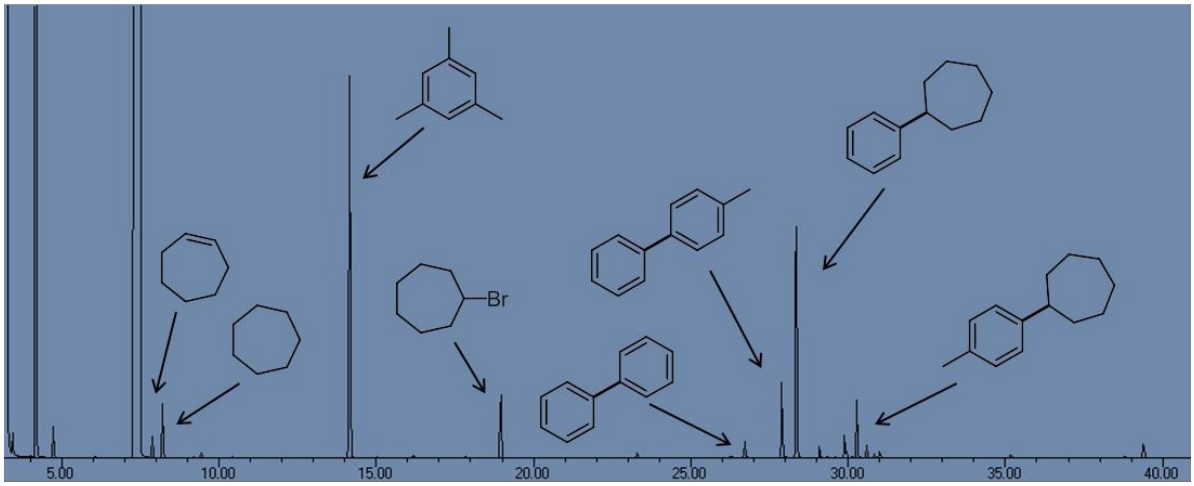

Figure S35. GC-MS trace of the quenched reaction mixture after 16h at 85°C. GC-MS retention times: 7.48 minutes, cycloheptene; 7.90 minutes, cycloheptane; 14.17 minutes, mesitylene; 18.97 minutes, bromocycloheptane; 27.89 minutes, 4-phenyltoluene; 28.35 minutes, phenylcycloheptane; 30.27 minutes, 4-methylphenylcycloheptane.

12. Boron-to-Zinc Transmetallation Studies

12a. $ZnCl_2$ (0.5 equiv.) + 2a (generated *in-situ* from KH) in THF:

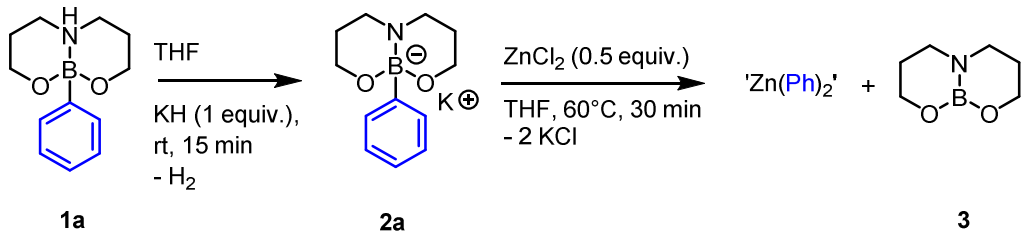

In a glovebox an oven dried J. Youngs NMR tube equipped with a DMSO-d_6 capillary insert was loaded with **1a** (40 mg, 0.183 mmol), KH (7.3 mg, 0.183 mmol) and protio-THF (0.8 mL) followed by agitation until the reaction mixture became completely homogeneous and hydrogen evolution had ceased (*ca.* 10-15 mins). After this time an $^{11}B\{^1H\}$ NMR spectrum was taken prior to the addition of anhydrous $ZnCl_2$ (12.6 mg, 0.092 mmol) in a glovebox. The reaction mixture was heated at 60°C for 30 minutes followed by $^{11}B\{^1H\}$ NMR analysis to demonstrate complete hydrocarbyl transfer from **2a** (δ_{11B} = 2.6 ppm) to afford **3** (δ_{11B} = 20.0 ppm) (*Figure S36*).

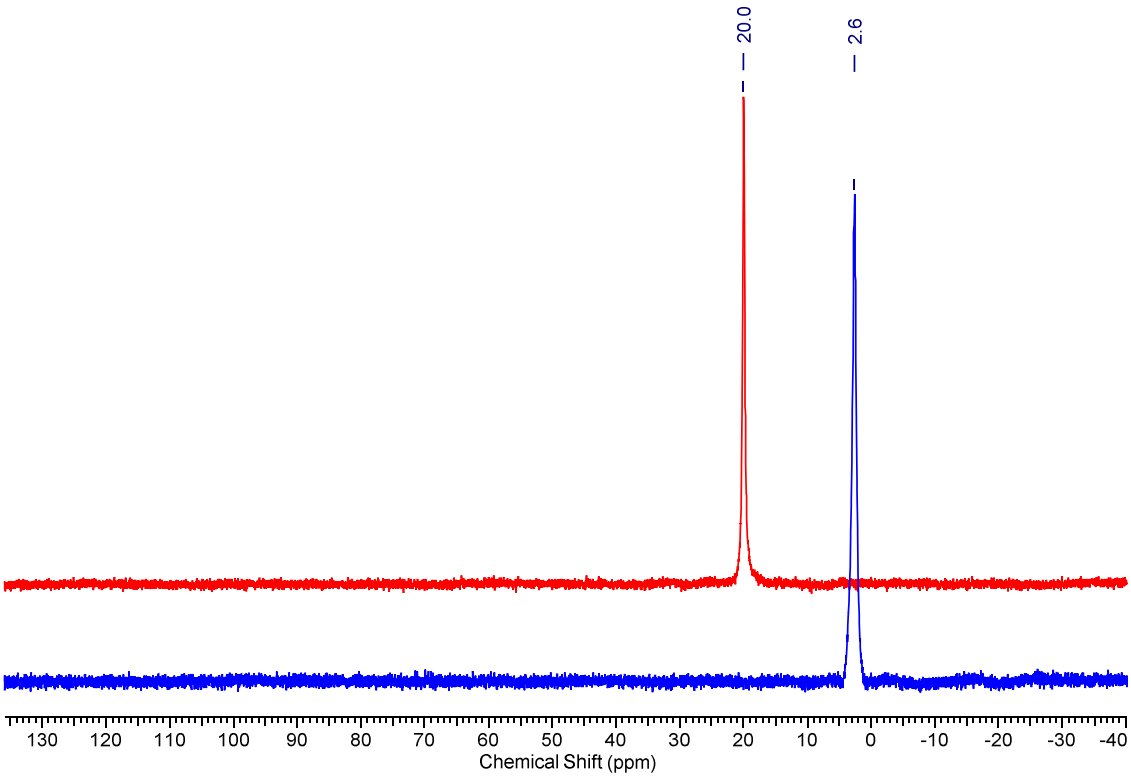

Figure S36. Collected $^{11}B\{^1H\}$ NMR spectra (baseline corrected): *In-situ* generated **2a** (*blue*); reaction mixture after 30 minutes at 60°C (*red*).

12b. $ZnCl_2$ (0.5 equiv.) + potassium phenyltrifluoroborate in THF:

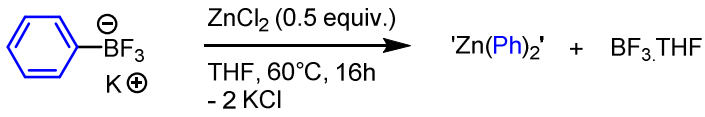

In a glovebox an oven dried J. Youngs NMR tube equipped with a DMSO-d_6 capillary insert was loaded with potassium phenyltrifluoroborate (36.8 mg, 0.2 mmol) and $ZnCl_2$ (13.6 mg, 0.1 mmol) *protio*-THF (0.8 mL) followed by heating at 60°C for 16h. Analysis by $^{11}B\{^1H\}$ NMR demonstrated the presence of the a minor amount of BF_3.THF adduct (δ_{11B} = 3.4 ppm), however, the poor solubility of potassium phenyltrifluoroborate in THF precludes its observation. The generation of BF_3.THF is indicative of a transmetallation event but the degree of hydrocarbyl transmetallation is low given the poor solubility of potassium phenyltrifluoroborate in THF (*Figure S37*). Significant solid was still observed after 16 h and dissolution of the entire sample in d_6-DMSO (in which both BF_3 and Ph-BF_3 are soluble) confirmed the major product to be $[PhBF_3]^-$.

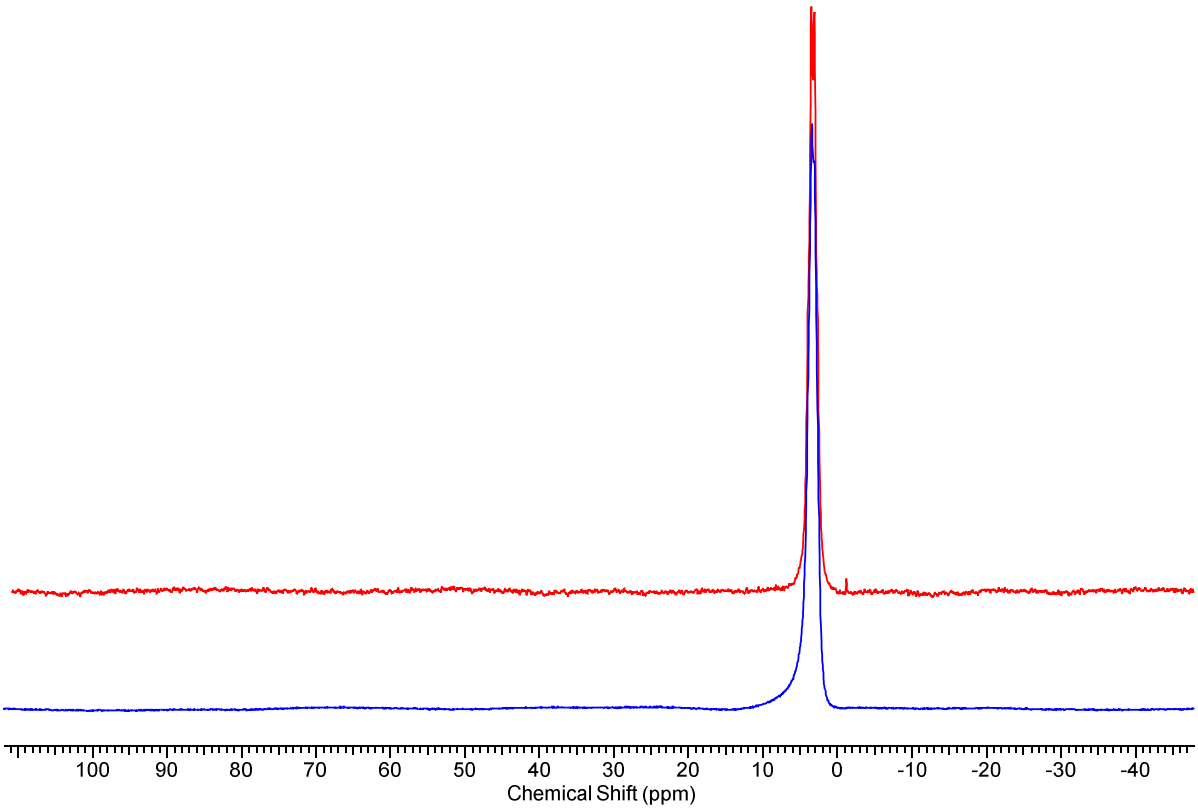

Figure S37. Collected $^{11}B\{^1H\}$ NMR spectra (baseline corrected) of: potassium phenyltrifluoroborate (blue); and the reaction mixture after 16h at 60°C in d_6-DMSO.

12c. $ZnCl_2$ (0.5 equiv.) + triolborate in THF:

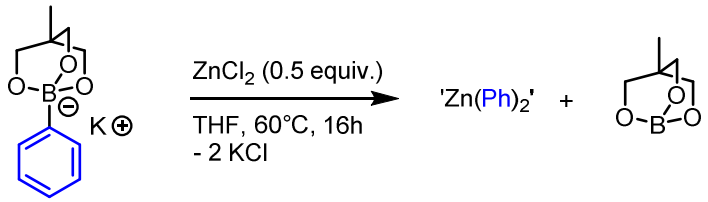

In a glovebox an oven dried J. Youngs NMR tube equipped with a DMSO-d_6 capillary insert was loaded with phenyltriolborate (44.8 mg, 0.2 mmol) and $ZnCl_2$ (13.6 mg, 0.1 mmol) *protio*-THF (0.8 mL) followed by heating at 60°C for 16h. Analysis by $^{11}B\{^1H\}$ NMR demonstrated the presence of the triolborate (δ_{11B} = 26.6 ppm), however, the poor solubility of the 3-coordinate borane by-product of transmetallation in THF precludes its observation. The persistence of the triolborate resonance (δ_{11B} = 26.6 ppm) is indicative of at least incomplete hydrocarbyl transmetallation under the reaction conditions (*Figure S38*). After 16 hours the reaction mixture was dried and analysed in d_6-DMSO in which it is fully homogenous, which revealed that no transmetallation had occurred.

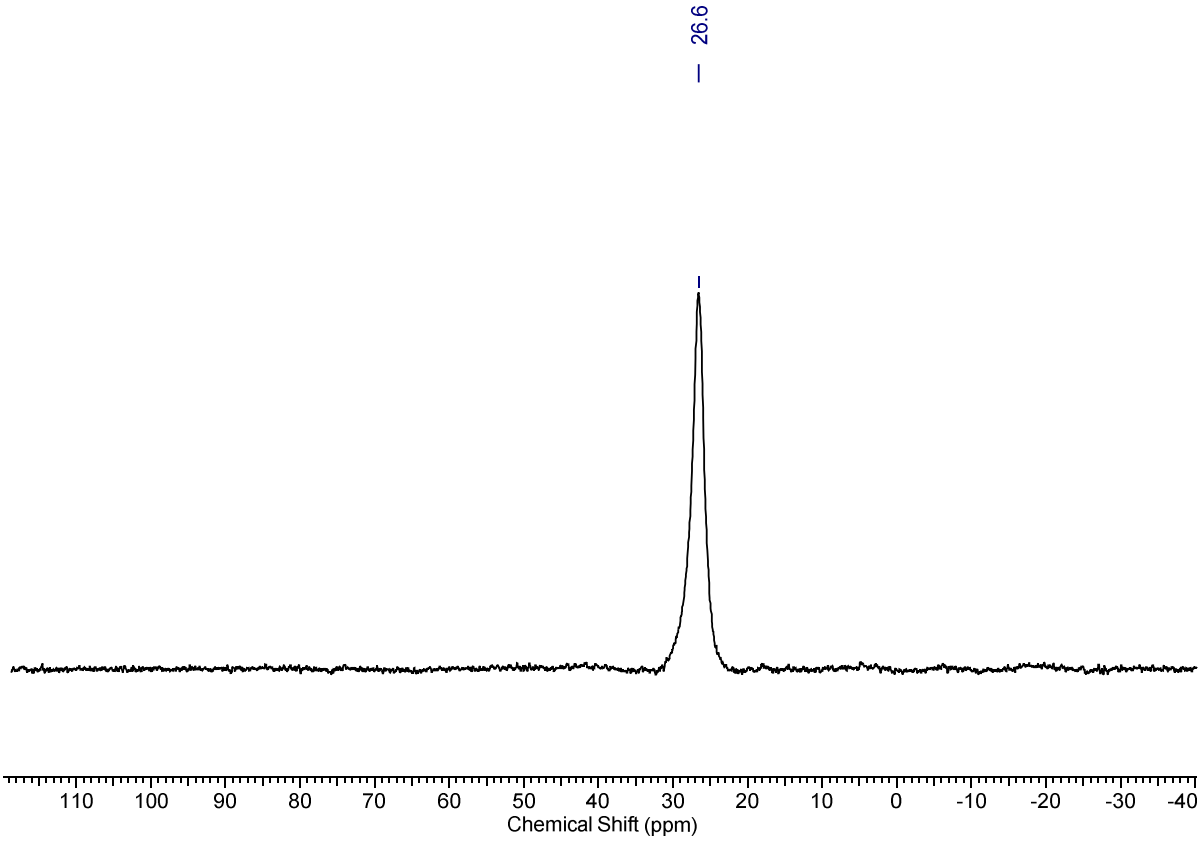

Figure S38. $^{11}B\{^1H\}$ NMR spectra (baseline corrected) of the reaction mixture after 16h at 60°C.

13. Boron-to-Magnesium Transmetallation Studies:

13a. $MgBr_2$ (0.5 equiv.) + 2a (generated *in-situ* from KH) in THF:

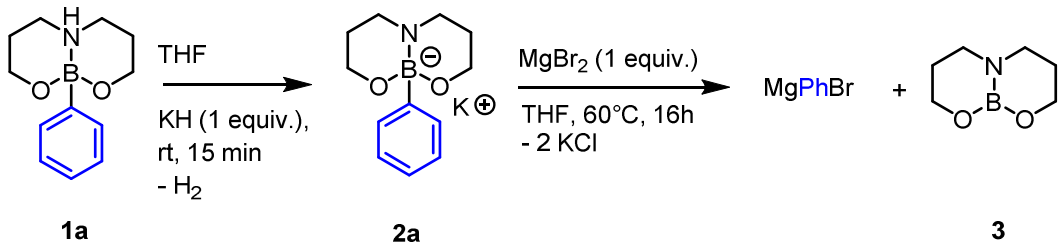

In a glovebox an oven dried J. Youngs NMR tube equipped with a DMSO-d_6 capillary insert was loaded with **1a** (40 mg, 0.183 mmol), KH (7.3 mg, 0.183 mmol) and protio-THF (0.8 mL) followed by agitation until the reaction mixture became completely homogeneous and hydrogen evolution had ceased (*ca*. 10-15 mins). After this time an $^{11}B\{^1H\}$ NMR was taken prior to the addition of anhydrous $MgBr_2$ (17 mg, 0.092 mmol) in a glovebox. Heating the reaction mixture at 60°C for 10 minutes afforded no change in $^{11}B\{^1H\}$ NMR, with no evidence of any of the 3-coordinate by-product of aryl transfer, **3** (20.0 ppm). Heating at 60°C for a further 16h afforded no evidence of transmetallation, with only **2a** (2.7 ppm) observed by $^{11}B\{^1H\}$ NMR spectroscopy (*Figure S39*).

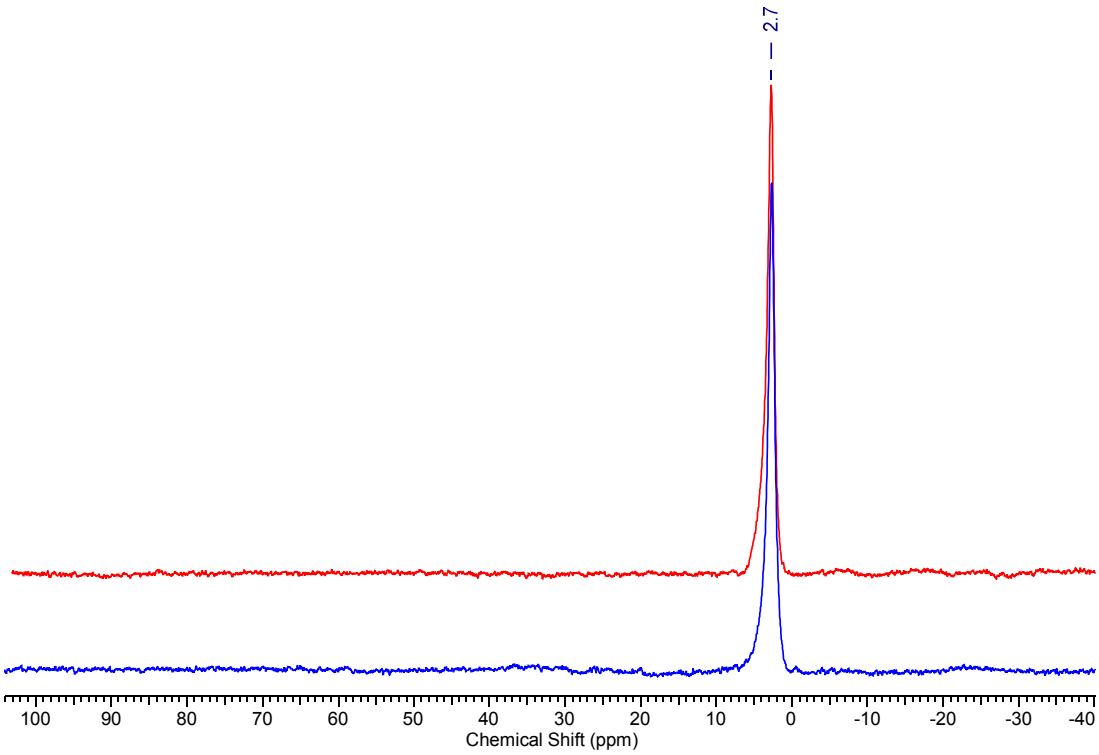

Figure S39. Collected $^{11}B\{^1H\}$ NMR spectra (baseline corrected): 10 minutes at 60°C (blue); 16h at 60°C (red).

14. Crystallographic Data

Data for compounds **1a**, K[**2a**] and **4** were recorded on an Agilent Supernova diffractometer, with Mo Kα radiation (mirror monochromator, λ =0.7107). Data for **1b** was recorded on an Oxford Xcalibur Sapphire2 diffractometer, with Mo Kα radiation (graphite monochromator, λ=0.71073). The CrysAlisPro[11] software package was used for data collection, cell refinement and data reduction. The CrysAlisPro software package was also used for empirical absorption corrections, which were applied using spherical harmonics, implemented in SCALE3 ABSPACK scaling algorithm. Structures were solved using direct methods and refined against F^2 using the OLEX2[12] software package. Non-hydrogen atoms were refined anisotropically. Hydrogen atoms were all located in a difference map and repositioned geometrically. The data obtained for K[**2a**] was of insufficient quality, however the connectivity map obtained confirms its assignment.

Crystallographic data for **1a**, **1b** and **4** have been deposited with the Cambridge Crystallographic Data Center under the references: 1010524, 1010526 and 1058782. These data can be obtained free of charge from The Cambridge Crystallographic Data Centre (CCDC) *via* www.ccdc.cam.ac.uk/data _request/cif.

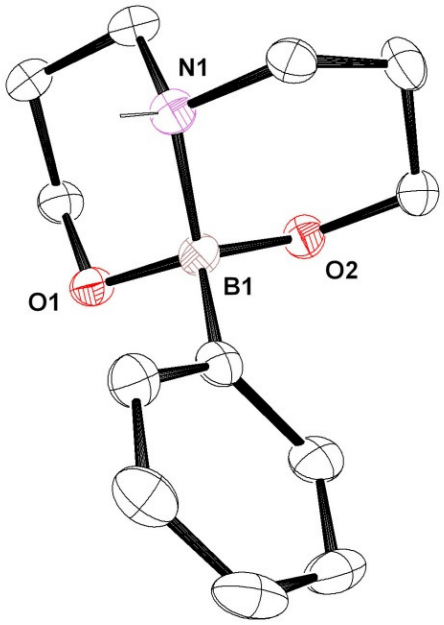

Figure S40. ORTEP[13] representation of **1a** at 50% the probability level with most hydrogen atoms omitted for clarity.

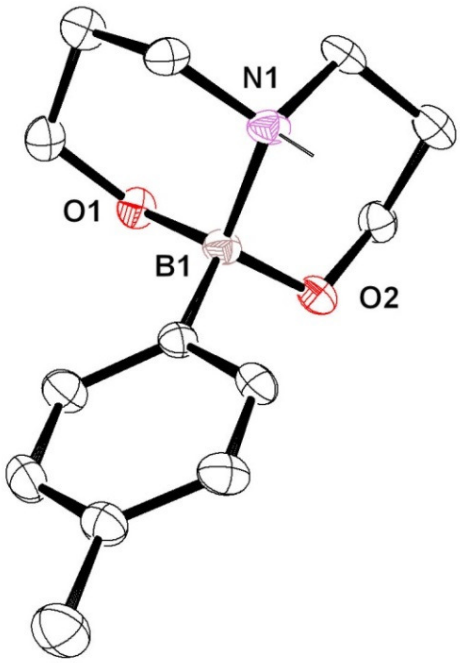

Figure S41. ORTEP[13] representation of **1b** at 50% the probability level with most hydrogen atoms omitted for clarity.

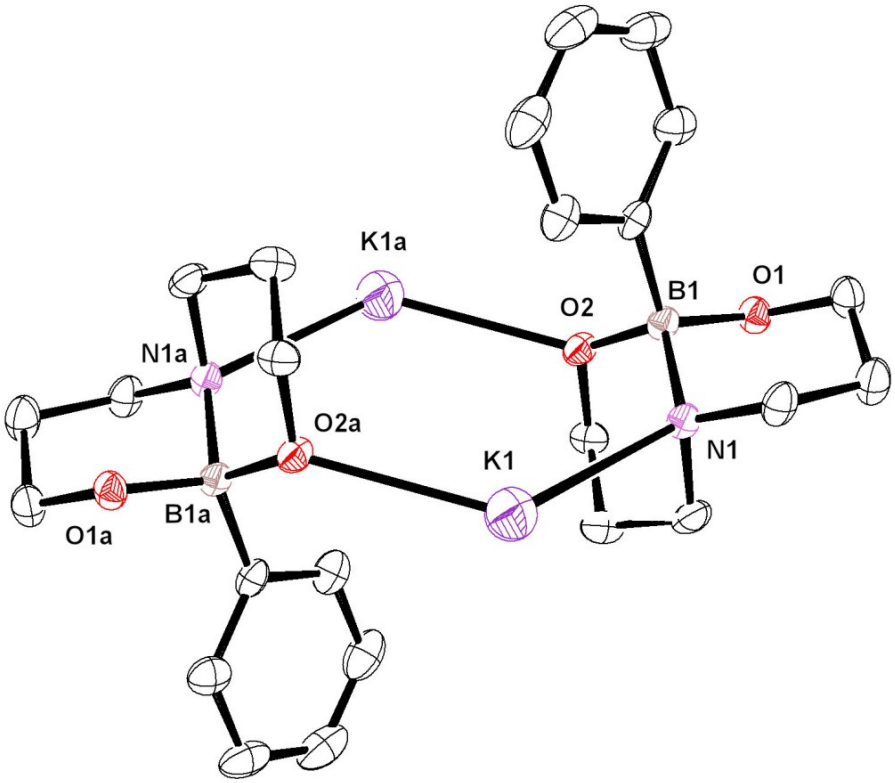

Figure S42. ORTEP[13] representation of part of the extended solid state structure of K[**2a**] at 50% the probability level with all hydrogen atoms omitted for clarity.

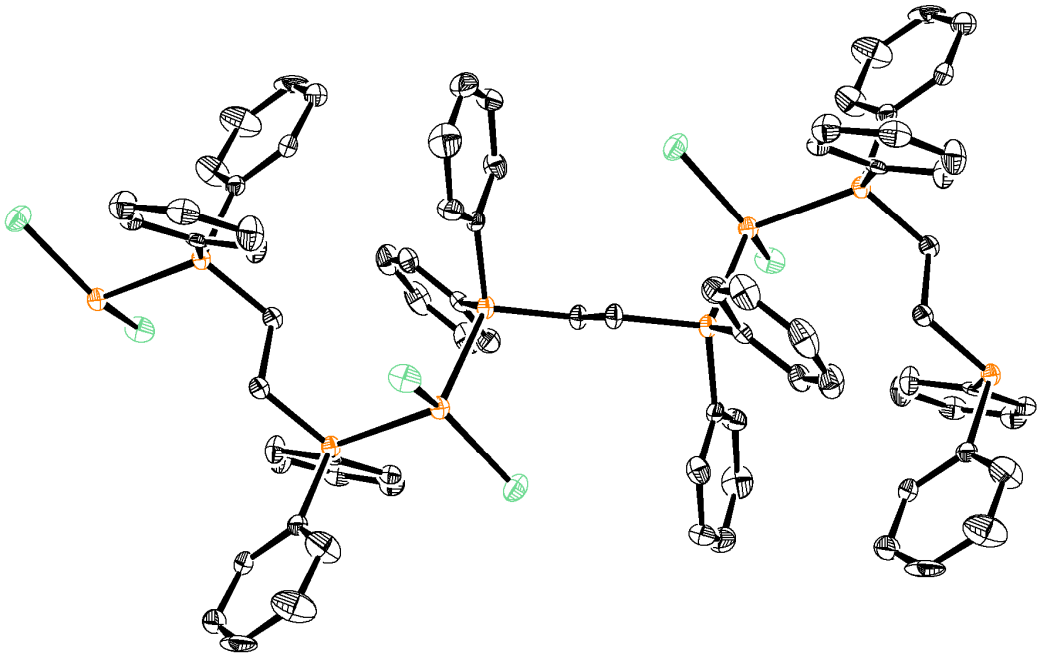

Figure S43. ORTEP[13] representation of polymeric **4** at 50% the probability level with all hydrogen atoms omitted for clarity.

Table S3. Crystal Structure Refinement Data for Compounds **1a**, **1b** and **4**

	1a	**1b**	**4**
Empirical Formula	$C_{12}H_{18}BNO_2.H_2O$	$C_{13}H_{20}B_1N_1O_2$	$C_{26}H_{24}Cl_2FeP_2$
Fw/g mol^{-1}	237.12	233.11	525.18
Cryst syst, space Group	Monoclinic, $P2_1/n$	Monoclinic, C2/c	Monoclinic, $P2_1/n$
a/Å	9.7171(19)	18.416(4)	12.9849(6)
b/Å	11.890(2)	9.961(2)	11.4495(7)
c/Å	11.565(2)	13.900(3)	16.7344(8)
α/deg	90	90	90
β/deg	113.84(3)	91.41(3)	100.206(4)
γ/deg	90	90	90
Vol/Å^3	1222.2(5)	2549.0(9)	2448.5(2)
Z, calc density (Mg m^{-3})	4, 1.2885	8, 1.215	4, 1.4245
abs coeff (mm^{-1})	0.090	0.079	0.977
F(000)	512.0	1008.0	1083.7
cryst, colour	Block, colourless	Block, colourless	Block, colourless
cryst dimens /mm^3	0.3 × 0.3 × 0.2	0.2 × 0.2 × 0.1	0.3 x 0.2 x 0.2
θ range (deg)	8.24 to 50.68	8.184 to 50.696	6.1 to 57.98
no. of reflns collected / unique	4143 / 2206	8224 / 2322	9720 / 5409
R_{int}	0.0507	0.0710	0.0411
no. of data/restraints/ parameters	2206 /0 / 156	2322 / 0 / 159	5409 /0 / 279
final R indicies [F^2 < 2σ(F^2)]:	0.0686, 0.1176	0.0601, 0.1311	0.0532, 0.0899
R indicies (all data) : R1, wR2	0.1208, 0.1539	0.1068, 0.1519	0.0796, 0.1012
Largest diff peak and hole/e Å^{-3}	0.46 / -0.45	0.28 / -0.20	1.14 / -1.12

15. VT-NMR Measurements of 1a (in DMSO-d_6)

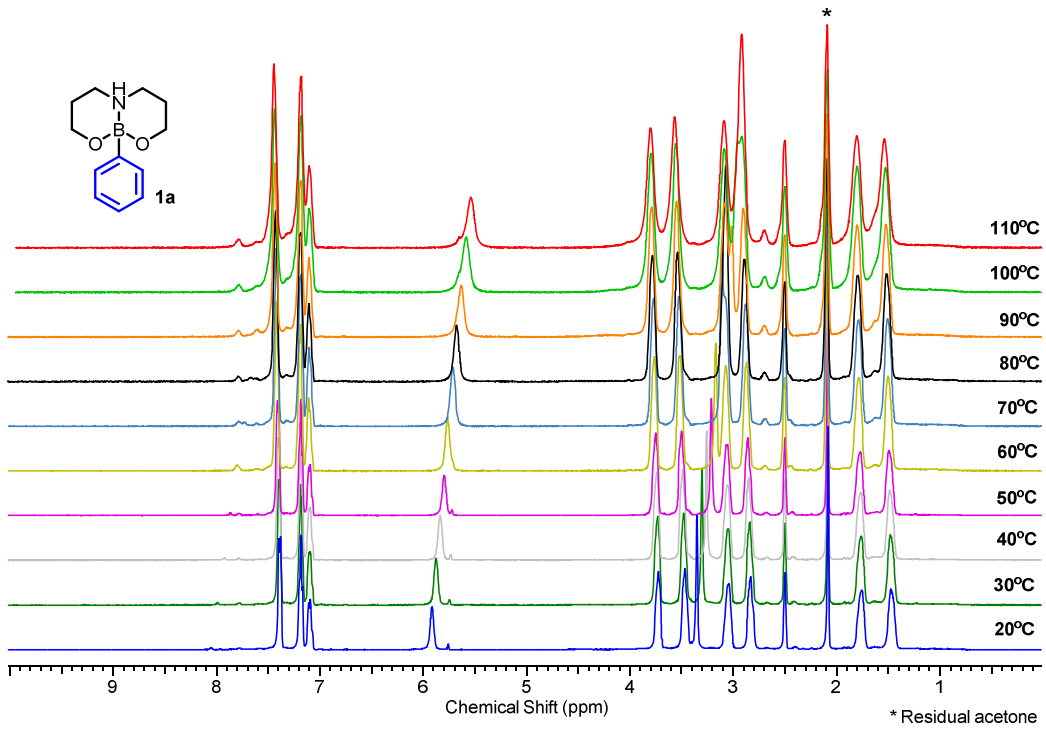

Figure S44. Collected ^{1}H NMR spectra of **1a** in DMSO-d_6 from 20-110°C.

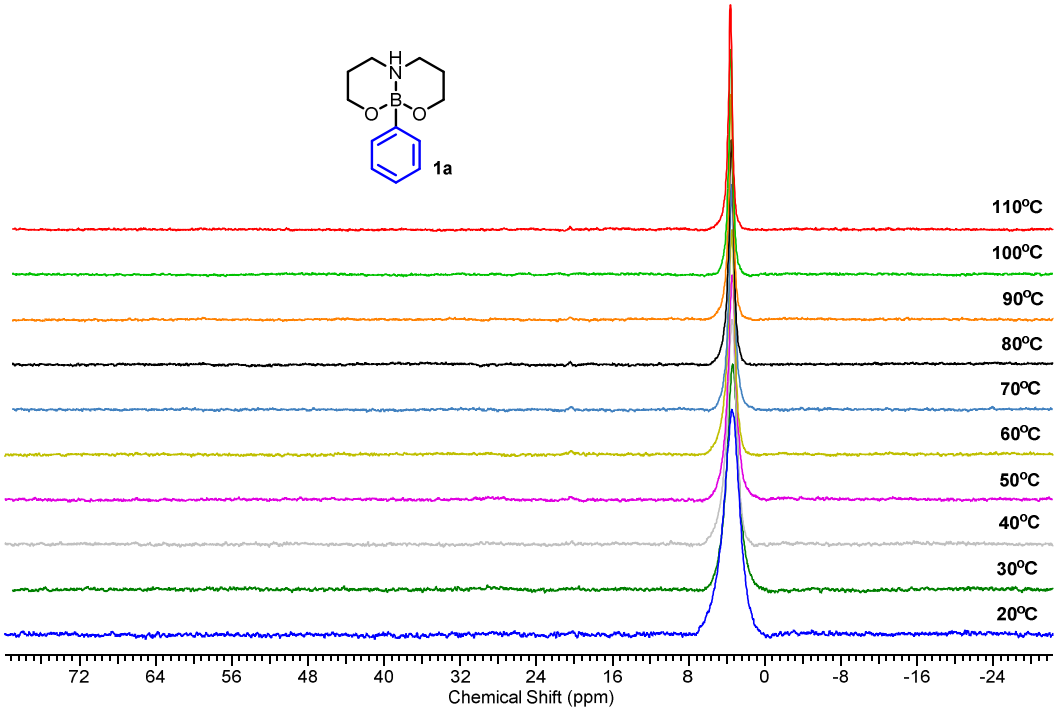

Figure S45. Collected ^{11}B{^{1}H} NMR spectra of **1a** in DMSO-d_6 from 20-110°C.

16. References

[1] Granier, C.; Guilard, R. *Tetrahedron*, 1995, *51*, 1197-1208.

[2] Evans, D. J.; Hitchcock, P. B.; Leigh, G. J.; Nicholson, B. K.; Niedwieski, A. C.; Nunes, F. S.; Soares, J. F. *Inorg. Chim. Acta*. **2001**, *319*, 147-158.

[3] Bedford, R. B.; Carter, E.; Cosgwell, P. M.; Harvey, J. N.; Gower, N. J.; Haddow, M. F.; Harvey, J. N.; Murphy, D. M.; Neeve, E. C.; Nunn, J. *Angew. Chem. Int. Ed*., **2013**, 52, 1285-1288.

[4] Adams, C. J.; Bedford, R. B.; Carter, E.; Gower, N. J.; Haddow, M. F.; Harvey, J. N.; Huwe, M.; Angeles-Carter, M.; Mansell, S. M.; Mendoza, C.; Murphy, D. M.; Neeve, E. C.; Nunn, J. *J. Am. Chem. Soc*. **2012**, *134*, 10333-10336.

[5] Csuk, R.; Hönig, H.; Romanin, C. *Monatshefte für Chemie* **1982**, 113, 1025-1035.

[6] Hatakeyama, T.; Hashimoto, T.; Kondo, Y.; Fujiwara, Y.; Seike, H.; Takaya, H.; Tamada, Y.; Ono, T.; Nakamura, M. *J. Am. Chem. Soc*. **2010**, *132*, 10674-10676.

[7] Clark, E. R.; Del Grosso, A.; Ingleson, M. J.; *Chem. Eur. J.* **2013***, 19,* 2462-2466.

[8] Gaussian 09, Revision C1, Frisch, M. J.; Trucks, G. W.; Schlegel, H. B.; Scuseria, G. E.; Robb, M. A.; Cheeseman, J. R.; Scalmani, G.; Barone, V.; Mennucci, B.; Petersson, G. A.; Nakatsuji, H.; Caricato, M.; Li, X.; Hratchian, H. P.; Izmaylov, A. F.; Bloino, J.; Zheng, G.; Sonnenberg, J. L.; Hada, M.; Ehara, M.; Toyota, K.; Fukuda, R.; Hasegawa, J.; Ishida, M.; Nakajima, T.; Honda, Y.; Kitao, O.; Nakai, H.; Vreven, T.; Montgomery, Jr., J. A.; Peralta, J. E.; Ogliaro, F.; Bearpark, M.; Heyd, J. J.; Brothers, E.; Kudin, K. N.; Staroverov, V. N.; Kobayashi, R.; Normand, J.; Raghavachari, K.; Rendell, A.; Burant, J. C.; Iyengar, S. S.; Tomasi, J.; Cossi, M.; Rega, N.; Millam, J. M.; Klene, M.; Knox, J. E.; Cross, J. B.; Bakken, V.; Adamo, C.; Jaramillo, J.; Gomperts, R.; Stratmann, R. E.; Yazyev, O.; Austin, A. J.; Cammi, R.; Pomelli, C.; Ochterski, J. W.; Martin, R. L.; Morokuma, K.; Zakrzewski, V. G.; Voth, G. A.; Salvador, P.; Dannenberg, J. J.; Dapprich, S.; Daniels, A. D.; Farkas, Ö.; Foresman, J. B.; Ortiz, J. V.; Cioslowski, J.; Fox, D. J. Gaussian, Inc., Wallingford CT, **2009**.

[9] [10] http://comp.chem.umn.edu/info/DFT.htm

[10] Dunsford, J. J.; Cade, I. A.; Fillman, K. L.; Neidig, M. L.; Ingleson M. J. *Organometallics* **2014**, *33*, 370-377.

[11] CrysAlisPro, Agilent Technologies, Version 1.171.35.19 (release 27-10-2011 CrysAlis171 .NET) (compiled Oct 27 2011,15:02:11)

[12] Olex2.refine (L.J. Bourhis, O.V. Dolomanov, R.J. Gildea, J.A.K. Howard, H. Puschmann, in preparation, 2011).

[13] L. J. Farrugia, *J. Appl. Cryst*. **2012**, *45*, 849-854.

17. NMR Data

3,3'-azanediyl*bis*(propan-1-ol) (400 MHz, $CDCl_3$, 298K):

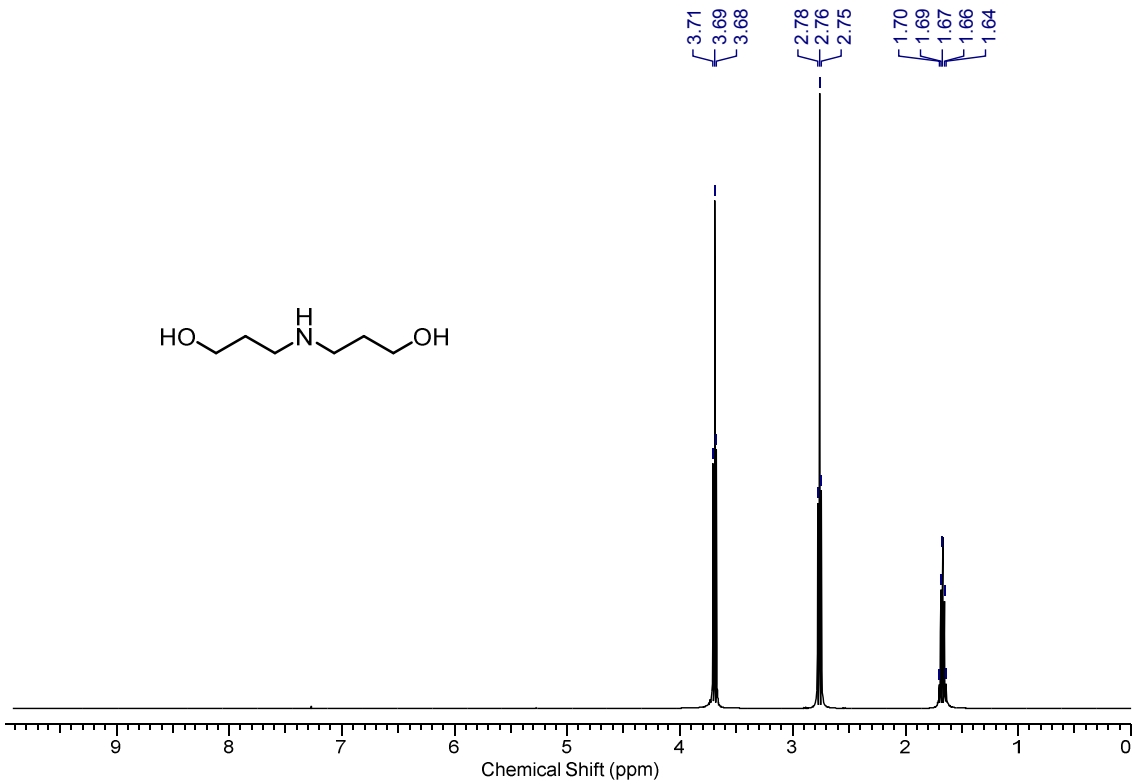

3,3'-azanediyl*bis*(propan-1-ol) (100 MHz, $CDCl_3$, 298K):

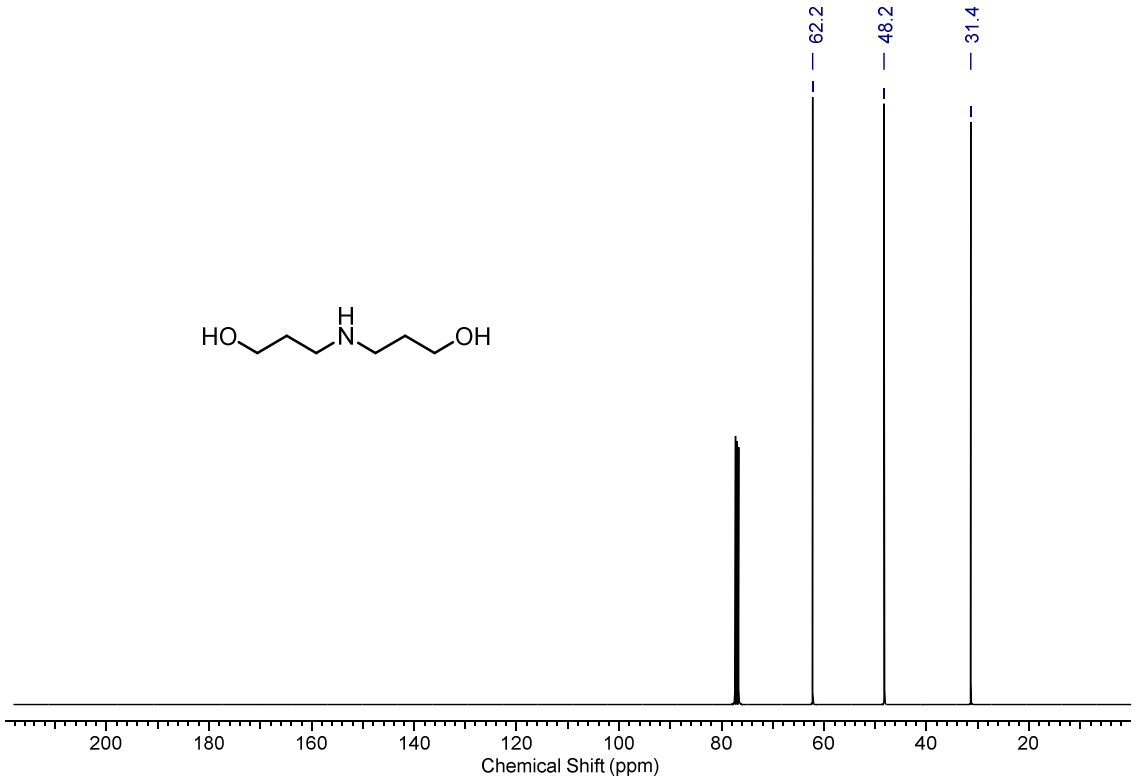

1a. (1H NMR, 400 MHz, DMSO-d_6, 298K):

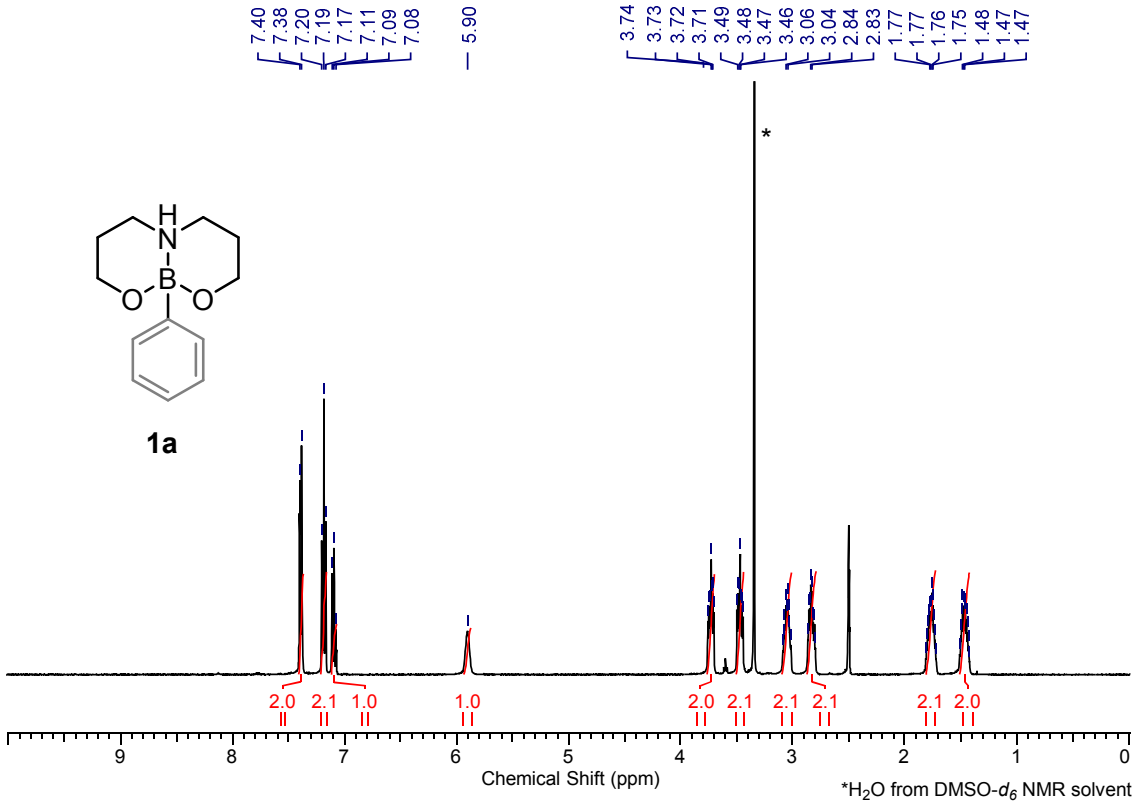

1a. (^{13}C{^{1}H} NMR, 100 MHz, DMSO-d_6, 298K):

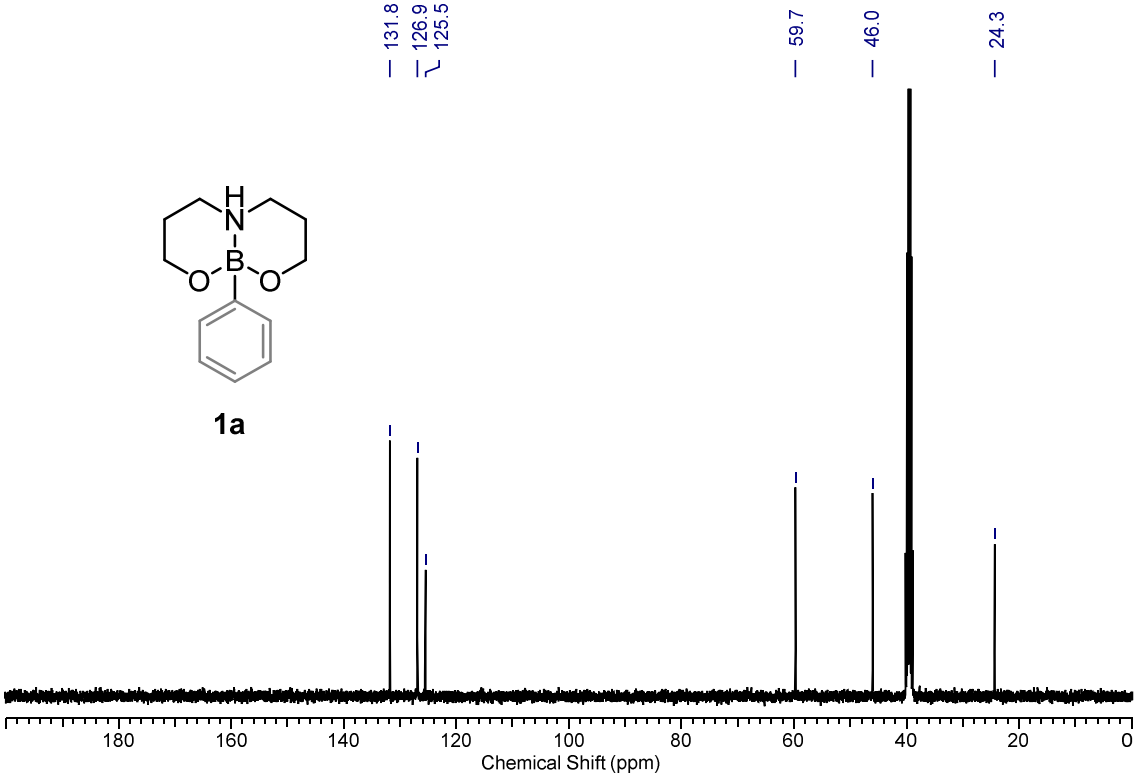

1a. ($^{11}B\{^1H\}$ NMR (baseline corrected), 128.4 MHz, DMSO-d_6, 298K):

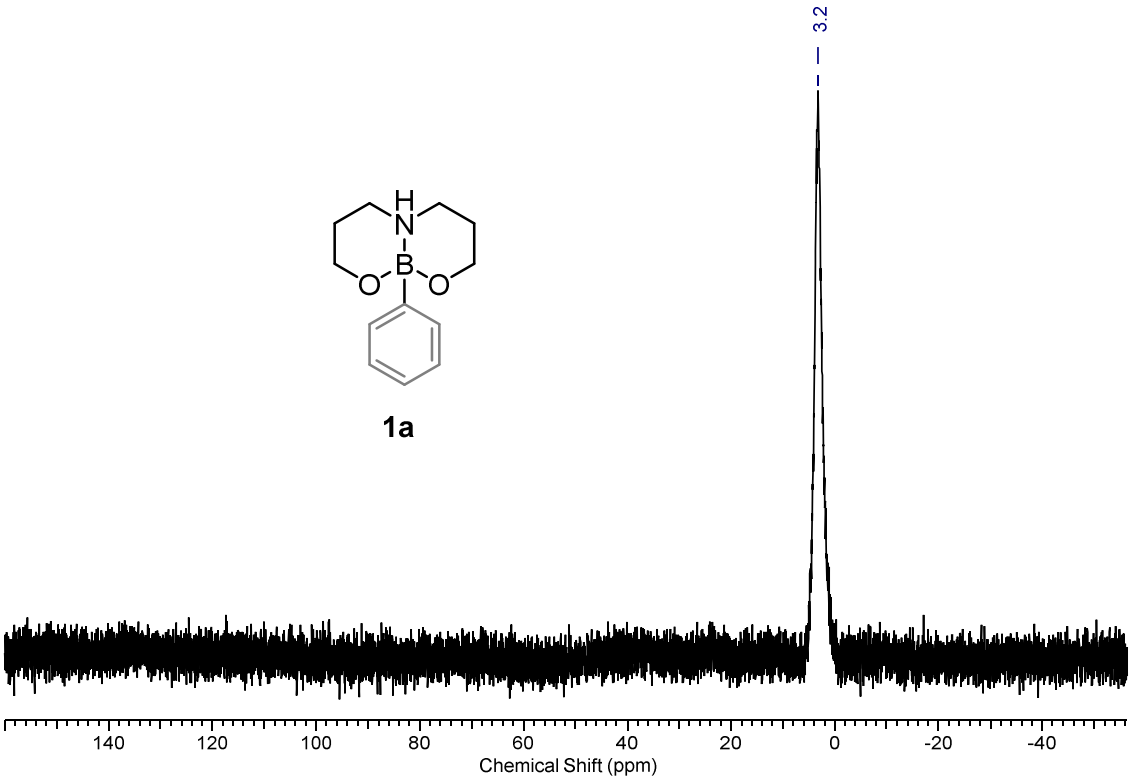

1b. (^1H NMR, 400 MHz, DMSO-d_6, 298K):

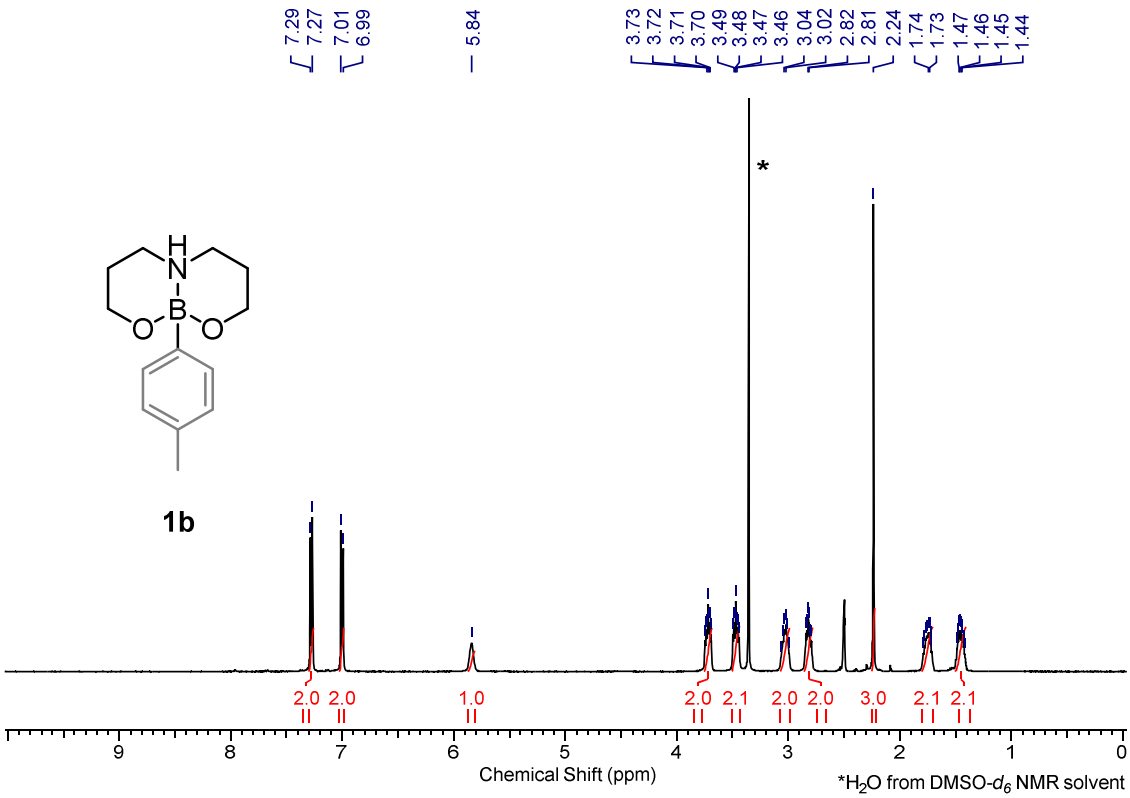

1b. ($^{13}C\{^{1}H\}$ NMR, 100 MHz, DMSO-d_6, 298K):

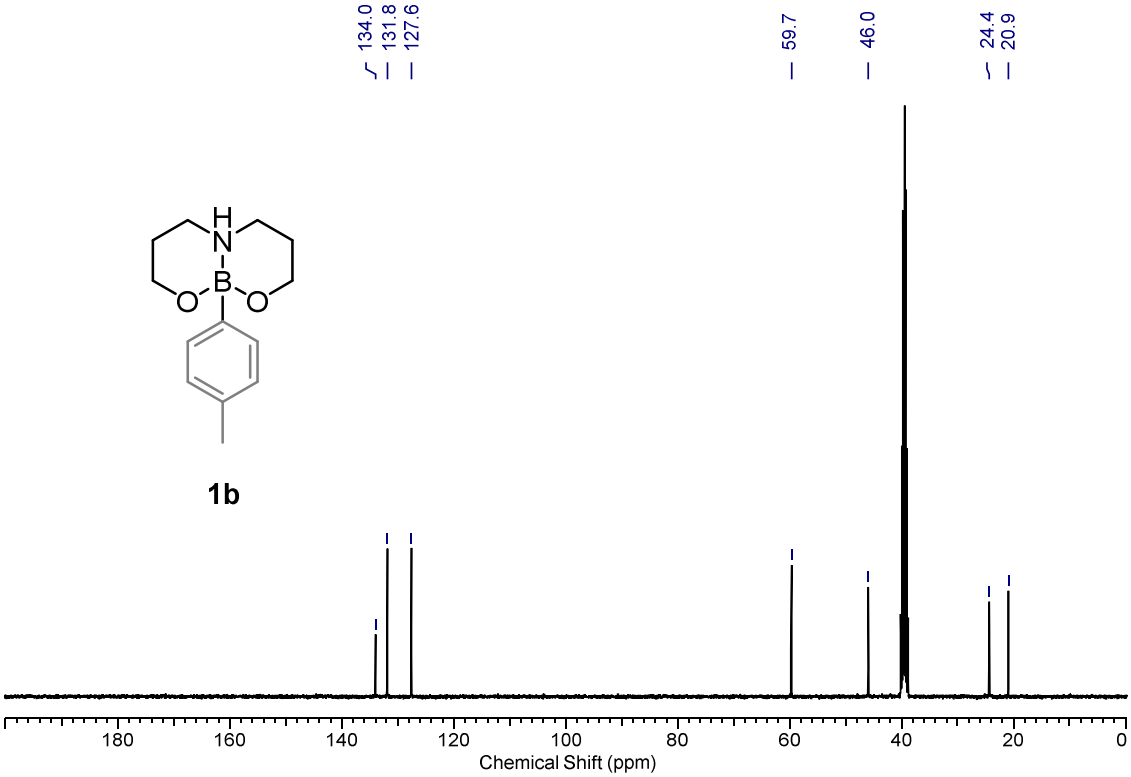

1b. ($^{11}B\{^{1}H\}$ NMR (baseline corrected), 128.4 MHz, DMSO-d_6, 298K):

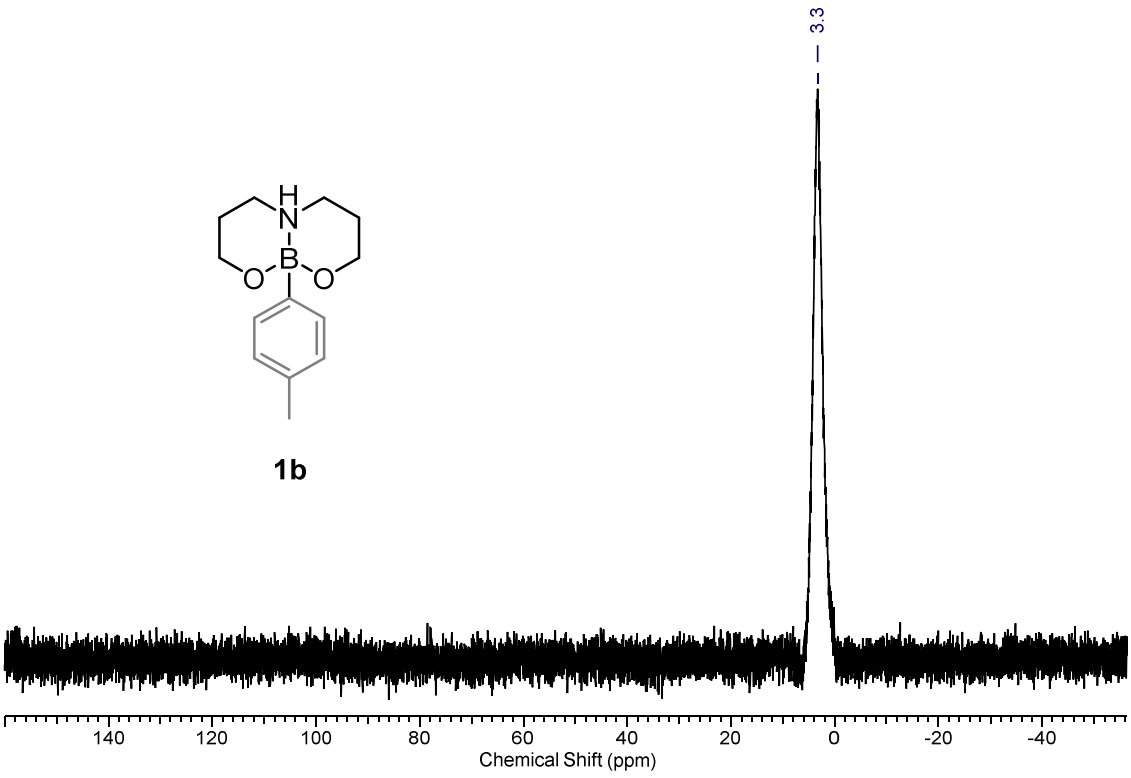

1c. (^{1}H NMR, 400 MHz, DMSO-d_6, 298K):

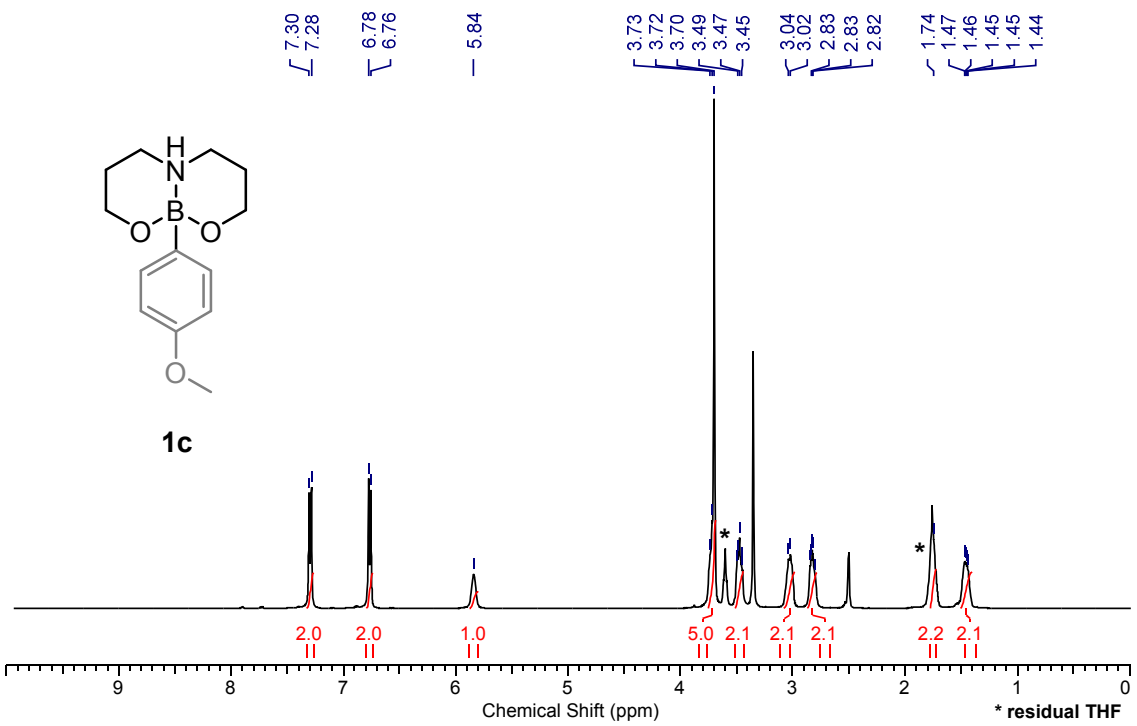

1c. (^{13}C{^{1}H}{ NMR, 100 MHz, DMSO-d_6, 298K):

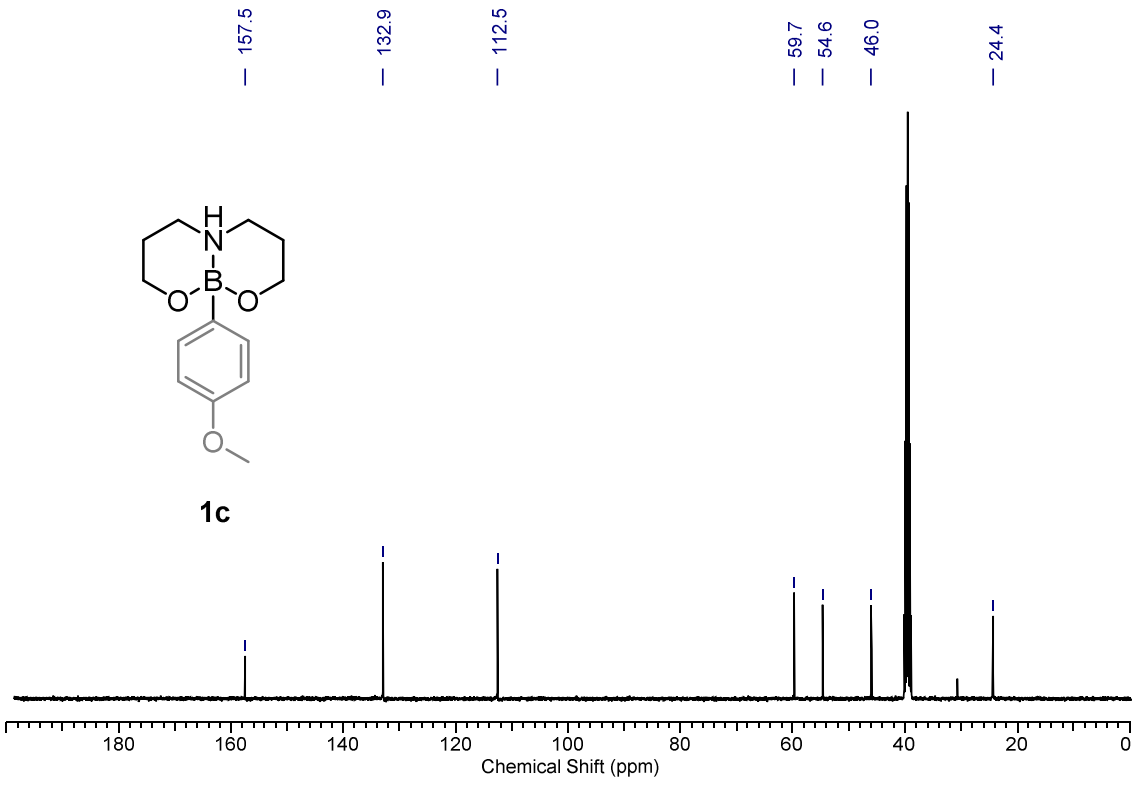

1c. ($^{11}B\{^1H\}$ NMR (baseline corrected), 128.4 MHz, DMSO-d_6, 298K):

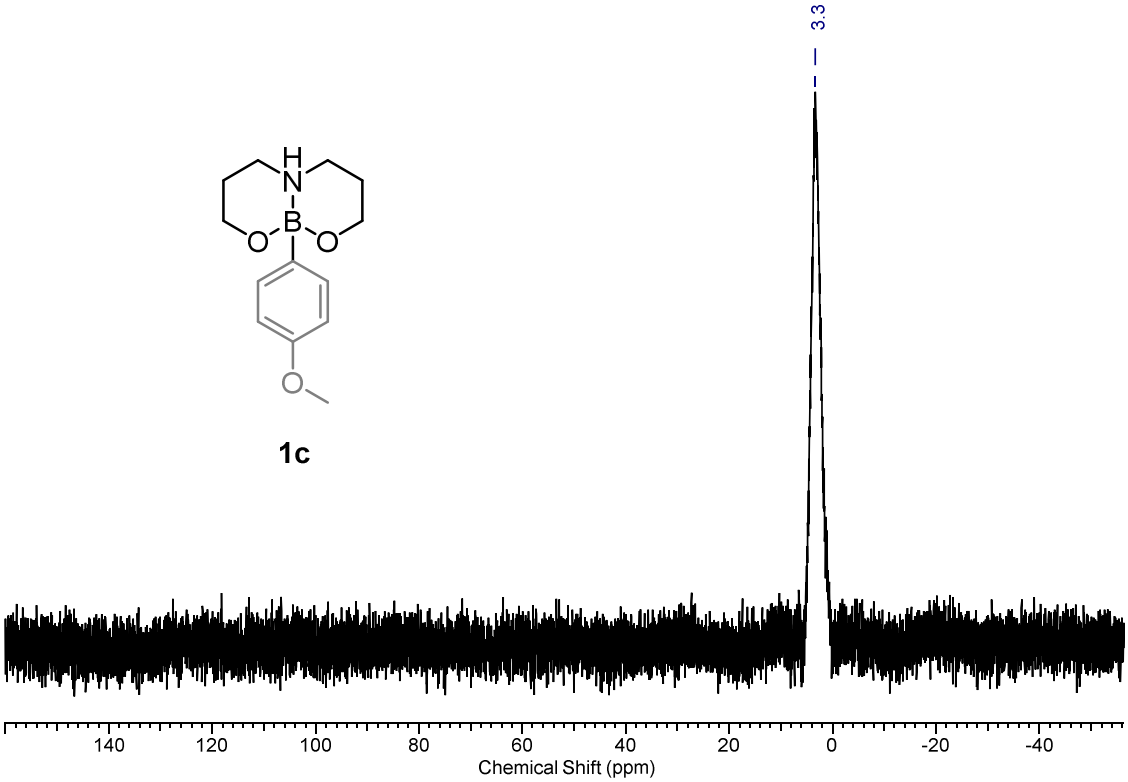

1d. (^1H NMR, 400 MHz, DMSO-d_6, 298K):

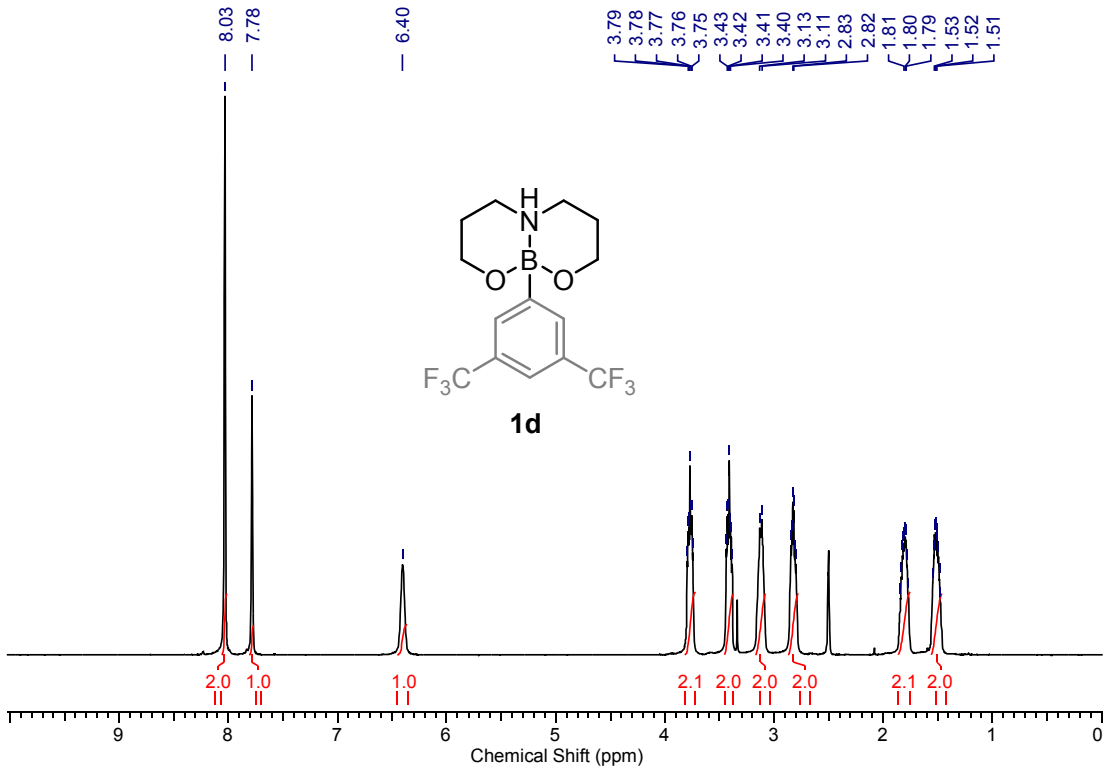

1d. ($^{13}C\{^{1}H\}$ NMR, 100 MHz, DMSO-d_6, 298K):

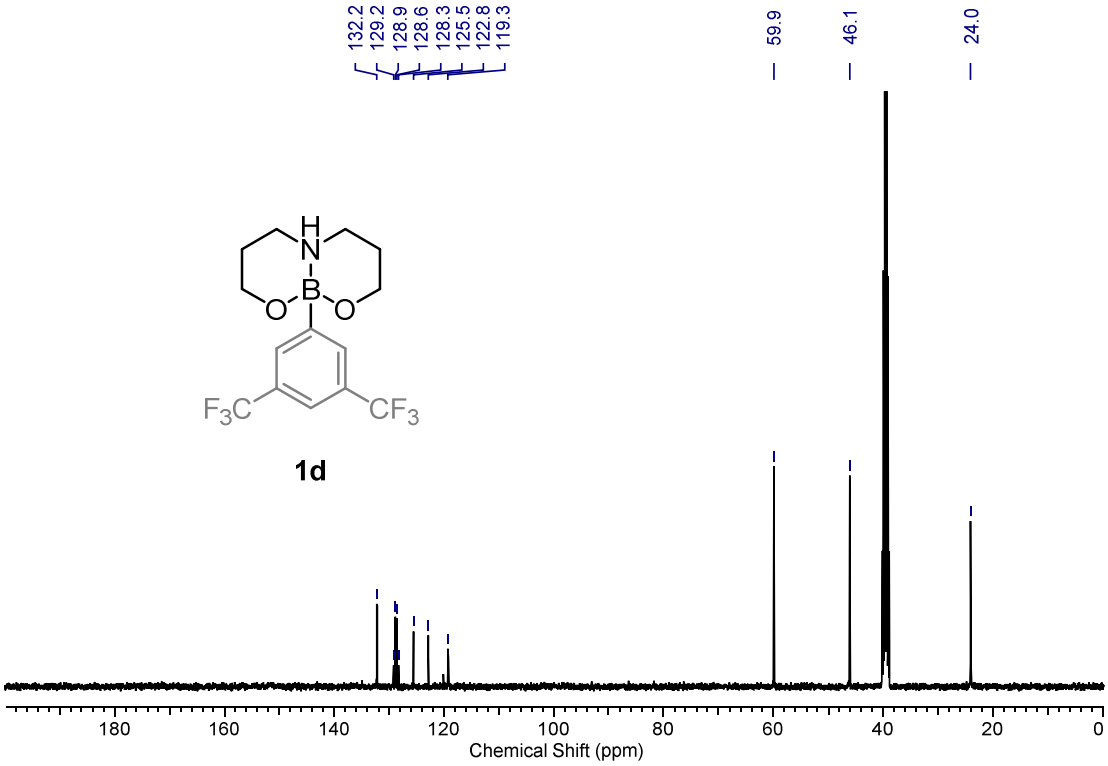

1d. ($^{11}B\{^{1}H\}$ NMR (baseline corrected), 128.4 MHz, DMSO-d_6, 298K):

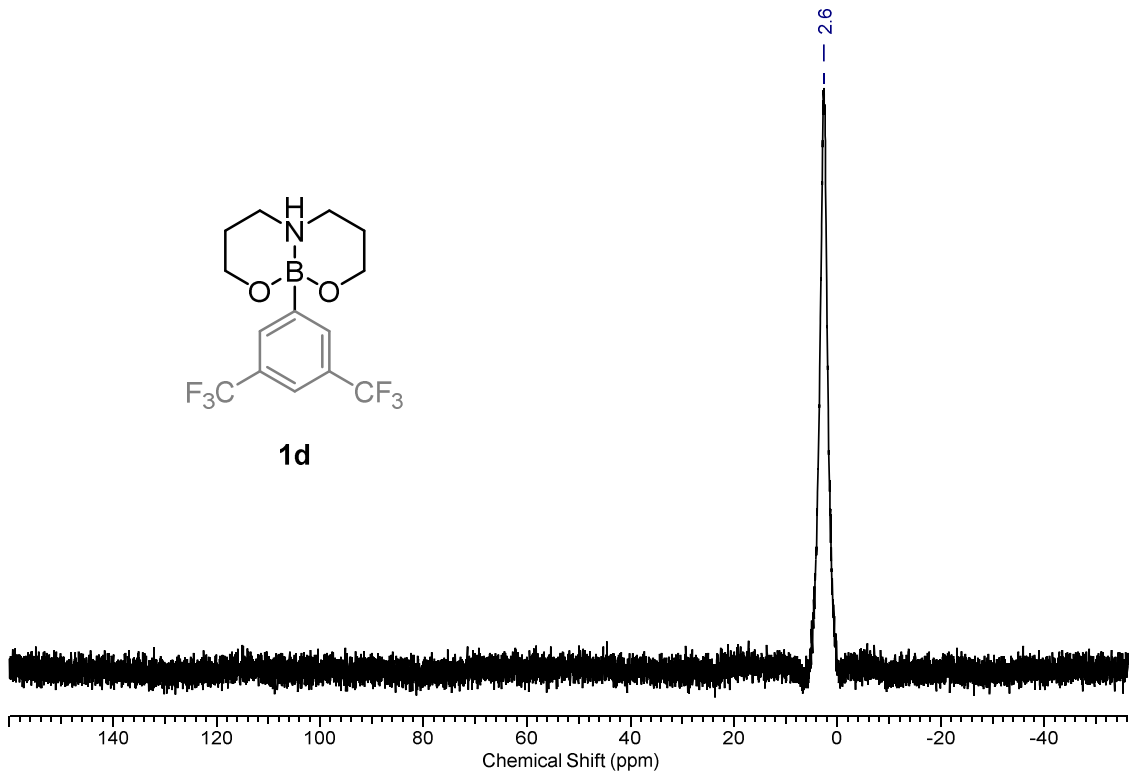

1d. ($^{19}F\{^{1}H\}$ NMR, 376.5 MHz, DMSO-d_6, 298K):

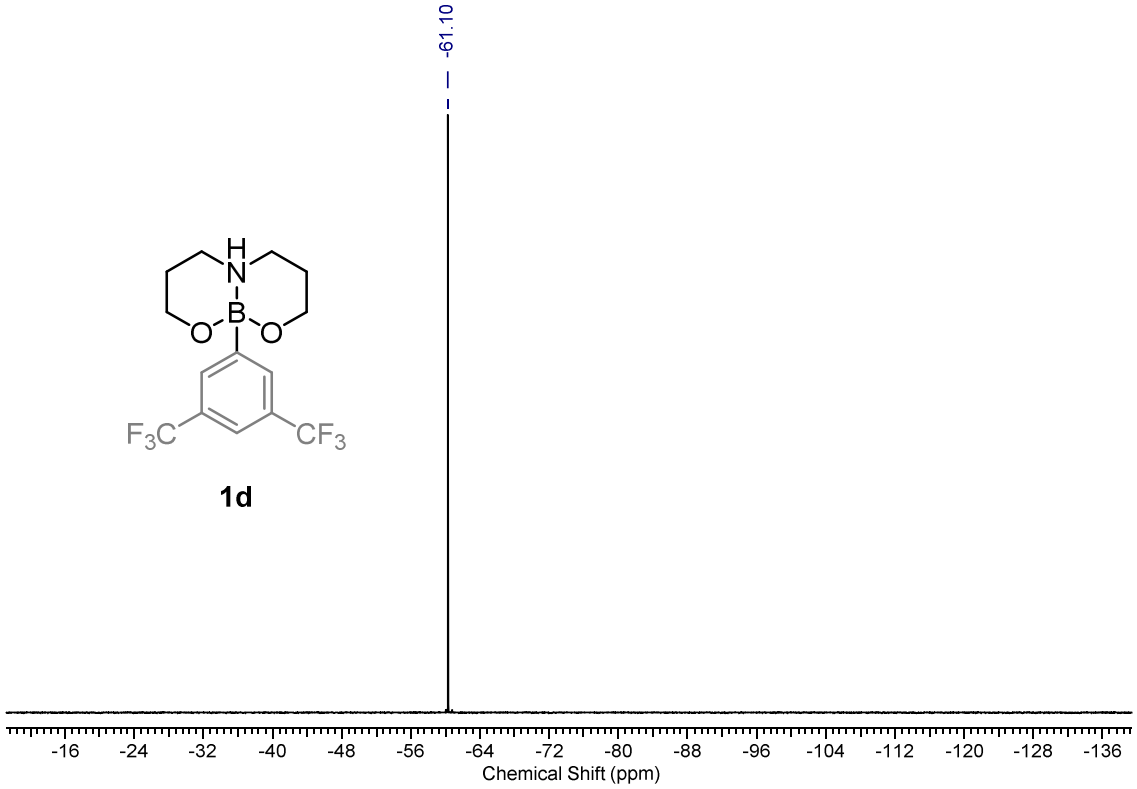

1e. (^{1}H NMR, 400 MHz, DMSO-d_6, 298K):

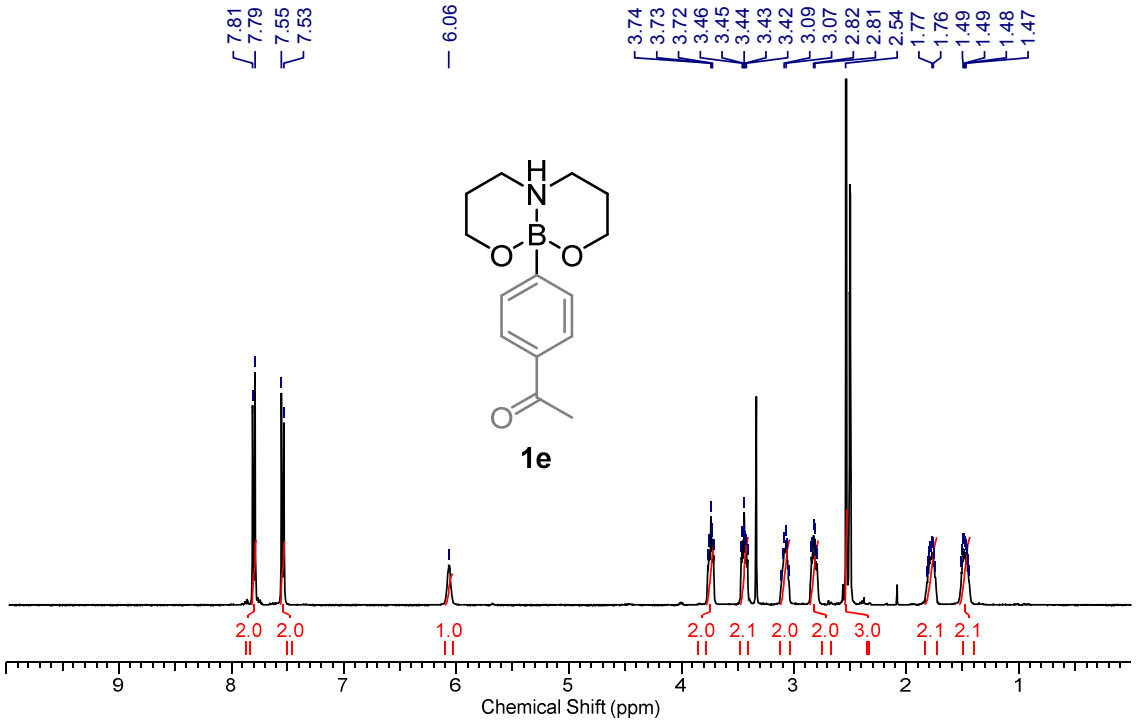

1e. ($^{13}C\{^{1}H\}$ NMR, 100 MHz, DMSO-d_6, 298K):

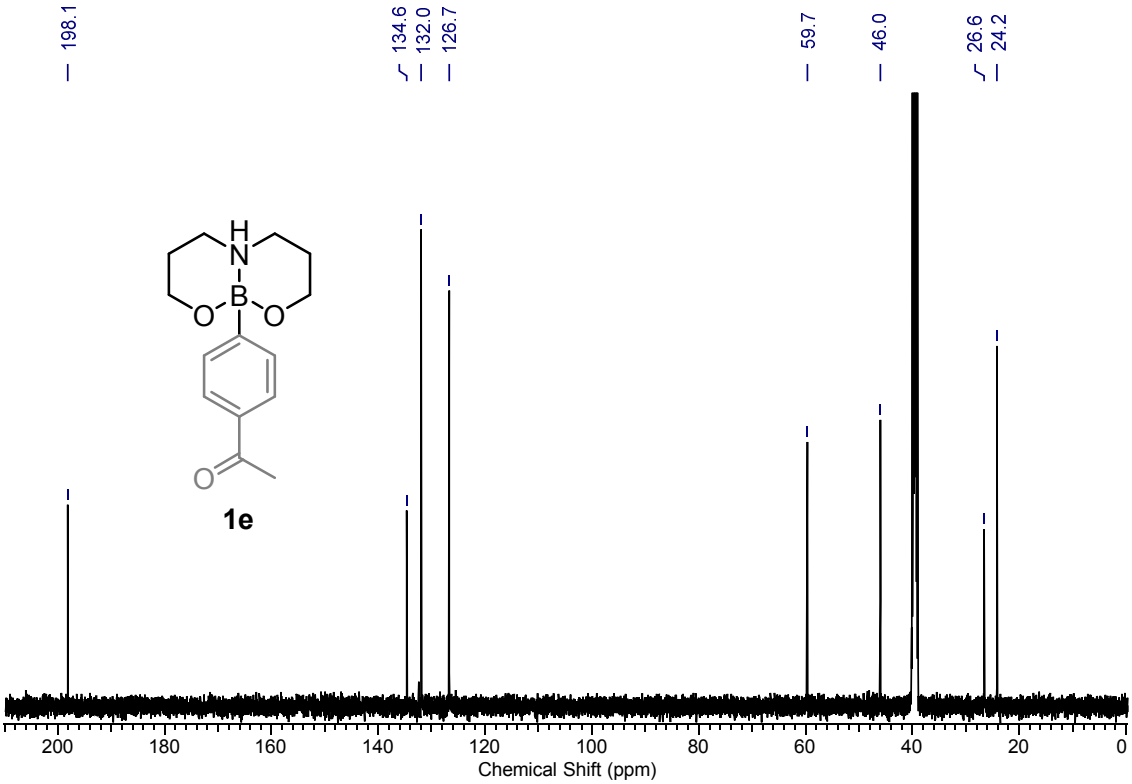

1e. ($^{11}B\{^{1}H\}$ NMR (baseline corrected), 128.4 MHz, DMSO-d_6, 298K):

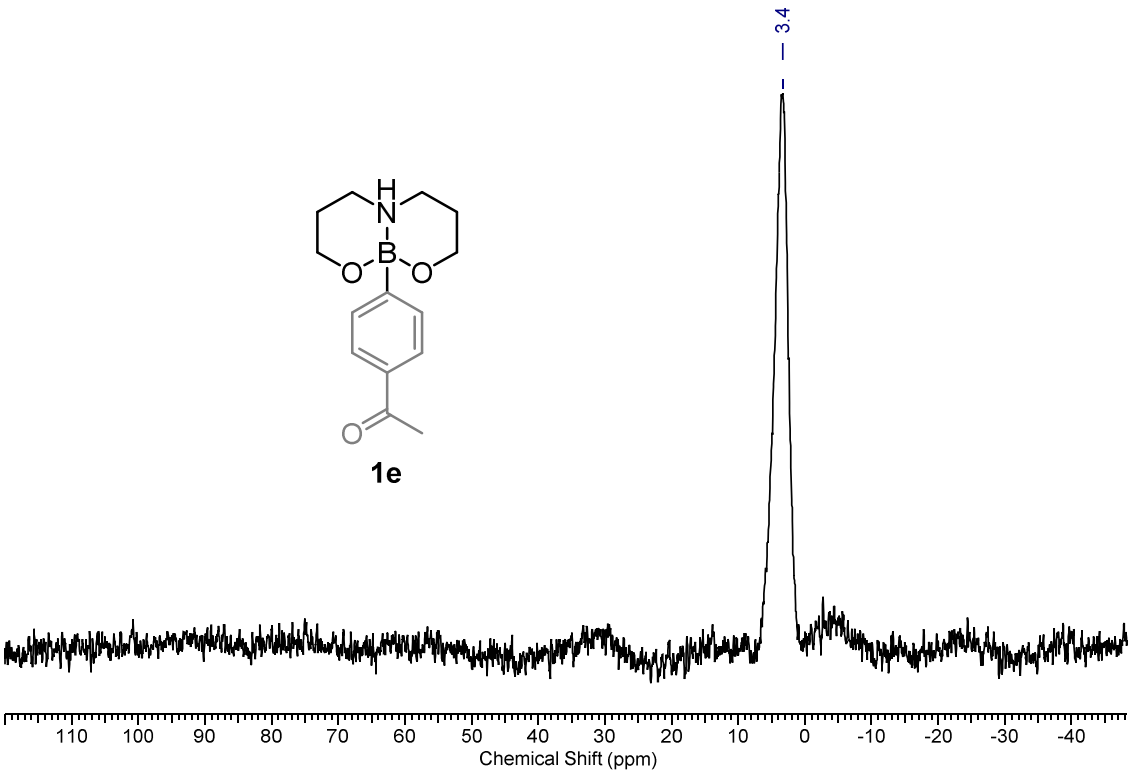

1f. (^{1}H NMR, 400 MHz, DMSO-d_6, 298K):

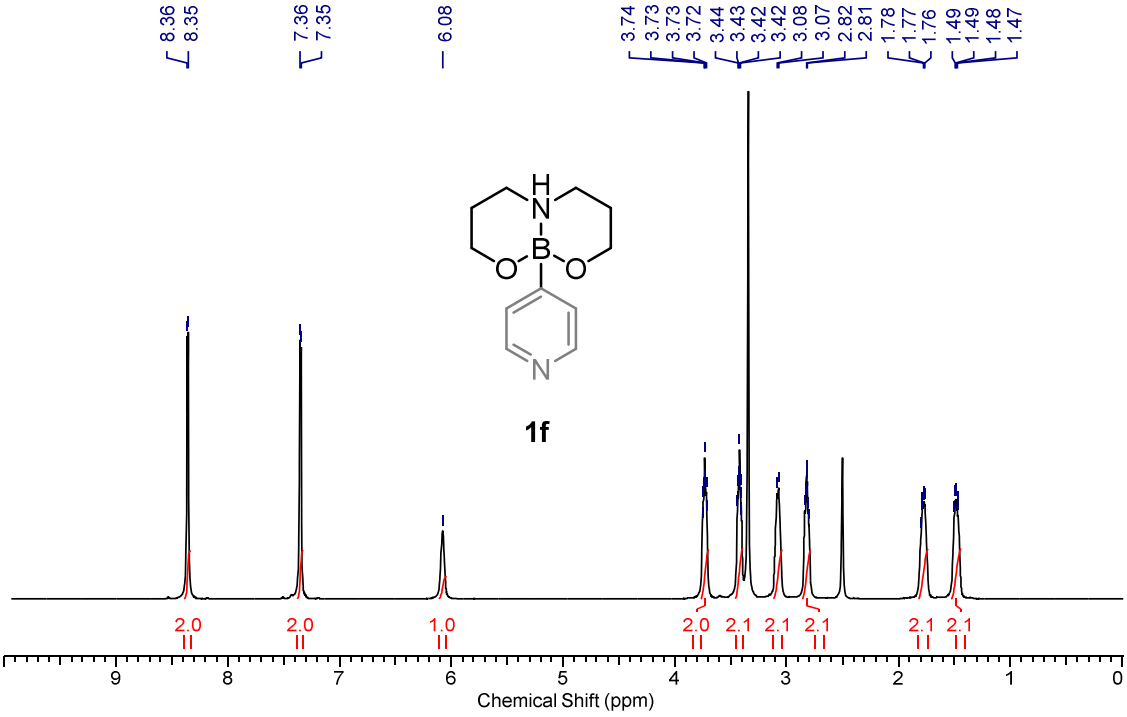

1f. (^{13}C{^{1}H} NMR, 100 MHz, DMSO-d_6, 298K):

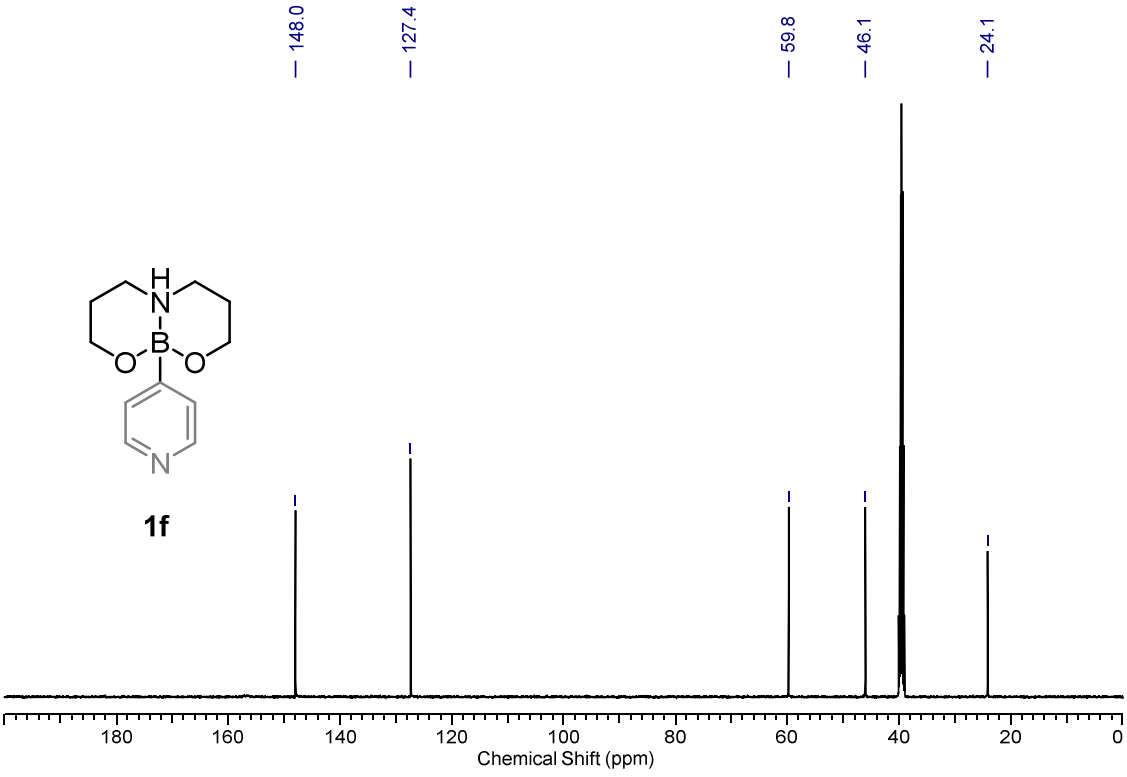

1f. ($^{11}B\{^1H\}$ NMR (baseline corrected), 128.4 MHz, DMSO-d_6, 298K):

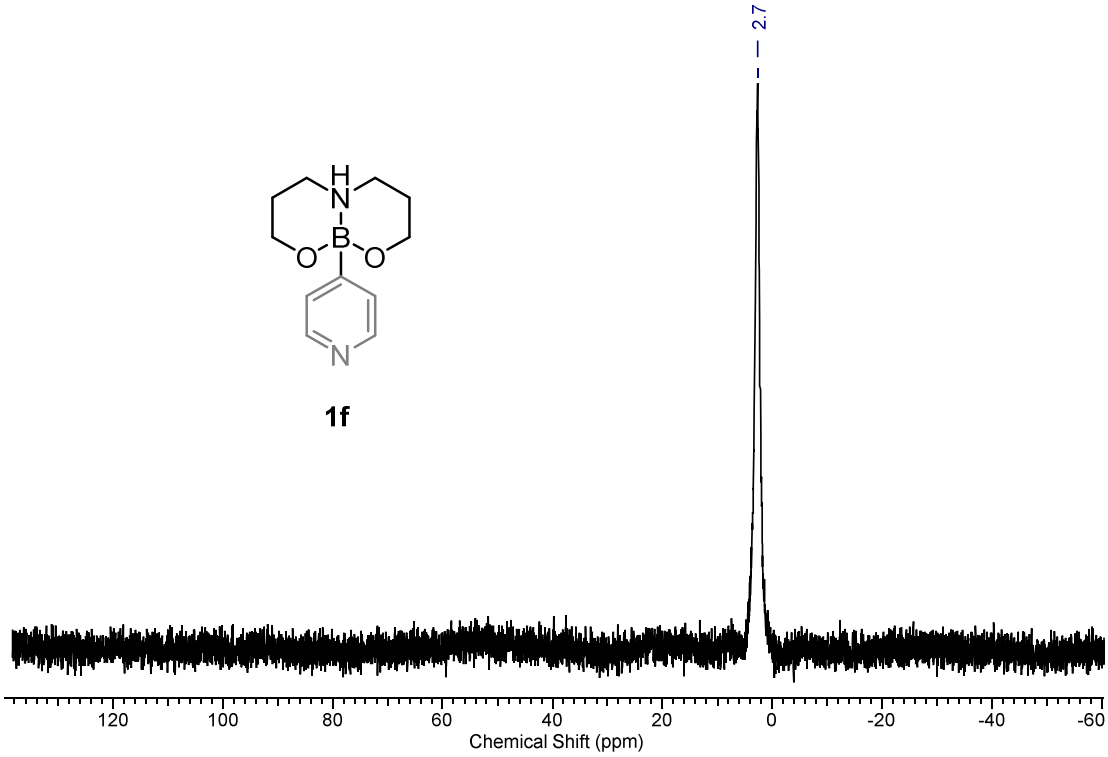

1g. (^1H NMR, 400 MHz, DMSO-d_6, 298K):

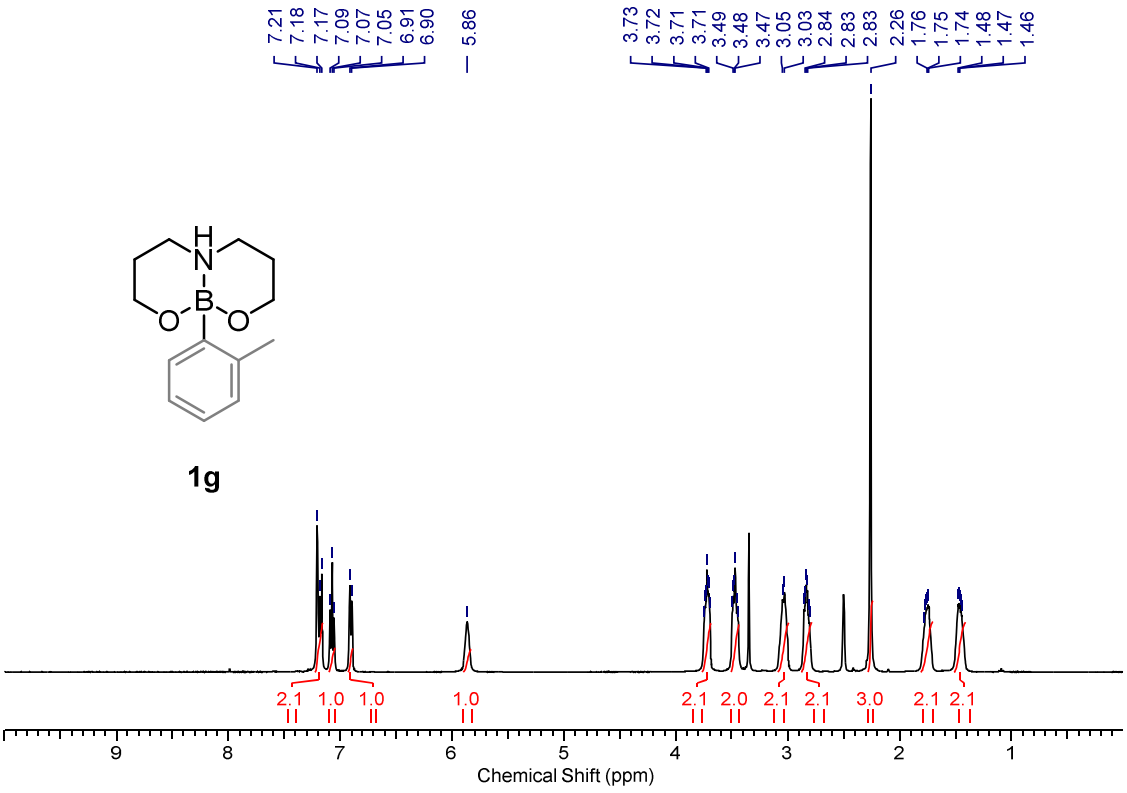

1g. ($^{13}C\{^{1}H\}$ NMR, 100 MHz, DMSO-d_6, 298K):

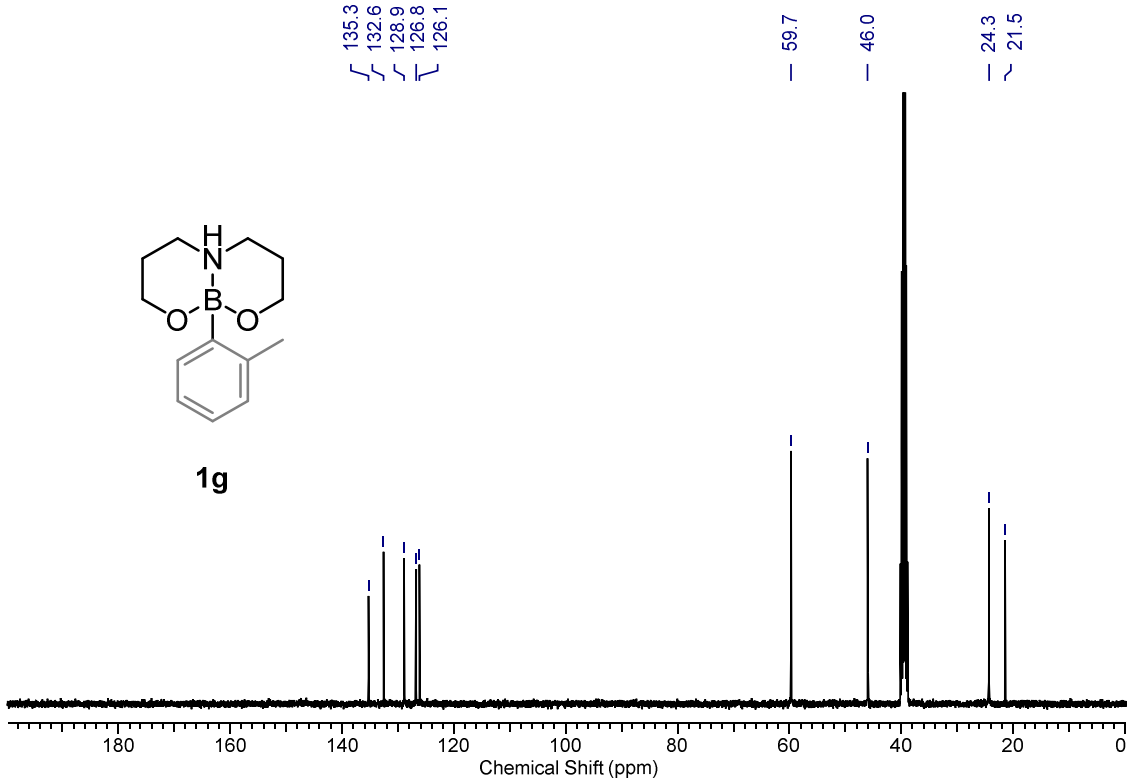

1g. ($^{11}B\{^{1}H\}$ NMR (baseline corrected), 128.4 MHz, DMSO-d_6, 298K):

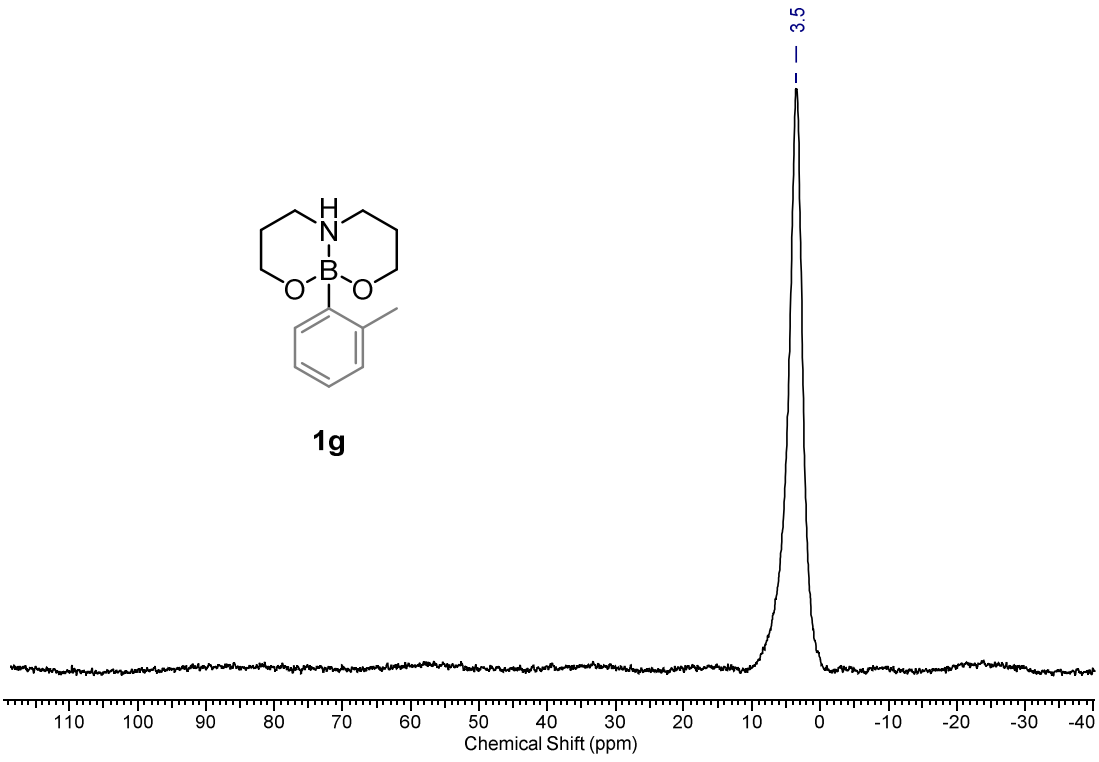

1h. (^{1}H NMR, 400 MHz, DMSO-d_6, 298K):

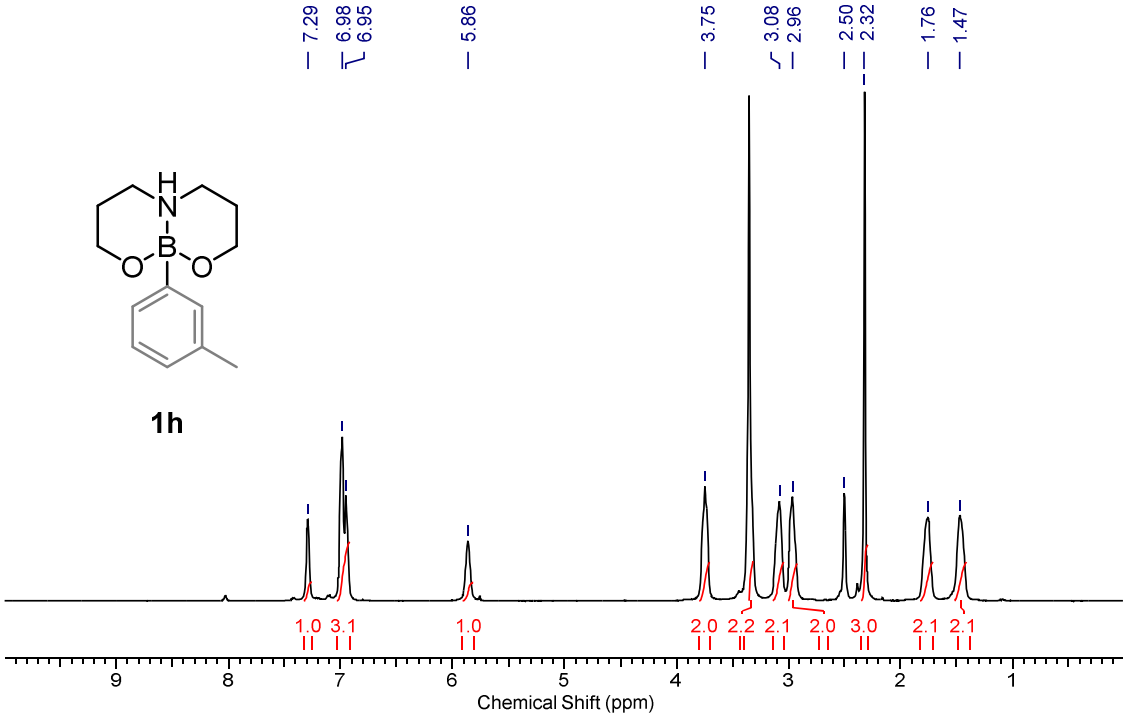

1h. (^{13}C{^{1}H} NMR, 100 MHz, DMSO-d_6, 298K):

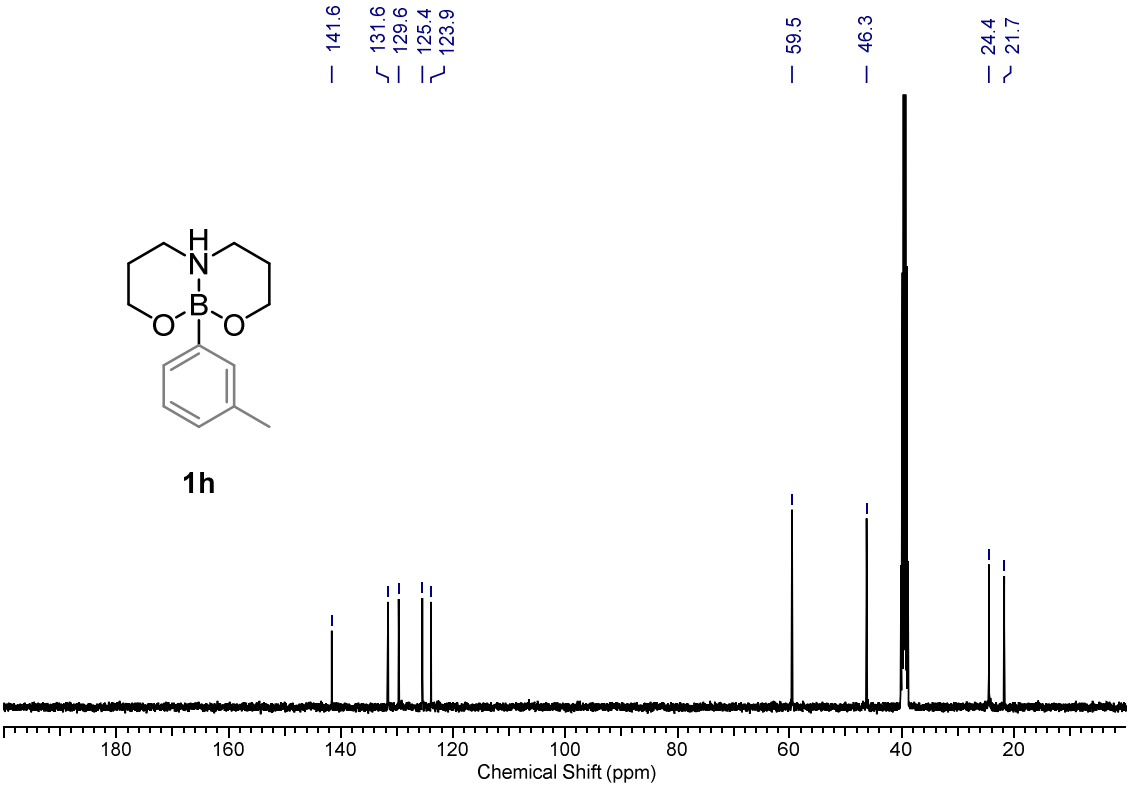

1h. ($^{11}B\{^1H\}$ NMR (baseline corrected), 128.4 MHz, DMSO-d_6, 298K):

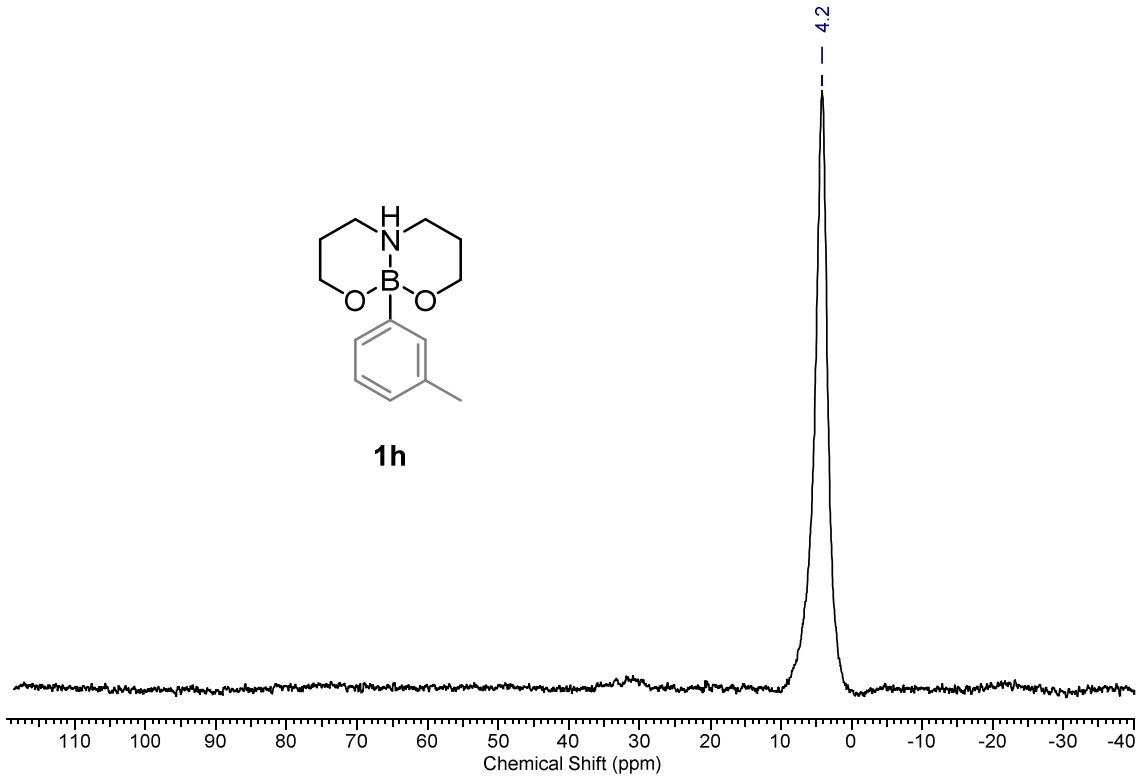

1i. (^1H NMR, 400 MHz, DMSO-d_6, 298K):

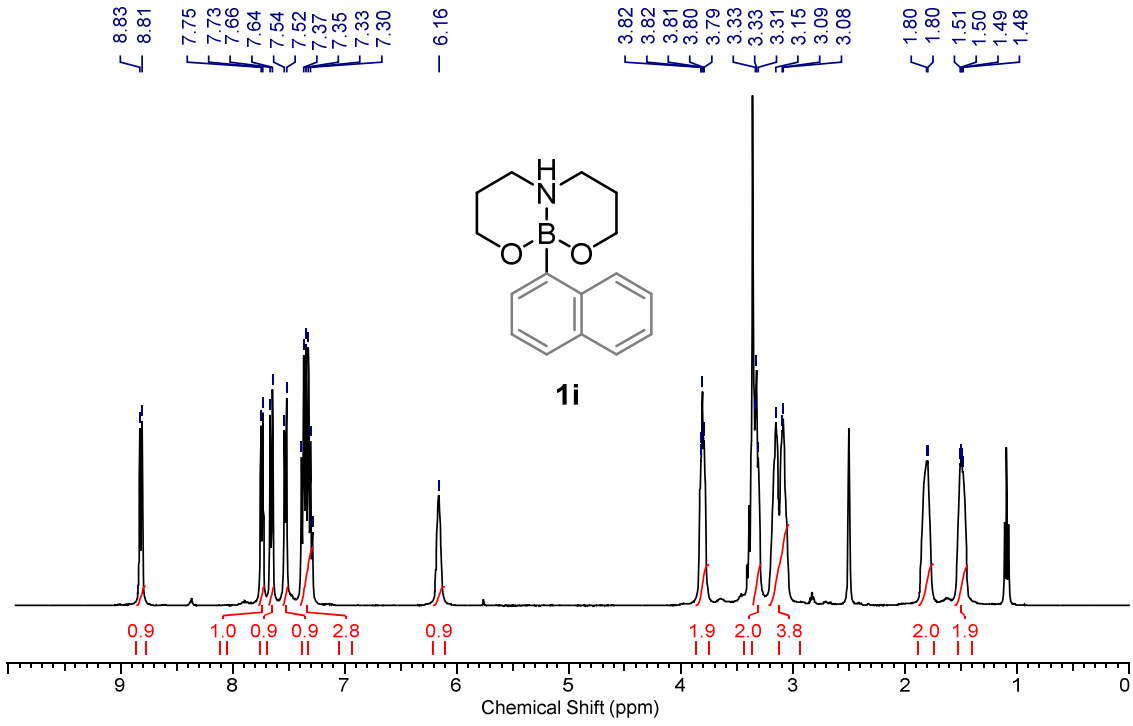

1i. ($^{13}C\{^{1}H\}$ NMR, 100 MHz, DMSO-d_6, 298K):

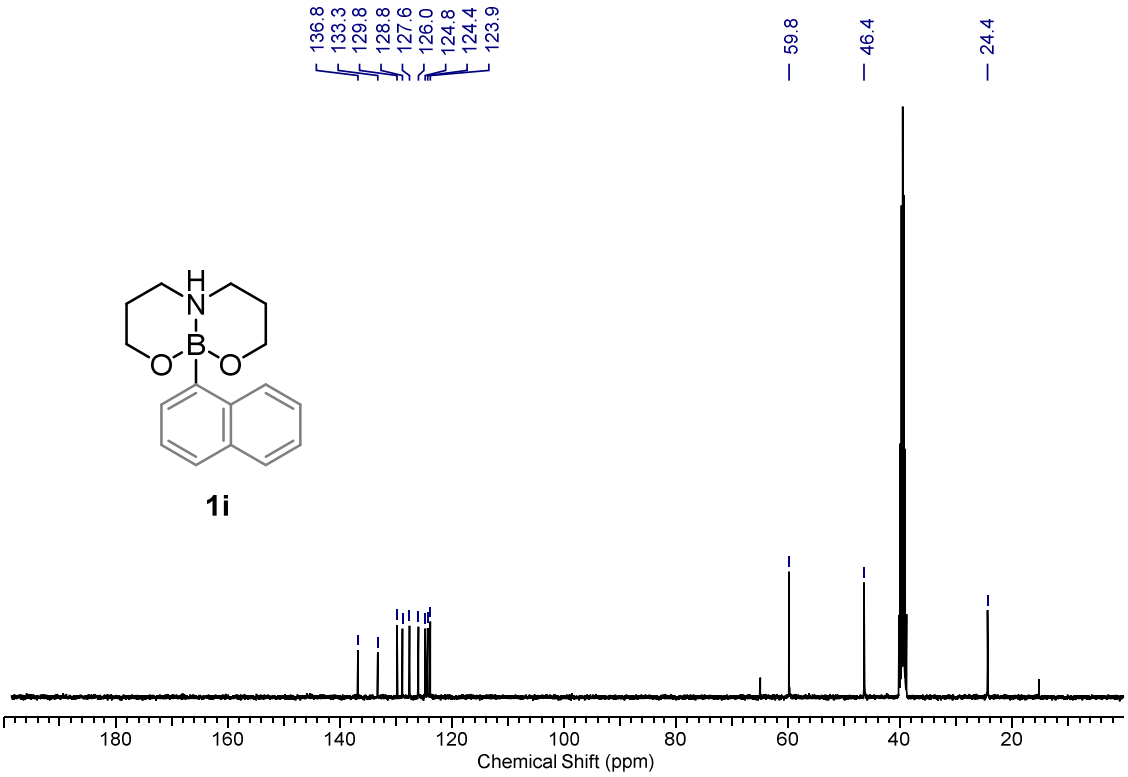

1i. ($^{11}B\{^{1}H\}$ NMR (baseline corrected), 128.4 MHz, DMSO-d_6, 298K):

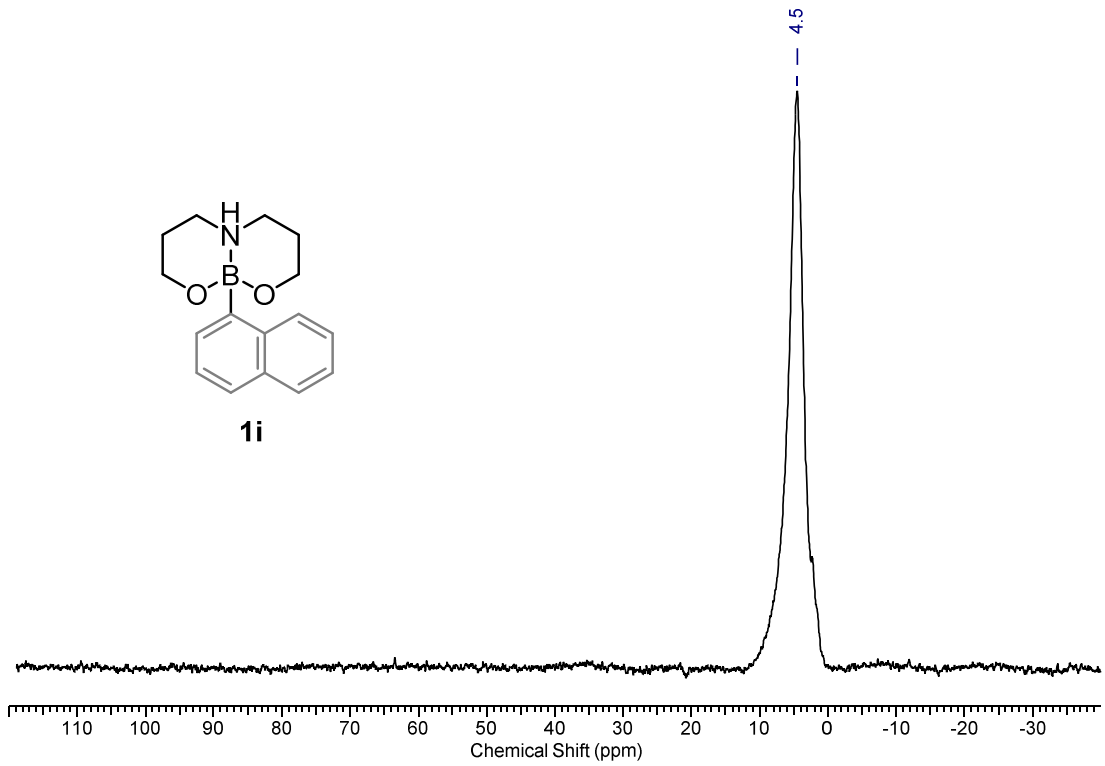

1j. (^{1}H NMR, 400 MHz, DMSO-d_6, 298K):

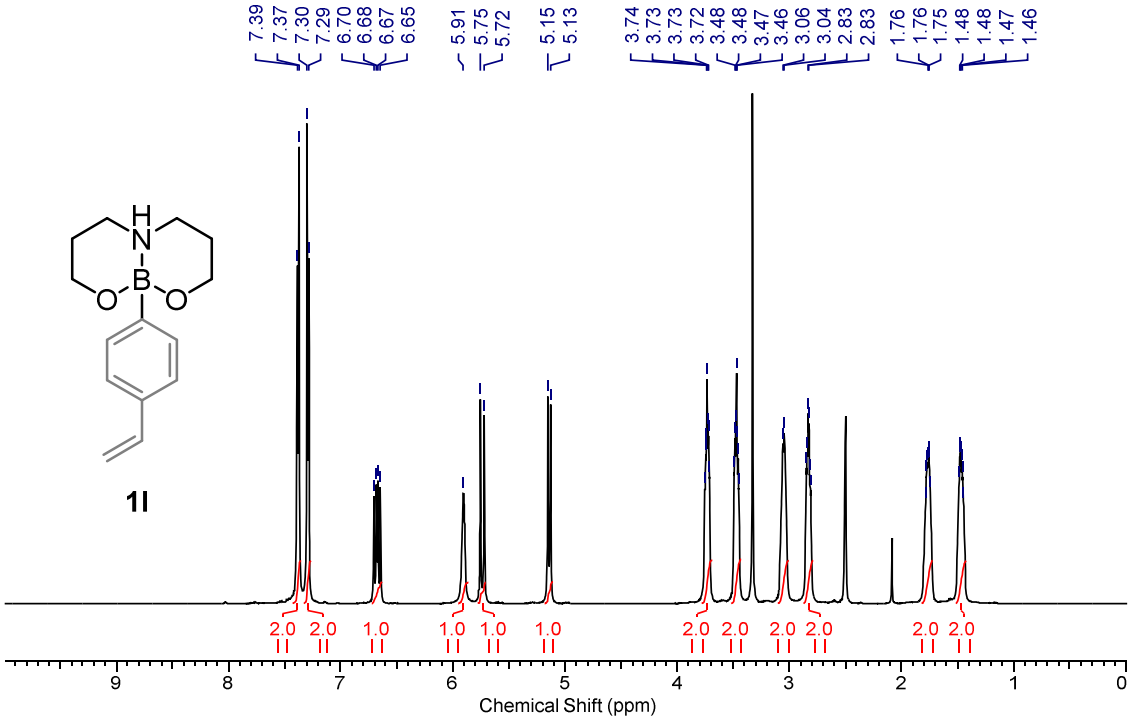

1j. (^{13}C{^{1}H} NMR, 100 MHz, DMSO-d_6, 298K):

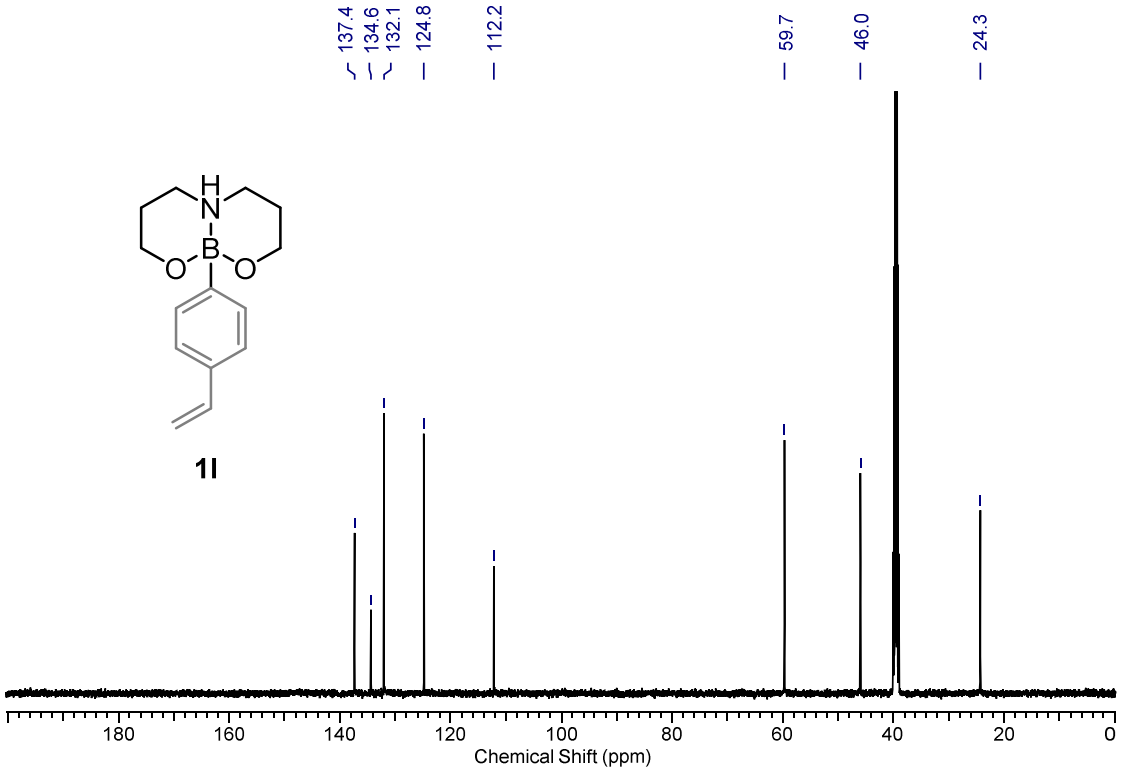

1j. ($^{11}B\{^1H\}$ NMR (baseline corrected), 128.4 MHz, DMSO-d_6, 298K):

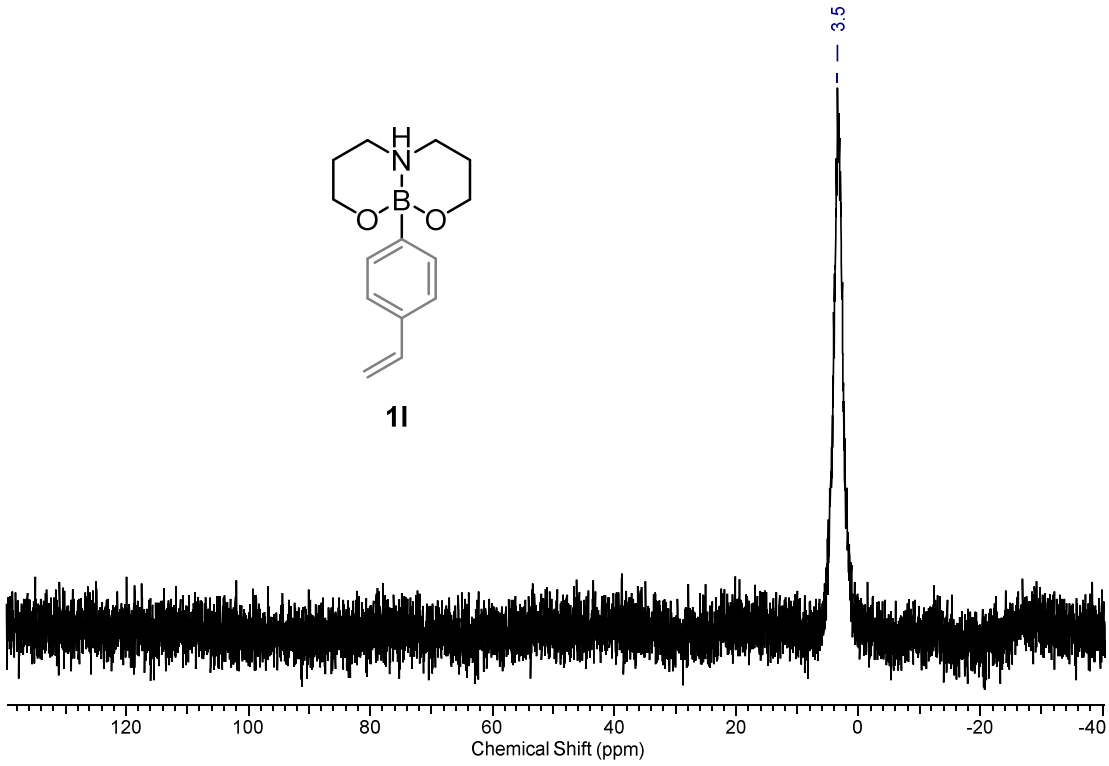

1k. (^1H NMR, 400 MHz, DMSO-d_6, 298K):

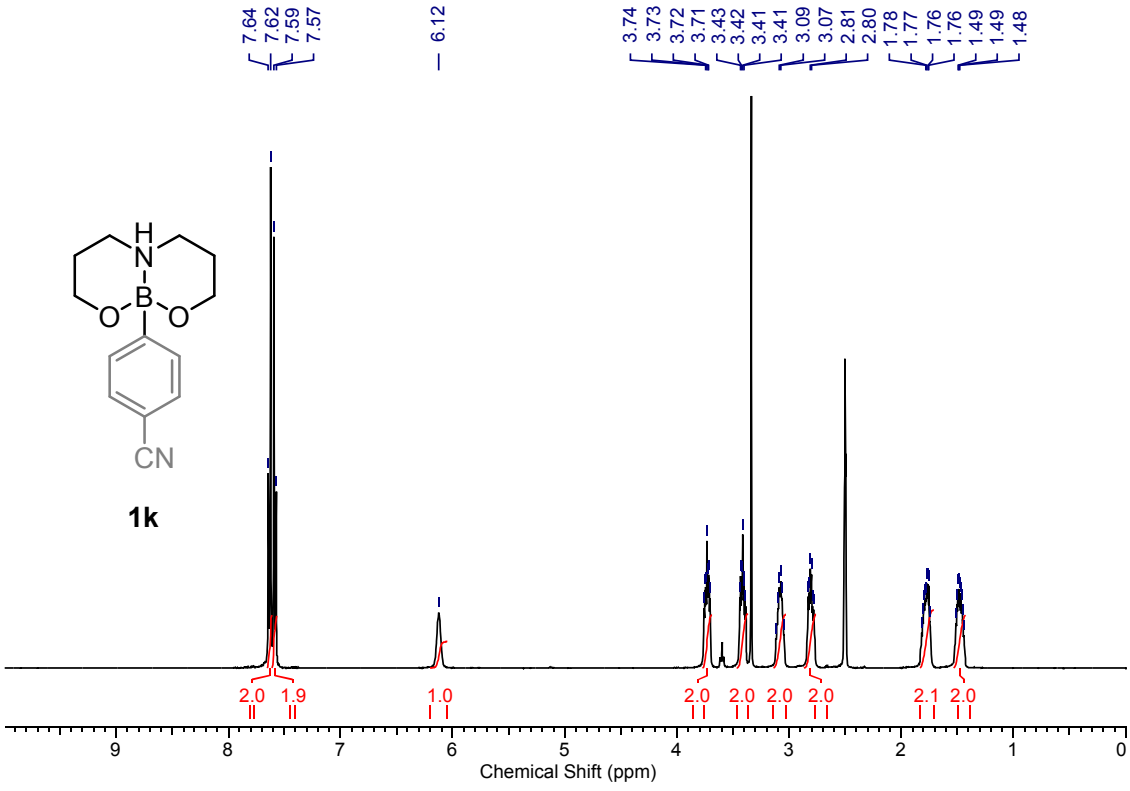

1k. ($^{13}C\{^{1}H\}$ NMR, 100 MHz, DMSO-d_6, 298K):

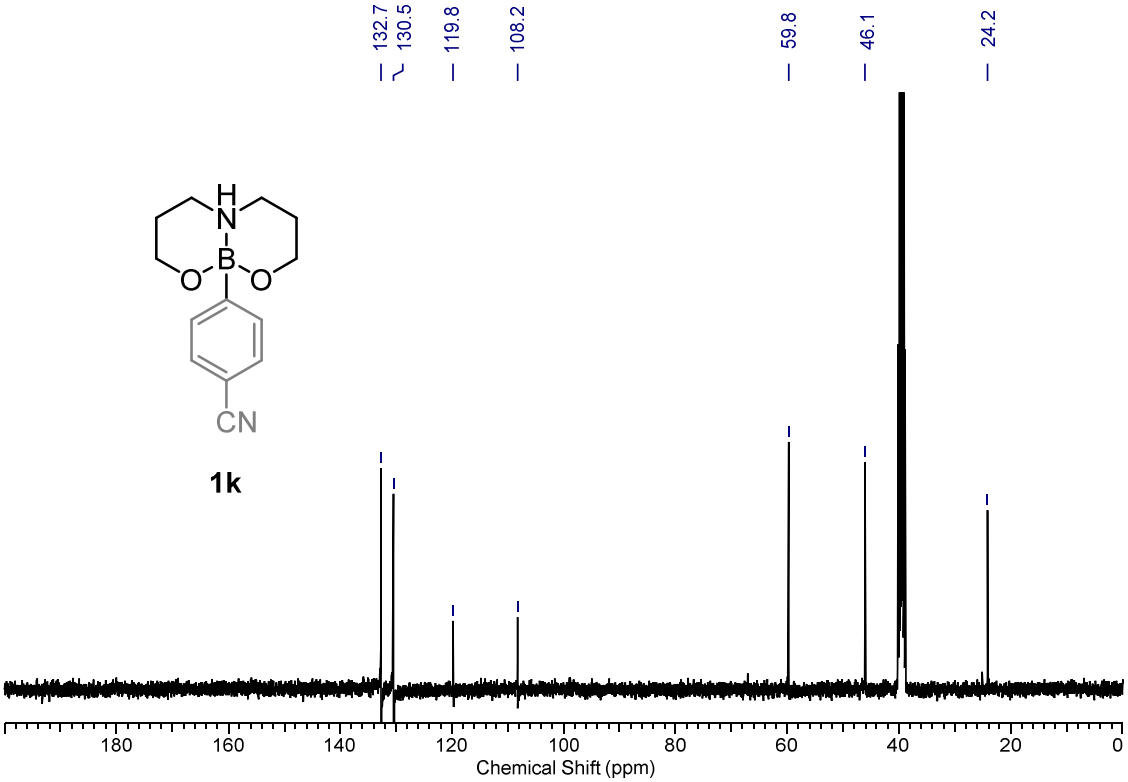

1k. ($^{11}B\{^{1}H\}$ NMR (baseline corrected), 128.4 MHz, DMSO-d_6, 298K):

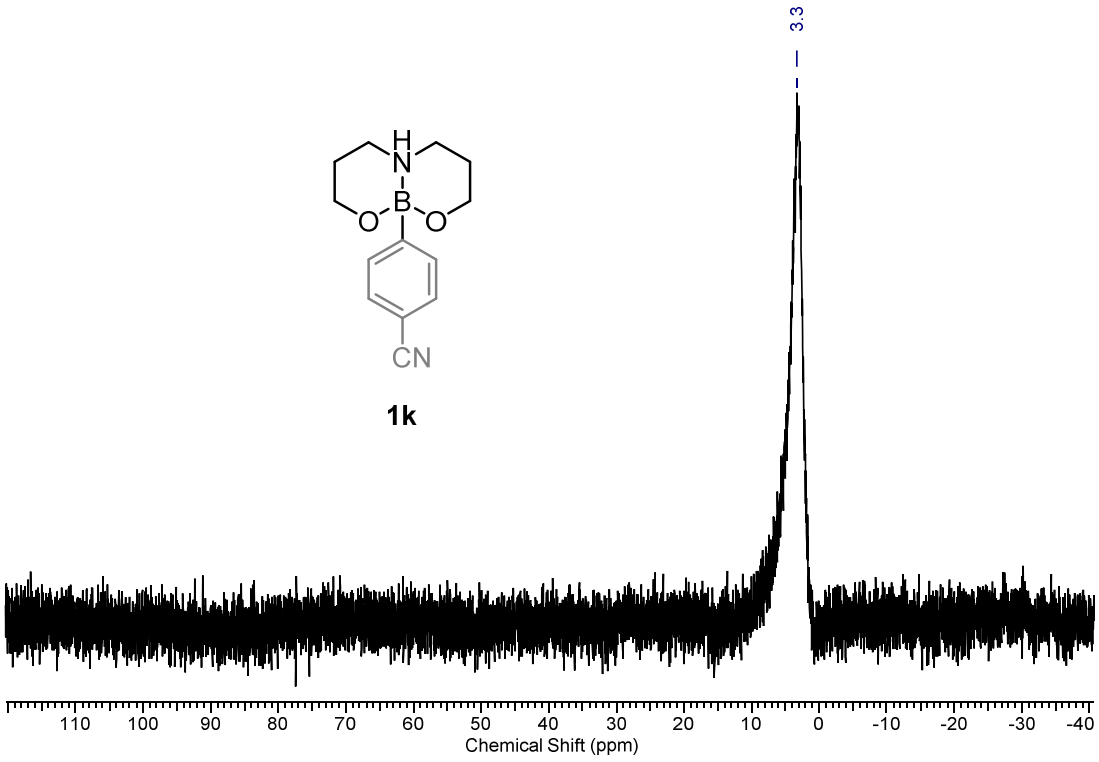

1l. (^{1}H NMR, 400 MHz, DMSO-d_6, 298K):

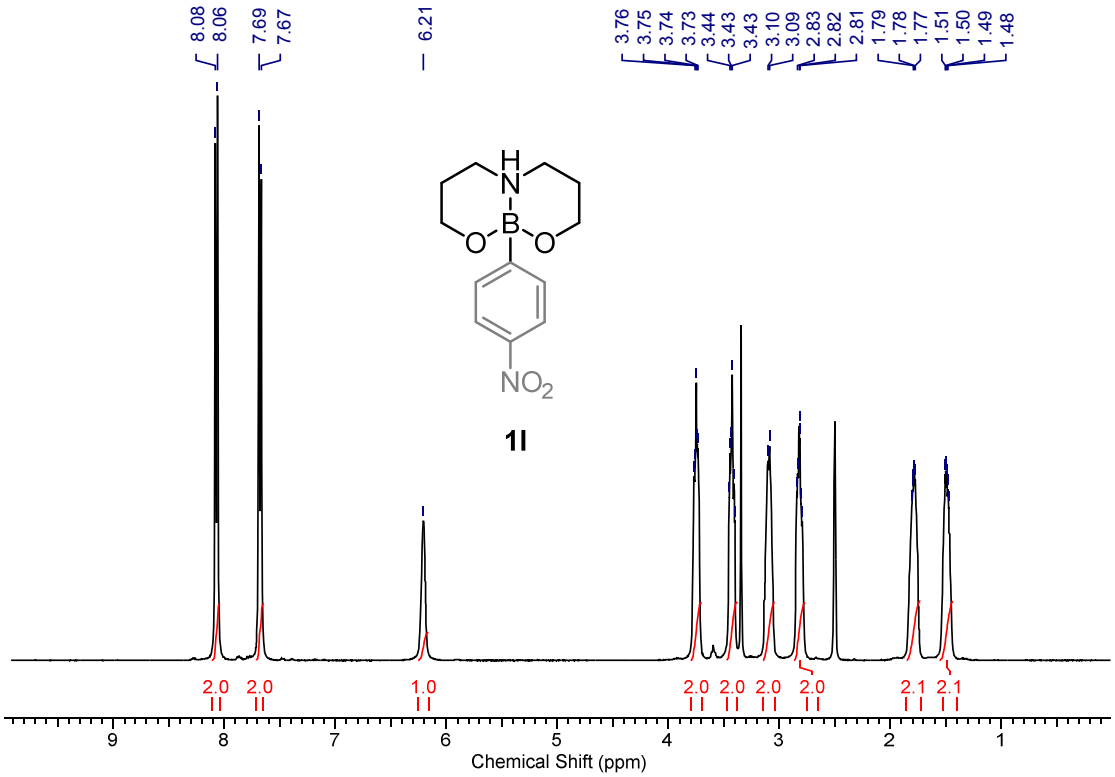

1l. (^{13}C{^{1}H} NMR, 100 MHz, DMSO-d_6, 298K):

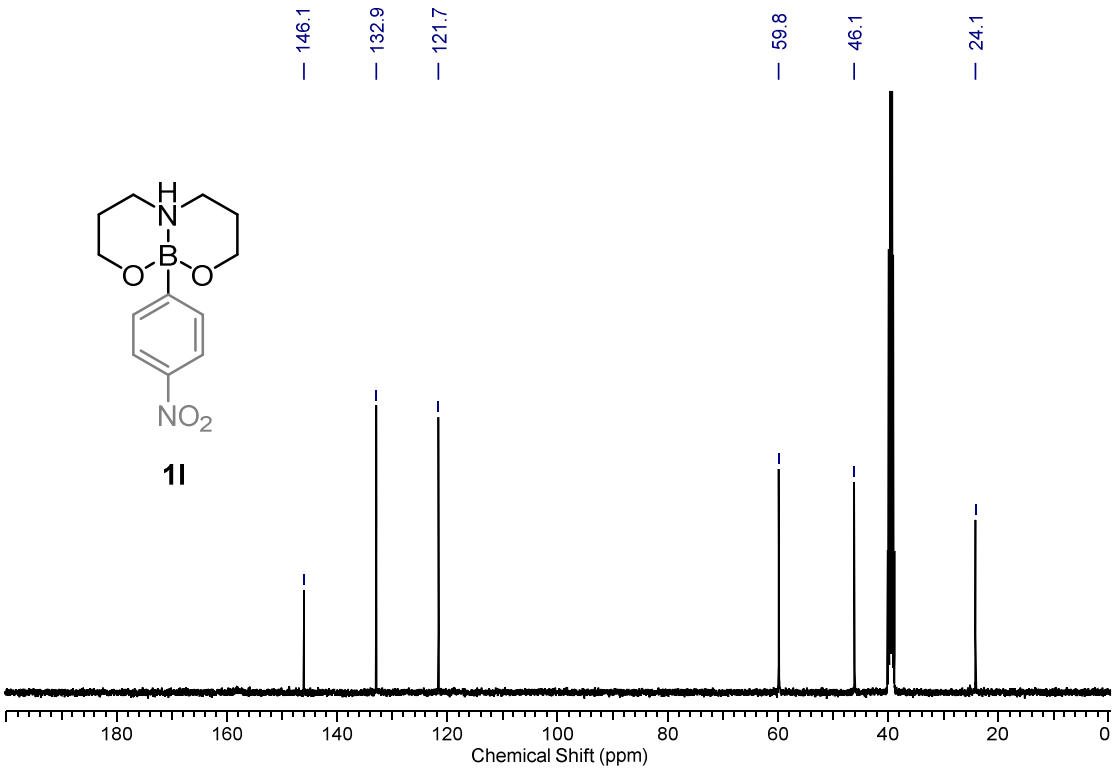

1l. ($^{11}B\{^{1}H\}$ NMR (baseline corrected), 128.4 MHz, DMSO-d_6, 298K):

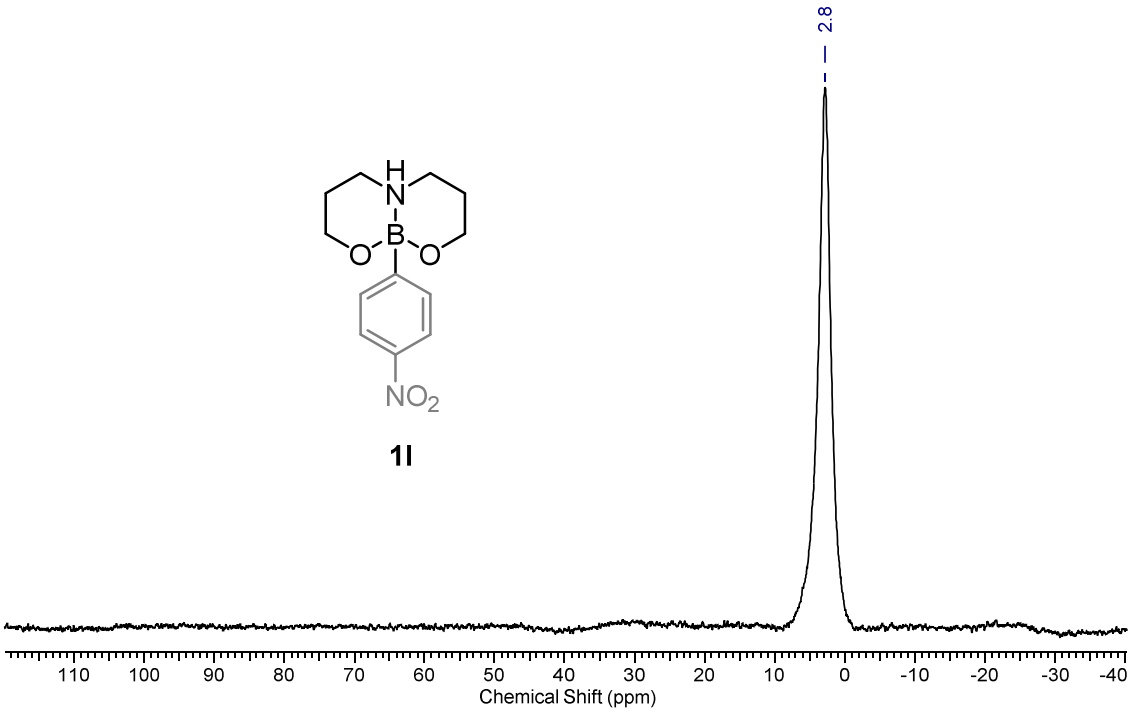

1m. (^{1}H NMR, 400 MHz, DMSO-d_6, 298K):

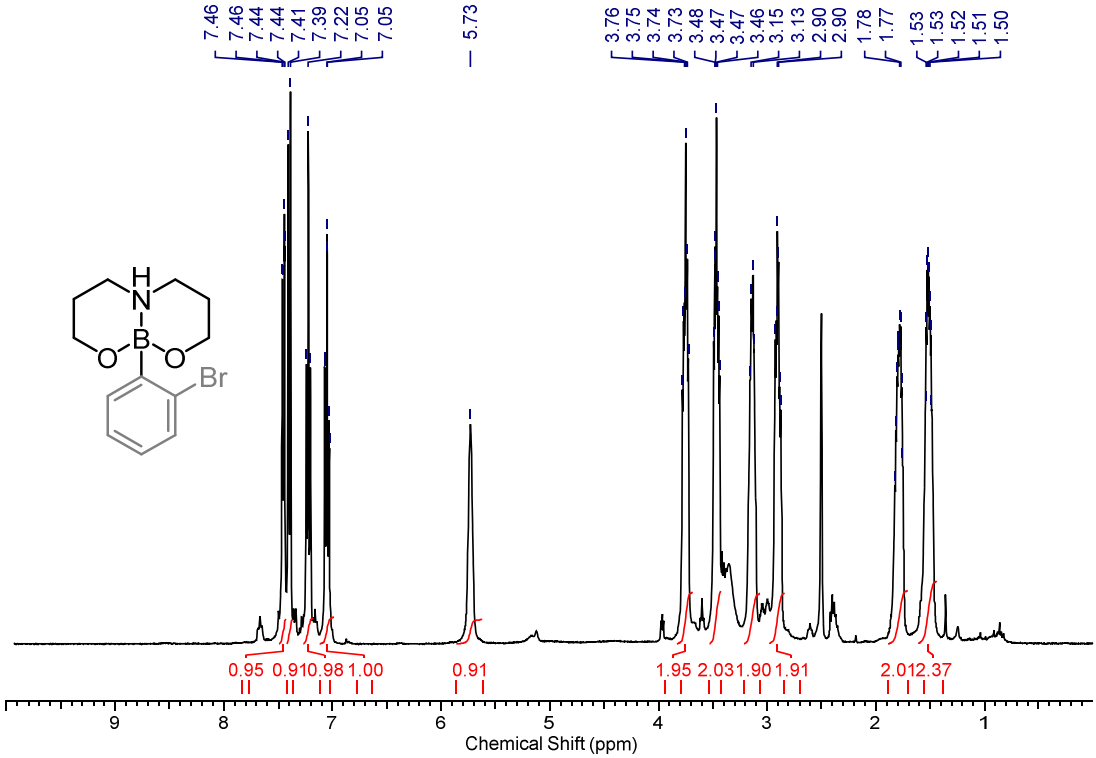

1m. ($^{13}C\{^{1}H\}$ NMR, 100 MHz, DMSO-d_6, 298K):

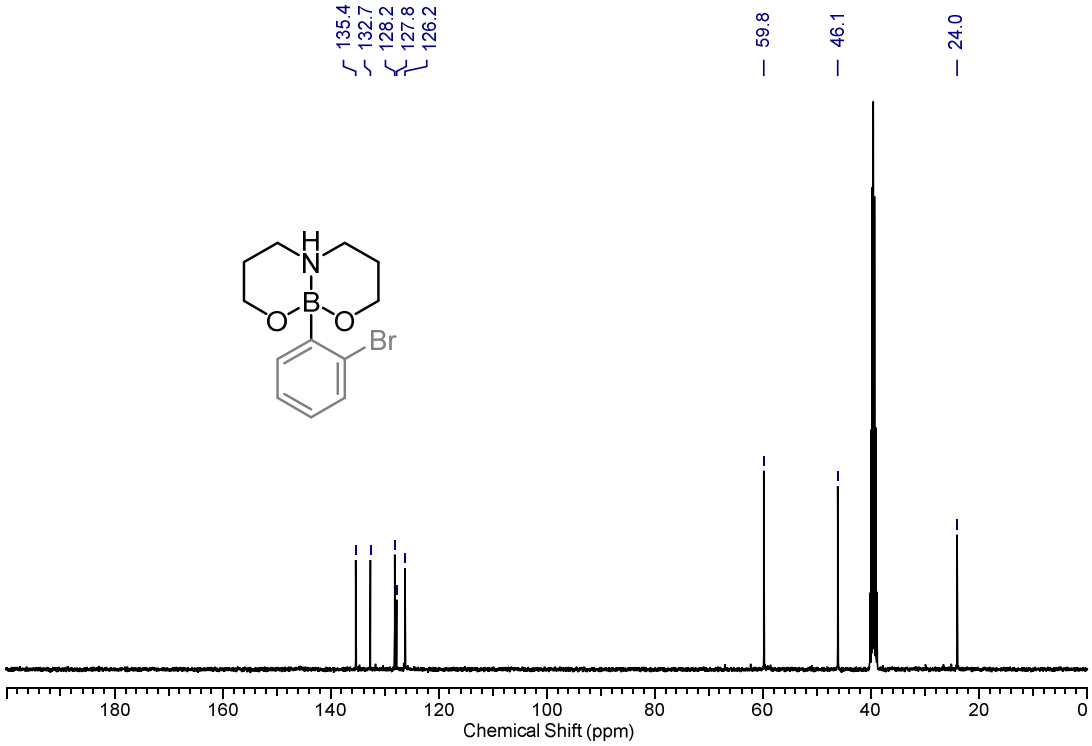

1m. ($^{11}B\{^{1}H\}$ NMR (baseline corrected), 128.4 MHz, DMSO-d_6, 298K):

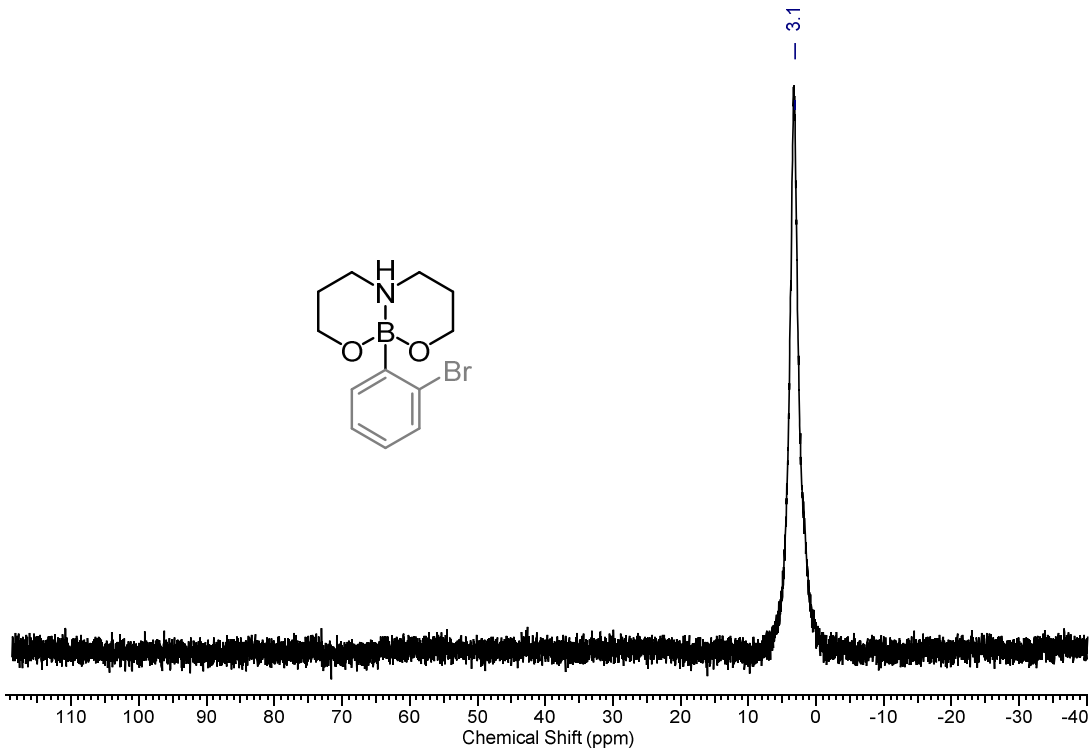

1n. (^{1}H NMR, 400 MHz, DMSO-d_6, 298K):

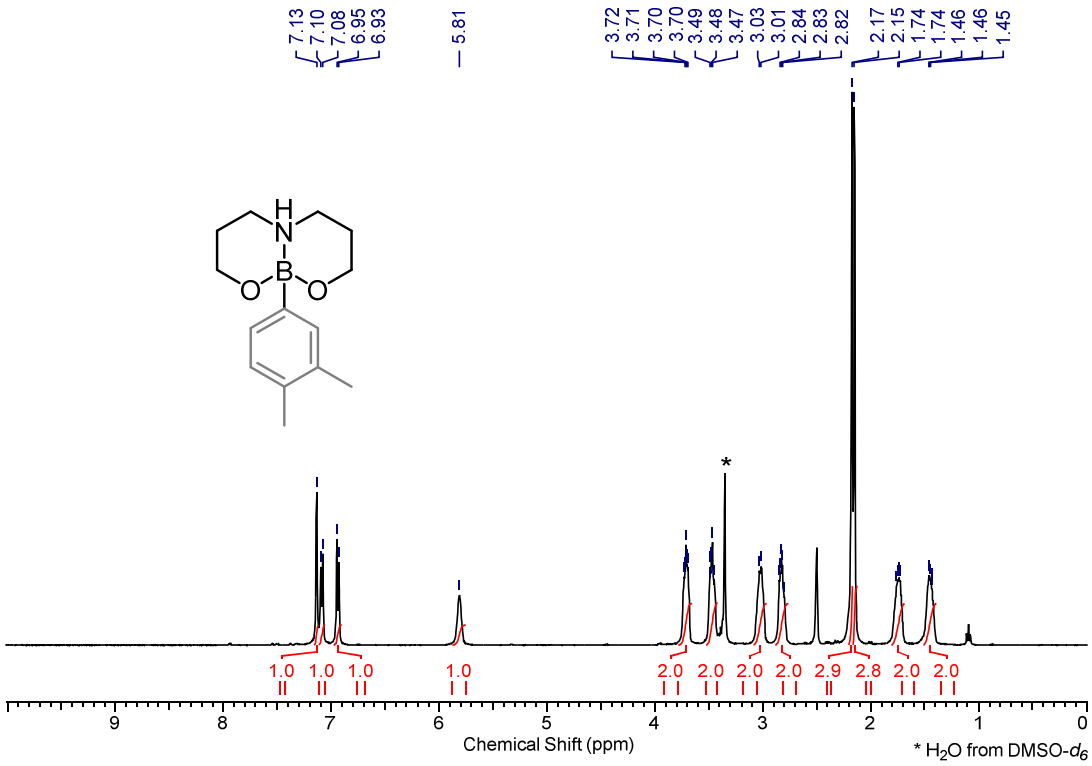

1n. (^{13}C{^{1}H} NMR, 100 MHz, DMSO-d_6, 298K):

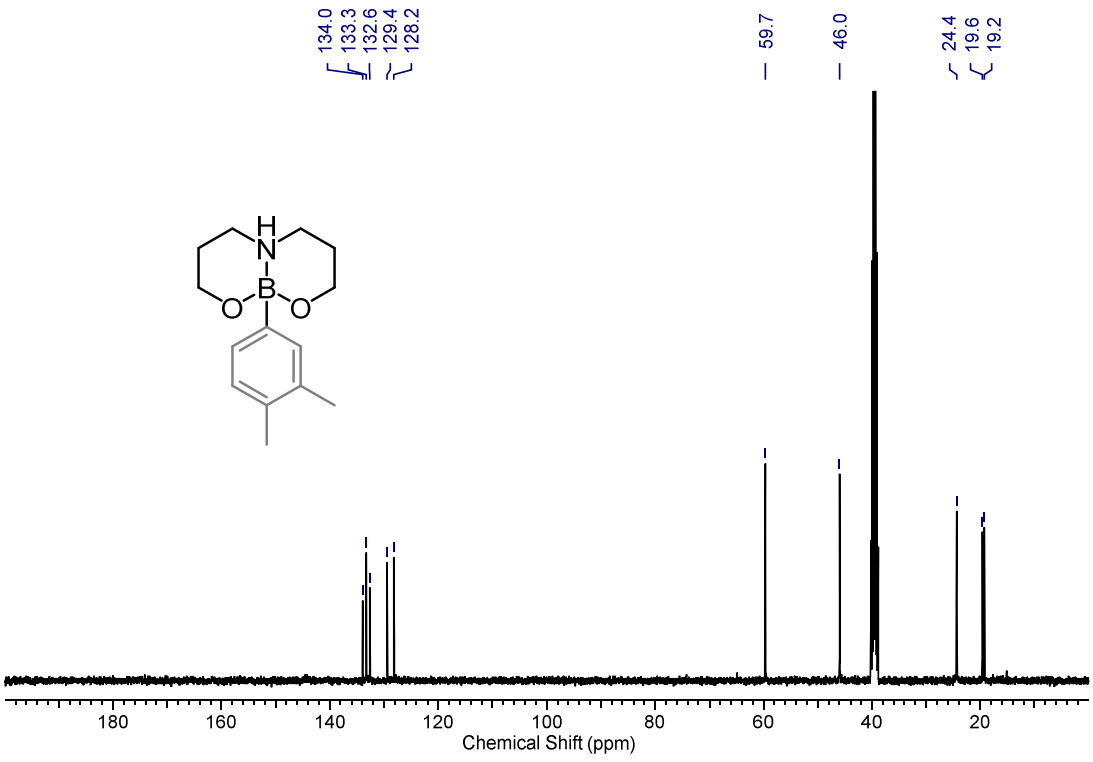

1n. ($^{11}B\{^1H\}$ NMR (baseline corrected), 128.4 MHz, DMSO-d_6, 298K):

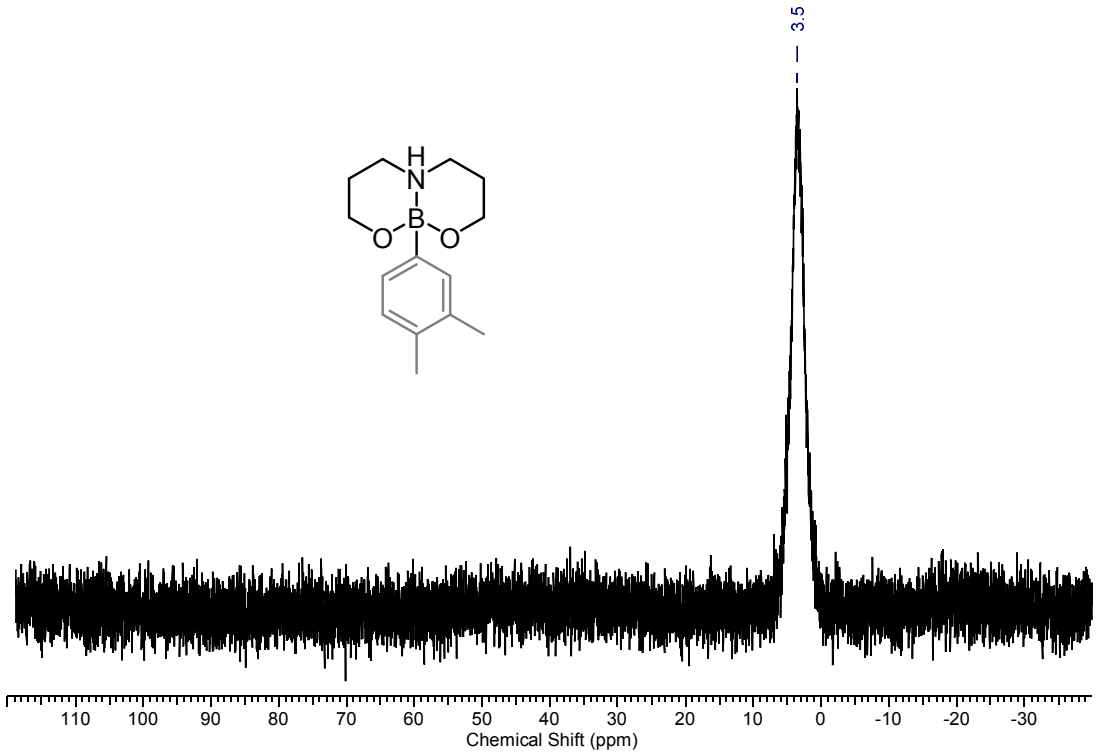

1o. (^1H NMR, 400 MHz, DMSO-d_6, 298K):

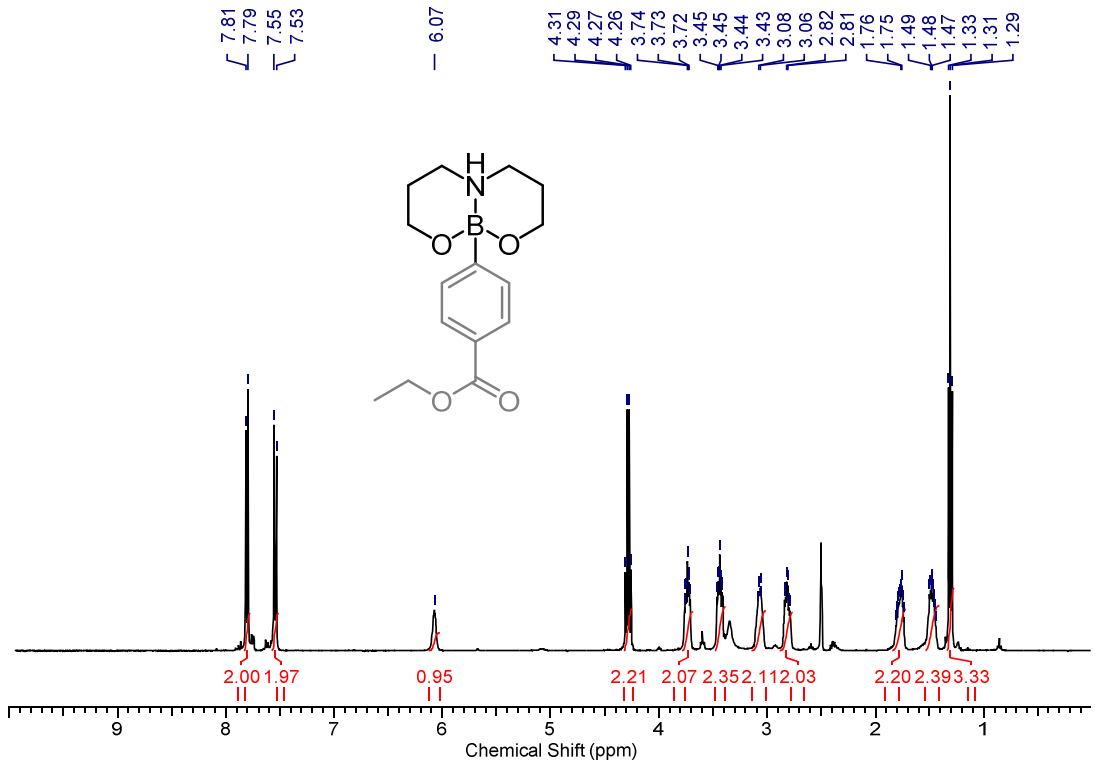

1o. ($^{13}C\{^{1}H\}$ NMR, 100 MHz, DMSO-d_6, 298K):

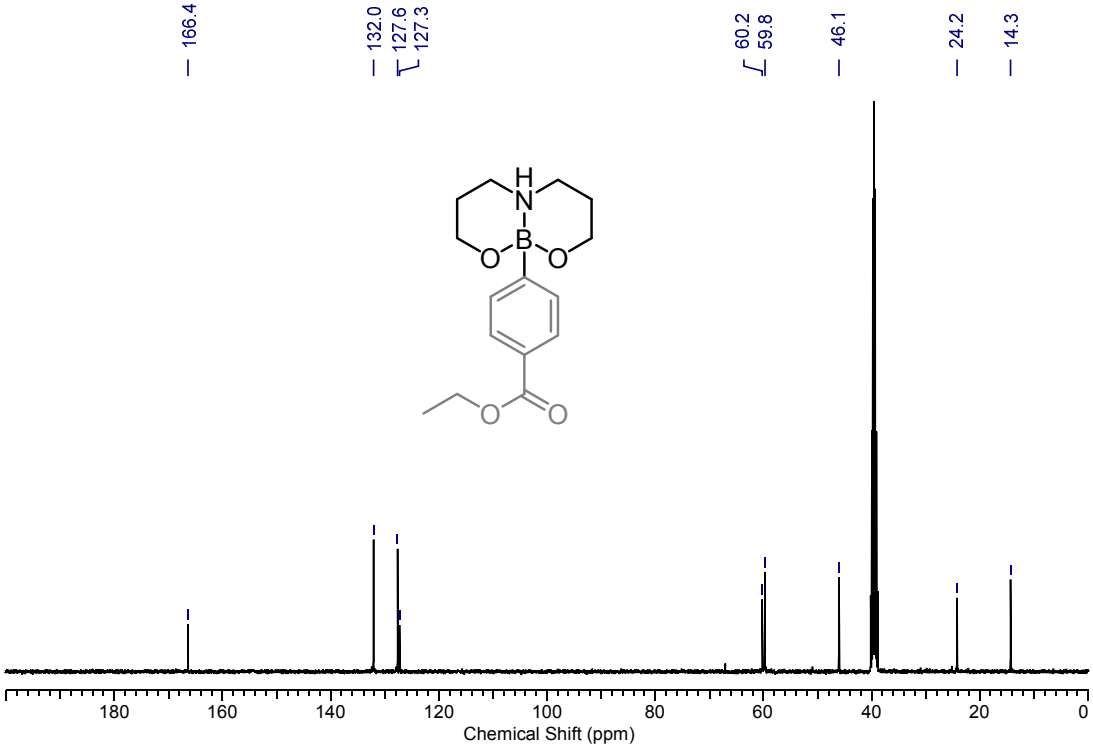

1o. ($^{11}B\{^{1}H\}$ NMR (baseline corrected), 128.4 MHz, DMSO-d_6, 298K):

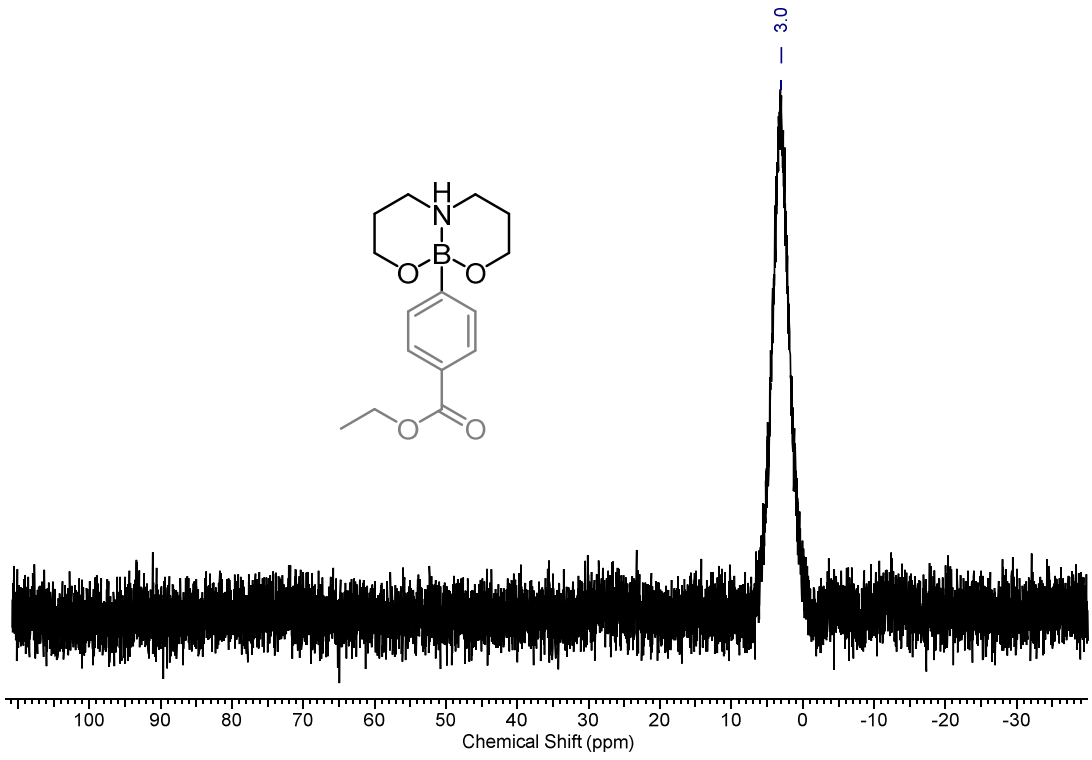

1p. (^{1}H NMR, 400 MHz, DMSO-d_6, 298K):

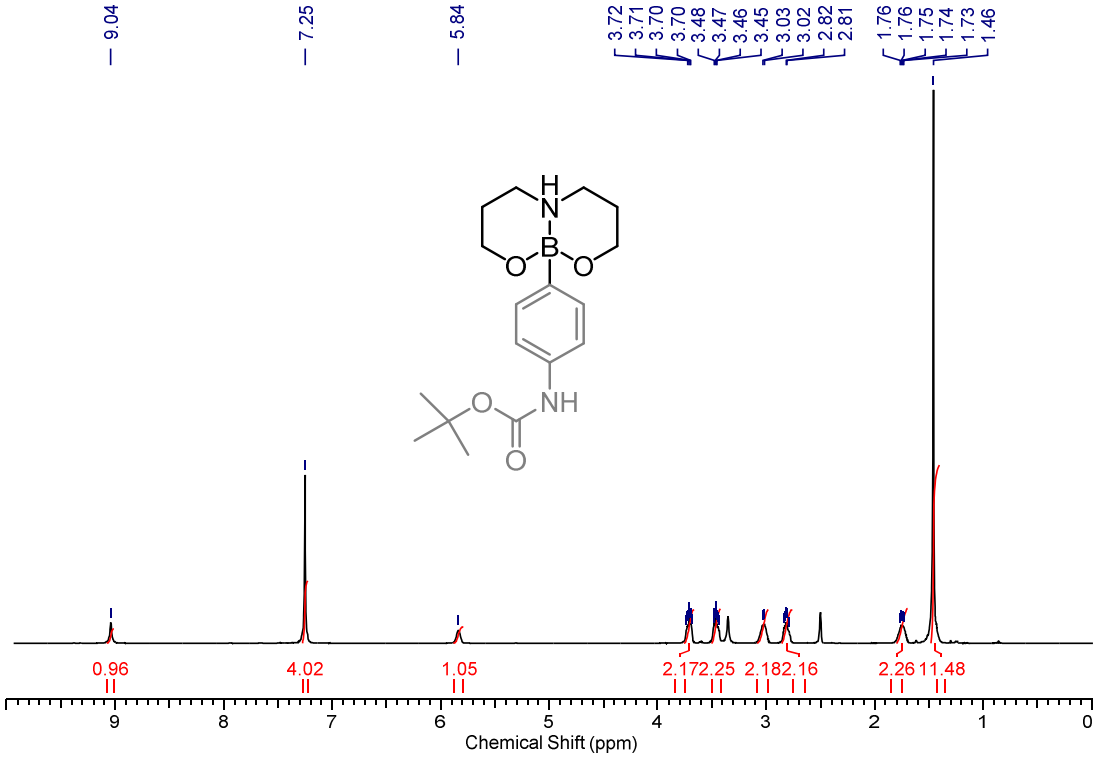

1p. (^{13}C{^{1}H} NMR, 100 MHz, DMSO-d_6, 298K):

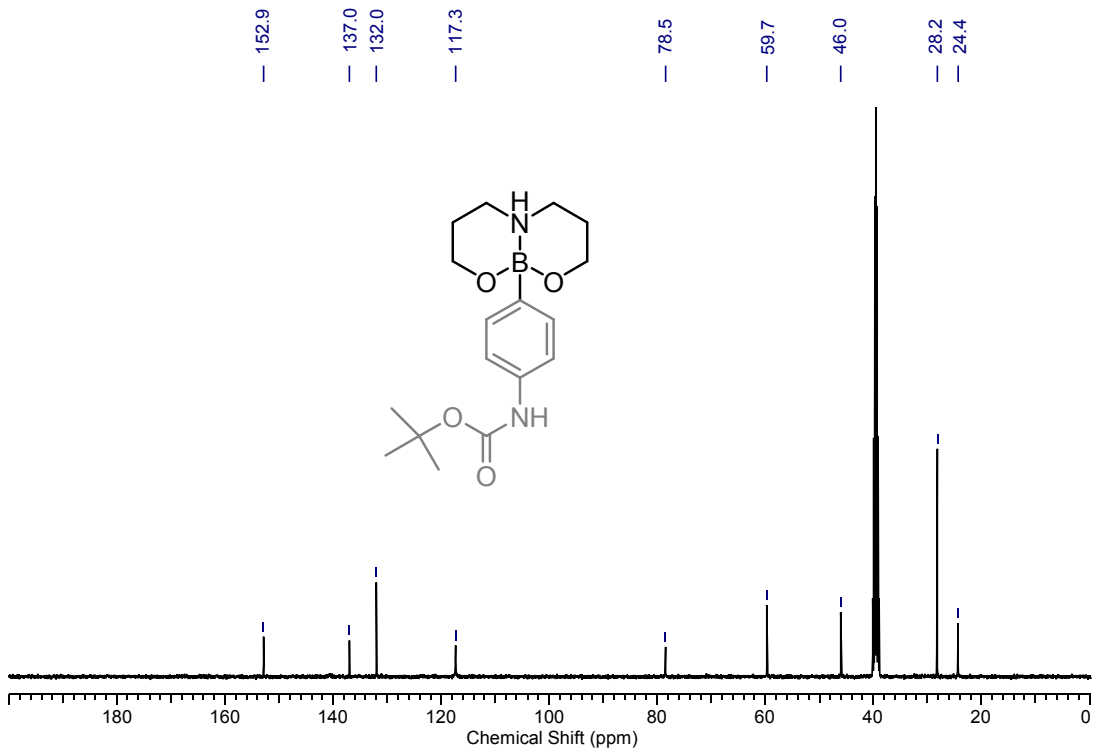

1p. ($^{11}B\{^1H\}$ NMR (baseline corrected), 128.4 MHz, DMSO-d_6, 298K):

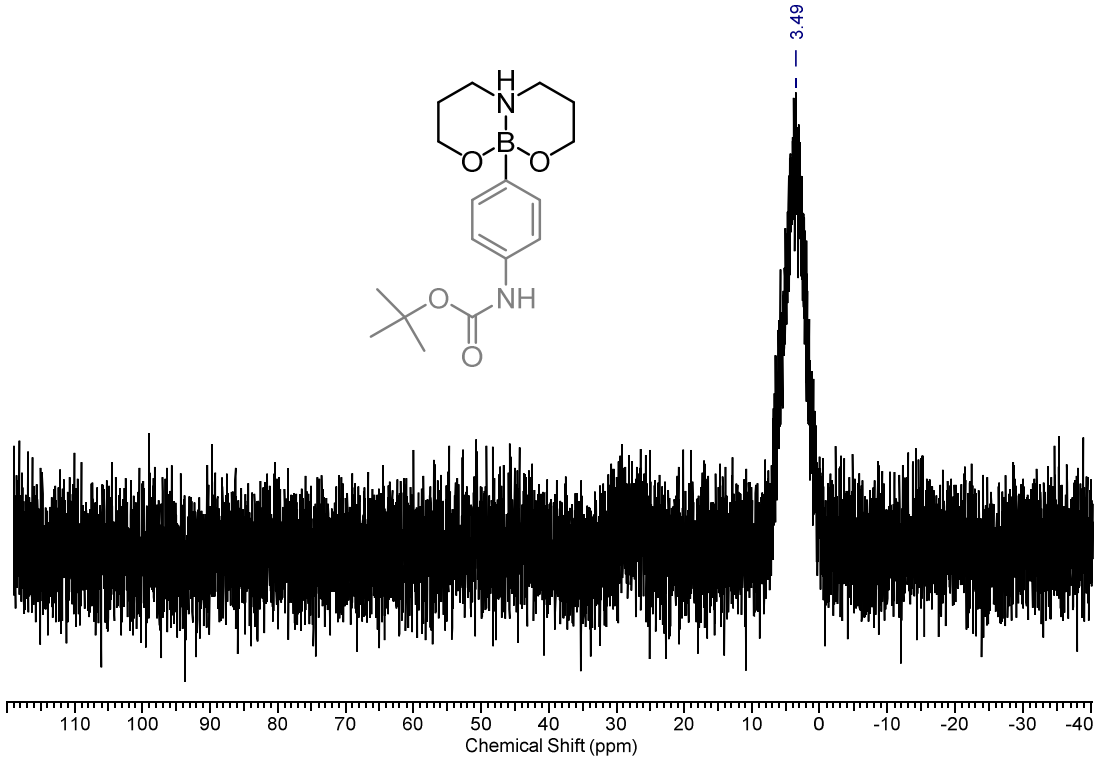

1q. (^1H NMR, 400 MHz, DMSO-d_6, 298K):

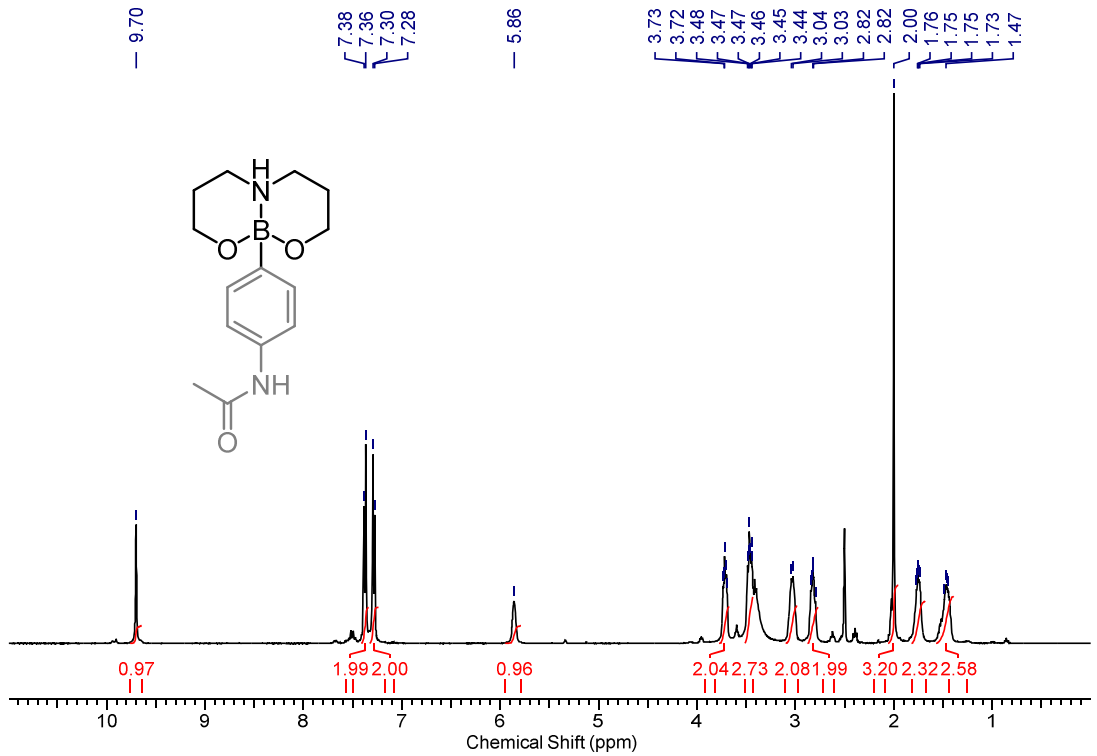

1q. ($^{13}C\{^{1}H\}$ NMR, 100 MHz, DMSO-d_6, 298K):

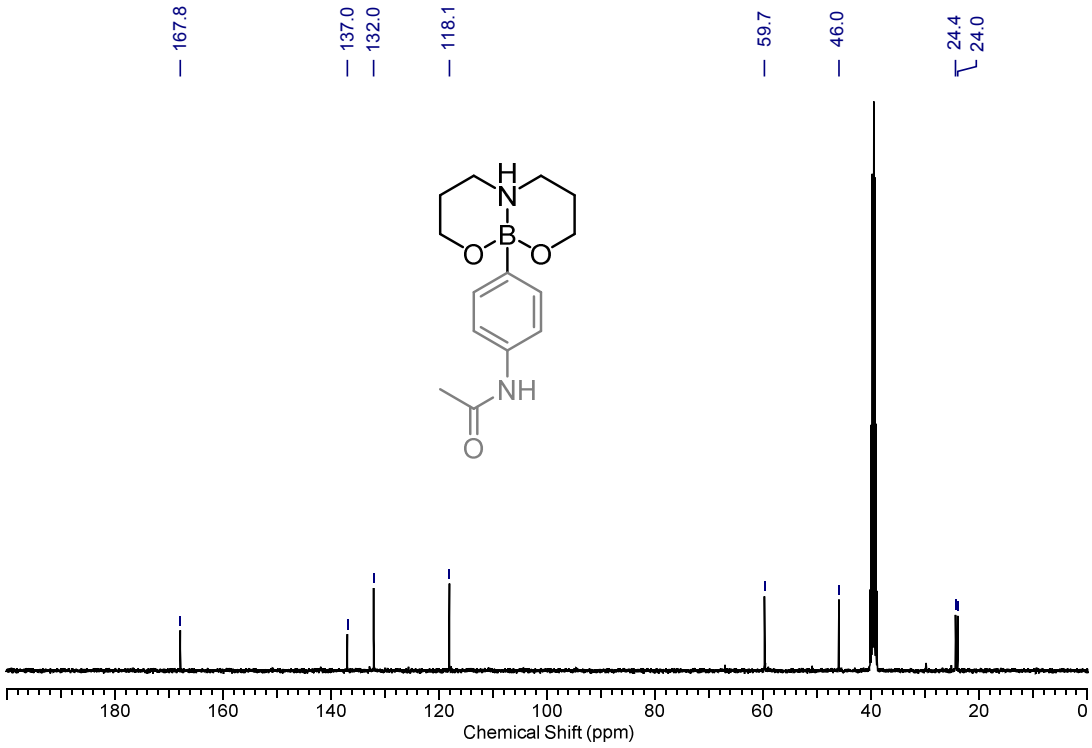

1q. ($^{11}B\{^{1}H\}$ NMR (baseline corrected), 128.4 MHz, DMSO-d_6, 298K):

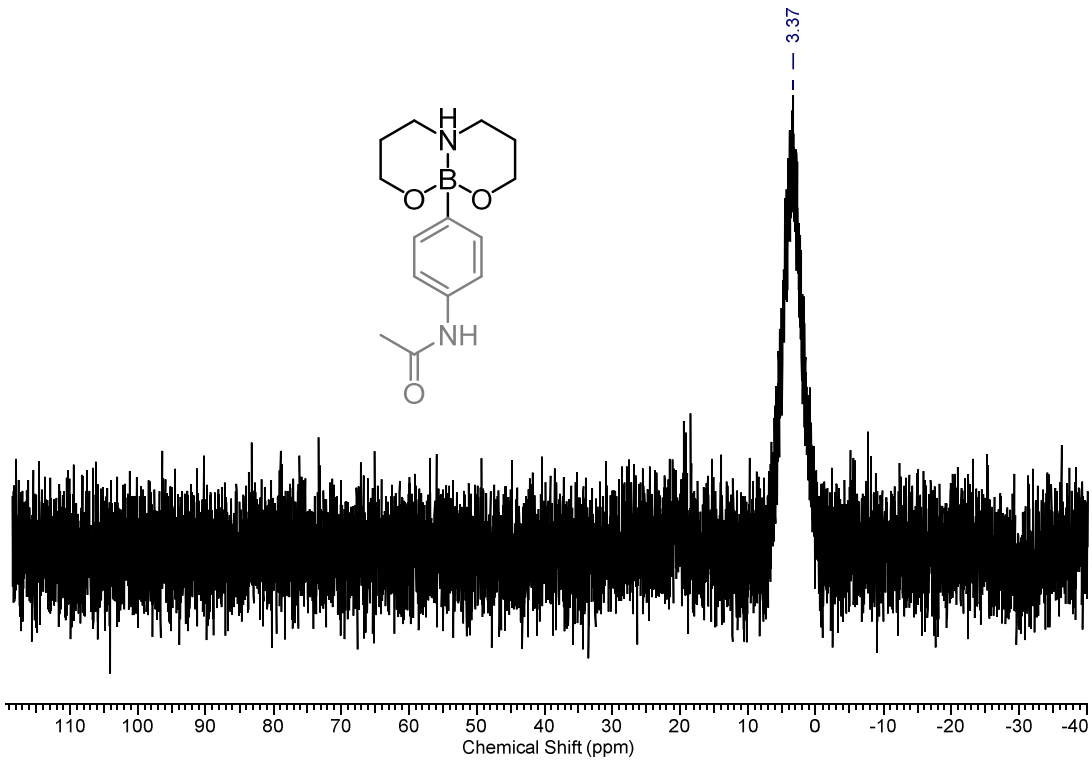

K[2a]. (^{1}H NMR, 400 MHz, THF-d_8, 298K):

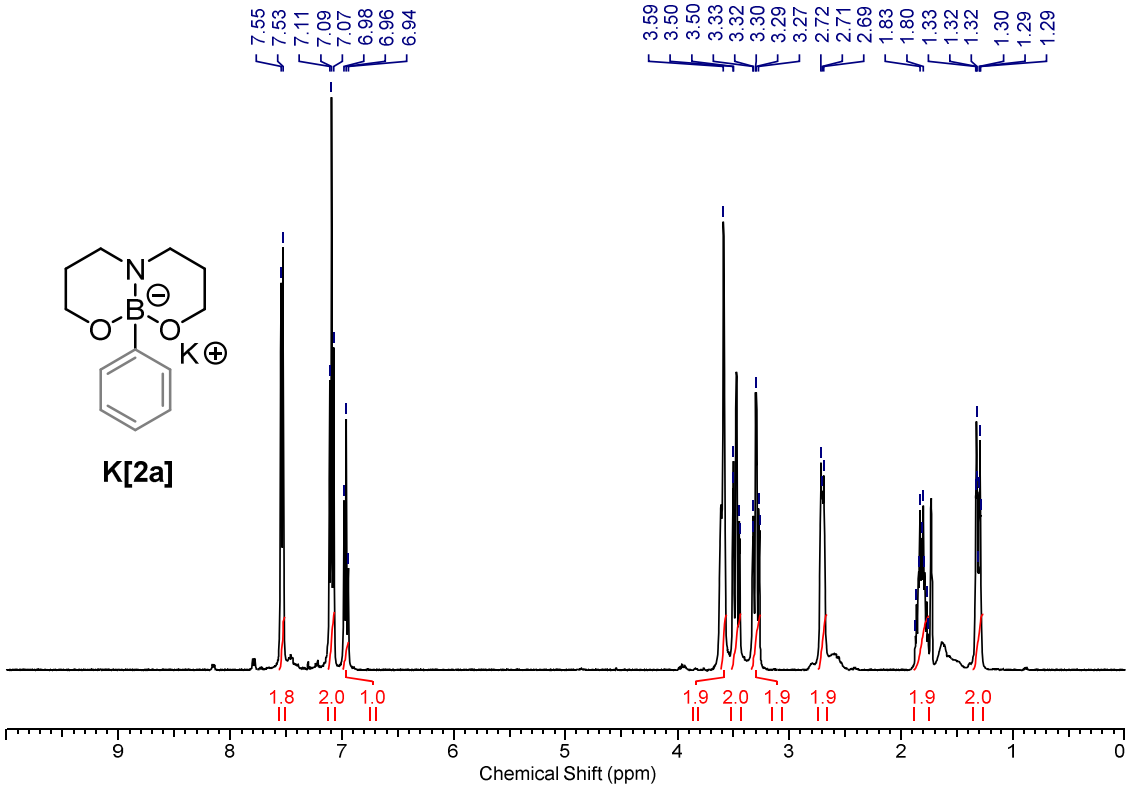

K[2a]. (^{13}C{^{1}H} NMR, 100 MHz, THF-d_8, 298K):

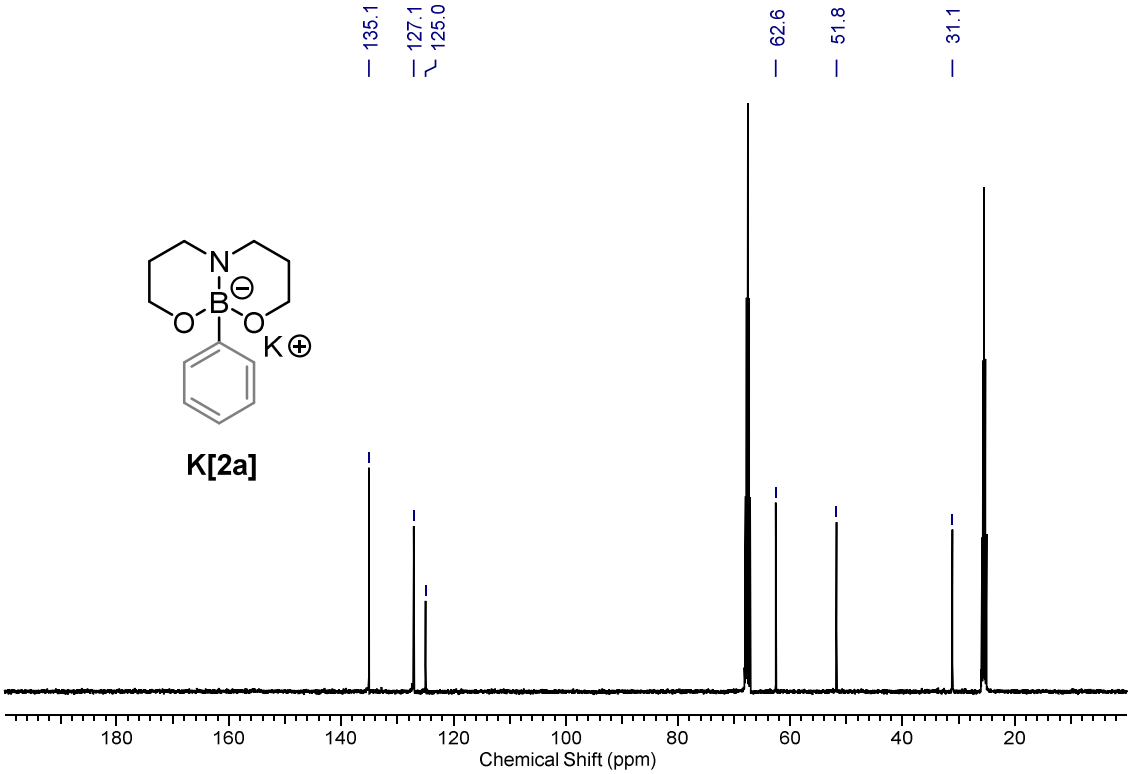

K[2a]. ($^{11}B\{^{1}H\}$ NMR (baseline corrected), 128.4 MHz, THF-d_8, 298K):

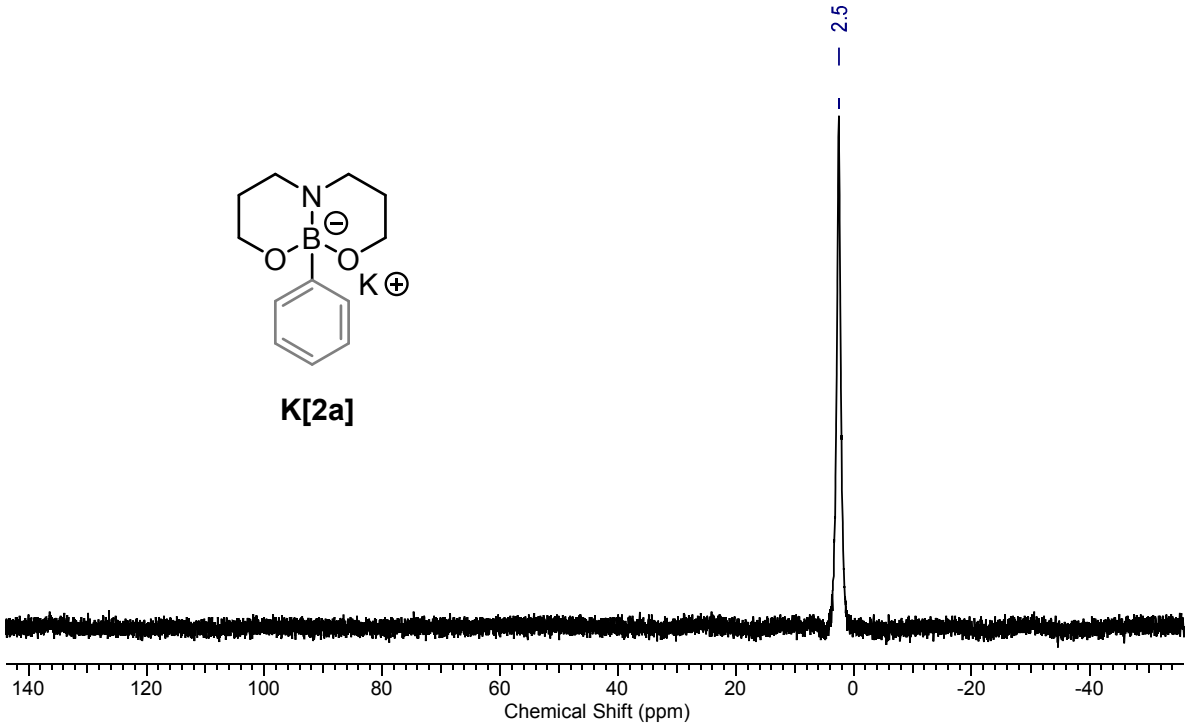

Li[2a]. (^{1}H NMR, 400 MHz, C_6D_6, 298K):

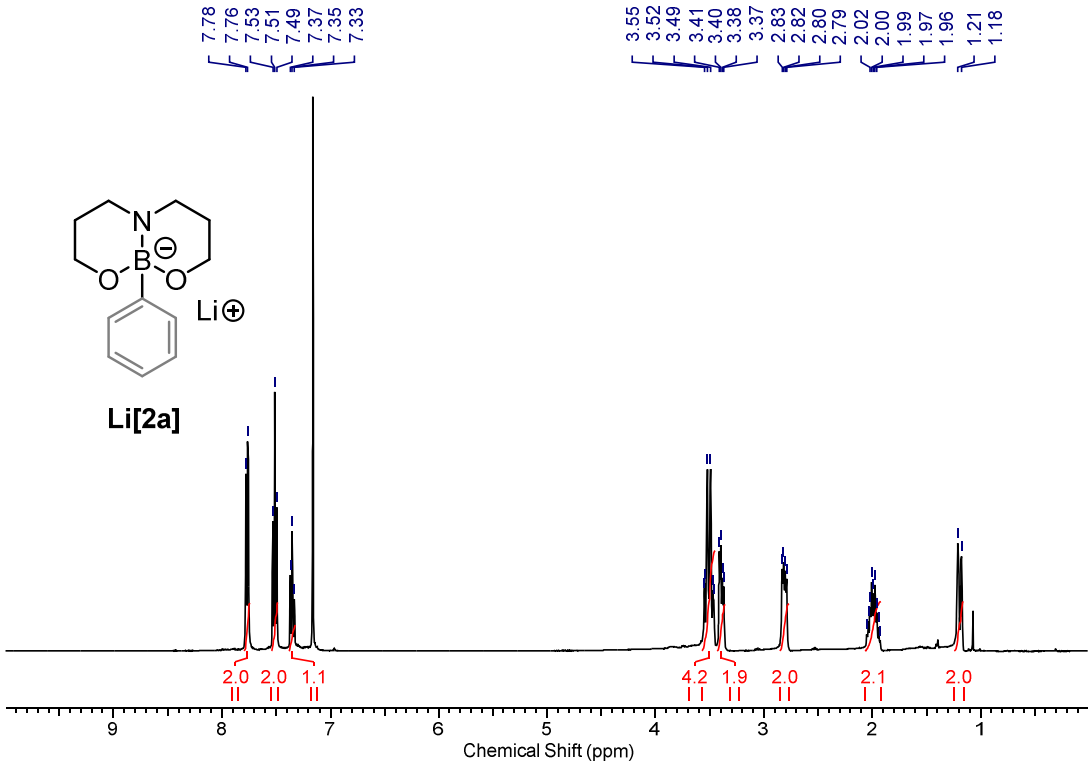

Li[2a]. ($^{13}C\{^{1}H\}$ NMR, 100 MHz, C_6D_6, 298K):

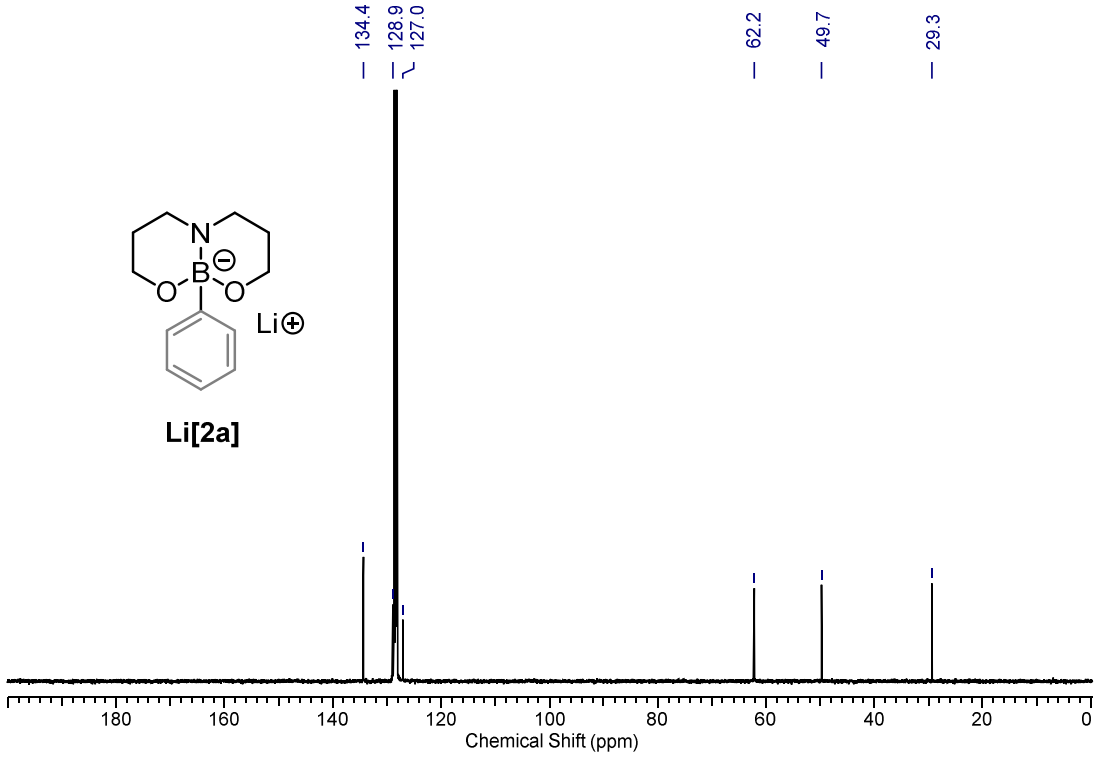

Li[2a]. ($^{11}B\{^{1}H\}$ NMR (baseline corrected), 128.4 MHz, C_6D_6, 298K):

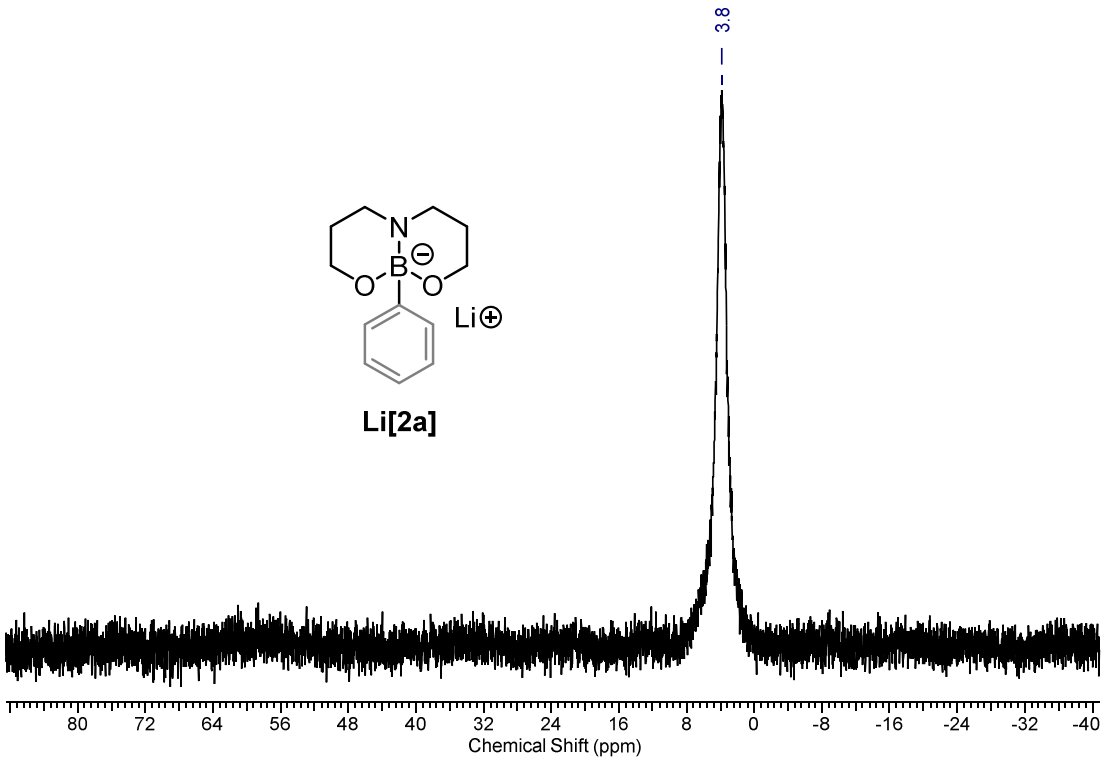

Li[2a]. (^{7}Li NMR, 155.51 MHz, C_6D_6, 298K):

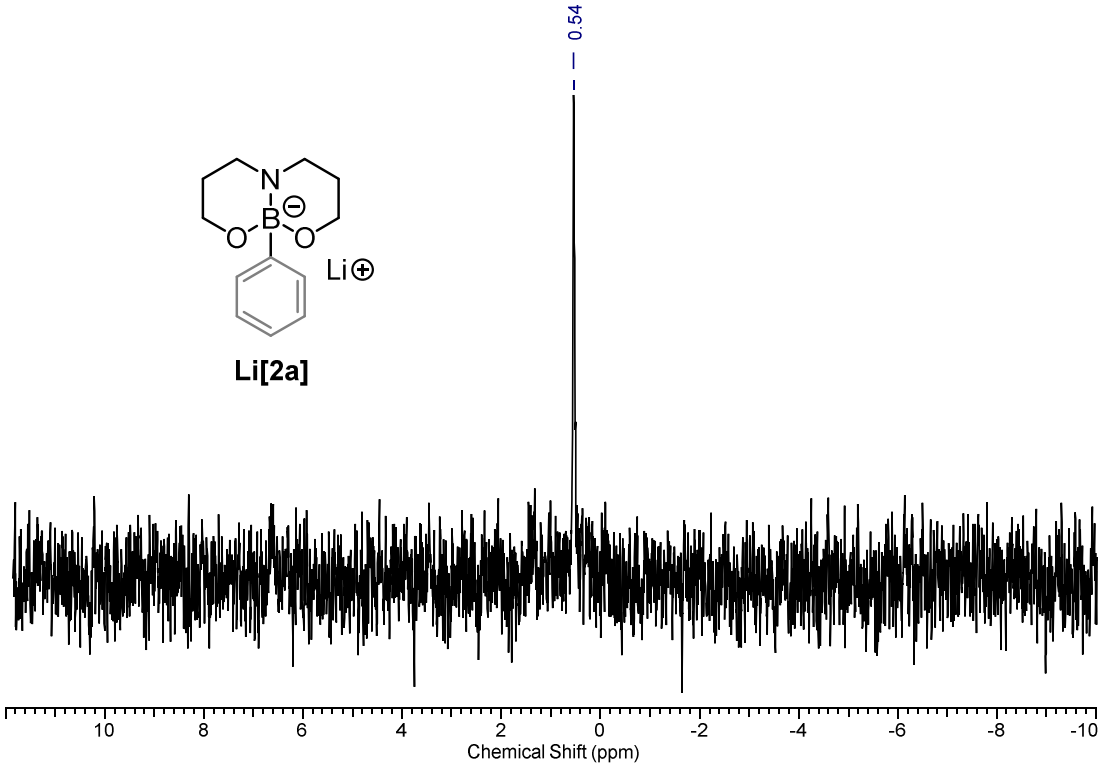

3. (^{1}H NMR, 400 MHz, $CDCl_3$, 298K):

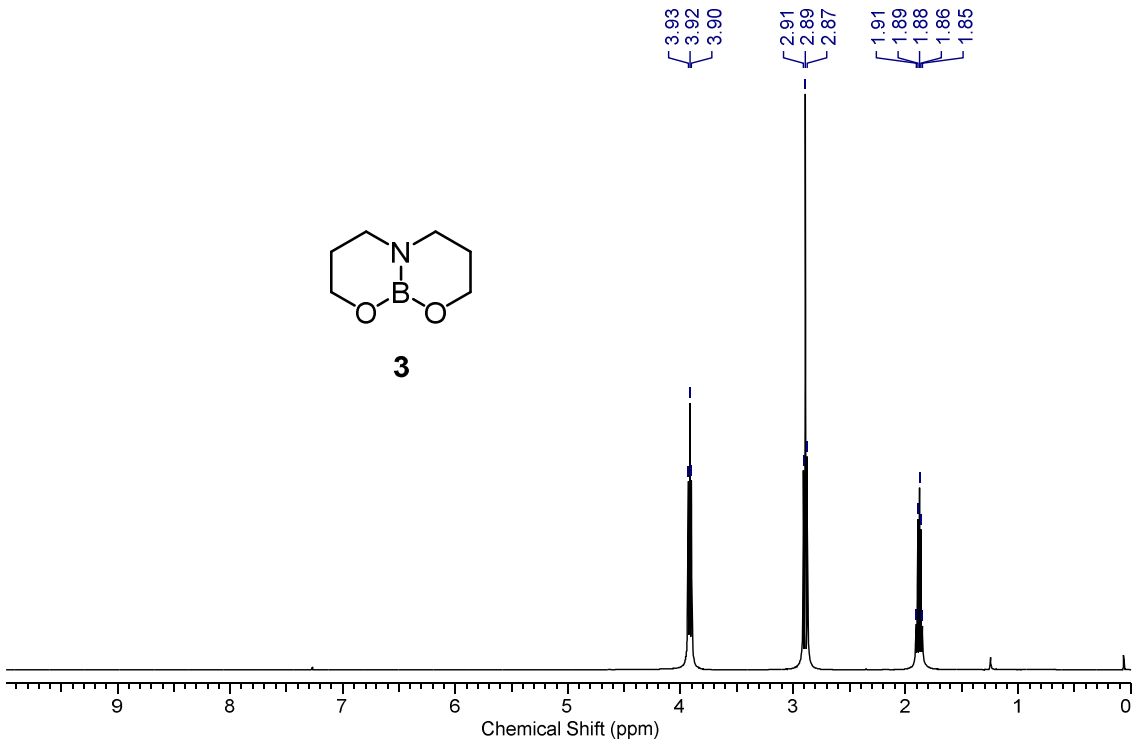

3. ($^{13}C\{^{1}H\}$ NMR, 100 MHz, $CDCl_3$, 298K):

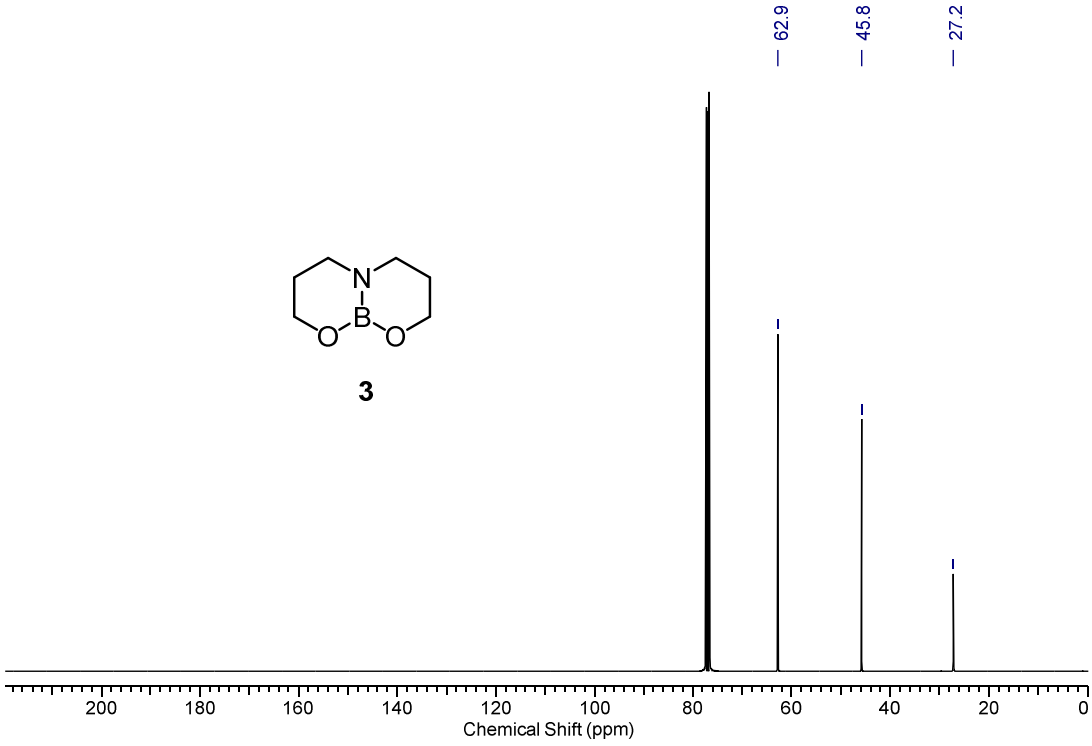

3. ($^{11}B\{^{1}H\}$ NMR (baseline corrected), 128.4 MHz, $CDCl_3$, 298K):

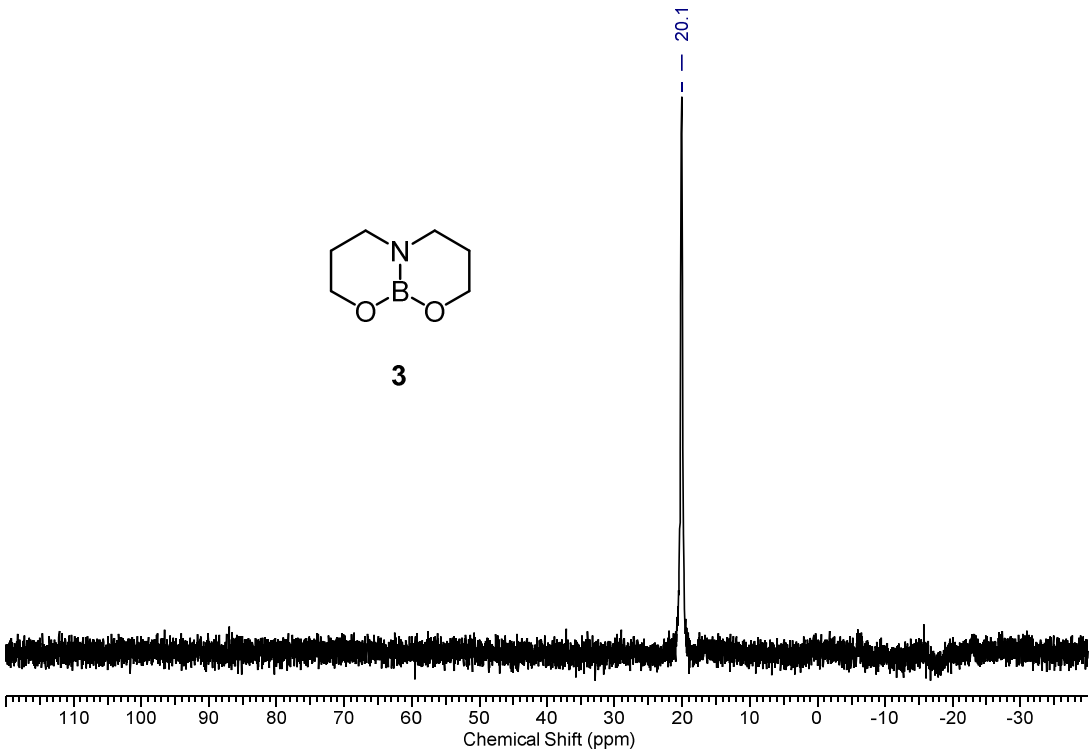

5. (^{1}H NMR, 400 MHz, protio-THF, 298K):

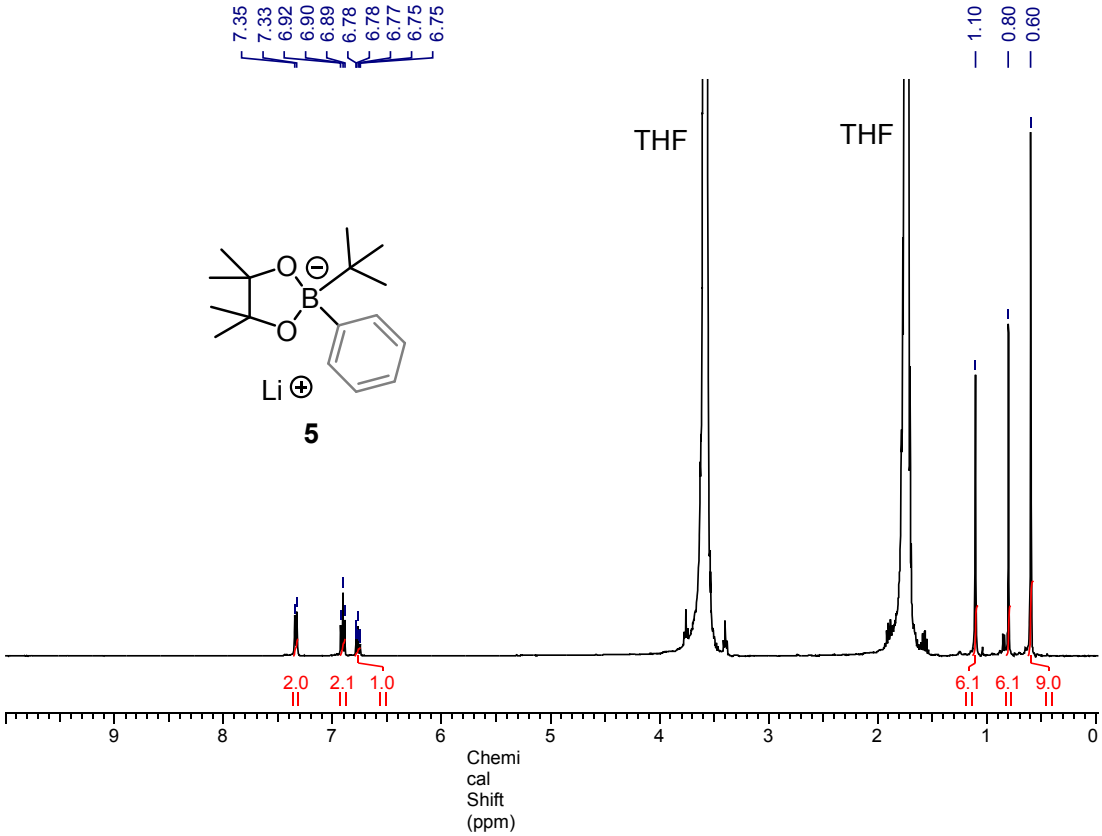

5. (^{13}C{^{1}H} NMR, 100 MHz, protio-THF, 298K):

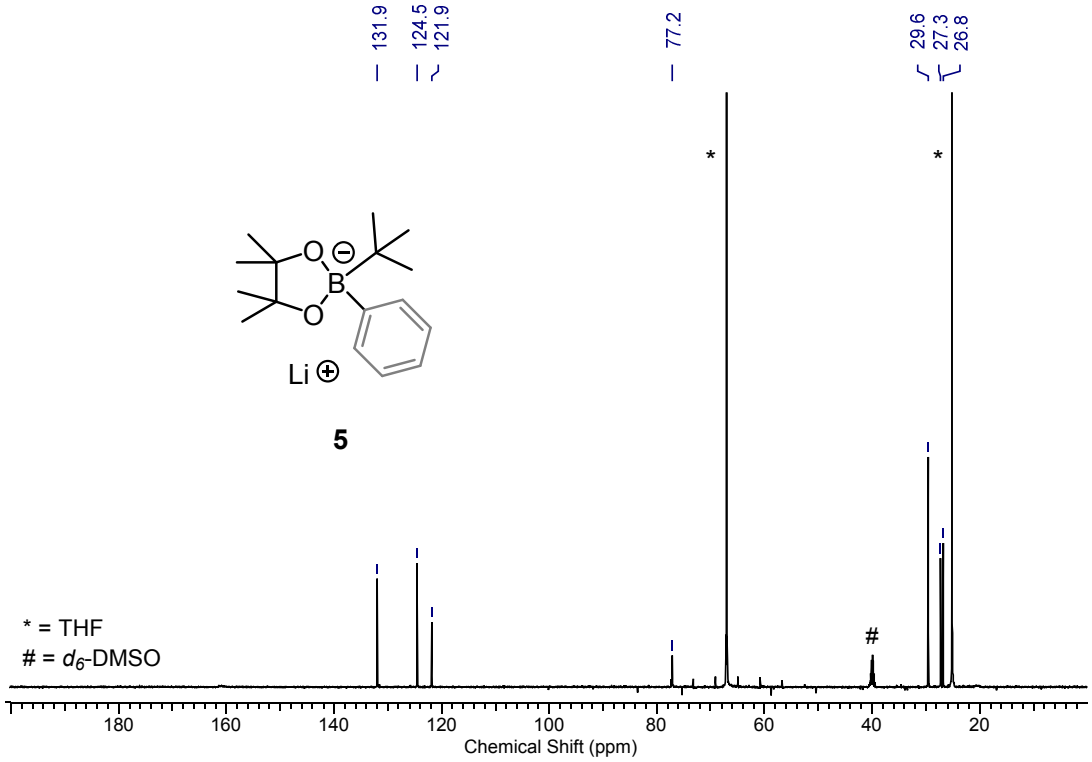

5. ($^{11}B\{^{1}H\}$ NMR (baseline corrected), 128.4 MHz, protio-THF, 298K):

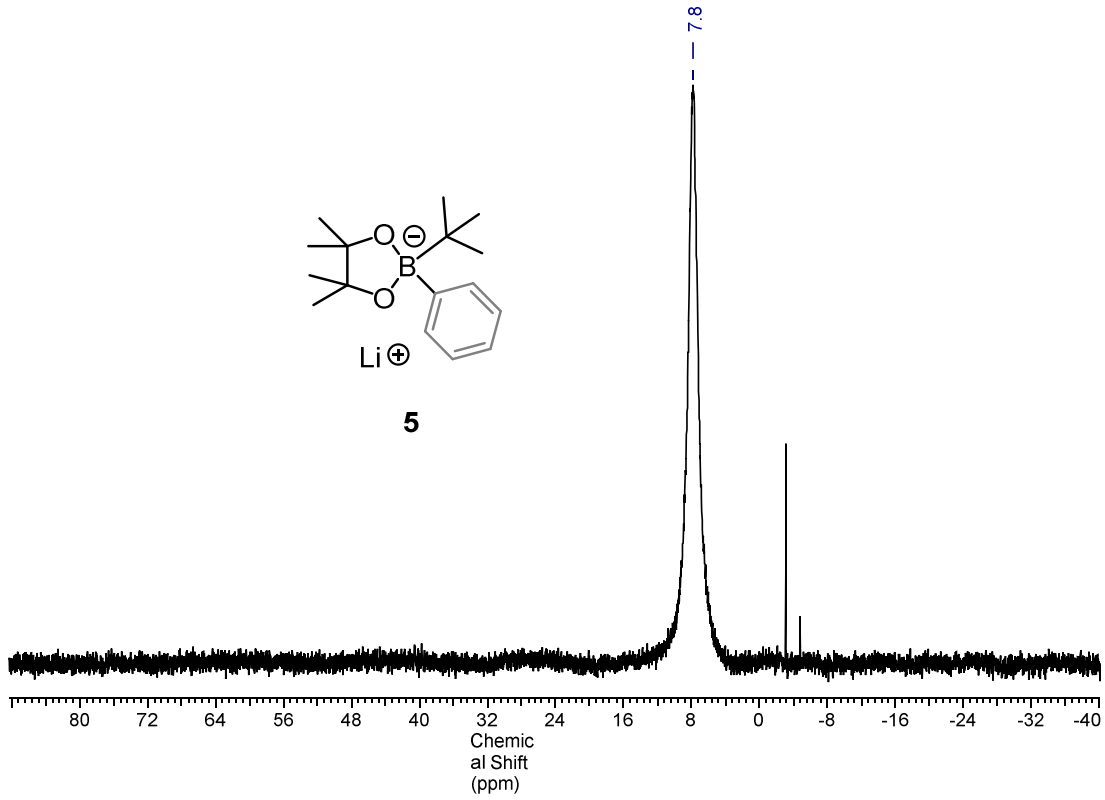

5. (^{7}Li NMR, 155.51 MHz, protio-THF, 298K):

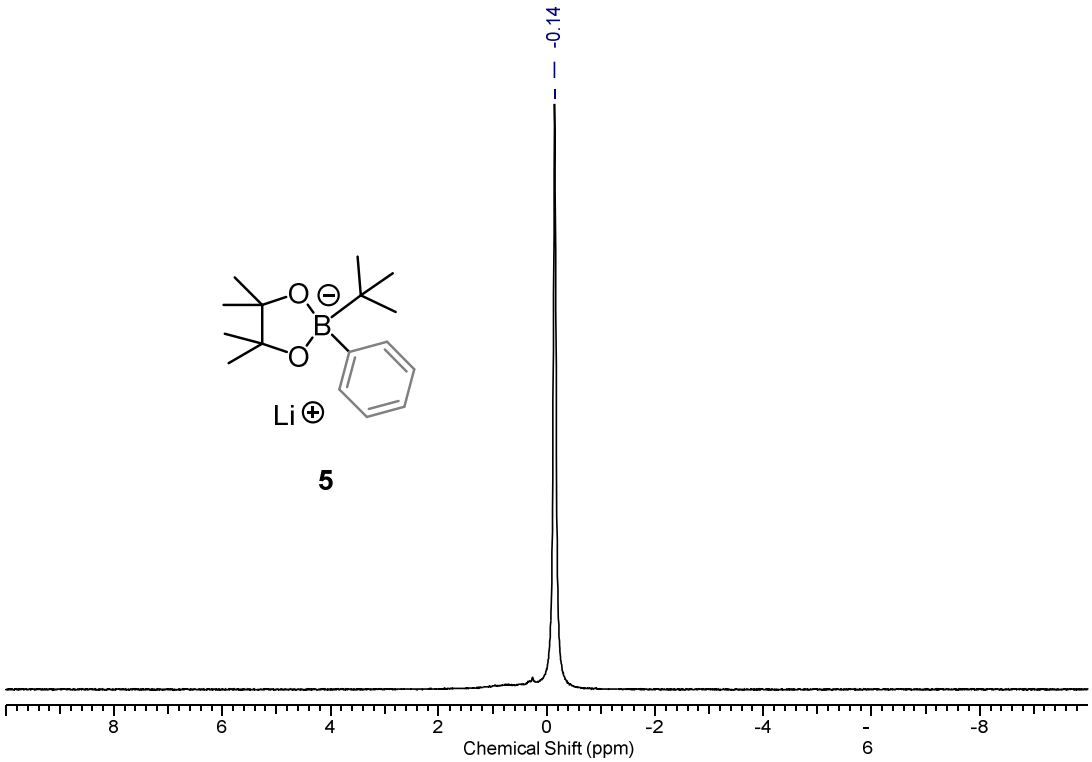

18. Full Cartesian coordinates for all M06-2X/6-311G+(d,p) structures:

18a. [BF_3]

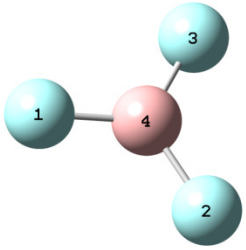

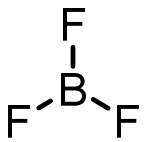

Centre Number	Atomic Number	Coordinates (Angstroms) X	Y	Z
1	9	-1.804805	-1.707334	-1.747601
2	9	0.052453	-3.020630	-1.747612
3	9	0.054147	-1.048370	-2.881291
4	5	-0.565908	-1.925250	-2.125324

18b. [$PhBF_3$]$^-$

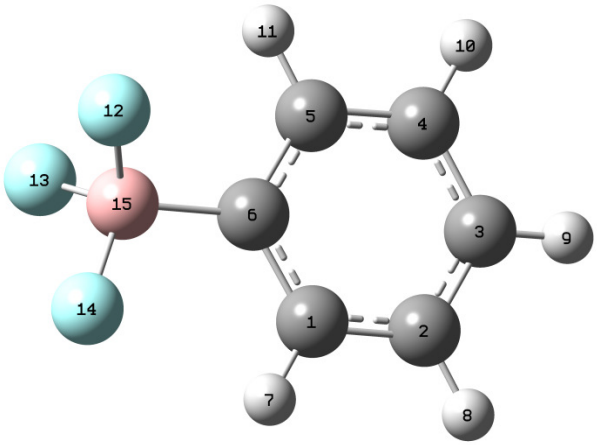

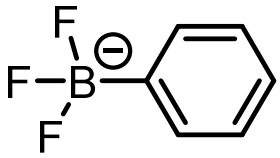

Centre Number	Atomic Number	Coordinates (Angstroms) X	Y	Z
1	6	1.864420	-2.588732	0.082683
2	6	3.259350	-2.591697	0.072251
3	6	3.957071	-1.389910	-0.008087
4	6	3.249458	-0.190725	-0.074955
5	6	1.856794	-0.203587	-0.062600
6	6	1.130873	-1.399809	0.014624
7	1	1.330065	-3.531470	0.149601
8	1	3.801952	-3.529695	0.127166
9	1	5.041354	-1.386099	-0.016766
10	1	3.785440	0.750689	-0.135456
11	1	1.319222	0.739575	-0.111806
12	9	-1.004784	-0.458412	0.945883
13	9	-0.983098	-1.004058	-1.281178
14	9	-1.017143	-2.670475	0.303111
15	5	-0.483790	-1.388001	-0.000548

Selected Bond Lengths: B15-C6 1.61478 Å

18c. [BPh_3]

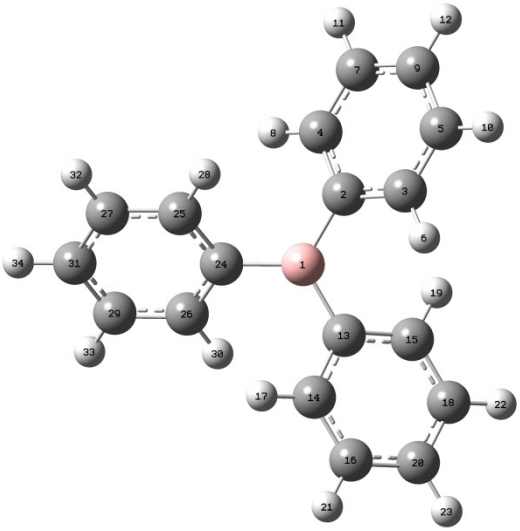

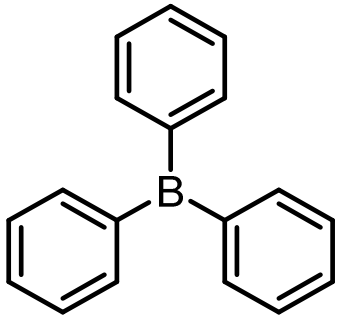

Centre Number	Atomic Number	Coordinates (Angstroms) X	Y	Z
1	5	0.933994	-1.767606	-0.004966
2	6	0.915043	-1.011513	1.366271
3	6	0.474877	-1.645402	2.540891
4	6	1.340960	0.323793	1.470984
5	6	0.445781	-0.976016	3.759403
6	1	0.137945	-2.675922	2.494771
7	6	1.344644	0.989874	2.691843
8	1	1.688145	0.842518	0.583197
9	6	0.889176	0.342050	3.837419
10	1	0.086410	-1.481074	4.648569
11	1	1.695383	2.013759	2.750941
12	1	0.880337	0.862935	4.788093
13	6	1.215351	-3.307650	-0.042046
14	6	0.624405	-4.136135	-1.011318
15	6	2.067879	-3.914371	0.896377
16	6	0.858180	-5.507087	-1.033478

17	1	-0.040653	-3.700377	-1.749950
18	6	2.330748	-5.279637	0.861721
19	1	2.542380	-3.303067	1.657104
20	6	1.718550	-6.079721	-0.099672
21	1	0.376782	-6.128172	-1.780010
22	1	3.005951	-5.720974	1.585802
23	1	1.911527	-7.146226	-0.121598
24	6	0.674100	-0.985245	-1.336053
25	6	-0.189013	0.123340	-1.375989
26	6	1.297580	-1.365241	-2.536840
27	6	-0.431237	0.811039	-2.560385
28	1	-0.687427	0.442176	-0.466216
29	6	1.084143	-0.663813	-3.718580
30	1	1.970371	-2.216625	-2.540597
31	6	0.211776	0.421751	-3.732855
32	1	-1.113054	1.653538	-2.569846
33	1	1.589676	-0.965695	-4.628588
34	1	0.033409	0.962685	-4.655244

18d. $[BPh_4]^-$

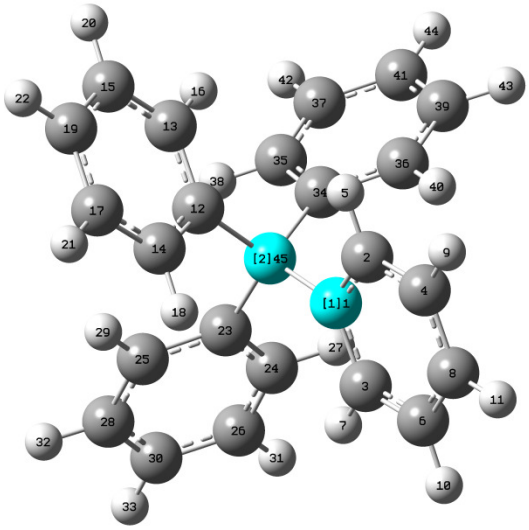

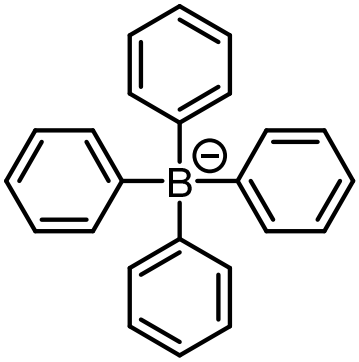

Center Number	Atomic Number	Coordinates (Angstroms) X	Y	Z
1	6	0.994220	-0.500982	1.209463
2	6	2.094503	-1.329517	0.917582
3	6	0.820403	-0.179576	2.562754
4	6	2.951296	-1.817131	1.899702
5	1	2.284784	-1.596732	-0.119363
6	6	1.673065	-0.655332	3.562571
7	1	-0.001877	0.467227	2.852697
8	6	2.743391	-1.481127	3.237518
9	1	3.785370	-2.455196	1.624798
10	1	1.500046	-0.375942	4.597215
11	1	3.409107	-1.852860	4.008765
12	6	0.946479	0.515364	-1.251140
13	6	0.742870	0.174598	-2.595488
14	6	2.038854	1.366739	-0.998353
15	6	1.560274	0.653343	-3.622881
16	1	-0.074442	-0.490582	-2.856374

17	6	2.860619	1.857729	-2.008083
18	1	2.250924	1.648721	0.030382
19	6	2.623856	1.501596	-3.335930
20	1	1.365533	0.358143	-4.649273
21	1	3.690001	2.513594	-1.762586
22	1	3.262504	1.875052	-4.128860
23	6	-0.967028	1.228146	0.522891
24	6	-2.051107	0.947902	1.376270
25	6	-0.786140	2.579673	0.197839
26	6	-2.885618	1.938776	1.884160
27	1	-2.246465	-0.087324	1.646229
28	6	-1.616491	3.588322	0.693888
29	1	0.023329	2.861456	-0.468307
30	6	-2.670866	3.274472	1.544125
31	1	-3.707928	1.672370	2.540746
32	1	-1.438898	4.621186	0.410770
33	1	-3.319516	4.052655	1.931139
34	6	-0.972925	-1.233062	-0.493422
35	6	-2.082923	-0.968591	-1.318145
36	6	-0.775168	-2.579531	-0.157661
37	6	-2.927452	-1.969619	-1.788046
38	1	-2.291072	0.062076	-1.596175
39	6	-1.615215	-3.598196	-0.615467
40	1	0.055945	-2.848909	0.486833
41	6	-2.696382	-3.299886	-1.437188
42	1	-3.769940	-1.715253	-2.423597
43	1	-1.424093	-4.626612	-0.324994
44	1	-3.352475	-4.085978	-1.794605
45	5	0.000157	0.002810	-0.004045

Selected Bond Lengths: B45-C1 1.64760 Å

18e. [B(4-ClPh)$_3$]

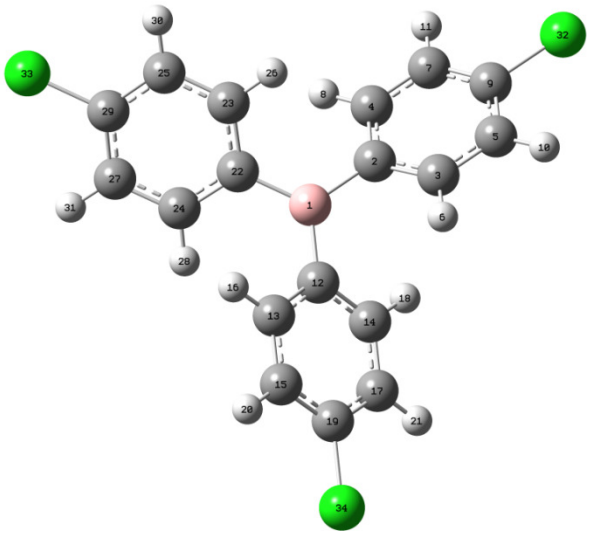

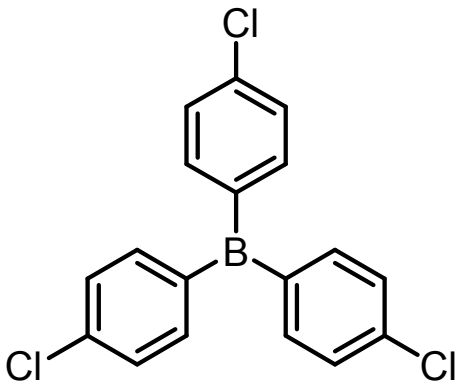

Centre Number	Atomic Number	Coordinates (Angstroms) X	Y	Z
1	5	0.930442	-1.769583	-0.005398
2	6	0.912317	-1.013022	1.364092
3	6	0.475934	-1.645359	2.539940
4	6	1.336796	0.321944	1.467228
5	6	0.446923	-0.982807	3.760642
6	1	0.136409	-2.674916	2.501101
7	6	1.346351	0.995211	2.682580
8	1	1.684043	0.844490	0.582194
9	6	0.892707	0.331674	3.815197
10	1	0.093190	-1.475337	4.657574
11	1	1.693489	2.018260	2.753454
12	6	1.212822	-3.307995	-0.041613
13	6	0.628245	-4.136711	-1.013362
14	6	2.060894	-3.914498	0.899700
15	6	0.859129	-5.506595	-1.042273
16	1	-0.036388	-3.707443	-1.755558

17	6	2.330350	-5.277259	0.872439
18	1	2.535551	-3.307974	1.663580
19	6	1.716301	-6.057936	-0.098263
20	1	0.389559	-6.138403	-1.785560
21	1	2.999670	-5.730002	1.593086
22	6	0.670893	-0.987834	-1.335303
23	6	-0.189414	0.121872	-1.374725
24	6	1.293246	-1.366673	-2.536025
25	6	-0.434444	0.816467	-2.552821
26	1	-0.691783	0.443536	-0.468592
27	6	1.087383	-0.668848	-3.719707
28	1	1.967259	-2.216540	-2.546300
29	6	0.216336	0.413028	-3.711714
30	1	-1.111228	1.661201	-2.574673
31	1	1.586840	-0.959313	-4.635316
32	17	0.883735	1.171451	5.347674
33	17	-0.066189	1.290617	-5.195739
34	17	2.030534	-7.776068	-0.134527

18f. $[PhB(4\text{-}ClPh)_3]^-$

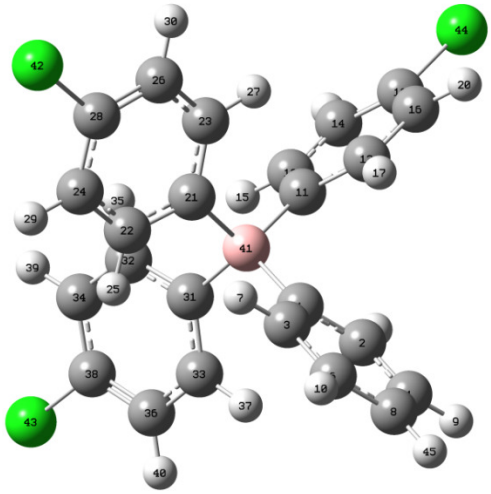

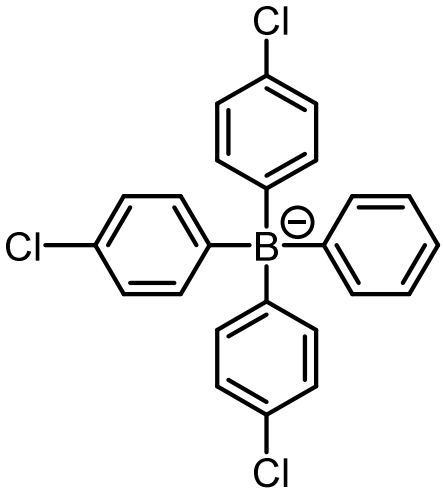

Centre Number	Atomic Number	Coordinates (Angstroms) X	Y	Z
1	6	0.776655	-0.818860	1.039338
2	6	0.510205	-1.549753	2.211895
3	6	1.233146	0.492031	1.230122
4	6	0.670437	-1.011456	3.484533
5	1	0.165823	-2.577179	2.119406
6	6	1.403919	1.047307	2.499855
7	1	1.471474	1.103192	0.365026
8	6	1.121087	0.299087	3.636140
9	1	0.446807	-1.612449	4.360159
10	1	1.763851	2.066351	2.598769
11	6	1.130304	-3.031530	-0.404895
12	6	0.485651	-4.155332	-0.936278
13	6	2.397694	-3.266190	0.158357
14	6	1.054522	-5.429437	-0.925943
15	1	-0.502062	-4.048950	-1.372553
16	6	2.997023	-4.520544	0.181729
17	1	2.935260	-2.433065	0.603333

18	6	2.309943	-5.594613	-0.367230
19	1	0.528607	-6.280129	-1.342625
20	1	3.976299	-4.667617	0.621727
21	6	1.242802	-0.622990	-1.613904
22	6	0.668824	0.588979	-2.038045
23	6	2.444759	-0.976872	-2.238948
24	6	1.248104	1.405939	-3.002565
25	1	-0.272971	0.905885	-1.598027
26	6	3.051988	-0.183992	-3.213914
27	1	2.934475	-1.906899	-1.970065
28	6	2.443983	1.003507	-3.581486
29	1	0.782092	2.335731	-3.306239
30	1	3.980593	-0.486924	-3.682711
31	6	-1.098067	-1.550984	-0.760164
32	6	-1.539603	-1.825866	-2.066891
33	6	-2.105546	-1.343047	0.189648
34	6	-2.883759	-1.908954	-2.412595
35	1	-0.799903	-1.976721	-2.848883
36	6	-3.464083	-1.413168	-0.122320
37	1	-1.832558	-1.110365	1.213727
38	6	-3.836171	-1.700099	-1.424131
39	1	-3.191322	-2.126601	-3.428458
40	1	-4.220869	-1.244636	0.634662
41	5	0.513943	-1.505740	-0.431263
42	17	3.192736	2.017018	-4.811678
43	17	-5.545077	-1.793046	-1.837830
44	17	3.044859	-7.194886	-0.341247
45	1	1.252657	0.725494	4.624517

Selected Bond Lengths: B41-C1 1.64423 Å

18g. [Triolborane]

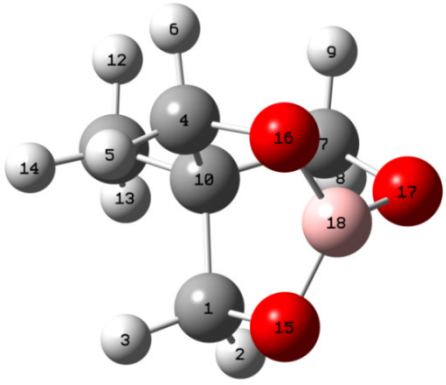

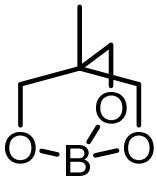

Centre Number	Atomic Number	Coordinates (Angstroms) X	Y	Z
1	6	-2.744440	-0.790327	0.738628
2	1	-2.981846	-1.706759	0.191025
3	1	-3.206109	-0.817982	1.727433
4	6	-2.578250	1.691868	0.636242
5	1	-2.809085	1.702313	1.705102
6	1	-2.928019	2.615165	0.170938
7	6	-2.592846	0.358339	-1.466277
8	1	-3.053364	-0.452265	-2.033798
9	1	-2.706965	1.303054	-2.005188
10	6	-3.216088	0.457362	-0.050398
11	6	-4.731658	0.556164	-0.103703
12	1	-5.040704	1.388903	-0.739414
13	1	-5.162143	-0.362727	-0.507886
14	1	-5.142396	0.716831	0.895577
15	8	-1.299862	-0.695253	0.929706
16	8	-1.131322	1.625650	0.449836
17	8	-1.173624	0.045348	-1.324553
18	5	-1.013376	0.313061	0.024695

18h. [Triolborate]$^-$

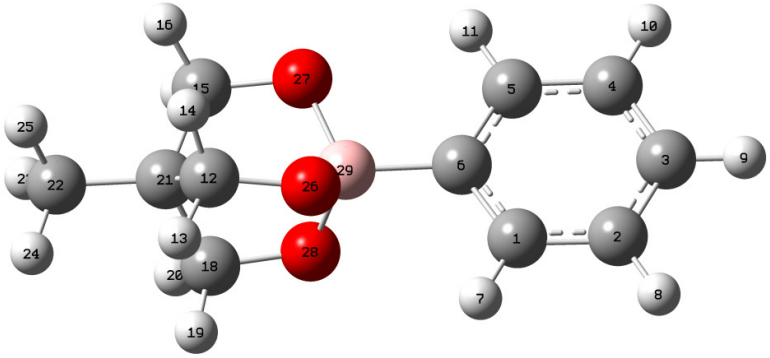

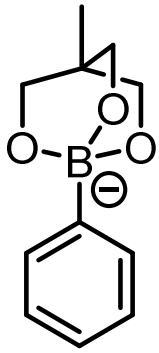

Centre Number	Atomic Number	Coordinates (Angstroms) X	Y	Z
1	6	1.524129	-1.018154	-0.260902
2	6	2.910723	-1.149788	-0.226374
3	6	3.701760	-0.078782	0.187734
4	6	3.090497	1.114672	0.562729
5	6	1.700331	1.230149	0.522866
6	6	0.883222	0.171486	0.110960
7	1	0.917951	-1.860132	-0.583530
8	1	3.377919	-2.084212	-0.520462
9	1	4.781762	-0.174855	0.216824
10	1	3.697677	1.954335	0.885941
11	1	1.230760	2.163027	0.819112
12	6	-2.747787	-0.659196	0.899656
13	1	-3.267072	-1.596239	0.648944
14	1	-3.025694	-0.392937	1.933021
15	6	-2.567055	1.756434	0.438003
16	1	-3.050785	2.077370	1.372346
17	1	-2.737493	2.546609	-0.312061
18	6	-2.602165	0.142856	-1.424002
19	1	-2.911509	-0.867904	-1.738376

20	1	-2.992247	0.853881	-2.167205
21	6	-3.212162	0.452422	-0.050674
22	6	-4.725856	0.555573	-0.110660
23	1	-5.034592	1.415883	-0.712407
24	1	-5.161118	-0.343357	-0.557582
25	1	-5.149771	0.674382	0.891135
26	8	-1.352322	-0.844003	0.788699
27	8	-1.186035	1.567304	0.660441
28	8	-1.194490	0.241127	-1.365222
29	5	-0.723494	0.291012	0.051510

Selected Bond Lengths: B29-C6 1.61225 Å

18i. [BPin^{t}Bu]

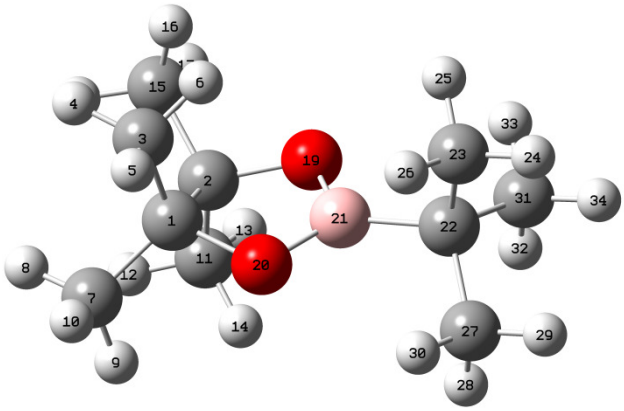

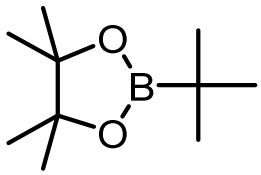

Centre Number	Atomic Number	Coordinates (Angstroms) X	Y	Z
1	6	-1.851129	2.168611	-1.068748
2	6	-0.364670	2.333383	-1.519038
3	6	-2.331228	3.317171	-0.186077
4	1	-2.453221	4.235758	-0.763240
5	1	-3.295747	3.047771	0.247910
6	1	-1.625851	3.504121	0.627641
7	6	-2.833507	1.916209	-2.198245
8	1	-2.828745	2.756812	-2.897248
9	1	-2.589868	1.004592	-2.743112
10	1	-3.840891	1.817263	-1.789429
11	6	-0.017121	1.481819	-2.736546
12	1	-0.481274	1.879089	-3.641380
13	1	1.065871	1.487208	-2.870993
14	1	-0.343597	0.448396	-2.598420
15	6	0.080024	3.769595	-1.729108
16	1	-0.002541	4.349420	-0.810273
17	1	1.121169	3.785030	-2.056968
18	1	-0.529619	4.243898	-2.502487

19	8	0.356032	1.771538	-0.392792
20	8	-1.780187	0.992656	-0.223655
21	5	-0.494190	0.909354	0.253652
22	6	-0.074643	-0.015403	1.454046
23	6	-0.465913	0.732129	2.744906
24	1	-0.201453	0.128146	3.620018
25	1	0.057256	1.689597	2.827548
26	1	-1.541478	0.926973	2.780782
27	6	-0.835261	-1.347726	1.400923
28	1	-0.576323	-1.920800	0.505776
29	1	-0.584075	-1.958995	2.274841
30	1	-1.916001	-1.186450	1.397156
31	6	1.436160	-0.273880	1.458353
32	1	1.749220	-0.815727	0.561330
33	1	1.997744	0.662912	1.495842
34	1	1.715813	-0.875142	2.330416

18j. [PhBPin^{t}Bu]$^{-}$

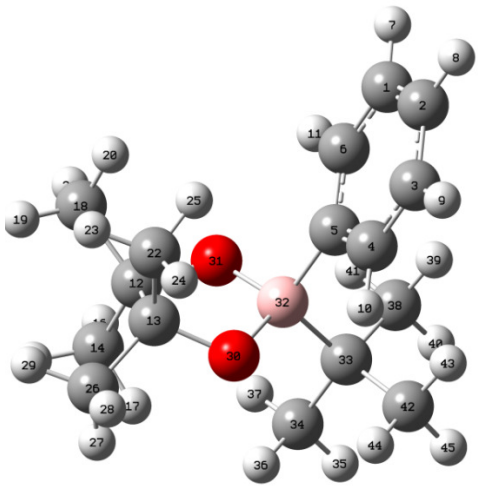

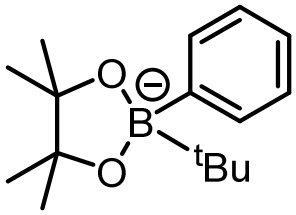

Centre Number	Atomic Number	Coordinates (Angstroms) X	Y	Z
1	6	-0.963684	-3.145792	-2.388241
2	6	0.316943	-3.406575	-2.871708
3	6	1.359664	-2.550449	-2.520240
4	6	1.114502	-1.454290	-1.694097
5	6	-0.162153	-1.162730	-1.192128
6	6	-1.188448	-2.041820	-1.565328
7	1	-1.786708	-3.800463	-2.658820
8	1	0.499353	-4.259316	-3.516902
9	1	2.360981	-2.736600	-2.896875
10	1	1.935318	-0.786655	-1.444716
11	1	-2.196056	-1.840575	-1.211408
12	6	-1.864471	1.894046	-1.053511
13	6	-0.401098	2.064029	-1.598572
14	6	-2.208223	2.955088	-0.000158
15	1	-2.355357	3.940793	-0.451891
16	1	-3.135320	2.661682	0.499431
17	1	-1.422667	3.026486	0.751466

18	6	-2.938532	1.932456	-2.140694
19	1	-2.905886	2.873347	-2.699696
20	1	-2.817673	1.103728	-2.839449
21	1	-3.925812	1.846510	-1.677931
22	6	-0.242786	1.488487	-3.015472
23	1	-0.741999	2.117853	-3.757945
24	1	0.823093	1.448182	-3.256212
25	1	-0.641984	0.476257	-3.084670
26	6	0.093997	3.508647	-1.613965
27	1	0.143930	3.917425	-0.604096
28	1	1.097600	3.544579	-2.046643
29	1	-0.559802	4.143301	-2.220483
30	8	0.370629	1.322271	-0.677107
31	8	-1.856227	0.615959	-0.449619
32	5	-0.443610	0.148967	-0.235782
33	6	-0.128375	-0.208991	1.347332
34	6	-0.447459	0.986886	2.249603
35	1	-0.214395	0.759824	3.300218
36	1	0.134294	1.866940	1.957242
37	1	-1.507842	1.248773	2.189499
38	6	-0.979908	-1.393499	1.818781
39	1	-0.755302	-2.299145	1.246693
40	1	-0.799288	-1.614077	2.880865
41	1	-2.047387	-1.178450	1.699702
42	6	1.350899	-0.565684	1.537846
43	1	1.621214	-1.464811	0.975710
44	1	1.995677	0.250162	1.194011
45	1	1.579773	-0.753979	2.596936

Selected Bond Lengths: B32-C5 1.64753 Å

18k. [BPin^{n}Bu]

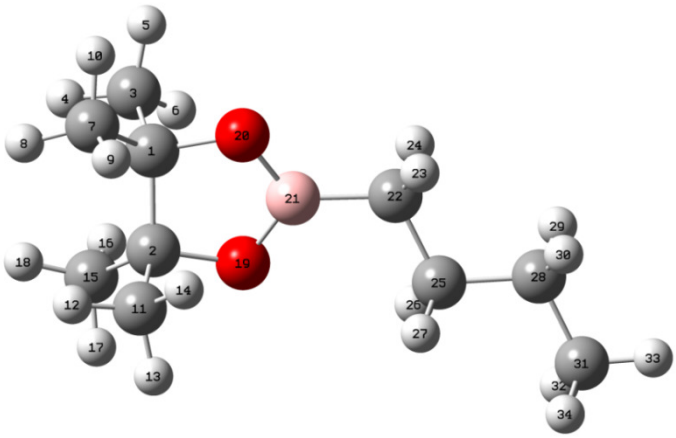

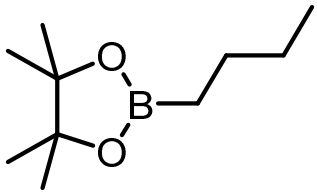

Centre Number	Atomic Number	Coordinates (Angstroms) X	Y	Z
1	6	-1.999269	2.073316	-1.337479
2	6	-0.541466	2.595081	-1.124699
3	6	-3.058672	3.099733	-0.946747
4	1	-3.092702	3.924124	-1.661699
5	1	-4.034056	2.610224	-0.934456
6	1	-2.864464	3.506434	0.048515
7	6	-2.280584	1.523172	-2.724294
8	1	-2.128554	2.301149	-3.477236
9	1	-1.633885	0.677598	-2.956988
10	1	-3.319019	1.191227	-2.780650
11	6	0.489917	1.813813	-1.933764
12	1	0.404972	2.035210	-2.999441
13	1	1.488829	2.097560	-1.597964
14	1	0.368626	0.737909	-1.787755
15	6	-0.363686	4.087342	-1.337214
16	1	-0.985539	4.665329	-0.654298
17	1	0.680498	4.357535	-1.168640
18	1	-0.624928	4.354848	-2.364548

19	8	-0.307822	2.279544	0.271120
20	8	-2.078185	0.995661	-0.371628
21	5	-1.152593	1.252066	0.611168
22	6	-1.080862	0.468783	1.962462
23	1	-1.265819	-0.593982	1.765662
24	1	-1.926529	0.793316	2.584065
25	6	0.225003	0.645819	2.742033
26	1	0.396732	1.711158	2.931448
27	1	1.068995	0.309472	2.128552
28	6	0.237746	-0.110555	4.068254
29	1	-0.602522	0.231308	4.682940
30	1	0.064758	-1.175070	3.874638
31	6	1.545550	0.068559	4.835072
32	1	1.720789	1.123520	5.062929
33	1	1.538590	-0.482189	5.777981
34	1	2.393526	-0.288045	4.243896

18l. [PhBPin^{n}Bu]$^{-}$

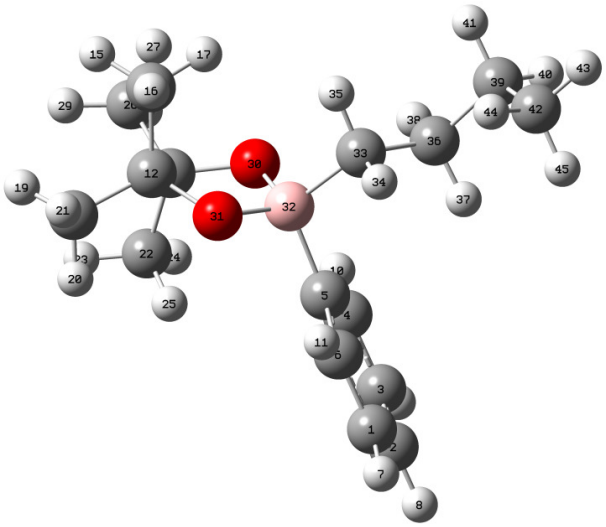

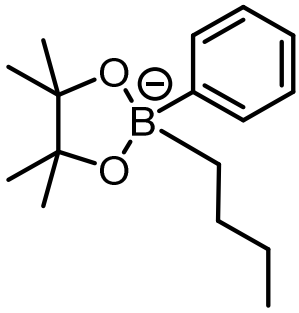

Centre Number	Atomic Number	Coordinates (Angstroms) X	Y	Z
1	6	-0.735709	-3.440511	-1.880716
2	6	0.474939	-3.600155	-2.553529
3	6	1.386182	-2.545914	-2.566730
4	6	1.082735	-1.351614	-1.913275
5	6	-0.124473	-1.160242	-1.226744
6	6	-1.020104	-2.239864	-1.230177
7	1	-1.455589	-4.253246	-1.865816
8	1	0.703087	-4.531257	-3.060956
9	1	2.331786	-2.657122	-3.088927
10	1	1.794051	-0.530219	-1.940610
11	1	-1.971998	-2.134148	-0.714227
12	6	-1.831580	2.011984	-1.131127
13	6	-0.406546	2.147804	-1.757367
14	6	-2.003343	2.947777	0.073752
15	1	-2.099606	3.994032	-0.231547
16	1	-2.909447	2.660107	0.613095

17	1	-1.153792	2.855695	0.752898
18	6	-2.972624	2.254305	-2.115085
19	1	-2.900534	3.251366	-2.561547
20	1	-2.964566	1.510514	-2.912738
21	1	-3.930462	2.184838	-1.592059
22	6	-0.365057	1.557839	-3.174036
23	1	-0.870942	2.206024	-3.895698
24	1	0.679483	1.446696	-3.476585
25	1	-0.833596	0.572115	-3.192012
26	6	0.131681	3.574270	-1.793241
27	1	0.255108	3.969125	-0.784357
28	1	1.106912	3.586665	-2.287929
29	1	-0.540201	4.234349	-2.351001
30	8	0.386279	1.368555	-0.885332
31	8	-1.858140	0.669083	-0.695674
32	5	-0.448237	0.220547	-0.402324
33	6	-0.201678	-0.036362	1.193266
34	1	-0.918448	-0.791638	1.546727
35	1	-0.432608	0.889398	1.742999
36	6	1.222404	-0.477890	1.540093
37	1	1.413342	-1.462255	1.092320
38	1	1.930108	0.211375	1.062426
39	6	1.541964	-0.549648	3.037646
40	1	2.600960	-0.797679	3.175043
41	1	1.395483	0.441811	3.482897
42	6	0.690217	-1.571570	3.789934
43	1	0.986787	-1.646539	4.839265
44	1	-0.367896	-1.303036	3.759247
45	1	0.793501	-2.563658	3.339047

Selected Bond Lengths: B32-C5 1.64045 Å

18m. [6-ONO]

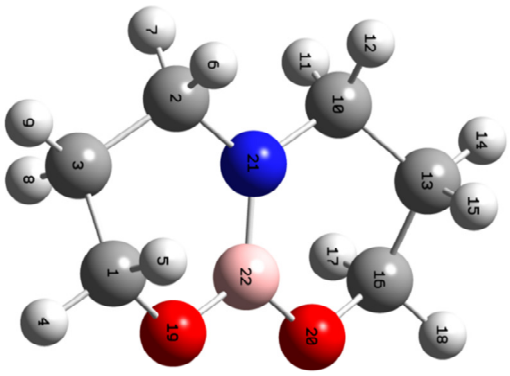

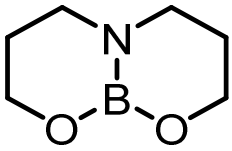

Centre Number	Atomic Number	Coordinates (Angstroms) X	Y	Z
1	6	-1.675601	-2.143206	-0.666678
2	6	-3.132004	-0.223241	-0.011236
3	6	-2.544076	-1.005112	-1.179974
4	1	-1.254244	-2.720093	-1.490537
5	1	-2.269627	-2.820101	-0.041433
6	1	-3.954953	-0.786904	0.449261
7	1	-3.550230	0.725790	-0.366450
8	1	-1.926313	-0.344537	-1.796074
9	1	-3.344091	-1.400617	-1.809047
10	6	-2.442341	1.040978	1.988596
11	1	-2.455128	2.043869	1.539952
12	1	-3.453922	0.842119	2.361419
13	6	-1.441860	0.987480	3.136705
14	1	-1.561132	1.860696	3.781463
15	1	-1.621368	0.094019	3.742610
16	6	-0.022117	0.933113	2.594696
17	1	0.184634	1.820175	1.984360
18	1	0.706999	0.899279	3.404868
19	8	-0.580713	-1.643577	0.096449

20	8	0.178505	-0.235097	1.802884
21	7	-2.100139	0.048532	0.979563
22	5	-0.845231	-0.603716	0.959409

Selected Bond Lengths (Angstroms):		**Selected Bond Angles (Degrees):**
B22-N21	1.41444	N21-B22-O20 121.839
B22-O20	1.37672	N21-B22-O19 121.844
B22-O19	1.37695	O20-B22-O19 116.316

Sum of Angles about Boron (Degrees): 359.999

18n. [Ph6-ONO]$^-$

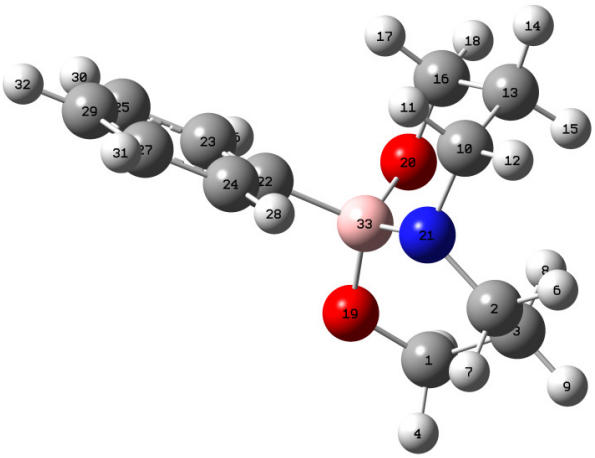

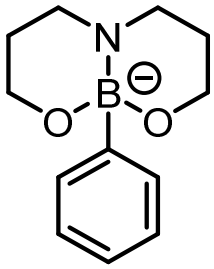

Center Number	Atomic Number	Coordinates (Angstroms) X	Y	Z
1	6	-3.168998	-2.122525	1.485475
2	6	-3.105490	0.373441	1.614220
3	6	-2.868021	-0.924507	2.393480
4	1	-4.246856	-2.332164	1.520757
5	1	-2.654335	-3.016154	1.866704
6	1	-2.930818	1.235557	2.270011
7	1	-4.171146	0.405573	1.337977
8	1	-1.829406	-0.959062	2.726445
9	1	-3.514479	-0.966178	3.277225
10	6	-1.193006	1.448852	0.523259
11	1	-0.867160	1.715583	-0.492797
12	1	-1.554314	2.374510	0.989720
13	6	0.031291	0.907488	1.273315
14	1	0.847419	1.639799	1.265198
15	1	-0.227674	0.706158	2.319426
16	6	0.488401	-0.386782	0.598583
17	1	0.836096	-0.138108	-0.421126
18	1	1.343383	-0.819342	1.132437

19	8	-2.829079	-1.901262	0.132591
20	8	-0.535661	-1.342813	0.547813
21	7	-2.276516	0.484458	0.413977
22	6	-1.543192	-0.815026	-1.754259
23	6	-0.767774	-1.792518	-2.394448
24	6	-2.089951	0.181117	-2.571658
25	6	-0.556749	-1.789369	-3.772356
26	1	-0.314329	-2.571386	-1.787680
27	6	-1.885096	0.205531	-3.952164
28	1	-2.684276	0.957925	-2.098608
29	6	-1.116921	-0.784752	-4.560201
30	1	0.045837	-2.565031	-4.234913
31	1	-2.321955	0.995898	-4.554921
32	1	-0.954205	-0.773160	-5.632602
33	5	-1.802276	-0.883995	-0.133138

Selected Bond Lengths: B33-C22 1.64314 Å

18o. [Ph6-ONO]$^-$ (calculated from the solid state structure of 2a)

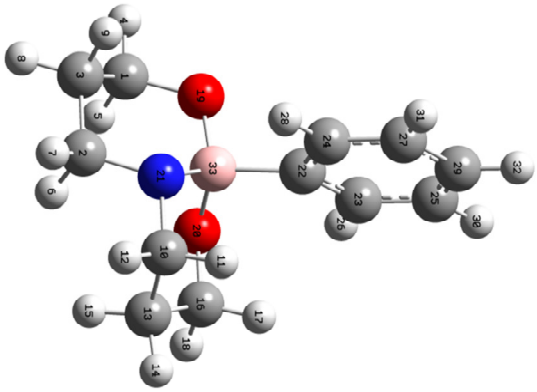

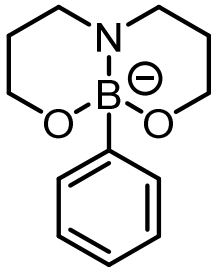

Centre Number	Atomic Number	Coordinates (Angstroms) X	Y	Z
1	6	-3.374020	-2.108088	1.374573
2	6	-3.000027	0.320906	1.727206
3	6	-4.043605	-0.788617	1.738895
4	1	-4.104412	-2.925133	1.372894
5	1	-2.615928	-2.344680	2.138588
6	1	-2.291587	0.116891	2.552351
7	1	-3.469052	1.289316	1.956391
8	1	-4.510861	-0.860629	2.726788
9	1	-4.825767	-0.570702	1.003618
10	6	-1.301000	1.409987	0.426118
11	1	-1.027593	1.620323	-0.616209
12	1	-1.687632	2.346863	0.851572
13	6	-0.031923	0.969302	1.174259
14	1	0.755788	1.723681	1.066603
15	1	-0.237964	0.861393	2.243968
16	6	0.452158	-0.367930	0.612558
17	1	0.811050	-0.201165	-0.417860
18	1	1.305524	-0.736886	1.194375
19	8	-2.792532	-2.041329	0.097180

20	8	-0.553304	-1.348878	0.626670
21	7	-2.347999	0.395679	0.427666
22	6	-1.520939	-0.871545	-1.717159
23	6	-0.516717	-1.637637	-2.323676
24	6	-2.303807	-0.081233	-2.568750
25	6	-0.301837	-1.624617	-3.701783
26	1	0.115918	-2.255208	-1.691067
27	6	-2.104450	-0.054163	-3.948841
28	1	-3.083776	0.530865	-2.124133
29	6	-1.098535	-0.829318	-4.523216
30	1	0.486130	-2.231267	-4.137358
31	1	-2.730036	0.570984	-4.578802
32	1	-0.936096	-0.812391	-5.595548
33	5	-1.810621	-0.961491	-0.101759

Selected Bond Lengths: B33-C22 1.64363 Å

18p. [5-ONO]

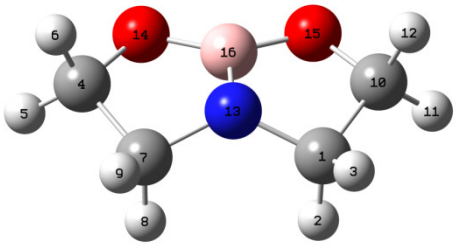

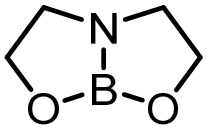

Center Number	Atomic Number	Coordinates (Angstroms) X	Y	Z
1	6	-2.306300	0.067699	-0.177126
2	1	-2.175937	-0.271038	-1.214258
3	1	-3.353324	0.337641	-0.026369
4	6	0.531224	2.419162	-0.178203
5	1	1.276132	2.693222	-0.923191
6	1	0.474243	3.198348	0.584935
7	6	-0.864171	2.142136	-0.784623
8	1	-0.778822	1.730840	-1.800012
9	1	-1.468757	3.050247	-0.824147
10	6	-1.855325	-1.021719	0.823886
11	1	-2.002473	-2.033640	0.450908
12	1	-2.369079	-0.907123	1.780663
13	7	-1.369961	1.138383	0.145223
14	8	0.944247	1.186919	0.462754
15	8	-0.439050	-0.807315	1.043107
16	5	-0.208321	0.476040	0.638115

Selected Bondlengths (Angstroms):

B(16)-O(14)	1.36547
B(16)-O(15)	1.36538
B(16)-N(13)	1.42515

Selected Bond Angles (Degrees):

O(14)-B(16)-O(15)	132.072
O(14)-B(16)-N(13)	113.681
O(15)-B(16)-N(13)	113.683

Sum of angles about boron (degrees): 359.436

18q. [Ph5-ONO]$^-$

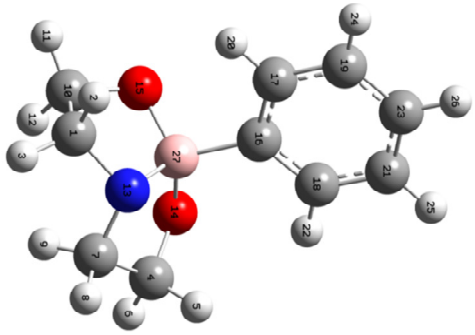

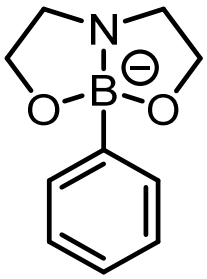

Center Number	Atomic Number	Coordinates (Angstroms) X	Y	Z
1	6	-1.794353	-0.376211	-0.621156
2	1	-1.417867	-1.397372	-0.755248
3	1	-2.444326	-0.142739	-1.471172
4	6	-0.275225	2.768834	0.146658
5	1	0.784058	2.859461	-0.145866
6	1	-0.688167	3.777819	0.247324
7	6	-1.024839	1.925543	-0.882034
8	1	-0.742358	2.175837	-1.912111
9	1	-2.105826	2.117633	-0.776056
10	6	-2.508158	-0.278985	0.733234
11	1	-3.123128	-1.155574	0.963121
12	1	-3.158948	0.609588	0.758428
13	7	-0.670162	0.554774	-0.510741
14	8	-0.400497	2.061574	1.355603
15	8	-1.458229	-0.164165	1.668386
16	6	1.075355	-0.047970	1.450679
17	6	1.262570	-1.437846	1.471304
18	6	2.196586	0.739171	1.742346
19	6	2.497699	-2.015265	1.758353
20	1	0.411882	-2.080485	1.259496

21	6	3.440670	0.178629	2.034248
22	1	2.082886	1.819744	1.747585
23	6	3.596992	-1.205275	2.041338
24	1	2.607554	-3.095217	1.765342
25	1	4.287996	0.818621	2.260157
26	1	4.560891	-1.648339	2.267284
27	5	-0.358243	0.606485	1.035717

Selected Bond Lengths (Angstroms):
B(27)-C(16) 1.62963

18r. [B(OMe)$_3$]

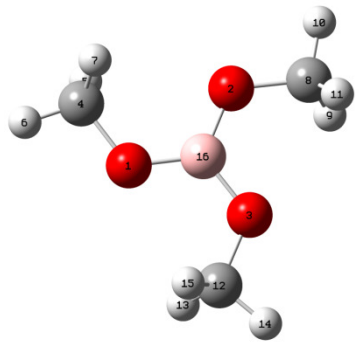

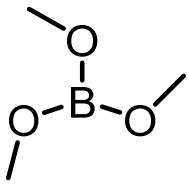

Center Number	Atomic Number	Coordinates (Angstroms) X	Y	Z
1	8	-1.063189	-0.455351	0.573089
2	8	0.526815	0.255381	-1.023438
3	8	1.018451	-1.560683	0.405710
4	6	-1.941713	0.570067	0.124381
5	1	-2.197382	0.428033	-0.927360
6	1	-2.845798	0.513121	0.728194
7	1	-1.484272	1.553624	0.246866
8	6	1.809630	0.105452	-1.620361
9	1	1.916086	-0.884733	-2.067409
10	1	1.900499	0.864922	-2.395052
11	1	2.599575	0.245417	-0.880078
12	6	0.618781	-2.431184	1.457831
13	1	-0.257893	-3.013302	1.167244
14	1	1.450393	-3.104727	1.657796
15	1	0.382977	-1.865751	2.361314
16	5	0.160401	-0.587228	-0.015017

18s. $[PhB(OMe)_3]^-$

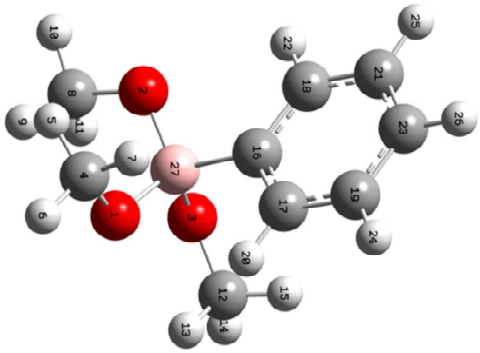

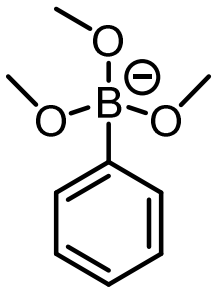

Center Number	Atomic Number	Coordinates (Angstroms) X	Y	Z
1	8	-0.839864	-0.873631	-0.015964
2	8	1.050410	0.423999	-0.869835
3	8	1.388679	-1.668581	0.227174
4	6	-1.764610	0.157887	-0.206340
5	1	-1.537383	0.754794	-1.101078
6	1	-2.763535	-0.273602	-0.328812
7	1	-1.794374	0.849734	0.647912
8	6	0.986816	-0.130906	-2.155485
9	1	-0.043866	-0.384985	-2.439983
10	1	1.370855	0.597841	-2.876235
11	1	1.586674	-1.045654	-2.234819
12	6	1.076977	-2.627695	1.196566
13	1	0.012161	-2.893908	1.181898
14	1	1.658932	-3.534433	1.001164
15	1	1.320935	-2.281927	2.212228
16	6	0.708863	0.388479	1.621112
17	6	-0.127190	0.137151	2.717845
18	6	1.719500	1.340803	1.811200
19	6	0.031074	0.791809	3.939012
20	1	-0.926128	-0.592131	2.603968

21	6	1.892737	2.006869	3.024493
22	1	2.381442	1.564870	0.979825
23	6	1.046632	1.732963	4.097288
24	1	-0.635198	0.571571	4.767208
25	1	2.685078	2.740545	3.136400
26	1	1.175850	2.246711	5.043792
27	5	0.563138	-0.443544	0.211809

Selected Bond Lengths (Angstroms):
B(27)-C(16) 1.64306